

1. Report No. FHWA/TX-00/1432-5F		2. Government Accession No.		3. Recipient's Catalog No.	
4. Title and Subtitle GUIDELINES FOR THE DESIGN AND CONSTRUCTION OF FLEXIBLE BASES TO CONTROL THERMAL CRACKING IN PAVEMENTS				5. Report Date December 1997	
				6. Performing Organization Code	
7. Author(s) Dallas N. Little, Mark N. Milton, Muhammad Arif Beg, Athar Saeed, Albert Yeung, Virgil Anderson, and Ronald Hudson				8. Performing Organization Report No. Report 1432-5F	
9. Performing Organization Name and Address Texas Transportation Institute The Texas A&M University System College Station, Texas 77843-3135				10. Work Unit No. (TRAIS)	
				11. Contract or Grant No. Project No. 0-1432	
12. Sponsoring Agency Name and Address Texas Department of Transportation Research and Technology Transfer Office P.O. Box 5080 Austin, Texas 78763-5080				13. Type of Report and Period Covered Final: September 1995 - December 1997	
				14. Sponsoring Agency Code	
15. Supplementary Notes Research performed in cooperation with the Texas Department of Transportation and the U.S. Department of Transportation, Federal Highway Administration. Research Project Title: Guidelines for the Design and Construction of Flexible Bases to Control Thermal Cracking in Pavements					
16. Abstract Many miles of pavements in Texas are constructed with aggregate bases. These pavements are typically comprised of a thin asphalt surface over a flexible or aggregate base layer. The base layer is, therefore, usually the primary structural layer. Thermal- and moisture-related effects can cause cracks and general distress within these layers, resulting in a general reduction in the serviceability and load-carrying capacity of the pavement. The cracks that may emanate from the flexible base will reflect through the hot mix asphalt surface and further compromise load-carrying capacity of the pavement. The complex and diverse environment within Texas provides a challenge to the proper design, construction, and maintenance of aggregate bases. This project identifies a simple and easy-to-use dielectric value measurement test as an aggregate is subjected to capillary soak as a primary tool for design and construction of acceptable bases. The dielectric value test, combined with an assessment of the effects of the environmental conditions (based on suction potential versus moisture content) at a specific location, can be used to improve the methods for design and construction of aggregate bases. A protocol for this approach to design and construction is presented. Finally, the report presents a protocol for field analysis of the structural capability and response of pavements containing distressed flexible bases. This field testing protocol is integrated with simple and direct lab testing to establish a method of flexible base rehabilitation and recycling alternatives.					
17. Key Words Flexible Base, Dielectric Value, Suction, Thermal-Moisture Sensitivity, Transverse Cracking			18. Distribution Statement No restrictions. This document is available to the public through NTIS: National Technical Information Service 5285 Port Royal Road Springfield, Virginia 22161		
19. Security Classif.(of this report) Unclassified		20. Security Classif.(of this page) Unclassified		21. No. of Pages 256	22. Price

**GUIDELINES FOR THE DESIGN AND CONSTRUCTION OF FLEXIBLE
BASES TO CONTROL THERMAL CRACKING IN PAVEMENTS**

by

Dallas N. Little, Texas Transportation Institute

Mark N. Milton, Center for Transportation Research

Muhammad Arif Beg, Center for Transportation Research

Athar Saeed, Center for Transportation Research

Albert Yeung, Texas Transportation Institute

Virgil Anderson, Center for Transportation Research

and

Ronald Hudson, Center for Transportation Research

Report 1432-5F

Project Number 0-1432

Research Project Title: Guidelines for the Design and Construction of
Flexible Bases to Control Thermal Cracking in Pavements

Sponsored by the
Texas Department of Transportation
In Cooperation with the
U.S. Department of Transportation
Federal Highway Administration

December 1997

TEXAS TRANSPORTATION INSTITUTE
Texas A&M University
College Station, Texas 77843-3135

and

CENTER FOR TRANSPORTATION RESEARCH
Bureau of Engineering Research
The University of Texas at Austin
Austin, Texas 78712

IMPLEMENTATION STATEMENT

GENERAL

This research has identified and developed laboratory tests and a testing and evaluation protocol that can effectively be used to enhance design and construction specifications for the use of aggregate bases. The design and construction tests supplement current TxDOT item 247 specifications of the *Standard Specifications for Construction of Highways, Streets and Bridges (1995)*. This testing can help to assure that bases, which are highly sensitive to thermal and moisture effects, are either not selected or are altered or treated in a manner to reduce thermal and moisture sensitivity to an acceptable level. This research has provided a field testing protocol using the Falling Weight Deflectometer (FWD) and Ground Penetrating Radar (GPR) which has the potential to define the structural capacity and deficiencies in flexible bases due to moisture and thermal damage. An important step at this time is to establish a list of test pavements with established flexible base moisture and/or thermal-moisture related deficiencies in selected districts that can be monitored over a long period of time. The flexible bases represented in the field case history studies should have similar properties (DV, suction, etc.) to the aggregates deemed problematic in the laboratory study and should cover the range of these properties. The selected field case history pavements must then be evaluated using the FWD and GPR techniques described in this report. This evaluation must occur over a sufficient period of time and through significant seasonal and weather episode variations. FWD and GPR testing should be done several times a year over at least a two-year period.

In this proposed implementation or monitoring study, it is imperative to test exactly the same material in the lab that was used in the field for the flexible base. It is equally important to monitor the field sections over at least a two-year period and frequently enough to assess the effects of significant swings in moisture state and significant thermal effects. The experiment design for the field testing and the approach for selecting the case history site locations presented in Chapters 3, 4, and 6 should be followed.

GUIDELINES FOR THE DESIGN AND CONSTRUCTION OF FLEXIBLE BASES TO CONTROL THERMAL CRACKING IN PAVEMENTS

General: The first phase of implementing the finding of this project will involve familiarizing TxDOT personnel with the testing of flexible base materials in an attempt to determine the pavement's susceptibility to thermal cracking. Construction practices that are believed to be either good or bad in regard to preventing cracking will be monitored. After testing the material and observing and possibly specifying construction practices, the completed pavements will be evaluated for cracking. If it can be determined that thermally induced cracks that originate within the base layer can be reliably predicted, testing and construction specifications will be recommended for inclusion in contracts.

Purchase and Distribution of Test Equipment: The project director will coordinate with the Materials and Tests (MAT) Section of the Construction Division to purchase dielectric value (DV) testing equipment for that section. With the approval of MAT, the testing equipment may be purchased for all districts most likely to be affected by thermal cracking so that screening may be accomplished at the district level. Initially, it is recommended that the following districts, as a minimum, be asked to participate in the testing and screening of base materials: Amarillo, Lubbock, Childress, Wichita Falls, Abilene, Paris, and San Angelo. (The problem statement originated in the San Angelo District.)

Lab Tests: Testing will be done on as many base materials as possible so that a catalog of good versus poor aggregates may eventually be obtained. Results will be recorded for each material source for each project having a specified minimum amount of flexible base. DV testing in the beginning will not be performed to determine specification compliance but will be for the purpose of gathering information. Accomplishing the successful screening of materials for their thermal cracking resistance will justify when testing will be done for compliance.

Monitoring of Construction: During construction of pavements containing DV tested base, construction techniques (or their absence) found to be critical in this study will be noted.

Evaluation of Pavements: Upon completion of each pavement project where the flexible bases were tested and the construction techniques were monitored as described above, a test section to monitor cracking will be set up and evaluated at prescribed time intervals. The test section may be established up using the SHRP-LTPP protocol and may be evaluated using PMIS techniques.

Analyzing Results: All data acquired will be sent to the project director for review. After evaluating the testing, construction practices and crack monitoring data, the project director will seek a recommendation from appropriate specification committees to determine if certain specifications need changing to reflect the findings of this project.

DISCLAIMER

The contents of this report reflect the views of the authors, who are responsible for the facts and the accuracy of the data presented herein. The contents do not necessarily reflect the official views or policies of the Texas Department of Transportation (TxDOT), or the Federal Highway Administration (FHWA). This report does not constitute a standard, specification, or regulation.

TABLE OF CONTENTS

	Page
List of Figures	xv
List of Tables	xix
Summary	xxi
Chapter 1. Introduction	1.1
Background	1.1
Study Objectives and Scope	1.2
Research Approach	1.3
Report Organization	1.5
Chapter 2. Summary of Pertinent Literature	2.1
General	2.1
Previous TxDOT Research	2.2
TxDOT Research Report 18-1	2.2
Chapter 3. Extent of Cracking in Texas, Experiment Design, and the Selection of Case Study Projects	3.1
Extent of Cracking in Texas	3.1
PMIS Database	3.1
Average Transverse Cracks per 30.48 m	3.2
Percent PMIS Sections with Three Transverse Cracks per 30.48 m	3.5
Discussion	3.5
Experiment Design	3.6
Temperature	3.6
Moisture	3.6
Soil Type	3.8
Screening of Districts	3.9
Identification and Selection of Case Study Projects	3.9

TABLE OF CONTENTS (CONTINUED)

Chapter 4. Field Condition Surveys	4.1
Sampling Plan	4.1
Distress Manifestation Types	4.1
Measurement Units for Distress Manifestations	4.2
Distress Severity Ratings	4.3
Condition Survey Procedures	4.4
Selection of Test Sections	4.4
Distress Mapping Procedure	4.4
Summary Results	4.4
Chapter 5. Laboratory Testing Program	5.1
Laboratory Testing to Satisfy Research Objectives	5.1
General Requirements of a Successful Flexible Base	5.2
Moisture Sensitivity of Flexible Bases	5.11
Thermal Sensitivity of Flexible Bases	5.16
Influence of Climatic Conditions on the Performance of Flexible Bases	5.24
Laboratory Testing Approach	5.25
Laboratory Testing Procedures Adopted for this Study	5.26
Gradation and Moisture - Density Analysis	5.26
Dielectric and Electrical Conductivity Measurements During Capillary Soak	5.26
Suction Measurements as a Function of Moisture	5.27
Volume Change Due to Freezing and Thawing	5.31
Strength Testing	5.35
Mineralogical Testing and Index Testing to Evaluate Mineralogical Effects	5.35
Materials Evaluated	5.36
Source Material and Site Specific Material	5.36
Selected Study to Determine Volumetric Effects of Freezing and Thawing	5.40
Finding from Laboratory Testing	5.41

TABLE OF CONTENTS (CONTINUED)

Source Material and Site Specific Studies	5.41
Selected Study to Determine Volumetric Changes During Freezing and Thawing Cycles	5.57
Chapter 6. Falling Weight Deflectometer (FWD) Testing and Data Collection	6.1
Falling Weight Deflectometer Apparatus	6.1
Analysis of FWD Deflection Data	6.1
Structural Evaluation of Pavement	6.2
Backcalculation of Moduli	6.3
Statistical Analysis	6.4
FWD Testing Protocol for Project	6.4
Tests in Areas Free of Distress	6.5
Tests at Cracked Locations	6.9
Winter Phase	6.9
Summer Phase	6.10
Data Collection	6.11
Variability within the Pavement Structure and Material	6.11
Variability Associated with the Testing Apparatus	6.12
Variability Associated with Human Error	6.12
Chapter 7. Structural Evaluation of Case Study Pavements Using FWD Data	7.1
Parameters Considered in the Evaluation	7.1
Ground Penetration Radar Analysis	7.1
Structural Evaluation	7.2
Results of Analysis	7.8
Discussion	7.11
Chapter 8. Statistical Analysis of FWD Data	8.1
Main Effects Considered	8.1
Classification (Class) Variables	8.1
Continuous Variables	8.2

TABLE OF CONTENTS (CONTINUED)

Interactions	8.2
Models	8.3
Statistical Analysis	8.4
Chapter 9. Synthesis of Results	9.1
Chapter 10. Summary and Conclusions and Recommendations	10.1
Guidelines for Design of Flexible Bases	10.1
Selection of Alteration or Stabilization Strategies to Eliminate or Mitigate Moisture and Thermal Problems in Flexible Bases	10.3
Field Testing Protocol to Evaluate the Structural Effects of Transverse Cracking . . .	10.3
Recommendations	10.4
References	R-1
Appendix A	A-1
Appendix B	B-1
Appendix C	C-1
Appendix D	D-1
Appendix E	E-1

LIST OF FIGURES

Figure	Page
1.1 Research Approach Used for Study 1432	1.4
3.1 Distribution of Average Transverse Cracks in Districts	3.4
3.2 Distribution of Percentage of PMIS Sections Having Three Transverse Cracks Per Section in Districts	3.4
3.3 Temperature (Freeze and No-Freeze) and Moisture (Wet and Dry) Categories	3.7
3.4 General Soil Classifications Used in This Study	3.10
3.5 Factorial Identifying Texas Districts	3.12
3.6 Potential Texas Districts for Case Study Projects Selection	3.13
3.7 Factorial Cells Showing the Number of Selected Case Study Projects	3.14
3.8 Selected Case Study Projects	3.15
4.1 Sampling Plan for Distress Mapping	4.1
4.2 Distress Manifestation Types for Condition Surveys	4.2
5.1 Predicted versus Observe Poission's Ratio	5.5
5.2 Schematic Illustration of the Point of Tertiary Deformation on a Plot of Accumulated Permanent Deformation versus Number of Cyclic Load Applications	5.10
5.3 Correlation between CBR-Value and Gravimetric Moisture Content of Texas and Finnish Aggregates	5.14
5.4 Correlation between CBR-Value and Dielectric Value of Texas and Finnish Aggregates	5.14
5.5 The Effect of Drying and Saturation in the Strength Properties and Dielectric Value of Some Texas Carbonate Aggregates	5.15
5.6 Correlation between Water Absorption and Specific Surface Area of Fine Factions (<0.074 mm) of Some Finnish Base Course Materials	5.17
5.7 Volume Change upon Freezing: (a) Volume Change of Most Materials; and (b) Volume Change of Water	5.20
5.8 Freezing Point Depression as a Function of Suction	5.22
5.9 Capillary Soak - Dielectric Value Test Setup and Typical Results	5.28

LIST OF FIGURES (CONTINUED)

Figure	Page
5.10a. The Probe Tip Containing the Sensing Elements (Transistors)	5.30
5.10b. The Probe and Thermally Insulated Container	5.30
5.11 Calibration of Probe 9-Transistor Psychrometer	5.32
5.12 Plots of Average Dielectric Values for Source and Pavement Site Materials in the Abilene District	5.47
5.13 Plots of Average Dielectric Values for Source and Pavement Site Materials in the Amarillo District	5.48
5.14 Plots of Average Dielectric Values for Source and Pavement Site Material in the Lufkin District	5.49
5.15 Plots of Average Dielectric Values for Source and Pavement Site Material in the San Angelo District	5.50
5.16 Plots of Average Dielectric Values for Source and Pavement Site Materials in the Yoakum District	5.51
5.17 Plots of Average Texas Triaxial Strength Plots (7 kPa confinement) for Materials in the Abilene and Amarillo Districts.	5.52
5.18 Plot of Average Texas Triaxial Strengths (7 kPa confinement) for Materials from the Lufkin and Yoakum Districts	5.53
5.19 Plot of Average Texas Triaxial Strengths (7 kPa confinement) for Materials from the Bryan and Corpus Christi Districts	5.54
5.20 Compaction Moisture-Density Relationships for Selected Aggregates Used in the Freeze-Thaw Volume Change Analysis	5.59
5.21 Percent Height Change of Coon Pit Aggregate versus Temperature	5.59
5.22 Percent Diameter Change of Coon Pit Aggregate versus Temperature	5.60
5.23 Percent Volume Change of Coon Aggregate versus Temperature	5.60
5.24 Suction versus Water Content of Box Canyon Aggregates	5.66
5.25 Suction versus Water Content of Buckles Pit Aggregates	5.66
5.26 Suction versus Water Content of Coon Pit Aggregates	5.67
5.27 Suction versus Water Content of Lindsey Aggregates	5.67

LIST OF FIGURES (CONTINUED)

Figure	Page
5.28 Suction versus Water Content of Victoria Aggregates	5.68
5.29 Suction versus Water Content of Yoakum Crushed Limestone	5.68
5.30 Suction versus Water Content of Lime Treated Fayette County Gravel	5.69
5.31 Master Curve of Suction versus Water Content for All Seven Aggregates	5.69
5.32 Master Curve of Soil Suction versus Water Content Normalized	5.70
5.33 Variation of Suction Capacity with Maximum Water Content	5.70
5.34 Variation of Water Content with Time during Suction Test for Box Canyon Aggregate	5.71
5.35 Variation of Water Content with Time during Suction Test for Buckles Pit Aggregate	5.71
5.36 Variation of Water Content with Time during Suction Test for Coon Pit Aggregate	5.72
5.37 Variation of Water Content with Time during Suction Test for Lindsey Aggregate .	5.72
5.38 Variation of Water Content with Time during Suction Test for Victoria Aggregate .	5.73
5.39 Variation of Water Content with Time during Suction Test for Yoakum Limestone .	5.73
5.40 Variation of Water Content with Time during Suction Test for Yoakum Lime-Treated Limestone	5.74
5.41 Static Equilibrium and Steady-State Flow Conditions in the Zone of Negative Pore-Water Pressure.	5.77
5.42 Predicted Suction in Subgrade below a Pavement (Upper Value), $pF = \log(\text{mm of H}_2\text{O})$ Based on Thornthwaite Moisture Index (Lower Value) for a Clay Subgrade	5.81
5.43 Approximate Construction of a Suction (pF) versus Volumetric Water Content Curve	5.82
6.1 Typical Deflection Bowl from FWD Deflection Data	6.2
6.2a CASE 1: No Visible Cracks in Pavement	6.7
6.2b CASE 2: Crack between Loading Plate (Sensor #1) and Sensor #2	6.7
6.2c CASE 3: Crack behind Loading Plate (Sensor #1); Normal Sensor Positioning	6.7

LIST OF FIGURES (CONTINUED)

Figure	Page
6.2d	CASE 4: Crack behind Loading Plate (Sensor #1) and Additional (Sensor #4) 6.8
6.2e	CASE 5: Crack between Sensor #2 and Sensor #3 6.8
7.1	Average Maximum Deflections (Y_1) for Winter Phase of Testing 7.4
7.2	Average Maximum Deflections (Y_1) for Summer Phase of Testing 7.4
7.3	Average SCI Calculations for Winter Phase of Testing 7.5
7.4	Average SCI Calculations for Summer Phase of Testing 7.5
7.5	Average BCI Calculations for Winter Phase of Testing 7.6
7.6	Average BCI Calculations for Summer Phase of Testing 7.6
7.7	Average LTE Calculations for Winter Phase of Testing 7.7
7.8	Average LTE Calculations for Summer Phase of Testing 7.7

LIST OF TABLES

Table		Page
3.1	Pavement Types in PMIS Database Used in Determining the Extent of Transverse Cracking in Texas	3.2
3.2	Extent of Cracking in Flexible Pavements in Texas	3.3
3.3	General Soil Classification of Texas Used in this Study	3.8
3.4	Summary of the Selected Case Study Projects	3.16
4.1	Distress Severity Levels Used in Field Surveys	4.3
4.2	Summary Statistics for the Distress Types in Outside Lane of the Case Study Projects	4.5
4.3	Summary Statistics for the Distress Types in Inside Lane of the Case Study Projects	4.6
5.1	Material Properties K_1 to K_5 for Soil at Minus 2% Optimum Moisture	5.6
5.2	Material Properties K_1 to K_2 for Soil at Optimum Moisture	5.6
5.3	A Proposed Relationship between Electrical Properties and Field Performance of Granular Base Material	5.29
5.4	Material Used in Laboratory Dielectric Testing from the Abilene District	5.37
5.5	Material Used in Laboratory Dielectric Testing from the Amarillo District	5.37
5.6	Material Used in Laboratory Dielectric Testing from the Lufkin and Bryan Districts	5.38
5.7	Material Used in Laboratory Dielectric Testing from the San Angelo District	5.38
5.8	Material Used in Laboratory Dielectric Testing from the Yoakum District	5.38
5.9	Study of the Effects on Additives and Selective Gradation Alterations on Selected Aggregates	5.39
5.10	Seven Aggregate Systems Selected for Volumetric Change Testing Due to Freeze-Thaw	5.41
5.11	Relationship between Suction and Water Content	5.62
5.12	Estimates of Wet Suction Values	5.79
5.13	θ_{sat} for Various Soil Classifications	5.82
7.1	Y_1 Mean and Standard Deviation for Case 1 Configurations	7.2

LIST OF TABLES (CONTINUED)

Table		Page
8.1	Significance of Main Effects on Y_1	8.5
8.2	Significance of Main Effects on SCI	8.6
8.3	Significance of Main Effects on LTE	8.6
8.4	Significance of Effect of Pavement Temperature * Phase	8.7
8.5	Significance of Effect of Pavement Temperature * Asphalt Thickness	8.8
8.6	Significance of Main Effects and Interactions on Y_1 , SCI, and LTE	8.8
8.7	Significance of Main Effects and Interactions on Y_1 , SCI, and LTE Using Only Case 1 Data	8.9

SUMMARY

Aggregate bases provide the major structural component, or at least a primary structural component, of many miles of Texas pavements. Thermal- and moisture-related effects sometimes cause these aggregate bases to crack or lose strength, resulting in a reduction of pavement life. It is, therefore, imperative to identify design and construction protocols that will help ensure better performing aggregate bases with greater resistance to moisture and thermal effects.

This project evaluated the extent of transverse cracking in Texas and found it to be widespread based on a review of PMIS data. The review demonstrated that while much of the transverse cracking is thermally induced in the hot mix asphalt concrete surface, much also originates in the aggregate base as a result of volume change triggered by thermal cycling or moisture cycling. Previous TxDOT research on this issue has documented the mechanisms that are responsible for transverse cracking due to thermal cycling. The previous research also pointed out the climatic and environmental diversity within the state of Texas and how the climatic conditions compounded with subgrade soil conditions affect the potential for cyclic thermal- or moisture-related cracking within aggregate bases.

The major research objective of this project was to develop design and construction protocols to reduce the potential for thermal or moisture cracking within flexible bases. The researchers identify laboratory design and quality control tests that will supplement current item 247 specification tests for flexible bases. These tests include a capillary soak test with dielectric value measurement. The maximum or equilibrium value of the dielectric value following at least 250 hours of soak is a good parameter by which to assess moisture sensitivity of unbound aggregates. The test is sensitive to the fines component of the aggregate, the mineralogy of the aggregate, and chemical stabilization techniques used to improve the properties of the aggregate. The dielectric value recorded following long-term soak (250 hours) is compared to criteria to determine if the aggregate possesses good, fair, or poor moisture and thermal susceptibility.

If the aggregate base meets the criteria associated with the capillary soak screening test, then the threshold moisture of the aggregate base is determined. This threshold is the maximum moisture content that the aggregate base can tolerate either during construction or after the base reaches

moisture equilibrium with the environment without suffering destructive expansion due to the effects of freezing or thermal cycling (freeze-thaw) effects. The selection of the threshold or boundary moisture is determined based on aggregate suction-moisture content relationships and climatic conditions of the region in question based on the Thornthwaite Index and other environmentally related criteria.

A dielectric value is determined for each level of molding moisture content during the development of the moisture-density relationship. This dielectric value versus moisture content relationship can then be used for quality control purposes during construction of the flexible base.

Case history pavement sections were identified for field testing using the falling weight deflectometer (FWD) and ground penetrating radar (GPR). These studies illustrated the range in severity of thermal cracking among various districts. A testing protocol was developed for the FWD which makes it possible to define the load transfer efficiency (LTE) across pavement cracks and to identify the structural significance of the cracks. The testing protocol can be effectively used to assess field structural conditions and as an input to determine the need for rehabilitation of the pavement structure. Such rehabilitation may include recycling and/or upgrade of the base course through, for example, chemical stabilization. If this choice is made, the laboratory tests can be used to assess the ability of the corrective or stabilization processes to improve strength and stability and also to reduce thermal and moisture sensitivity.

CHAPTER 1. INTRODUCTION

BACKGROUND

Many miles of pavements in Texas are constructed with aggregate bases. These pavements are typically comprised of a thin asphalt concrete surface over a flexible base layer. The base layer is therefore often the major structural component in such pavements. Thermal- and moisture-related effects can sometimes cause cracks in these base layers. Because these cracks reflect through the asphalt surface, the load carrying capability of the entire pavement structure is thereby reduced. Thermal- and/or moisture-related cracking within the base layer is a problem that must be addressed to improve our ability to construct and manage structurally adequate pavements.

Texas' diverse environment includes regions with and without freezing temperatures and varying amounts of rainfall. Frost depth ranges from 12 to 50 cm in freezing regions in Texas [Jumikis 1977], which indicates that thermal activity is typically limited in surface and base layers in pavements in Texas. A low temperature cracking mechanism of asphalt concrete, however, cannot explain the large amount of transverse cracking observed in the no-freeze regions of Texas. Where it occurs, the alternate freezing and thawing brings about severe thermal stresses in pavement materials that can contribute to cracking. Carpenter and Lytton [1977] report that thermal fatigue caused by freeze-thaw cycling is a major cause of transverse cracking in flexible bases in west Texas.

The problem of cracking in bases is observed in different climatic regions throughout the state. It is likely that different distress mechanisms, which may or may not be thermal related, are active in Texas.

There have always been concerns regarding the quality of base materials in Texas. Sometimes for economic reasons, relatively lower quality materials are used to take advantage of local materials for pavement construction. These materials may be susceptible to thermal- and/or moisture-related cracking. Moreover, different coarse aggregate types — for example, limestone, gravel, and caliche — are used in construction in Texas. It is important to investigate the effect of coarse aggregate type on the cracking potential of bases.

Premature cracking in road bases in some of the newly constructed projects was observed in the San Angelo and Yoakum Districts. It is possible that base layers compacted at wet of optimum moisture content might have experienced shrinkage cracking on drying. Both transverse and random cracking are manifested on such prematurely cracked projects. At this stage, no conclusive explanation can be given for premature cracking in flexible bases.

It is essential to understand how such factors as the aggregates' physical and mineralogical properties, state construction practices, and the state's environment influence cracking in road bases. Developing such an understanding is critical in developing design and construction specifications for the Texas Department of Transportation (TxDOT) which will help in minimizing the problems of thermal and premature cracking in road bases.

STUDY OBJECTIVES AND SCOPE

Study 1432, entitled "Guidelines for the Design and Construction of Flexible Bases to Control Thermal Cracking in Pavements" was commissioned to investigate the problem of thermal- and/or moisture-related cracking in flexible bases — a problem prevalent in many regions in Texas. The following summarizes the objectives set forth for the study:

- Determine the extent of thermal cracking in flexible bases in Texas.
- Develop comprehensive design specifications for flexible bases that will minimize thermal cracking yet fulfill other design criteria.
- Develop improved flexible base construction specifications that can account for such factors as moisture content, compaction density, and other construction and design parameters.
- Investigate methods of improving poor performing aggregates (e.g., the use of stabilizers).
- Develop guidelines to structurally evaluate cracked pavements, and to propose optimum repair strategies for cracked pavements based on technical and economic considerations.

RESEARCH APPROACH

The research approach for Study 1432 is primarily based on a comprehensive field and laboratory testing program to investigate base materials from selected case study projects. Figure 1.1 shows the flowchart for the research approach used in this study. The researchers conducted a literature search for the study and documented the relevant references and important conclusions found.

The researchers utilized the PMIS database to help determine the extent of thermal cracking in roadbases in Texas. The PMIS database contains detailed distress data for most of the pavement sections in the state. Transverse cracking observed on the pavement surface was the primary focus when reviewing the database.

The next step developed was an experimental design for the study that included three important factors: temperature, moisture, and soil type. A screening of districts was conducted to identify candidate districts for study projects. Several TxDOT district offices were contacted; field visits were carried out, and case study projects were selected.

A comprehensive field evaluation program was conducted to investigate the case study projects. The program consisted of visual condition surveys, falling weight deflectometer (FWD) testing, and ground-penetrating radar (GPR) surveys. The purpose of the field evaluation program was to obtain information about pavements' condition and to estimate in situ properties of base materials in the case study projects. In future condition surveys, results will be examined in conjunction with the results obtained from other field and laboratory tests. This will help in understanding the relationship among the observed distresses, in situ pavement properties, and laboratory test results.

Base material samples were obtained from each case study project or representative samples from quarries within that district. The material samples were subjected to a comprehensive laboratory testing program aimed at investigating thermal susceptibility and strength properties of the materials.

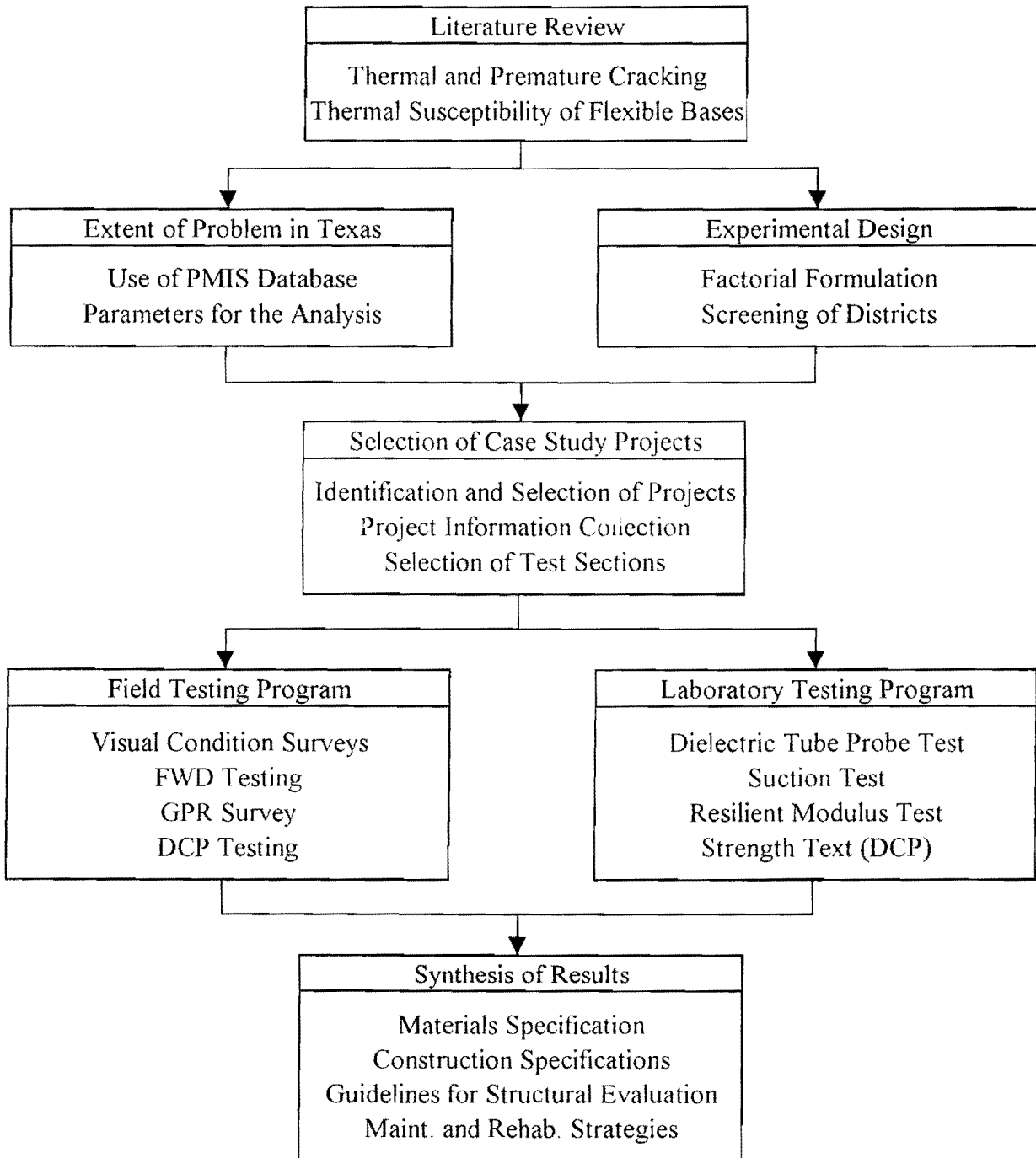


Figure 1.1 Research Approach Used for Study 1432

Results from the field and laboratory evaluation were synthesized in an effort to identify the cause of thermal cracking in flexible bases. Specifications were then developed for base materials to control thermal cracking. Finally, guidelines were developed for structural evaluation of cracked pavements which can be used with the laboratory testing protocol identified herein to select optimum repair strategies proposed to maintain and rehabilitate cracked pavements.

REPORT ORGANIZATION

Report 1432-5 is the final report for this study. It documents background, the literature review, extent of transverse cracking observed in Texas, experiment design, selection of case study projects, the field and laboratory evaluation programs, and presents the conclusions and recommendations of the study. The report is organized in chapters as follows.

Chapter 1 has presented some background, the objectives and scope of the study, and the research approach.

Chapter 2 presents a brief summary of the pertinent literature.

Chapter 3 describes the analysis of PMIS data conducted to determine the extent of transverse cracking in pavements in Texas. It also describes the experimental design developed for the study and the selection of the case study projects. It details the screening of districts and the selection of case study projects for field evaluations.

Chapter 4 describes the condition survey procedures and reports summary results for the surveys the researchers conducted on case study projects.

Chapter 5 presents the laboratory dielectric, strength, thermal susceptibility, and field ground penetrating radar (GPR) studies done to support the development of improved design and construction protocol for flexible bases.

Chapter 6 presents a general description of falling weight deflectometer (FWD) measurements and an overview of FWD data analysis. Also presented in this chapter is the testing protocol the researchers adopted for this study and some of the data collection problems that were encountered.

Chapters 7 and 8 are dedicated to our analysis of the FWD data for this study. Chapter 7 presents the results of the structural type evaluation of the data. Chapter 8 describes the methodology used in the statistical analysis of the data and presents the results.

Chapter 9 develops a synthesis of the results of both the laboratory and field testing programs.

Chapter 10 presents the researchers' conclusions for the improved design and construction of flexible bases with the goal of eliminating or at least mitigating moisture and/or thermally reduced cracking in these bases.

CHAPTER 2. SUMMARY OF PERTINENT LITERATURE

GENERAL

Very few Texas pavements were originally designed and constructed with thick asphalt surface layers (greater than about 200 mm); therefore, the base layer is often the major structural component of the pavement. Consequently, it is imperative to treat this layer as a critically important structural contributor. Since cracking within the base layer can certainly diminish its load-carrying capability, the problems associated with thermal and traffic load induced cracking within the base layer greatly impact the performance of the entire pavement structure. Thermal- or moisture-related cracking within the base is a problem that must be addressed, as this cracking reflects through the asphalt surface layer.

Concerns have been raised regarding the quality of base materials in Texas and that these lower quality materials are susceptible to freeze-thaw damage. Economical sources of type 1 bases do not exist in many parts of Texas, particularly along the Gulf Coast, south Texas, the High Plains, and in east Texas. Since local aggregate sources in those regions may not meet the rather tight specification requirements of type 1 bases (with regard to Texas triaxial strength, abrasion resistance, plasticity, etc.), it is essential to understand how their highly variable physical properties and mineralogical properties will influence their behavior in the pavement environment. In other areas, stabilizers are used to bring marginal materials up to type 1 specification; in some instances, these stabilizers may be the cause of some of the reported cracking.

This section summarizes the literature review conducted for Study 1432. Reports from earlier research conducted for TxDOT by the Texas Transportation Institute (TTI) [Carpenter 1974, 1977] were reviewed, and important conclusions are documented.

PREVIOUS TXDOT RESEARCH

TxDOT Research Report 18-1 [Carpenter, Lytton, Epps]

Carpenter et al. [Carpenter 1974] investigated environmental factors related to thermal cracking in west Texas and identified the following environmental factors to be significant for their study:

- rate of temperature drop,
- number of freeze-thaw cycles,
- solar radiation, temperature averages and ranges, and
- long-term moisture balance.

Shahin and McCullough [Shahin 1972] considered eight environmental and material parameters for their study of thermal fatigue cracking in pavements; they concluded that the following factors are most important in characterizing asphalt concrete cracking caused by thermal fatigue:

- average air temperature,
- solar radiation, and
- pavement surface absorptivity.

Carpenter et al. [Carpenter 1974] report that the thermal susceptibility of the base course is a valid deterioration mechanism, and that cyclic freeze-thaw contraction of base course materials is the major cause of thermal cracking in west Texas. Granular base course materials experience a volumetric contraction on freezing in a condition of constant moisture content. This contraction is similar to that which occurs in shrinkage drying of stabilized material, except that this freeze deformation is cyclic. A portion of this deformation remains after the material is thawed. This periodic volume change with freeze-thaw cycling is termed to be thermal susceptibility. Two components of thermal susceptibility are identified:

- freeze coefficient, which represents the contraction on freezing, and
- residual coefficient, which represents the permanent deformation.

The observed freeze coefficients were greater than the thermal coefficient of asphalt concrete, indicating that the base course is more thermally active than asphalt in west Texas.

Moisture in soil and unbound materials is one of the principal factors governing the soils' physical and mechanical properties and performance under thermal loading. Soil suction is used to characterize the effect of moisture on the volume and strength properties of unsaturated soils. Soil moisture suction is the process of soil moisture transfer through a porous medium of soil brought about by means of a thermal potential [Jumikis 1977]. Carpenter et al. [Carpenter 1974] mention that soil moisture suction is a parameter that directly relates the influence of the environment to the engineering behavior of the soil. Moreover, the freeze coefficients and residual coefficients mentioned above are related to the suction. Freeze coefficients increase 10 to 20 times from their initial value during freezing and then drop below the initial value during the thaw cycle.

Carpenter et al. [Carpenter 1974] conclude that thermal contraction of road bases is also affected by the proportion and mineralogy of clay particles present in the base material. The freezing process forces clay particles to reorient (significant volume contraction was observed through a scanning electron microscope). The amount of reorientation, and thus volume change, was shown to be controlled by the surface area of clay particles.

Electrical parameters, such as the dielectric constant and electrical conductivity, can also assist in the study of thermal behavior of pavement materials. Saarenketo and Little [Saarenketo 1995] evaluated eight different Texas fine aggregates (<0.074 mm) and two Finnish aggregates in order to relate their dielectric value and electrical conductivity at different moisture contents and densities to their strength and deformation properties. It was found that the dielectric constant correlates with the California Bearing Ratio (CBR), a measure of shear strength of compacted base, better than does compaction moisture content.

CHAPTER 3. EXTENT OF CRACKING IN TEXAS, EXPERIMENT DESIGN, AND THE SELECTION OF CASE STUDY PROJECTS

EXTENT OF CRACKING IN TEXAS

Following the literature review, the next step in the study was to assess the extent of cracking in road bases in Texas. This analysis provided the general trend of thermal cracking in Texas and helped to identify candidate districts to be used as case study projects for our field investigations. The best available data source to assist in this analysis was the PMIS database.

PMIS DATABASE

The PMIS database contains information about most of the pavement sections in the state of Texas, including detailed data on such distresses as transverse cracking. The latest survey, conducted in fiscal year 1995, was used for examining previously observed transverse cracking. Of course, given the many causes of transverse cracking in pavements, there is no reason to believe that transverse cracking observed in the PMIS results solely from problems in the base course. However, performing this preliminary survey helped to identify areas of potential study—areas where significant transverse cracking had been observed in recent years. The PMIS visual distress data are collected on a sample of the total pavement network of Texas. Each PMIS section is 0.88 km (0.5 m) long, and distresses are measured on only one of the lanes.

The PMIS Rater's Manual [PMIS 95] describes transverse cracking as cracks that are at right angles to the centerline and that (1) are at least 3.2 mm wide, (2) show evidence of spalling or pumping, or (3) have been sealed. In the PMIS, transverse cracks are recorded in terms of number per station (that is, the number of cracks in each 30.48 m of surface).

Ten pavement types, including different forms of rigid, flexible, and composite pavements, are defined in the PMIS database. Among these, the five pavement types that relate to flexible pavements are used in determining the extent of cracking in Texas. These pavement types are listed in Table 3.1.

Table 3.1. Pavement Types in PMIS Database Used in Determining the Extent of Transverse Cracking in Texas

Pavement Type Code in PMIS	Pavement Type Description
4	Thick asphalt concrete pavement (greater than 13.5 mm)
5	Intermediate thickness asphalt concrete pavement (61 to 135 mm)
6	Thin surfaced flexible base pavement (less than 61 mm)
9	Overlaid and/or widened old flexible pavement
10	Thin surfaced flexible base pavement (surface treatment-seal coat combination)

Since this analysis was used to identify candidate districts from which case study projects could be selected, the analysis was performed on a district basis. We defined two parameters for establishing the extent of transverse cracking in Texas. They are as follows:

- average transverse cracks per 30.48 m (100 ft), and
- percent PMIS sections with at least three transverse cracks per 30.48 m (100 ft).

The two parameters were determined by manual counts using hard copies of PMIS distress data sheets.

Average Transverse Cracks per 30.48 m

Transverse cracking data in the PMIS database are available for pavement sections in the form of cracks per 30.48 m (100 ft). Average transverse cracks per section were calculated by dividing the total number of transverse cracks by the total number of PMIS sections for each district. This indicator gave a general picture of the extent of cracking in the districts. The mean value of the indicator for the state was 3.01 cracks per section. Table 3.2 lists the Texas districts and the corresponding value of the calculated parameter.

Table 3.2. Extent of Cracking in Flexible Pavements in Texas

District No.	District	Total No. of PMIS Cracked Sections	Total Observed Trans. Cracks in PMIS Sections	Average Trans. Cracks Per Section	% PMIS Sections with 3 Trans. Cracks
1	Paris	232	879	3.79	49
2	Ft. Worth	240	399	1.66	6
3	Wichita	284	1154	4.06	20
4	Amarillo	2192	7685	3.51	34
5	Lubbock	1410	3958	2.81	27
6	Odessa	546	1221	2.24	14
7	San Angelo	317	665	2.10	14
8	Abilene	773	1398	1.81	8
9	Waco	267	701	2.63	24
10	Tyler	152	392	2.58	36
11	Lufkin	255	851	3.34	34
12	Houston	1323	5042	3.81	42
13	Yoakum	110	621	5.65	26
14	Austin	181	475	2.62	22
15	San	244	545	2.23	15
16	Corpus	165	340	2.06	13
17	Bryan	747	2577	3.45	36
18	Dallas	395	945	2.39	15
19	Atlanta	171	327	1.91	4
20	Beaumont	230	780	3.39	40
21	Pharr	435	2329	5.35	54
22	Laredo	103	276	2.68	21
23	Brownwood	247	576	2.33	21
24	El Paso	539	2378	4.41	44
25	Childress	850	2130	2.51	23

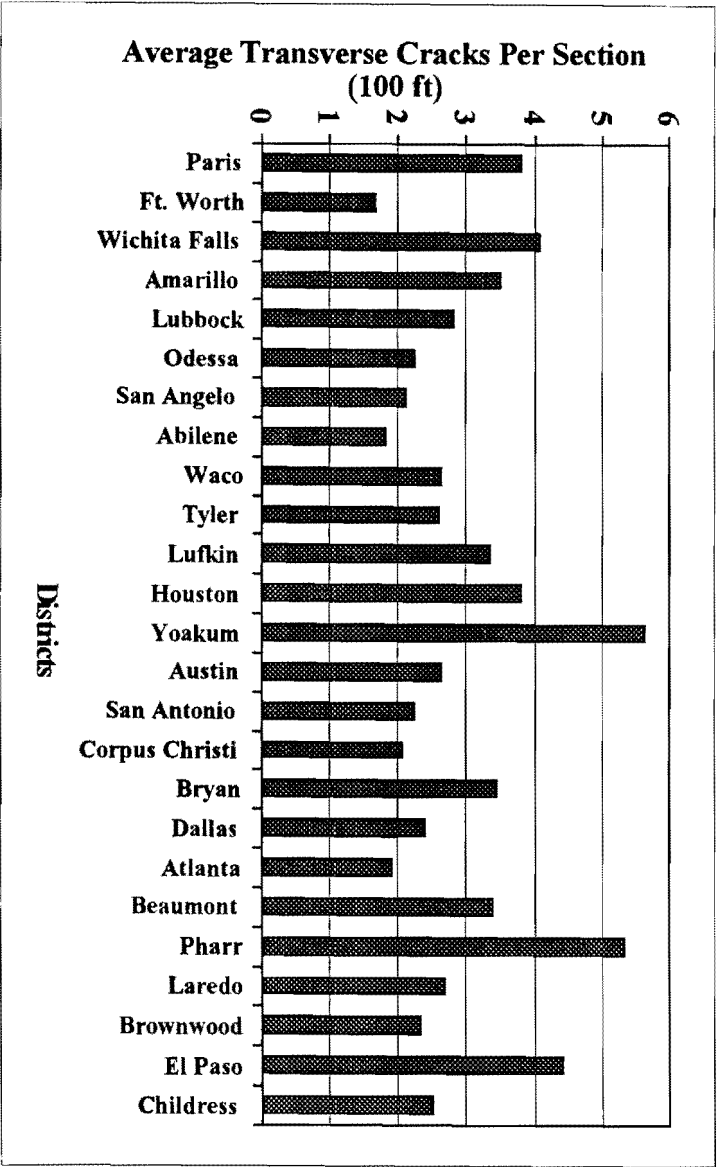


Figure 3.1. Distribution of Average Transverse Cracks in Districts

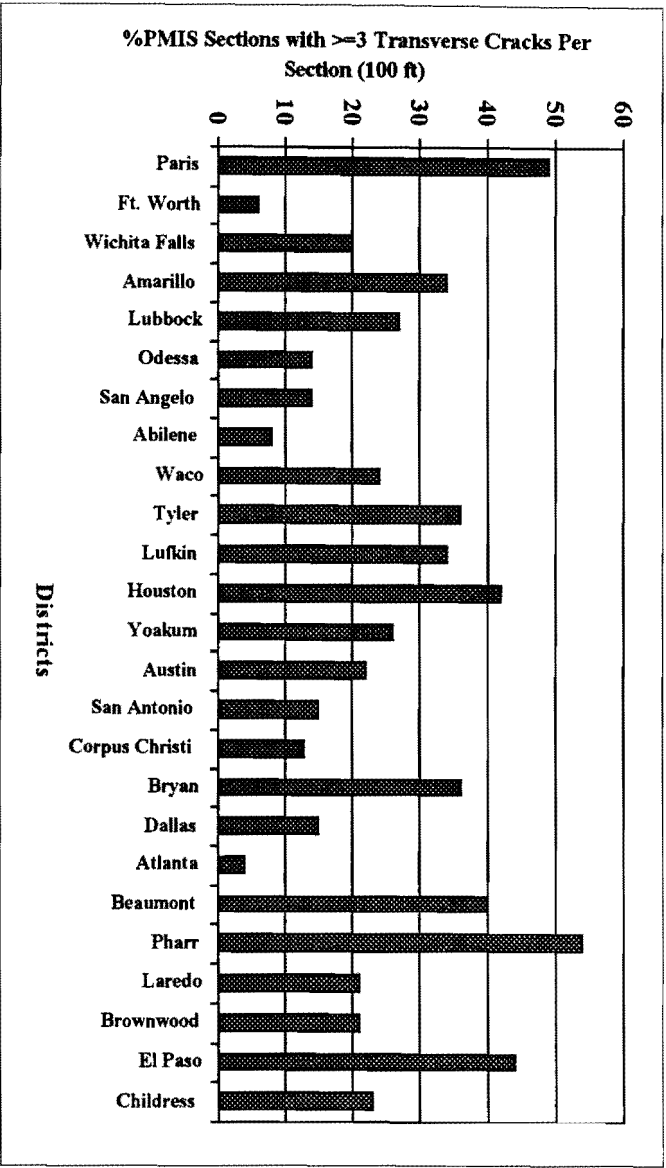


Figure 3.2. Distribution of Percentage of PMIS Sections Having Three Transverse Cracks Per Section in Districts

Percent PMIS Sections with Three Transverse Cracks per 30.48 m

The percentage of PMIS sections having three transverse cracks was also calculated for each district. This parameter gave a measure of the distribution of severely cracked sections in the districts. The boundary value of 3 was chosen because it was the average value for the first parameter, namely, average transverse cracks per section. Table 3.2 and Figures 3.1 and 3.2 show Texas districts and the corresponding value of the calculated parameters.

Discussion

The results show that every district in Texas has some level of transverse cracking in pavements. Moreover, a range of 1.66 to 5.65 cracks per 30.48 m (100 ft) was observed, which suggests a considerable variation among the districts. Similarly, a wide range of 4% to 54% was observed among the districts for the second parameter, namely, PMIS sections having three transverse cracks per 30.48 m (100 ft).

A higher extent of cracking was observed in the Amarillo, El Paso, Pharr, and Paris Districts. These districts are located remotely from each other and have very different climatic conditions. It is an interesting result and shows that transverse cracking is not confined to specific geographical locations or climatic conditions in Texas. This trend indicates that some other factors, in addition to a specific set of climatic factors, are influential in causing transverse cracking in road bases in Texas.

No data are available in the PMIS database for pavement age, pavement structure, stabilized layers, and coarse aggregate types. It was, therefore, not possible to assess the role of these factors on the observed transverse cracking.

There is a general trend that the districts having a larger average of transverse cracks per section also have a larger percentage of sections having three transverse cracks. Yoakum and Wichita Falls, however, are exceptions; they have a larger value for average cracks per section, but a rather low percentage of sections with three transverse cracks. This indicates the presence of a small proportion of heavily cracked sections in the sampled PMIS sections in these two districts.

EXPERIMENT DESIGN

In establishing the experiment design, temperature and moisture served as the two climatic variables. Two levels were defined for each of the factors. Subgrade soil type was also included in the factorial, since it has an indirect effect on the occurrence and further propagation of cracking in bases.

We used a simple experiment design for this study, the main purpose of which was to conduct a quick screening of the districts in Texas. Also ensuring a simple experimental design was the non-availability of information for some other potential factors, including coarse aggregate type, pavement structure, pavement age, and traffic.

Temperature

Texas is divided into freeze and no-freeze regions based on the mean freezing index [Ruiz-Huerta and McCullough 1994]. These two levels of the temperature variable, freeze and no-freeze, were used in the experiment design. Figure 3.3 shows the division of Texas into freeze and no-freeze regions.

Moisture

The two levels of the moisture variable used in the experiment design were wet and dry. Based on the Thornthwaite Moisture Index (TMI), Texas is divided into wet and dry regions [Ruiz-Huerta and McCullough 1994]. Figure 3.3 shows the division of Texas into wet and dry regions.

Texas Climatic Zones

The division of Texas into freeze/no-freeze and wet/dry regions resulted in the formation of four distinct climatic zones. The four climatic zones, with their origin in Bryan [Ruiz-Huerta and McCullough 1994] are:

Zone 1	Wet - Freeze	North-East Texas
Zone 2	Wet - Freeze	East Texas
Zone 3	Dry - No Freeze	South and South-West Texas
Zone 4	Dry - Freeze	North and North-West Texas

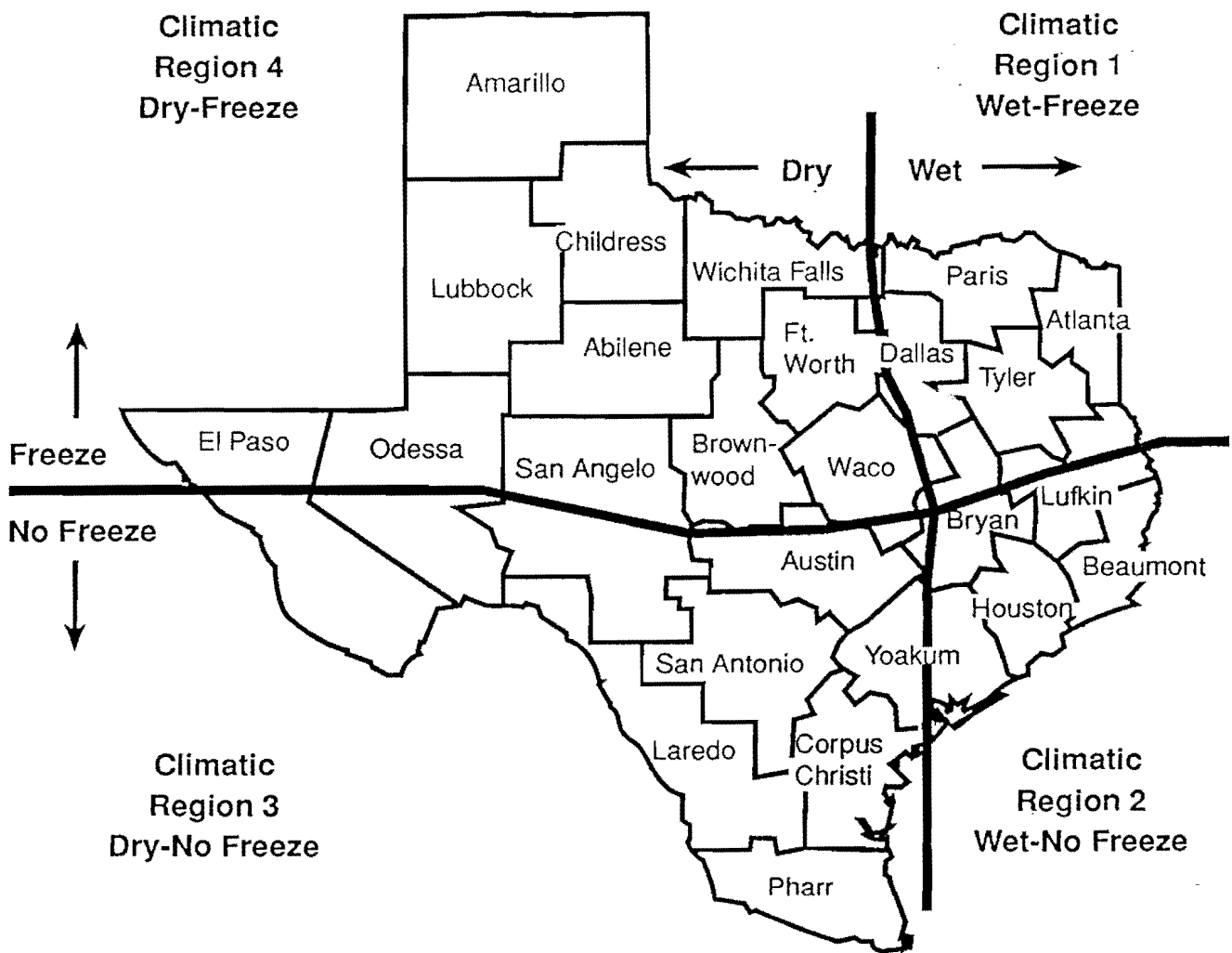


Figure 3.3. Temperature (Freeze and No-Freeze) and Moisture (Wet and Dry) Categories

Soil Type

Because no simple classification of soils was available for Texas that could be used directly in this study, it was necessary to derive a simple soil classification for the experiment design. The most relevant available source was the General Soil Map of Texas, published by the Texas Agricultural Experiment Station, Texas A&M University [Texas 1973]. Some of the terminology used in this map is described below.

Soil Orders are the most general level of soil classification represented in the map; they reflect in a general way the geographic distribution of soils similar in degree and kind of horizon development. Map Units are the smallest soil groups defined on the map; they represent a relatively homogeneous composition of soil having consistent properties.

Table 3.3. General Soil Classification of Texas Used in this Study

Soil Classification	Grouped Soil Orders	Description
Clay	VERTISOLS	Clayey throughout, cracking
Clay Loam	ALFISOLS and ULTISOLS	Top horizon thin and loamy over
Loam (calcareous)	MOLLISOLS and NCEPTISOLS	Loamy surface layers
Sandy Loam (dry)	ARIDSOLS, ENTISOLS and Rockout Crops	Sandy and loamy soils calcareous

The “General Soil Map” represents the eight major Soil Orders and 73 Map Units for Texas. It is observed that map units representing one type of Soil Order also have relatively similar textural class and engineering properties. Based on our review of Soil Orders and Map Units, we derived the following classification of soils in Texas:

- Clay (clayey soils, high shrink-swell)
- Clay Loam (clayey to loamy soils)
- Loam (loamy soils, calcareous, gravely)
- Sandy Loam (loamy to sandy soils, dry, calcareous, gravely)

Table 3.3 summarizes the soil classifications developed for this study, while Figure 3.4 shows the distribution of soil classes in Texas.

SCREENING OF DISTRICTS

A screening of districts was conducted to identify candidate districts from each cell in the factorial for actual selection of case study projects. Districts presented in each factorial cell were therefore scrutinized, and candidate districts were identified for further investigations.

Figure 3.5 shows the factorial of the Texas districts. The fact that many districts are represented in multiple cells is due to the occurrence of different levels of the factors in the same district. For example, because the freeze, no-freeze line crosses through El Paso, Odessa, San Angelo, and Bryan, these four districts are included in both freeze and no-freeze categories. Similarly, the wet-dry line crosses through Yoakum, which is therefore included in both wet and dry categories. Many districts also represent multiple soil types. Figure 3.6 shows the proposed candidate districts from each factorial cell.

IDENTIFICATION AND SELECTION OF CASE STUDY PROJECTS

Based on our screening, the districts of Paris, Atlanta, Waco, Amarillo, San Angelo, Abilene, El Paso, Yoakum, Houston, Bryan, Pharr, and Austin were identified for further consideration. Our target was to select 12 to 16 case study projects for field investigations. Contacts were made with Texas district offices; field visits were conducted, and, finally, case study projects were selected for field investigations.

After the first round of contacts with the TxDOT district offices, the number of districts that would provide case study projects was reduced to six. The other six districts — Paris, Houston, Waco, Bryan, Austin, and El Paso — were dropped from further consideration for various reasons. For example, TxDOT offices in Paris and Houston reported that most cracking problems in pavements in their districts are caused by drying shrinkage in cement-treated bases. Also, some projects in Waco that showed transverse cracking were later found to have cement-treated bases and, in some cases, older underlying

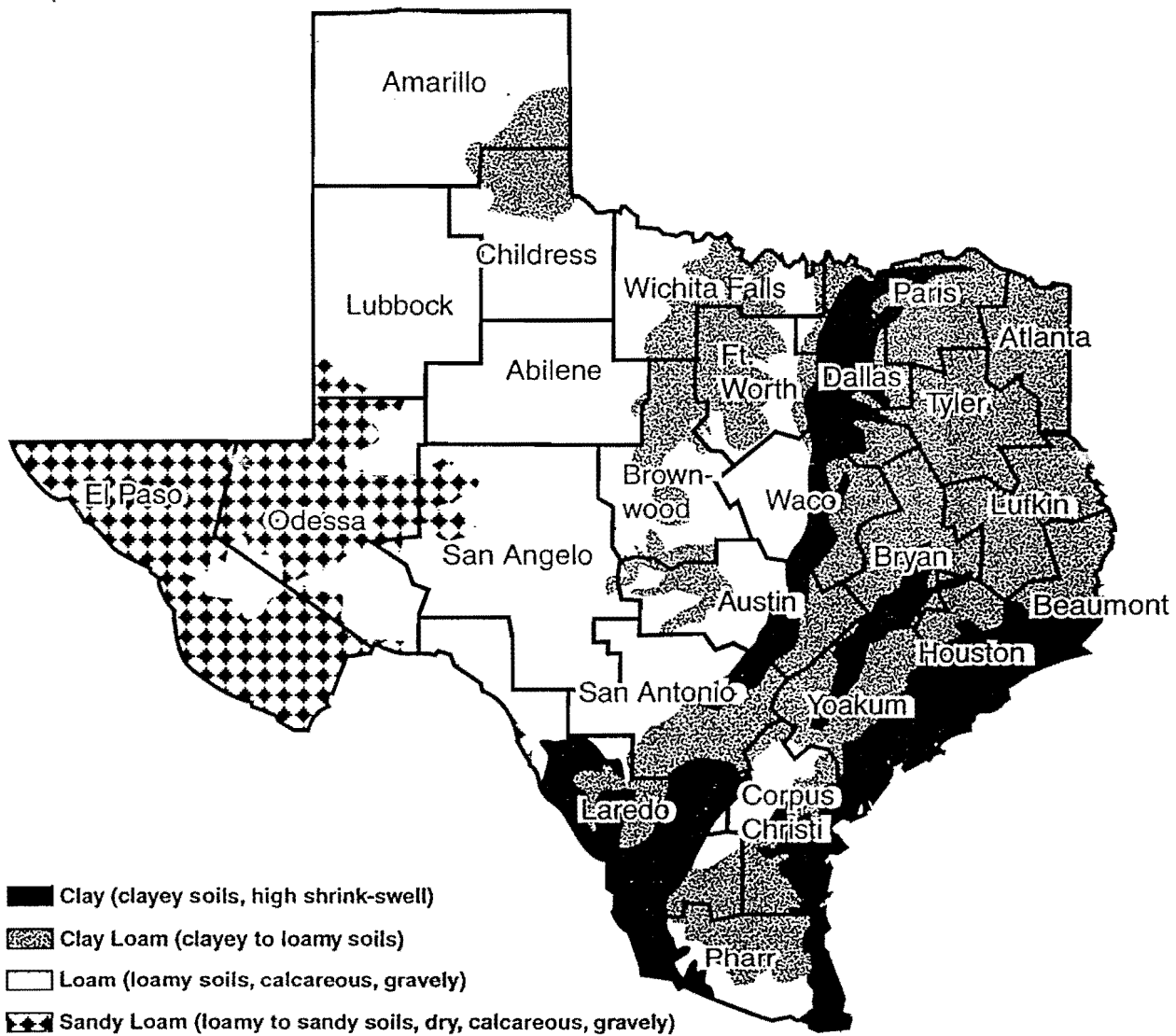


Figure 3.4. General Soil Classifications Used in This Study

jointed concrete pavements. TxDOT personnel in Bryan, Austin, and El Paso also reported that they had no evidences of thermal cracking in flexible bases in pavements in their districts.

Our target was to select two projects in each of the remaining qualified districts. After TxDOT district offices identified potential candidate projects, we then visited the specific case study projects selected in each district.

The selection of projects among the available choices in the districts was based on the following considerations. If possible, the projects selected had different coarse aggregate types, different ages, and a predominant trend of transverse and/or random cracking. Projects that were too old or extensively rehabilitated were not considered; the availability of identification and design information was also considered in each case. Figure 3.7 shows the factorial with the number of case study projects selected for each cell. Figure 3.8 shows the approximate locations of the case study projects.

An information sheet was developed, which recorded identification and design information for each of the selected projects. Appendix A of this report includes the completed information sheets. Table 3.4 presents each of the case study projects' information sheet.

Temperature Moisture Soil Classification		Freeze		No Freeze	
		Wet	Dry	Wet	Dry
		Clay	1 Paris Dallas	5 Waco	9 Yoakum Houston Beaumont
Clay Loam	2 Paris Bryan Lufkin Tyler Atlanta	6 Wichita Falls Amarillo Childress Brownwood Ft. Worth	10* Yoakum Houston Bryan Beaumont	14 Yoakum Pharr Laredo San Antonio Corpus Cristi	
Loam	3 .	7 Wichita Falls Amarillo Lubbock Childress San Angelo Abilene	11 .	15 Pharr Austin Odessa San Antonio San Angelo	
Sandy Loam	4 .	8 El Paso Odessa	12 .	16 El Paso Odessa	

Note: *No district in these cells

Figure 3.5. Factorial Identifying Texas Districts

Soil Classification		Freeze		No Freeze	
		Wet	Dry	Wet	Dry
		Temperature Moisture			
Clay	1 Paris	5 Waco	9 Yoakum Houston	13 Pharr Austin	
Clay Loam	2 Paris Atlanta	6 Amarillo	10 Yoakum Houston Bryan	14 Yoakum Pharr	
Loam	3 *	7 Amarillo San Angelo Abilene	11 *	15 Pharr Austin	
Sandy Loam	4 *	8 El Paso	12 *	16 El Paso	

Note: *No district in these cells

Figure 3.6. Potential Texas Districts for Case Study Projects Selection

Soil Classification	Temperature		Moisture	
	Freeze		No Freeze	
	Wet	Dry	Wet	Dry
Clay	1 **	5 **	9 One Project	13 **
Clay Loam	2 One Project	6 **	10 **	14 One Project
Loam	3 *	7 Six Projects	11 *	15 Two Projects
Sandy Loam	4 *	8 **	12 *	16 **

Note: *No district in these cells

**Case study projects are not available

Figure 3.7. Factorial Cells Showing the Number of Selected Case Study Projects

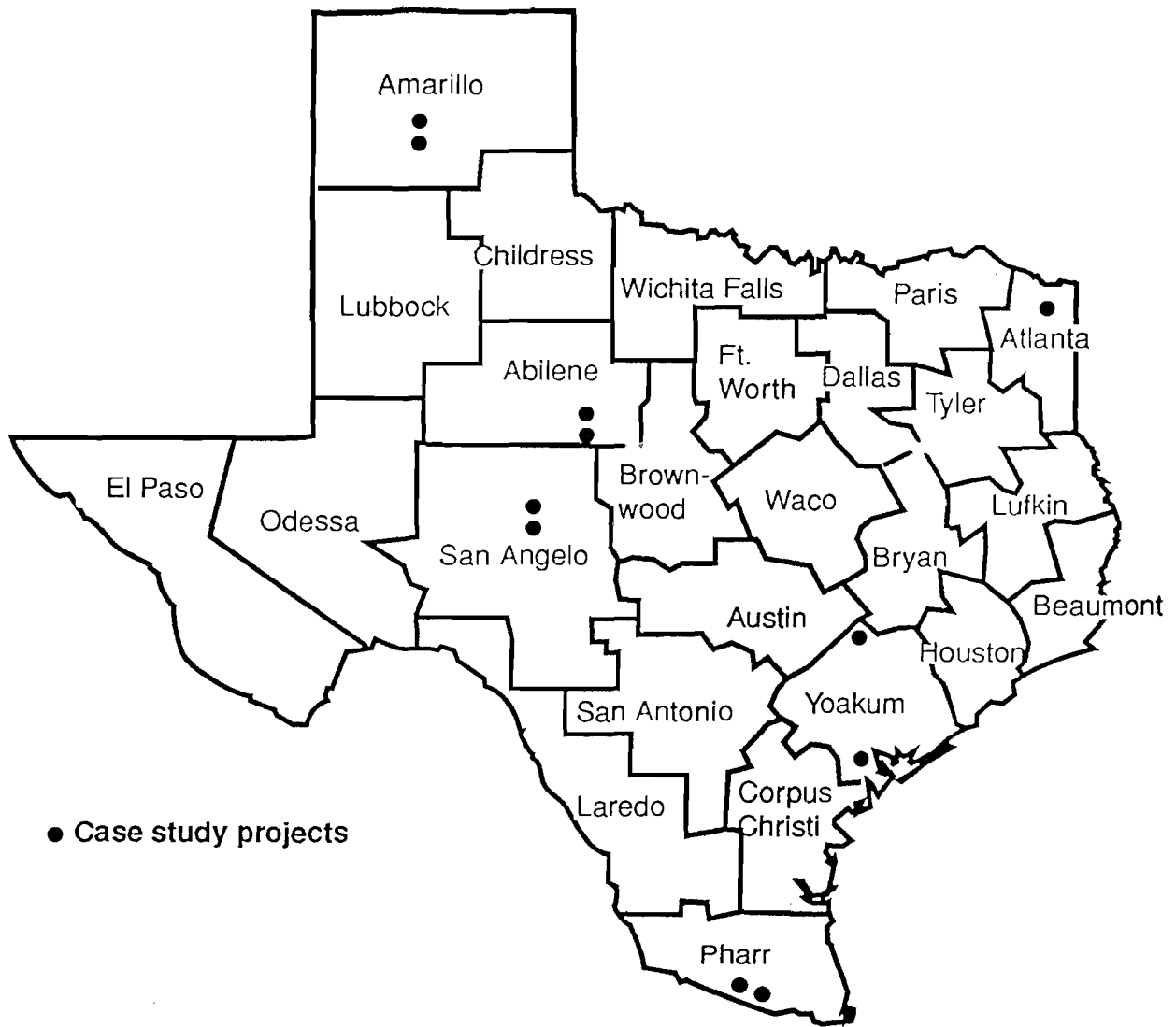


Figure 3.8. Selected Case Study Projects

Table 3.4. Summary of the Selected Case Study Projects

Project Code	District / Highway / Direction	Pavement Structure
AM1	Amarillo, US 87/287, NB Divided, two lanes in each direction	37 mm* Asphalt 20 mm Base, Gravel 100 mm Subbase, Gravel 150 mm Subgrade, 1.5% Lime
AM2	Amarillo, FM 1541, NB/SB Undivided, one lane in each direction	37 mm Asphalt 270 mm Base, Caliche
AB1	Abilene, US 83, SB Divided, two lanes in each direction	50 mm Asphalt 200 mm Base, Limestone 150 mm Subbase
AB2	Abilene, US 83 BU, NB Undivided, two lanes in each direction	37 mm Asphalt 300 mm Base, Limestone
SA1	San Angelo, US 67, NB Divided, two lanes in each direction	75 Asphalt 306 mm Base, Limestone 200 mm Subgrade, 2% Lime
SA2	San Angelo, SH 208, NB Undivided, two lanes in each direction	37 mm Asphalt 160 mm Base, Limestone 100 mm Subgrade
AT1	Atlanta, SH 08, NB/SB Undivided, one lane in each direction	50 mm Asphalt 250 mm Base, Gravel, 1% Lime & 2% Fly Ash
YO1	Yoakum, US 290, WB Divided, two lanes in each direction	61 mm Asphalt 200 mm Base, Limestone 300 mm Subbase, Gravel, 1.5% Lime 150 mm Subgrade, 4% Lime
YO2	Yoakum, LP 463, EB/WB Undivided, one lane in each direction	37 mm Asphalt 340 mm Base, Gravel, 2% Lime 200 mm Subbase, 5% Lime
PH1	Pharr, US 281, NB Divided, two lanes in each direction	50 mm Asphalt 250 mm Base, Caliche 300 mm Subgrade, 3% Lime
PH2	Pharr, FM 2128, EB Undivided, two lanes in each direction	50 mm Asphalt 200 mm Base, Caliche, 1% Lime 300 mm Subgrade, 3% Lime

CHAPTER 4. FIELD CONDITION SURVEYS

The field evaluation program began with visual condition surveys. This chapter (1) documents the methodology for measuring distress manifestations and (2) provides summary statistics of condition surveys conducted on the selected case study projects.

SAMPLING PLAN

A sampling plan was developed for conducting condition surveys on the case study projects. We decided to select a 500 m long test section on each project to conduct the surveys. These test sections were further subdivided into 100 m long subsections; distresses were then mapped on the first 15 m segment of each subsection. Figure 4.1 shows the sampling plan used for the condition surveys.

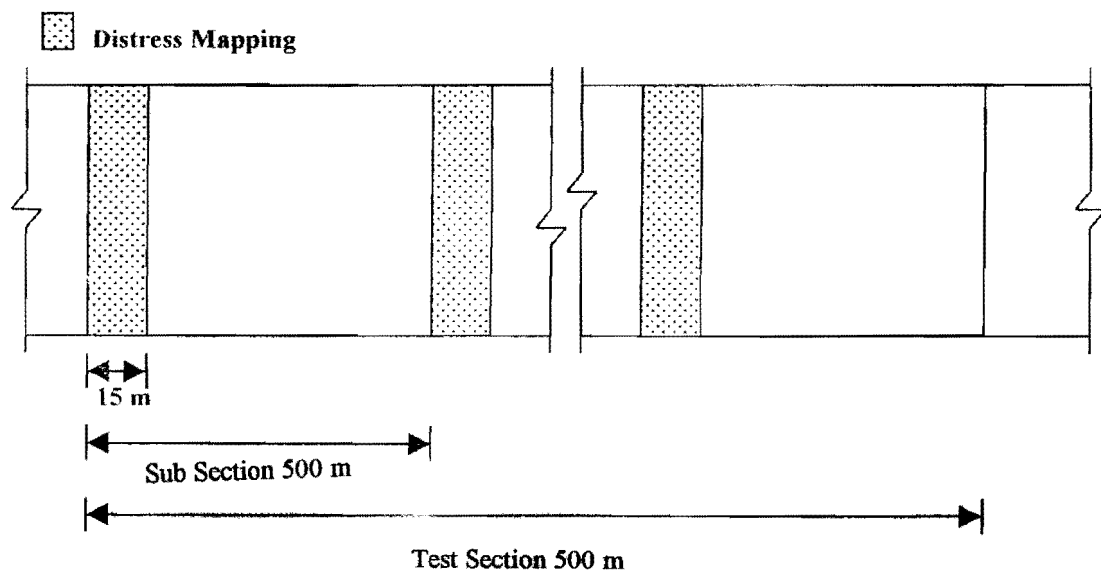


Figure 4.1 Sampling Plan for Distress Mapping

DISTRESS MANIFESTATION TYPES

Various cracking types, including transverse, longitudinal, random, and alligator, manifested on the pavement surface were mapped in the field to acquire information about

pavement conditions on case study projects. Figure 4.2 shows the distress types recorded in the condition surveys.

Measurement Units for Distress Manifestations

The “PMIS Rater’s Manual” [PMIS 95] and the “Distress Identification Manual for the Long-Term Pavement Performance (LTPP) Studies” [LTPP 95] were consulted for selecting appropriate units for reporting distress manifestations.

Transverse cracking is reported in number of cracks per kilometer, and longitudinal cracking is reported in linear meters per meter in this study. Alligator cracking is reported as percentage cracking, where percentage cracking is calculated by taking the ratio of the cracked wheel paths’ length to total wheel paths’ length.

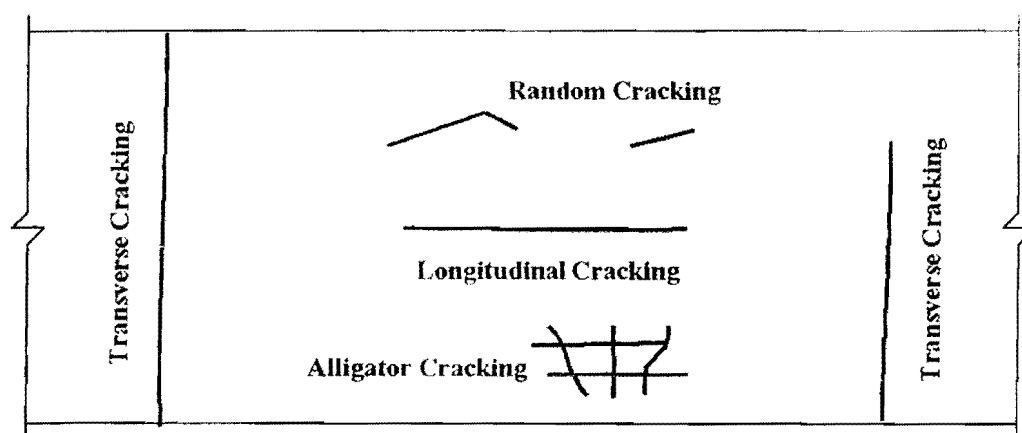


Figure 4.2. Distress Manifestation Types for Condition Surveys

Random cracking is not included among distress manifestations described in the PMIS and LTPP distress manuals. For this study, the researchers defined random cracking as cracks that may occur at any location on pavements and cannot be labeled as any of the other cracking manifestations (e.g., transverse, longitudinal, block, and alligator). In this study, random cracking is reported as number of cracks per kilometer.

Condition surveys were carried out over a total distance of 75 m at each test section. The observed values of distresses were linearly converted into the above-mentioned units for this report.

Distress Severity Ratings

Although the measurements described above address the extent of the distresses, some measurement of severity was also required. A distress severity rating scheme that includes three severity levels — high, moderate, and low — was therefore adopted for the condition surveys. The LTPP distress severity levels [LTPP 95] were adopted with minor modifications. Table 4.1 shows the distress severity descriptions used in this study.

Table 4.1. Distress Severity Levels Used in Field Surveys

Distress Types	Severity Levels		
	Low	Moderate	High
Transverse Cracking	No spalling and/or random cracking near the crack; sealant material in good condition	Low or moderate severity spalling and/or random cracking near the crack; sealant material in bad condition	High severity spalling and/or random cracking near the crack
Longitudinal Cracking	No spalling and/or random cracking near the crack; sealant material in good condition	Low or moderate severity spalling and/or random cracking near the crack; sealant material in bad condition	High severity spalling and/or random cracking near the crack
Random Cracking	No spalling and/or random cracking near the crack; sealant material in good condition	Low or moderate severity spalling and/or random cracking near the crack; sealant material in bad condition	High severity spalling and/or random cracking near the crack
Alligator Cracking	Disconnected hairline cracks running parallel and/or across to each other; may be a single crack in wheel path; cracks not spalled	A pattern of pavement pieces formed by interconnected cracks; cracks may be lightly spalled; cracks may be sealed	A pattern of pavement pieces more severely spalled at edges; loosely connected small pieces, pumping may exist

CONDITION SURVEY PROCEDURES

Selection of Test Sections

Several points were considered in selecting the test section on a case study project. The main consideration was to select a test section that was representative of distress manifestations on the project. Pavement sections close to or on a bridge and close to highway entrance or exit ramps were avoided. Moreover, availability of adequate sight distances was also considered for safety reasons.

Distress Mapping Procedure

1. Once the test section was identified, the odometer of the vehicle was used to roughly define the beginning and end of the test section. This helped to check if there were any obvious problems during distress mapping within the test section.

2. The beginning point was marked by painting a stripe on the outside shoulder and marking 0 m along the stripe. Distance was measured by using a measuring wheel. A paint stripe was marked every 100 m, and the cumulative distance from the starting point was marked along the stripe.

3. Distresses were mapped and rated within the first 15 m of each 100 m subsection on a distress mapping form. Any pertinent points relating to test sections were also noted, where required.

Two adjacent lanes were mapped at each test section. The outside lane and the adjacent inside lane were mapped for multiple lane projects; both outside lanes were mapped for single-lane undivided highway projects.

SUMMARY RESULTS

The summary results of the condition surveys are presented in Tables 4.2 and 4.3. In general, projects in freezing regions show more extensive transverse cracking. The projects located in the dry-freeze climatic zone — including Amarillo, Abilene, and San Angelo — show larger extents of transverse cracking, compared with other projects.

Both projects in Yoakum show a combination of significant transverse and random cracking, with the YO2 project the most heavily distressed among all projects. The project SA1 in San Angelo is representative of premature random cracking.

The projects represent three of the principal coarse aggregate types used in Texas: five projects were constructed with limestone aggregate; three were constructed with gravel, and three of caliche material.

Among all visited projects, the extent and severity of distresses observed in the outside lane were generally larger than distresses in the inside lane. Appendix B documents the distribution of distresses in the low, moderate, and high severity levels.

Table 4.2. Summary Statistics for the Distress Types in Outside Lane of the Case Study Projects

Case Study Projects	Transverse Cracking (No. / Km)	Long. Cracking (Lin. m /m)	Random Cracking (No. / Km)	Alligator Cracking (% Wh. path)
AM1, Amarillo, US 87, NB	293	0.544	307	10.20
AM2, Amarillo, FM 1541, NB	93	0.28	106	3.40
AB1, Abilene, US 83, SB	134	0	27	0
AB2, Abilene, US 83 BU, NB	267	0.272	160	3.40
SA1, San Angelo, US 67, NB	40	1.06	93	6
SA2, San Angelo, SH 208, NB	200	0.02	134	1.80
AT1, Atlanta, SH 08, NB	187	0.308	0	2
YO1, Yoakum, US 290, WB	133	0.868	133	0
YO2, Yoakum, LP 463, EB	307	1.188	213	0
PH1, Pharr, US 281, NB	53	0.04	53	40.60
PH2, Pharr, FM 2128, EB	107	0.632	200	8.20

**Table 4.3. Summary Statistics for the Distress Types in Inside Lane
of the Case Study Projects**

Case Study Projects	Transverse Cracking (No. / Km)	Long. Cracking (Lin. m/m)	Random Cracking (No. / Km)	Alligator Cracking (% Wh. path)
AM1, Amarillo, US 87, NB	53	0	0	0
AM2, Amarillo, FM 1541, SB	67	0.02	0	0
AB1, Abilene, US 83, SB	53	0	0	0
AB2, Abilene, US 83 BU, NB	134	0.624	26	2
SA1, San Angelo, US 67, NB	40	0.52	0	10
SA2, San Angelo, SH 208, NB	227	0	40	1.60
AT1, Atlanta, SH 08, SB	13	0	0	0
YO1, Yoakum, US 290, WB	80	0.056	13	0
YO2, Yoakum, LP 463, WB	240	1.764	133	0
PH1, Pharr, US 281, NB	0	0.072	0	0
PH2, Pharr, FM 2128, EB	240	0.392	147	5.60

CHAPTER 5. LABORATORY TESTING PROGRAM

LABORATORY TESTING TO SATISFY RESEARCH OBJECTIVES

The laboratory testing program was established to help satisfy the major research objectives of the 1432 study. These objectives, as stated on page 1.2 of Chapter 1, center around the development of improved design and construction guidelines for aggregate bases such that the bases selected and utilized in a specific environment will be satisfactorily resistant to fluctuations in moisture and temperature. Secondly, the research objective is to define laboratory tests which will assist in the selection and application of appropriate treatment or stabilization strategies to improve the structural performance and functionality of rehabilitated aggregate bases.

In general, design aggregate specifications address gradation, size, texture, soundness, compaction, and strength requirements to assure the construction of an acceptable unbound aggregate base course. Item 247 on flexible bases of the *Standard Specifications for Construction of Highways, Streets and Bridges (1995)* places a number of physical requirements on unbound aggregate bases or flexible bases. These include:

1. General classification according to geological type and degree of crushing (Types A through D).
2. Strength according to the Texas Triaxial test (Tex-117-E).
3. Gradation limits (Tex-110-E).
4. Atterberg limits (liquid limit, Tex-104-E, and plasticity index, Tex-106-E).
5. Wear resistance according to the wet ball mill test (Tex- 116-E).
6. Linear shrinkage (Tex-107-E).

Construction aggregate specifications in Item 247 address:

1. Subgrade preparation.
2. Application of the first flexible base course and successive flexible base courses.
3. Compaction of the flexible base to meet the density requirements of Tex-113-E.

The concern in Texas over the distress in flexible bases due to cracking originating in these bases and reflecting through the asphalt concrete surface indicates that the existing design and construction specifications may not, in and of themselves, be satisfactory to assure acceptable

performance of these bases. Additional specification tests in the design phase and/or field control phase may be necessary.

General Requirements of a Successful Flexible Base

The performance of flexible bases is predicated on acceptable strength and durability. The current Texas specifications, Item 247, do not fully address all the aspects of acceptable flexible base performance. However, it is beyond the scope of this research to address all of the areas of improvement needed to upgrade the flexible base design and construction specifications to optimize flexible base performance. Nevertheless, it is instructive to the task at hand to review the problems that must be addressed in the development of improved flexible base specifications. These areas include:

1. Strength and the effect of volumetric changes under load.
2. Loss of strength due to scour and liquefaction.
3. Loss of strength due to abrasion under load.
4. Plastic deformation or rutting.
5. Freeze, moisture, and thermal problems.

Strength and the Effect of Volumetric Changes Under Load - Flexible bases have long been considered in pavement design models to be elastic layers. This is true whether the structural model is a layered elastic model (LEM) or a finite element model (FEM). It is well known that the strength and resilient moduli of flexible bases are highly dependent on the moisture content within the layer and the stress state within the flexible layer. In fact, an often used illustration of this is the magnitude of change in the resilient modulus of the limestone flexible base used at the AASHTO Road Test under the variable conditions of the Road Test experiment. Here it was shown that the modulus of the crushed limestone base could vary between about 56 MPa (wet aggregate and poor subgrade support) and about 448 MPa (dry aggregate and strong subgrade support). These effects can be accounted for in more sophisticated LEM and FEM structural models by the use of iterative processes or simplified algorithms to adjust the modulus for the effects of internal stress state and/or internal moisture state. However, another factor which substantially affects the structural response

has not been adequately addressed, and that is the effect of the volumetric change or dilation of the unbound aggregate base under load.

Aggregate bases or flexible bases are not continual but are comprised of a collection of discrete particles. As such, the particulate mass behaves differently under load than would a continuum. The particulate mass responds to load by dilating. The amount of dilation is not confined to the levels of an elastic continuum but may be considerably larger. The dilation or expansion of the particulate mass or flexible base results in a “self-induced” confinement that is not accounted for in LEM and FEM systems. The result is that flexible bases are assumed to be unable to accommodate tensile stresses or strains induced by load. However, the effect of the particulate dilation is to mobilize shear stresses and strains among aggregate particles in lieu of tensile stresses and strains. A flexible base may then indeed be able to accommodate loading heretofore not accounted for by conventional LEM and FEM models.

Research on unbound aggregates between 1973 and 1997, i.e., [Allen 1973], [Lytton et al. 1997], and [Tutumluer and Thompson 1997], has helped to define the material properties that are directly related to plastic deformation. Each of these studies allude to the importance of the *self-induced confining pressure* within the aggregate to the ability of the aggregate to resist permanent deformation. The degree of the self-induced confinement or dilatancy is dependent on the gradation of the aggregate, the shape and size of the top-size aggregate, and the characteristics of the aggregate fines.

Lytton [1997] states that the ability of an aggregate to build up its own confining pressure stems principally from its gradation. Under load, particles in a well-graded aggregate will rotate and wedge against one another, and the collection of particles will increase in volume unless they are confined. The same collection of particles in a base course being prevented from changing volume will build up their own confining pressure. This increase in volume under little confinement results in Poisson’s ratios well above 0.5. Measured values of Poisson’s ratio on various gradations of aggregates ranged from below 0.5 for fairly open graded mixes to nearly 2.0 for well-graded mixes whose gradation closely follows the 0.45 power line. The value of Poisson’s ratio is limited to a maximum value of 0.5 by elastic theory. However, this is not the case for a particulate mass such as an aggregates system.

Poisson's ratio is directly related to the stiffness of an aggregate under load, i.e., its resilient modulus through the power law [Uzan 1985] is

$$M_R = K_1(\theta - 3u)_{K_2}(\tau_{oct})^{K_3} \quad [5.1]$$

Where K_1, K_2, K_3 = material properties of the unbound aggregate,

θ = sum of principal stresses,

u = pore water pressure in the fines in the aggregate which can be positive (compression) or, more usually, negative (tension), and

τ_{oct} = the octahedral shear stress acting on the aggregate.

Project A-005 [Lytton 1994] of the Strategic Highway Research Program (SHRP) showed that the Poisson's ratio also depends on the same material properties ($K_1, K_2,$ and K_3) and the same stress state. Figure 5.1 shows comparison values of Poisson's ratios that have been measured and predicted using the relation given in the SHRP A-357 report whose results were based on the A-005 SHRP project. The proximity of all points to the line of equality shows how well this important characteristic of aggregate behavior is understood. Table 5.1 gives values of $K_1, K_2, K_3,$ and $u,$ pore water pressure in the aggregate, that were measured on a set of aggregates widely used in Texas. These K-values and the pore pressures differed as the water content changed. Lytton [1994] explains that the importance of this is that if the K-values and the pore pressure are known for a given aggregate, the same equations may be used to calculate the confining pressure that builds up in the aggregate when it is allowed to change volume. Lytton [1994] explains that it is important to understand that the K-values all depend principally on the gradation of the aggregate and on the pore water pressure. The importance of this dependence is that:

1. The values of K_1 through K_3 can be found from correlations to the gradation of the aggregate. The confining pressure that is generated by the aggregate under load depends on these K-values.

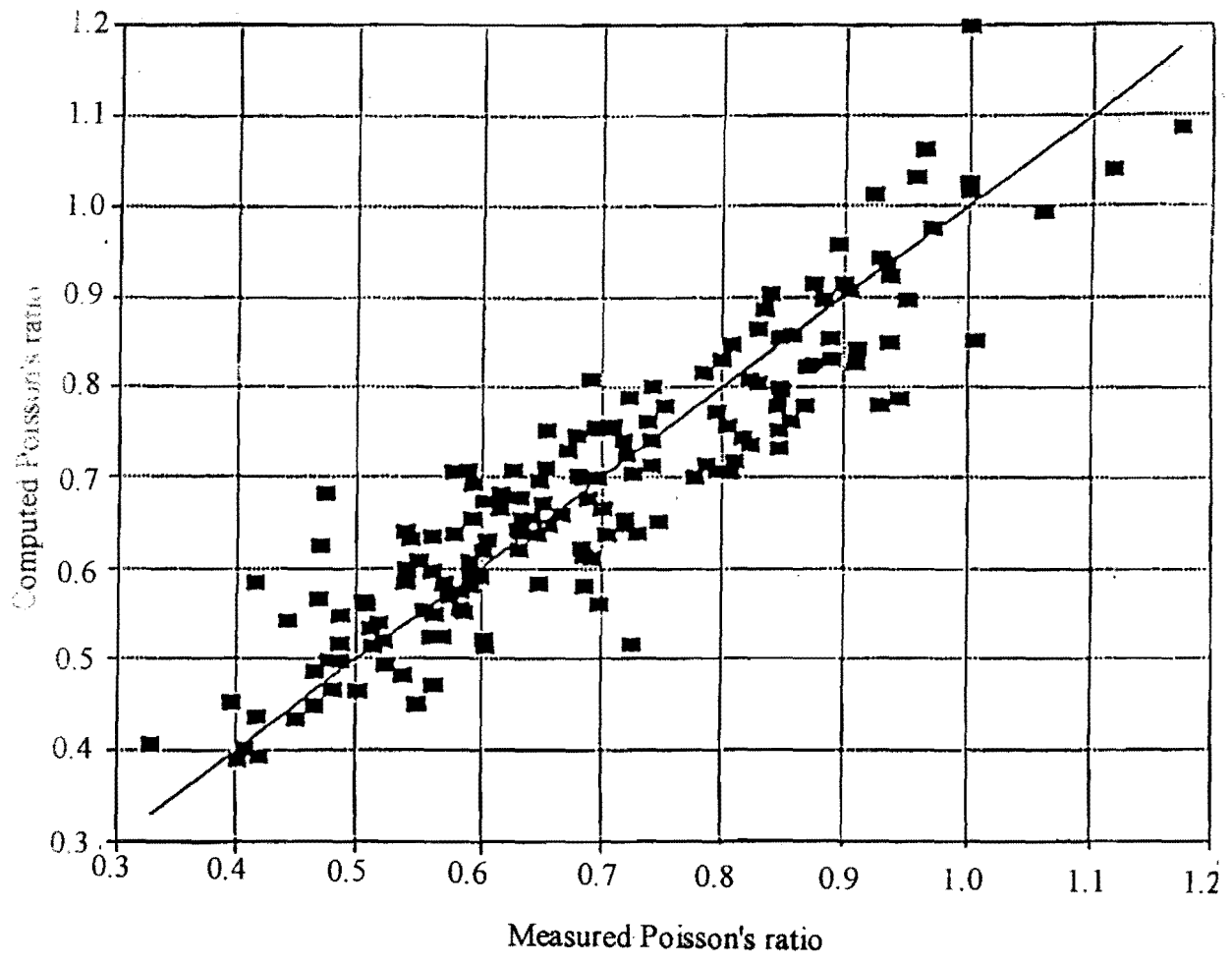


Figure 5.1 Predicted versus Observed Poisson's Ratio (After Allen 1973)

Table 5.1. Material Properties K_1 to K_5 for Soil at Minus 2% Optimum Moisture

Material	K_1	K_2	K_3	K_4	K_5	U (psi)
Limestone	1497.6	0.904	-0.326	2.297	-0.3395	-1.560
I.O. Gravel	2816.3	0.603	0.000	3.584	-0.5029	-2.533
S. Gravel	11288	0.631	-0.102	1.645	-1.6459	-0.003
Caliche	1443.4	1.184	0.000	0.791	-0.4366	-1.710
Shellbase	827.15	1.101	-0.0005	0.588	-0.201	-0.002
Sand	3118.4	0.439	-0.0001	1.537	-0.335	-0.238
Silt	823.73	1.195	-0.1107	1.034	-0.325	-1.45
Lean Clay	4096.53	0.000	-0.2674	0.0205	-0.7550	-0.002
Fat Clay	200.24	0.659	-1.4735	-0.944	0.3683	-2.107

Table 5.2. Material Properties K_1 to K_5 for Soil at Optimum Moisture

Material	K_1	K_2	K_3	K_4	K_5	U (psi)
Limestone	1656.87	0.9043	-0.3260	2.2975	-0.3395	-1.5640
I.O. Gravel	1271.02	0.4920	-0.0006	0.8856	-0.0064	-8.6666
S. Gravel	1574.07	0.6704	-0.2848	2.2230	-0.1849	-3.1403
Caliche	888.22	0.829	-0.0053	1.6233	-0.2767	-3.8608
Shellbase	815.14	0.5967	-0.0028	0.9288	-0.2133	-0.3273
Sand	6434.32	0.5116	0.0000	1.3370	-0.1186	-0.2455
Silt	1171.84	0.05185	-0.2041	1.7196	-0.0989	-0.0317
Lean Clay	105.50	0.3218	-0.1001	1.4895	-0.0112	-14.8380
Fat Clay	262.96	1.2488	-0.4978	1.2145	-0.2358	-8.5040

2. The plastic deformation of the aggregate under load is lubricated by the buildup of positive pore water pressure in the fines. This reduces the strength of the aggregate and increases plastic deformation.
3. The higher the confining pressure, the more rapidly positive pore water pressure will buildup.

Thus the selection of the gradation of an aggregate involves a balancing act — a trade off between its beneficial ability to develop its own confining pressure and its detrimental ability to convert the confining pressure to pore water pressure under repeated loading. The balancing act can be successfully resolved by selecting a gradation that deviates somewhat from the maximum density gradation, by limiting the amount of fines and by increasing the permeability of the aggregate which allows any buildup of pore water pressure to dissipate rapidly. As Lytton [1997] points out, an aggregate that powders under repeated loading and that absorbs water loses strength in service and contributes to increasing plastic deformation. Lytton [1997] points out that all the properties of an aggregate, e.g., plastic deformation, powdering, water absorption, pore water pressure buildup and resistance to degradation, are reflected in the values of K_1 through K_3 and the percent fines and ultimately the gradation. A good selection of an aggregate can be made by choosing:

1. A gradation that deviates somewhat from the maximum density in the particle size range from the #40 sieve (0.6 mm) to the #4 sieve (6 mm).
2. An aggregate that has less than about 10% plastic fines smaller than the #200 sieve (0.074 mm) and that does not develop them during repeated loading.
3. An aggregate that does not absorb more than about 20% of the volume of the fines in water.

Ultimately, the key to successfully integrating the important material properties of resilient modulus, dilatancy, and permanent deformation during cyclic loading is to develop the appropriate testing protocol and to select an FEM model capable of accounting for the dilatancy factors and material anisotropy. Fortunately, great strides have already been made in this direction. Tutumluer and Thompson [1997] have presented such an FEM model and have proposed a laboratory testing program to provide the needed material properties. The Tutumluer FEM model accounts for non-linearity, cross-anisotropy, residual stresses, and accounts for load transfer within the aggregate matrix by shear and not tension. Lytton [1997] has proposed improvements to the approach which

will provide more exact material properties which will produce more accurate predictive performance models. This work is being accomplished through the International Center for Aggregates Research (ICAR) at TTI. In essence, Lytton's approach is that the resilient dilatant properties of the unbound aggregate are not constant but depend on the stress state of the system. Lytton's approach establishes a methodology to account for the effects of changes in the stress state on the dilatant resilient properties of the unbound aggregate base.

Loss of Strength Due to Scour and Liquefaction - As discussed in the previous section, a precarious balance exists between the development of adequate self-induced confinement through dilation under load and the development of excessive self-induced confinement or excessive dilatancy. If self-induced confinement is too low, the mix will not develop the full strength nor optimal resilient properties. On the other hand, if the self-induced confinement is too high, the mix will degrade based on the development of excessive pore water pressures. The level of acceptability of the confining pressure is no doubt highly dependent on the quantity of fines and the mineralogical nature of the fines in the unbound aggregate. The goal should be to develop a methodology to calculate self-induced confining pressures through triaxial testing in which not only axial stresses and deformations are measured but also radial strains to account for dilatancy. These measurements will allow the K-values in Equation 5.1 to be determined and from these the level of self-induced confinement. Using this approach, a target self-induced confinement, ultimately, can be designed for through triaxial testing for a specific aggregate mineralogy and gradation.

Excessive pore pressures will cause loss of strength and even scour and liquefaction under repeated loading. The pore pressures induced in the aggregate mixture are a function of stress state (self-induced confinement), bulk modulus of the mixture and the relationship between suction of the aggregate system and moisture content of the aggregate system. Until more thorough research is completed in anisotropic triaxial testing and characterization of aggregate mixtures, the assessment of development of pore pressures within the aggregate mixture will have to be based on moisture content-soil suction relationships which will be addressed later in this chapter. This approach is simplistic and involves developing a relationship between aggregate suction and moisture content based on a simple testing protocol, and estimation of pore water pressure within the aggregate mixture in the pavement structure based on a simple algorithm relating pore pressure

to suction within the aggregate base. This algorithm can be incorporated into a simple LEM of the pavement structure, such as the Texas Flexible Pavement System (TFPS) structural model.

Water Problems - Durability Under Load - Loss of strength and general degradation can and does occur under repeated loading, especially in the presence of water which can act to soften the aggregate minerals. A test such as Los Angeles Abrasion [AASHTO T-96] or the Texas wet ball mill test [Tex-116-E] is not adequate to predict the effects of degradation under load. As fines are produced during cyclic loading, the mixture becomes more susceptible to scour and liquefaction and more sensitive to the effects of pore water pressure. More work must be done to improve the predictability of aggregate strength loss due to abrasion under load. Some of this work is being accomplished in NCHRP Study 4-23.

Plastic Deformation or Rutting - Plastic deformation of unbound aggregate systems has never been adequately accounted for in design testing protocols. The 1986 AASHTO Design Guide upgraded the assignment of the structural layer coefficient for unbound aggregate bases by linking that number to the resilient modulus of the aggregate base. As the 2002 AASHTO Design Guide is developed, it is clear that assigning a structural component of an unbound aggregate based solely on resilient properties is inadequate. Accumulated permanent deformation potential must also be characterized. The resilient properties and dilatant properties already discussed have a profound effect on the susceptibility of the aggregate system to permanently deform, as do the properties of the aggregate which affect its durability under cyclic loading or ability to resist abrasion or degradation. Perhaps the best approach to fully assess permanent deformation potential is a repeated load-deformation test where the log of permanent strain is plotted versus the number of loading cycles applied. The test should be performed at a specific ratio of confinement and axial stress to match a specific pavement structural application. A successful test under the specified stress state will be one in which the aggregate never exceeds the threshold permanent strain and never reaches tertiary deformation, as illustrated in Figure 5.2.

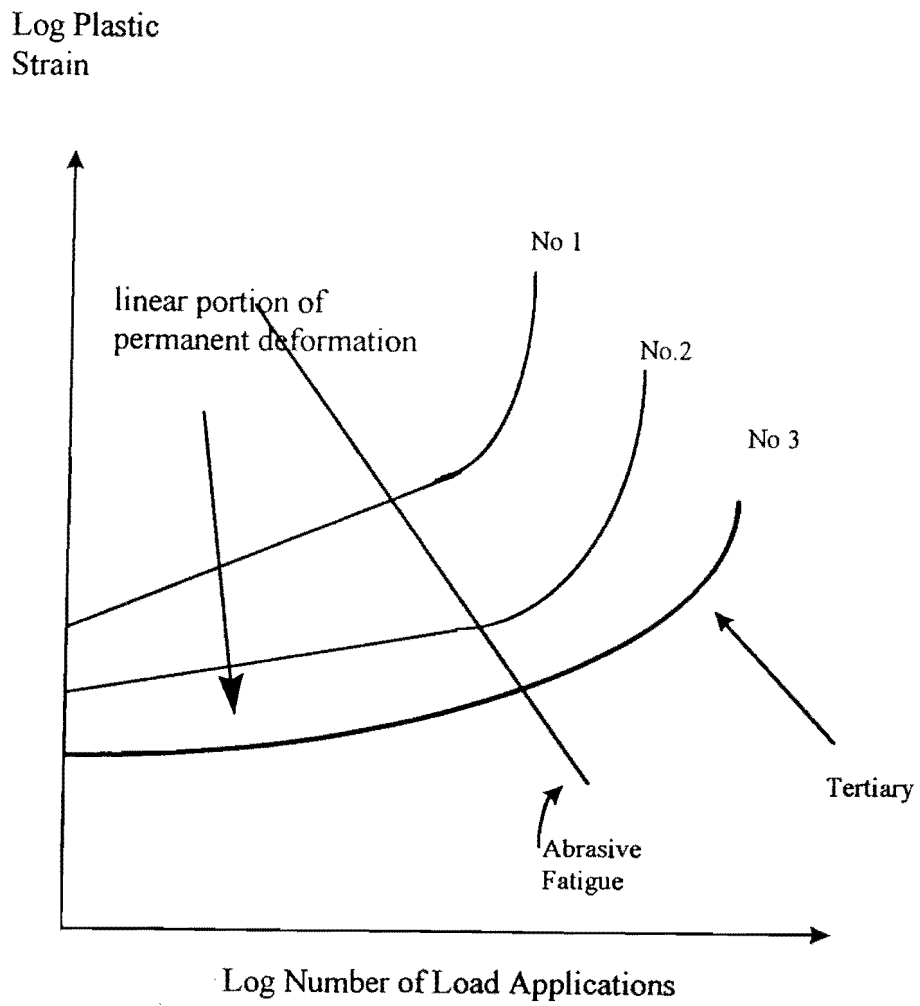


Figure 5.2. Schematic Illustration of the Point of Tertiary Deformation on a Plot of Accumulated Permanent Deformation versus Number of Cyclic Load Applications

Freeze and Thermal Problems - The final area of problems in unbound aggregate bases that must be addressed in a comprehensive assessment is volume changes that occur as a result of freezing or thermal changes. This is the focal area of this research effort. Volume changes which can be deleterious to the performance of the pavement containing the flexible base are affected by gradation, strength, abrasion resistance, mineralogy of fines, cementitious properties of the fines, and moisture sensitivity of the fines. Laboratory protocols to assess the properties of unbound aggregates related to freeze and thermally induced volume changes are addressed in this chapter.

Moisture Sensitivity of Flexible Bases

The granular base layer is often the primary structural layer in a flexible pavement system unless the asphalt is substantially thick (greater than about 200 mm). Very few pavements are originally designed and constructed with such thick asphalt surface layers. Consequently, it is imperative to treat the flexible base as the prime or at least a major structural contributor. Since cracking within the base layer can diminish its load-carrying capability, the problems associated with thermal and traffic load induced cracking within the base greatly impact the performance of the entire pavement system. Thermal- or moisture-related cracking within the base is a problem that must be addressed as this cracking reflects through the asphalt surface layer.

Carpenter and Lytton [1977] documented that transverse cracking in west Texas is largely a product of freeze-thaw cycling which acts primarily in the base course. The base course undergoes volumetric contraction upon freezing that is an order of magnitude larger than that which the asphalt concrete undergoes. Carpenter and Lytton [1977] concluded the following:

1. Thermal susceptibility of the base course is a valid deterioration mechanism, and the volumetric contraction activated by freezing and thawing is quite prevalent in the base course materials in west Texas and probably in other parts of Texas.
2. Soil moisture suction, which is a measure of the energy state of moisture within the soil, is a parameter that directly relates the environment to the engineering behavior of the soil. The relationship between soil suction and thermal susceptibility accentuates the need to fully characterize a material by testing it in the environment in which it is used.

3. Although clay contents in the base course are often relatively low and within specifications, the mineralogy of the clay fines has a significant impact on the mechanism of cracking and deterioration.

Evidence of thermal cracking of unstabilized granular bases has been reported in other countries. Saarenketo and Scullion [1995] who are employed by the Finnish National Roads Administration, have reported that the one factor which has a strong relationship with the eventual performance of a granular base is the level of suction that exists in the base. Materials that strongly attract and hold moisture are more susceptible to thermal cracking during freeze-thaw cycling. Work in Texas and Finland has shown that ground penetrating radar (GPR) is a useful tool to identify problems within existing sections of granular bases. The GPR wave is strongly affected by moisture in the base course, and GPR signal processing techniques developed by the Texas Transportation Institute can calculate the electrical conductivity properties and dielectric values in the in situ granular base materials. These layer dielectric values and electrical conductivities are strongly related to the moisture holding potential of the aggregate layer and can be used to assess in place base strength and deformation potential.

Saarenketo and Little [1995] showed that when one compares the correlation between dielectric value and soil strength (in terms of CBR), the relationship between strength and dielectric value is considerably stronger than the relationship between moisture content and strength. This fact is illustrated in Figures 5.3 and 5.4. The stronger relationship between strength and dielectric value is probably due to the fact that the dielectric value offers a more complete description of the way the water is held. Strongly or tightly held water has a lower dielectric value than does loosely held or free water. In other words, if we compare the strength of two different soils — a highly plastic clay and a sand — when compacted at the same moisture content, the strengths will be vastly different. Therefore, moisture content is very much soil or aggregate-type specific and is not a sufficient parameter, in and of itself, to correlate with the strength of the aggregate system. However, the dielectric value accounts not only for the amount of water held within the aggregate or soil matrix but also the way in which it is held; therefore, a stronger relationship between dielectric value and strength for a general material type is expected (than between moisture content and strength). This is illustrated in Figures 5.3 and 5.4.

Saarenketo and Little [1995] determined that low dielectric values (between about 5.5 and 6.5) in compacted aggregates indicate the presence of small amounts of absorption water and good to excellent strength properties (perhaps optimal properties). Higher dielectric values indicate that the strength and stiffness of the aggregate is sensitive to the effects of moisture. Dielectric values above 10 are identified by Saarenketo as “alarm values” as they indicate the threshold of significant potential loss of strength and increased deformation potential. If the dielectric value is greater than 16, the aggregate will become plastic and deform severely under traffic. High electrical conductivity values indicate high concentrations of dissociated ions in the free water, which can cause positive pore water pressures resulting in a rapid loss of strength.

The hysteretic effects of wetting and drying on strength and deformation of aggregates and soils in general are part of the literature [e.g., Yong and Warkentin 1966, Fredlund and Rahardjo 1993, and Lytton 1994]. Saarenketo demonstrated this hysteretic effect in a TTI study on carbonate aggregates. Figure 5.5 presents the CBR v. dielectric value during both wetting and drying cycles. These clearly defined hysteretic effects establish why substantially higher resilient moduli are measured in dry summer months than in wetter months of the year. It is not simply a function of moisture content but also whether the soil or aggregate is going through a wetting period or a drying period. The wetting period is the more deleterious, and lower strengths and stiffnesses result during wetting cycles than under drying regimes. Hence, the wetting mode is deemed the more conservative sequence and is the process followed in laboratory testing in this study.

The detrimental effects of water which give rise to volume changes within the aggregate system, and hence aggravate cracking, stem from water in the aggregate system in the form of either: (1) water within the mineral structure, (2) free water, or (3) bound water or adsorbed water. In adsorbed water, the dipole water molecules closest to the mineral surface are systematically arranged with respect to the mineral surface, which has a negative charge. The most tightly held water layer, approximately 10 Å thick, consists of about three molecular layers of water [Mitchell 1993] which has a higher density than free water and is much more tightly held [Mitchell 1993]. The thickness of the adsorbed water layer can extend to about 100 Å under the right conditions and depending on the mineralogy of the aggregate fines and the specific surface area of the aggregate fines. In a Finnish study, Saarenketo and Little [1995] related the specific surface area of selected

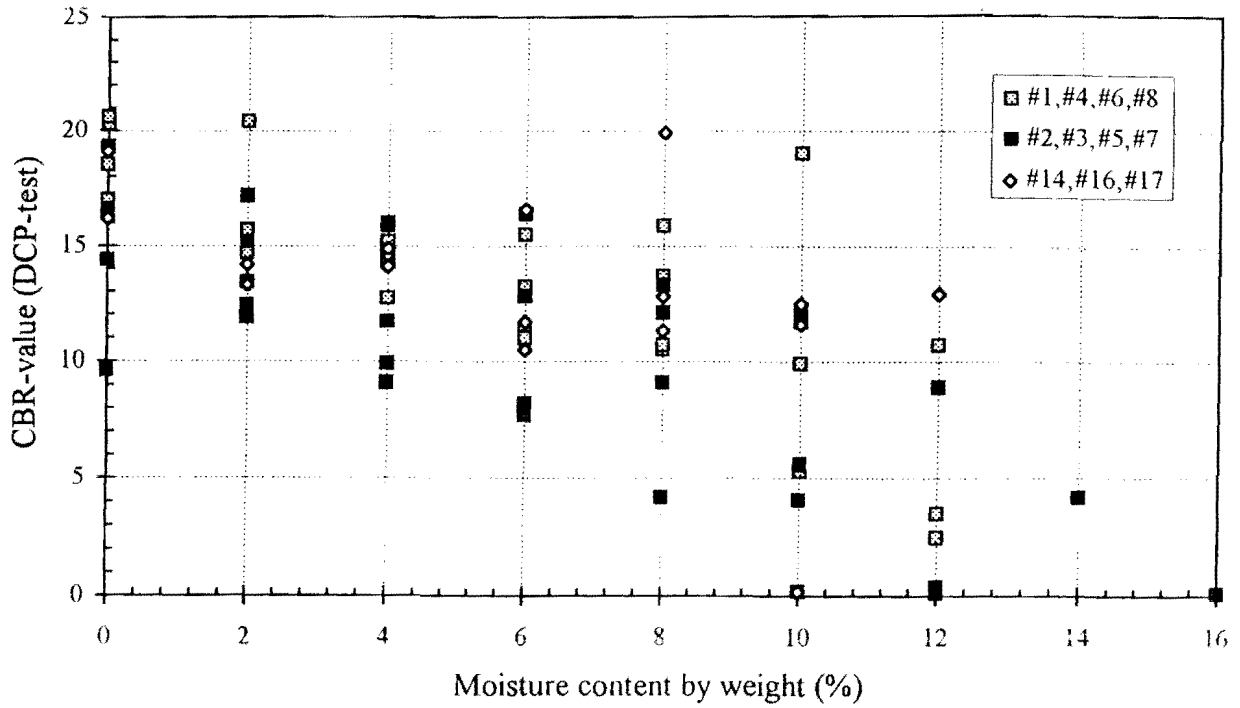


Figure 5.3. Correlation between CBR-Value and Gravimetric Moisture Content of Texas and Finnish Aggregates

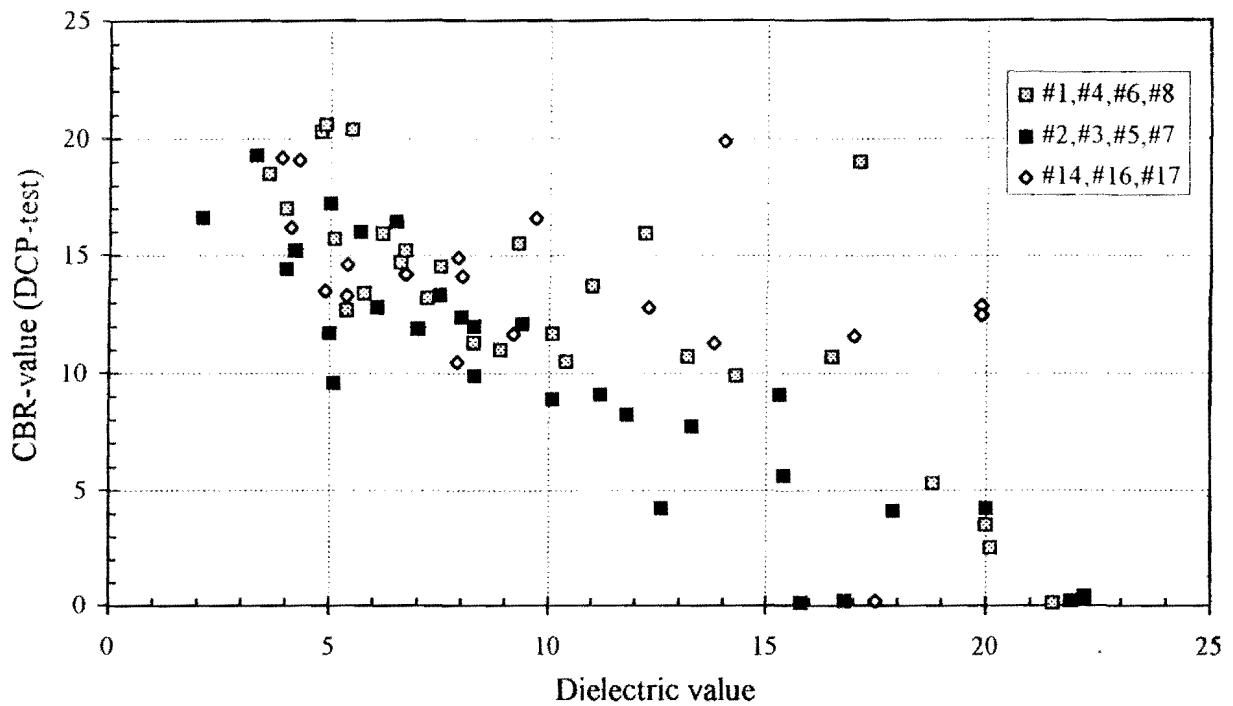


Figure 5.4. Correlation between CBR-Value and Dielectric Value of Texas and Finnish Aggregates

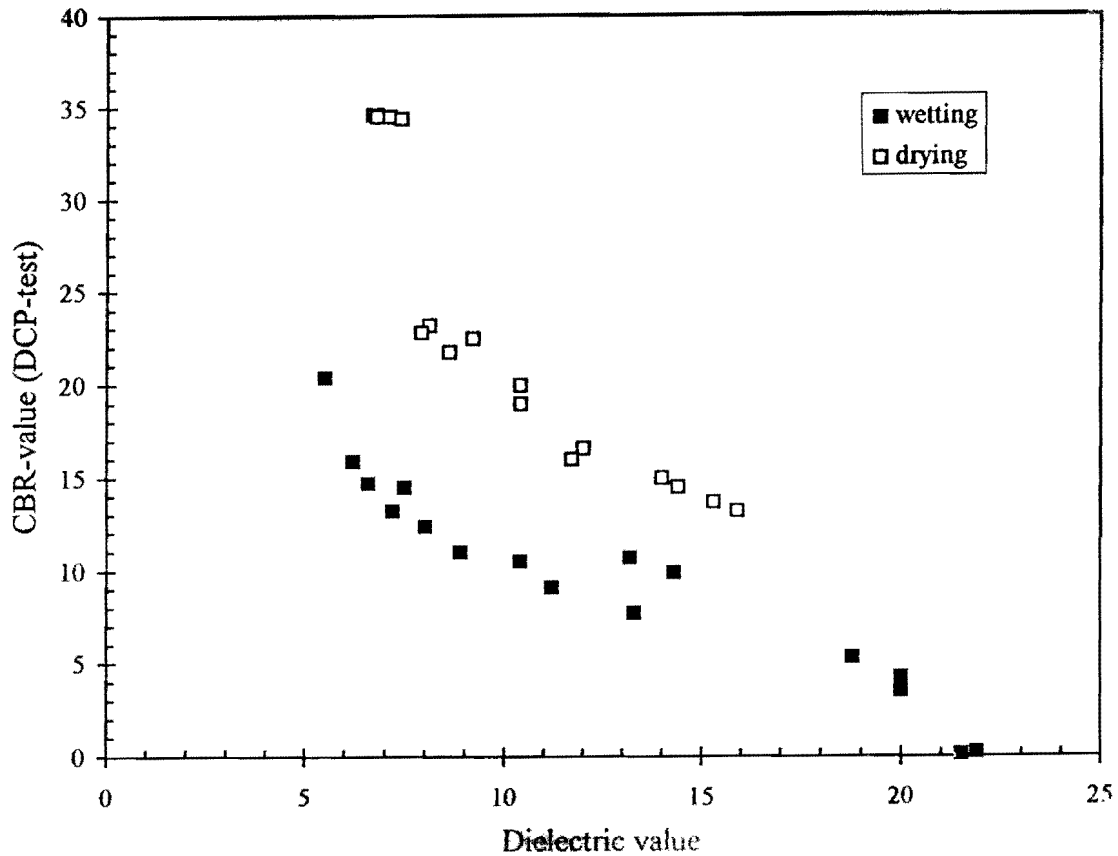


Figure 5.5. The Effect of Drying and Saturation in the Strength Properties and Dielectric Value of Some Texas Carbonate Aggregates

Finnish aggregates to water adsorption which is, in turn, related to performance. More highly adsorptive aggregates exhibited substantially poorer performance. This is especially true in the cold climate of Finland. This relationship between water adsorption and specific surface of the fine aggregate is illustrated in Figure 5.6.

When the soil temperature drops below 0 °C, free water forms hexagonal crystals and thus expands. During the freezing process, water molecules add one-by-one to the growing ice crystals, but they remain separated from the mineral surface by the thin adsorption layer [Anderson 1989]. This relatively narrow region below the nominal base of the ice lens is called the “frozen fringe”

[Ladanyi and Shen 1989]. At this same, time suction causes liquid water to migrate to the ice lens from the frozen soil through this unfrozen water layer [Konrad and Morgenstern 1980].

As the temperature in the soil continues to decrease, the bond water starts to freeze, but the tightly bound water remains unfrozen. At a temperature of -5°C , the amount of unfrozen water is still 12% of the total volume of unfrozen water [Anderson 1989]. The amount of the frozen adsorption water decreases with decreasing temperature until the water movement to the frozen fringe is significantly reduced. Small amounts of unfrozen water in the soil have been measured even at temperatures of -40°C [Anderson 1989].

The freezing process is also controlled by the amount of dissolved salts, by products of hydrolytic reactions, which according to Kujlala [1991], lower the free energy and thus the freezing temperatures of the aggregate-water system. On the other hand, many fine-grained base aggregates, such as argillaceous carbonates, volcanites, sandstones, and chert and shale impurities degrade with repeated wetting and drying and with freezing and thawing, especially under the influence of de-icing salts [Hudec and Achampong 1994] to worsen the destructive effects of both moisture and the freeze-thaw phenomenon.

The control of the moisture sensitivity of aggregate bases is primarily affected by the amount and nature of the material smaller than 74 microns. One popular approach to mitigate the effects of the fines is to either scalp and replace the fines or, more conveniently, to modify the fines through a stabilization process. Hydrated lime, lime, lime-fly ash, and portland cement are the most widely used additives to reduce moisture susceptibility. These calcium-based additives have the ability to change mineralogical properties of the clay fines. These changes result in reduced surface area of the fines, reduction in plasticity, agglomeration, and increased strength of the fines matrix.

Thermal Sensitivity of Flexible Bases

NCHRP Synthesis No. 26 provides a comprehensive summary of frost action technology. The full development of frost action requires: (1) a source of capillary water for large ice lenses to form, (2) a fine enough gradation of the material to produce a depression of freezing temperature in the smaller voids, and (3) a high enough permeability of the material to allow relatively free moisture movement to the zones where the ice lenses are formed. Particularly frost-susceptible

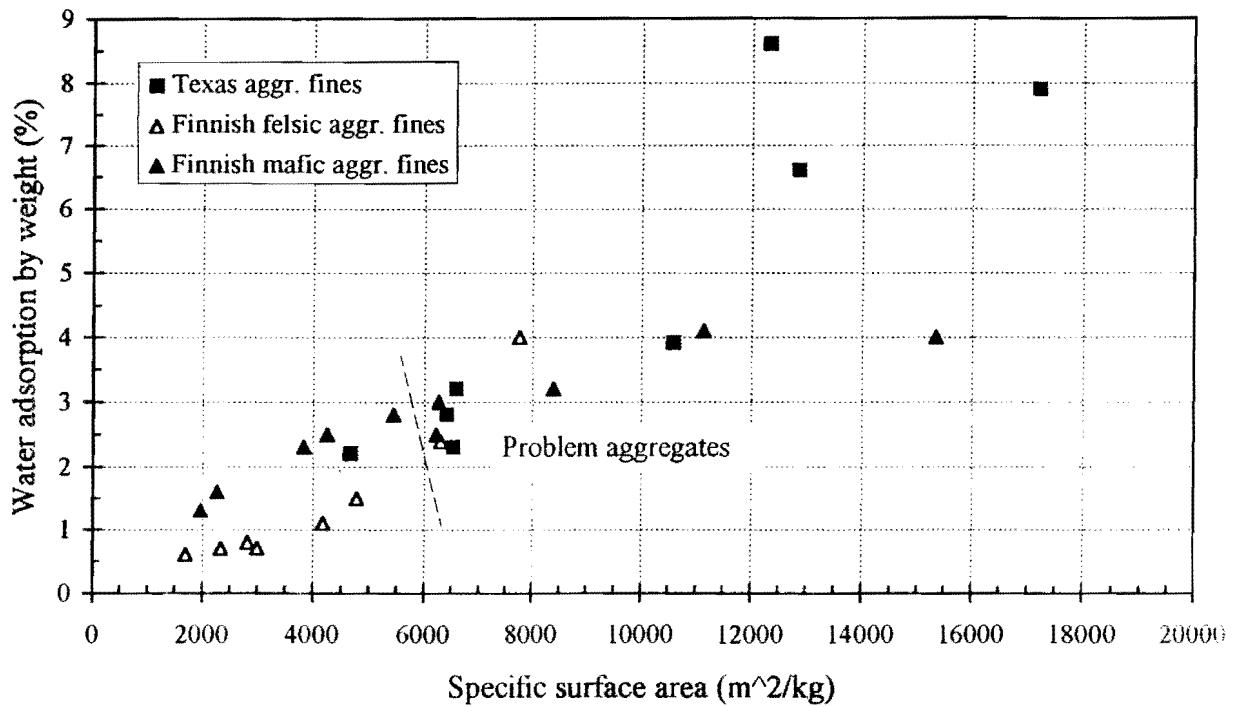


Figure 5.6. Correlation between Water Absorption and Specific Surface Area of Fine Fractions (<0.074 mm) of Some Finnish Base Course Materials

materials include soils and aggregates with intermediate permeabilities such as silty gravels, silty sands, sandy silts, and low plasticity clays

Frost susceptible materials can be modified as indicated in NCHRP Synthesis No. 26:

“Stabilization is widely used as a method of processing subgrade and base course material to improve their performance under traffic and climatic conditions. Effective stabilization of a frost-susceptible material usually involves (1) eliminating the effects of soil fines by their removal or by immobilization, such as cementitious binding, or (2) reducing the quantity of water available at the freezing plane by blocking migration passages. The commonly used stabilizing additives include portland cement, bitumen, lime, and lime-fly ash.”

The Role of Soil Suction - Soil suction is commonly referred to as the free energy state of soil water. The free energy of the soil water can be measured in terms of the partial vapor pressure of the soil water or relative humidity at 20 °C as [Fredlund and Rahardjo 1993]

$$\Psi = -135022 \times \ln(\text{RH}) \quad [5.2]$$

where Ψ = soil suction (kPa); RH = relative humidity (decimal) = u_v/u_{v0} ; u_v = partial pressure pore-water vapor (kPa); and u_{v0} = saturation pressure of water vapor over a flat surface of pure water at the same temperature (kPa). In most cases, soil suction is expressed in pF scale, which is the logarithm of soil suction in mm. The soil suction so measured is commonly called “total suction,” and it has two components, namely, matrix and osmotic suction. They are defined as follows [Aitchison 1965]:

Matrix or capillary component of free energy - In suction terms, it is the equivalent suction derived from the measurement of the partial pressure of the water vapor in equilibrium with the soil water, relative to the partial pressure of the water vapor in equilibrium with a solution identical in composition with the soil water. This suction component can be measured by the psychometric technique with an infinitely large drop of soil water placed on the wet bulb.

Osmotic (or solute) component of free water - In suction terms, it is the equivalent suction derived from the measurement of the partial pressure of the water vapor in equilibrium with a solution identical in composition with the soil water, relative to the partial pressure of water vapor in equilibrium with free pure water.

Total suction or free energy of the soil water - In suction terms, it is the equivalent suction derived from the measurement of the partial pressure of the water vapor in equilibrium with the soil water, relative to the partial pressure of water vapor in equilibrium with free pure water.

The matrix suction component is associated with the capillary phenomenon arising from surface tension of water. In soils, the pores with small radii behave as capillaries and cause soil water to rise above the water table. The capillary water thus has a negative pressure with respect

to the atmospheric pressure. The pore water pressure can be highly negative at low degrees of saturation. The surface of water in a capillary is curved and is called a meniscus. The same soil water will have a flat surface when placed in a large container. The partial pressure of the water vapor above the curved surface of soil water is less than the partial pressure of the water vapor above a flat surface of the same soil water. The relative humidity in a soil will thus decrease due to the presence of the curved water surface produced by the capillary phenomenon. The water vapor pressure or the relative humidity decreases with a decrease in the radius of curvature of the water surface in the capillary. The decrease in relative humidity due to the presence of the curved water surface in the capillary is referred to as the matrix suction.

The osmotic suction component is associated with dissolved salts in the pore water. The water vapor pressure over a flat surface of solvent is less than the water vapor pressure over a flat surface of pure water. The relative humidity decreases with an increase in dissolved salt concentration in the pore water. The decrease in relative humidity due to the presence of dissolved salts in the pore water is referred to as the osmotic suction.

When a soil desaturates, the soil water suction increases causing the inter-particle forces to increase. The increase in inter-particle forces causes a decrease in total volume of the soil or shrinkage.

Volume Change Due to Freezing - When the temperature of most materials is raised, their volumes increase due to thermal expansion. Similarly, when the temperature of these materials is lowered, their volumes decrease due to thermal contraction. Moreover, they expand when they change from the solid phase to the liquid phase and contract upon freezing from the liquid phase to the solid phase. However, the volume of a mass of water is at the minimum at 4 °C when its density attains the maximum value of 1000 kg/m³. Its volume increases when the temperature is lowered from 4 °C to 0 °C. Moreover, water expands approximately 9.2% during freezing, as the density of ice at 0 °C is only 916 kg/m³. The course of volume changes for most materials and water as a function of temperature is illustrated in Figure 5.7.

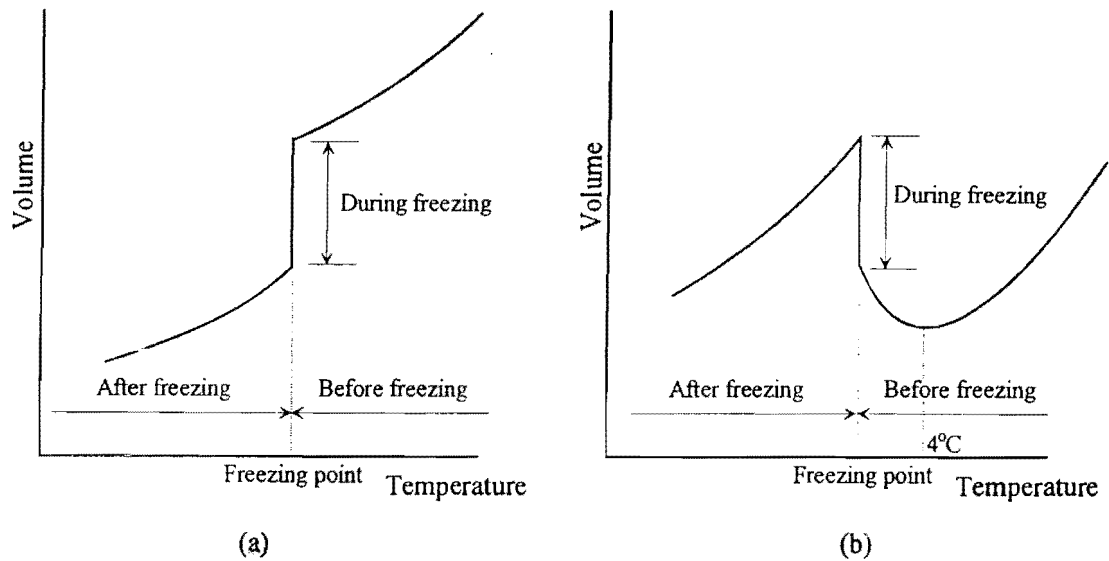


Figure 5.7. Volume Change upon Freezing: (a) Volume Change of Most Materials; and (b) Volume Change of Water

When the temperature of a compacted aggregate is lowered, the volume of the soil skeleton decreases as the pore water and aggregate particles contract thermally. However, when a compacted aggregate is frozen, its pore water will transform into ice, causing an increase in volume as shown in Figure 5.7. The compacted aggregate is also losing free water to the formation of ice, causing a decrease in unfrozen water content that increases soil suction. This mechanism is very similar to drying a compacted aggregate. The increased soil suction causes a decrease in volume [Yong 1965, Carpenter and Lytton 1975, Spaans and Baker 1996]. Similarity between soil freezing characteristics and soil moisture characteristics has been demonstrated by field measurements made by Spaans and Baker [1996]. Although freezing and drying can cause similar increase in soil

suction by decreasing the unfrozen water content to similar values, the decrease in volume caused by freezing may not be as much as that caused by drying as ice is still occupying the pore space. Freezing of pore water can thus increase or decrease the overall volume of a compacted aggregate depending on which of the two opposing mechanisms is dominant.

As a result, three mechanisms cause volume change of a compacted aggregate when it is lowered to below freezing temperature: (1) thermal contraction, (2) expansion due to ice formation, and (3) contraction due to increase in soil suction. It is instructional to evaluate the relative significance of these three mechanisms.

The coefficients of linear thermal expansion of natural aggregates widely used for base and subbase construction range from 4×10^{-6} to $13 \times 10^{-6}/^{\circ}\text{C}$ at ambient temperature [Verbeck and Hass 1951; Mindess and Young 1981]. The coefficient increases remarkably and nonlinearly with temperature [Mindess and Young 1981]. However, the thermal expansion coefficients of compacted aggregates are not readily available. If the pores between aggregate particles are empty, their volumetric characteristic as a function of temperature should be the same as the aggregate particles forming the pores. Therefore, the thermal expansion coefficient of the aggregate particles can be used to estimate the volume change of the compacted aggregate. If this range of values of thermal expansion coefficient are used as a first estimate for the percent volume change of compacted aggregates over a temperature range of 40°C and the effect of pore water is neglected, then

$$\text{Percent volume change} = 3 \times 13 \times 10^{-6} \times 40 \times 100\% = 0.156\% \quad [5.3]$$

The multiplier 3 is used to convert the coefficient of linear thermal expansion to the coefficient of volumetric thermal expansion. The volume change should thus be approximately 0.156% for a temperature difference of 40°C . Such a small volume change of compacted aggregates should not cause detrimental damage to pavement. Therefore, emphasis will be focused on the other two mechanisms.

Interrelationship between Soil Suction and Volume Change - Although the three mechanisms appear to be independent, they are interrelated. Soil suction causes the pressure in the pore water to be lower than the atmospheric pressure. When the pressure on water is increased, its freezing point is lowered. It is thus intuitive that a decrease in pressure will cause an increase in the freezing

point of the pore water. However, this is incorrect for the freezing of pore water in a soil. The decrease in pore water pressure is caused by the capillary action of the soil particles, and the pressure on any ice formed is still atmospheric. On the basis of this argument, the freezing point of pore water is actually lowered by soil suction. The relationship is given by [Hudson 1906; Schofield 1935; Williams 1963, 1964]

$$\Delta T = \frac{10^h \times T \times g}{100 \times L} \quad [5.4]$$

where ΔT = freezing point depression (K); h = soil suction in pF; T = freezing temperature of water (273.2° K); g = acceleration due to gravity (9.81 m/s²); and L = specific latent heat of fusion of ice (333.6×10³ J/kg). The relationship is shown graphically in Figure 5.8. Another relationship was developed by Edlefsen and Anderson [1943] based on theoretical considerations. However, the validity of the relationship presented has been established by numerous experimental studies [Williams 1963] while there are significant discrepancies between experimental data and the relationship developed by Edlefsen and Anderson [1943].

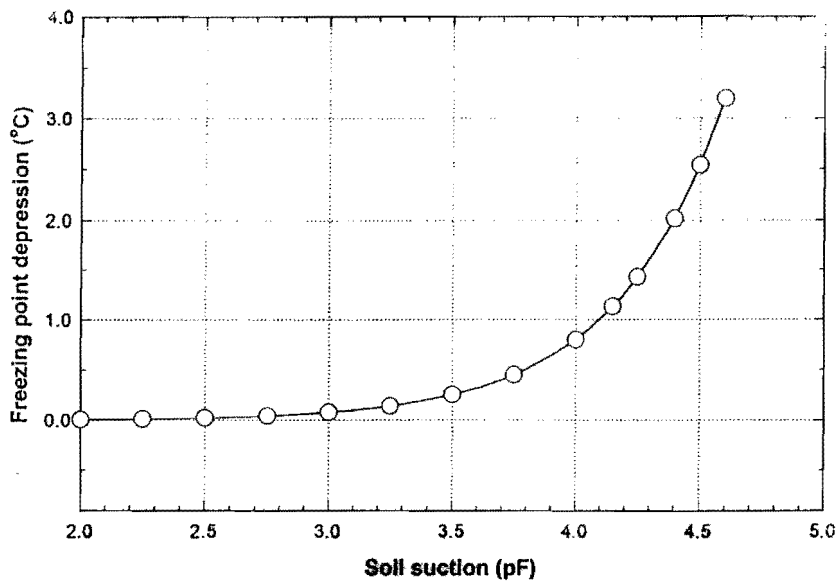


Figure 5.8. Freezing Point Depression as a Function of Suction

Soil suction also affects the unfrozen water content. A relationship proposed by Dillon and Andersland [1966] is as follows,

$$w_u = \frac{ST}{T_o} \times \frac{1}{A_c} \times \ell \times k \times 100\% \quad [5.5]$$

where w_u = unfrozen water content (% dry weight of aggregate); S = specific surface area (m^2/kg); T = temperature of frozen soil ($^{\circ}\text{K}$); T_o = temperature of initial freezing of soil pore water ($^{\circ}\text{K}$); A_c = activity ratio = $\text{PI}/(\% < 2 \mu\text{m})$; PI = plasticity index (%); $\ell = 1$ for non-expandable clays and 2 for expandable clays; and $k = \text{a constant} = 2.8 \times 10^{-7} \text{ kg of water}/\text{m}^2$. The prediction equation explicitly involves the specific surface area of the soil matrix, the plasticity index, and activity ratio. Although they did not emphasize it, the latter two parameters are closely related to the specific surface area of the soil matrix. As a result, Anderson and Tice [1972] refined the relationship as follows. The unfrozen water content can be related to the temperature below freezing,

$$w_u = \alpha \theta^\beta \quad [5.6]$$

where θ = temperature below 0° ($^{\circ}\text{C}$); and α and β = parameters characteristic of the soil. Their experimental results indicate that both α and β have a strong correlation with specific surface area S (m^2/g). They found that

$$\ln \alpha = 0.5519 \ln S + 0.2618 \quad [5.7]$$

with a correlation coefficient of 0.90 and

$$\ln(-\beta) = 0.2640 \ln S + 0.3711 \quad [5.8]$$

with a correlation coefficient of 0.86. Therefore, they developed a relationship relating unfrozen water content to specific surface area and temperature below freezing,

$$\ln w_u = 0.2618 + 0.5519 \ln S - 1.4495^{-0.264} \ln \theta \quad [5.9]$$

However, the expansion of some clay minerals when wetted exposes an “internal” surface area, which must be accounted for in S . Specific surface areas derived from nitrogen adsorption isotherms are unsatisfactory because they are a measure of ‘external’ surface only. When measured values of S are not available, it is possible to derive a “geometric” specific surface area from grain size distribution curves to obtain good estimates of w_u [Dillon and Andersland 1966]. Experimental results by Yong [1963] indicate the unfrozen water content of a soil at a given temperature increases with initial water content. Moreover, the unfrozen water content depends on temperature, soil type, and path of reaching the temperature. The unfrozen water content at a particular temperature below 0 °C during freezing can be considerably higher than that during thawing [Yong 1963]. As soil suction generally increases with plasticity index and specific surface area of soils, results from these previous studies indicate an increase in suction of soil water will lower the freezing point of pore water and increase the unfrozen water content at temperatures below freezing.

Influence of Climatic Conditions on the Performance of Flexible Bases

Environmental effects have long been recognized as being influential in the construction and performance of pavements. Environmental variables important in pavement cracking studies, such as the Thornthwaite moisture index, average annual frost penetration, mean annual minimum temperature, rate of temperature drop below 45 °F, annual average number of freeze thaw cycles, mean daily solar radiation, etc. have been catalogued by Carpenter et al. [1974]. Their results indicate that west Texas receives the most severe environmental changes. From the data collected for west Texas and the conclusions of previous studies, they drew the following conclusions [Carpenter et al. 1974]:

1. Low temperature thermal cracking of pavements is less influential than in other parts of the United States and Canada.
2. Stresses induced by rate of temperature drop are likely to be higher in west Texas than in Canada and probably in other parts of the United States.

3. Thermal fatigue would be more of a problem in west Texas and the United States than in Canada.
4. In all instances, west Texas appears to be subject to the more severe action of the climatic variables associated with low temperature, thermal fatigue, and shrinkage cracking.
5. The importance of having accurate measurements of climatic variables is borne out in all studies.
6. The base course and subgrade have not been adequately researched, recorded, or considered in previous studies.
7. Moisture redistribution and state of moisture (suction) in the base and subgrade materials is extremely important in studying the behavior of the pavement. A reliable relationship between an environmental indicator and the equilibrium suction beneath a highway in the subgrade exists. This environmental indicator (Thornthwaite moisture index) has been validated for the west Texas area by regression against similar known quantities derived specifically for the west Texas area.
8. The transverse cracking problem in west Texas is a much more complicated phenomenon than can be predicted by considering only the asphaltic concrete surface course. Much work remains to be done in relating the interactions of the various mechanisms.

LABORATORY TESTING APPROACH

In the laboratory testing phase of study 1432, aggregates from 24 sources were collected and evaluated. The sources included material from: (1) supply pits, stockpiles, or quarries (source materials) and (2) excavations from road bases.

A moisture-density relationship was determined for each material. Samples were then compacted in accordance with TEX-113-E, dried for 24 hours at 60 °C, and subjected to a capillary soak for 250 hours or until the material reached a moisture equilibrium. During this capillary soak period, the dielectric value, electrical conductivity, and moisture content were monitored. Texas triaxial strengths were then determined for each material.

Certain source materials were selected, and the effects of additives (stabilization) were evaluated. The screening dielectric tests as well as Texas triaxial testing were completed to evaluate

the effects of the additives in reducing moisture sensitivity and the sensitivity of the tests to the effects of changing the aggregate fines matrix through stabilization.

Seven aggregates representing different mineralogies and locations were selected from among the aggregate library of 24 materials for more detailed mineralogical and freeze-thaw sensitivity testing. On these aggregates, we determined the relationship between soil suction and moisture content, and we measured the volume change during temperature cycling between 20 °C and -10°C. In addition, for these materials, the mineralogy of the size fractions was determined from x-ray diffraction (XRD) analysis.

LABORATORY TESTING PROCEDURES ADOPTED FOR THIS STUDY

Gradation and Moisture - Density Analysis

Prior to any testing of the aggregate system, a gradation was produced which was typical of the gradation used in the district and which meets the requirements of item 247 grade 1 material. Typical district gradations were established through gradation analyses of materials collected from the pavement sections within each district. Based on the selected gradation for each district, a moisture-density relationship was developed for each material according to Tex-113-E.

Dielectric and Electrical Conductivity Measurements During Capillary Soak

The dielectric value test was performed by placing a 140 mm diameter by 280 mm high compacted sample held in a plastic tube in 20 mm of water. The sample was compacted in accordance with Tex-113-E at optimum moisture and maximum dry density prior to capillary soak; samples were dried for 24 hours at 60 °C. One mm holes were drilled into the bottom of the plastic mold to allow water to enter the compacted sample. A Adek electric probe was placed at the surface of the sample, and the dielectric value of the surface was monitored as a function of time of capillary soak. A schematic of this test is shown in Figure 5.9.

In addition to the dielectric value, the electric conductivity and the moisture content of the sample were continuously determined throughout the experiment.

Based on the results obtained using aggregates from Texas and Finland, the interpretation scheme in Table 5.3 was proposed by Saarenketo and Scullion [1995]. From this table, we conclude

that a dielectric value below 10 is representative of good quality granular materials in their normal operating range. Values above 10 are warning signs that the material has significant levels of free water and may be susceptible to stability loss and freeze-thaw damage. Values of dielectric of 16 or above represent critical values at which the shear strength of the material is significantly reduced, and the material will be extremely susceptible to damage by freezing.

Suction Measurements as a Function of Moisture

Soil suctions at different moisture contents were measured by a transistor psychrometer made by Soil Mechanics Instrumentation of Adelaide, South Australia, Australia. The instrument was designed to determine the relative humidity of the air within a confined space, where relative humidities ranged from 95% to 99.95%, by measuring the very small temperature difference between the wet bulb transistor and the dry bulb transistor. This enables the instrument to be used to measure soil suctions within the range of pF 3.0 to approximately 5.0. The instrument has 12 transistor probes, a thermally insulated container, and a data logger connected to a printer. Each transistor probe has a wet bulb transistor, a dry bulb transistor, a probe shaft containing a small electrical circuit board, and a probe head containing a trimming potentiometer used to zero the probe after temperature equilibrium is reached. Details of the equipment are shown in Figure 5.10.

The probes were cleaned with deionized water and dried. Standard sodium chloride solutions (NaCl) were prepared to give equivalent relative humidities between pF 2.0 to 5.0. Three drops of pF 2.0 solution were applied to each calibration cap containing two thicknesses of filter paper. A standard sized water drop was applied to the wet bulb transistor of every transistor probe using a screw-adjusted syringe. A calibration cap containing pF 2.0 solution impregnated filter papers was placed on the end of every probe and taped into position using electrical tape. The probes were inserted into the thermally insulated container to reach temperature equilibrium.

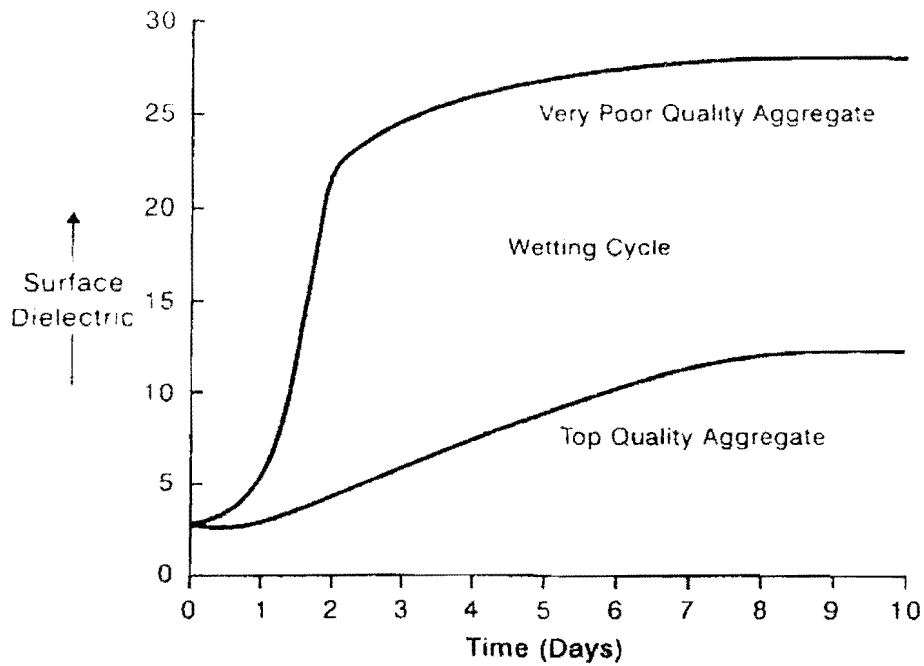
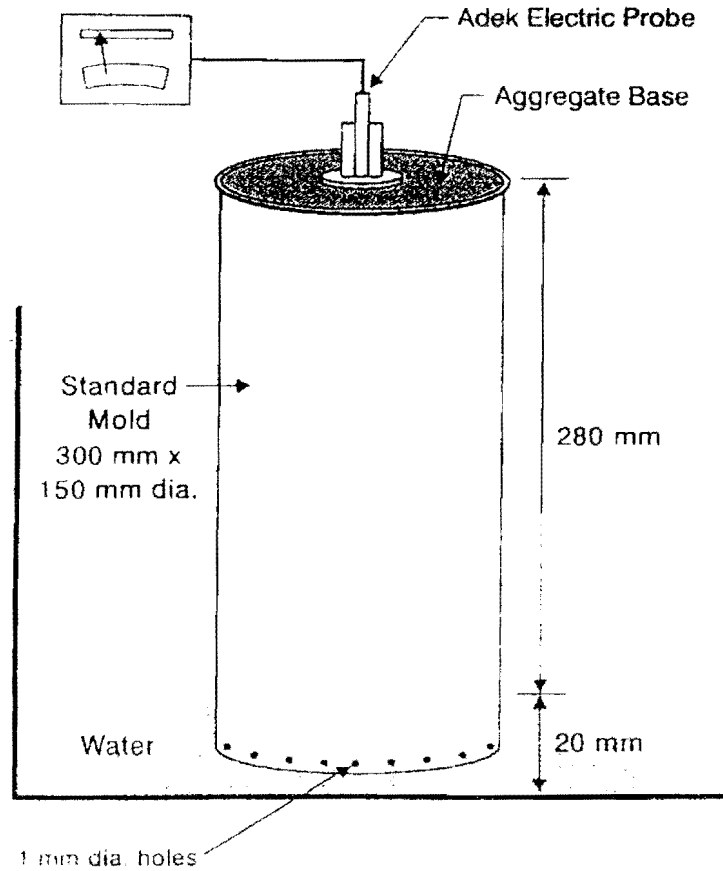


Figure 5.9. Capillary Soak - Dielectric Value Test Setup and Typical Results

Table 5.3. A Proposed Relationship between Electrical Properties and Field Performance of Granular Base Material [after Saarenketo and Scullion 1995]

Dielectric Value	Electrical Conductivity (1S/cm)	Material	Strength and Deformation Properties	Frost Susceptibility and Water Sensitive
<5	<10	-dry and open graded base with low water adsorption and large air-solid ratio	-low tensile strength, might be sensitive to permanent deformation by compaction	-non-frost susceptible, non-water sensitive
5 -7	<50	-dry base with low water adsorption value and optimum dry density	-optimum strength properties	-non-frost susceptible, non-water sensitive
7 - 10	<100	-slightly moist base with high suction value	-high shear strength because of suction, hysteresis has great effect on strength value	- might become water sensitive and frost susceptible if drainage stops working
10 - 16	<150	-moist base	-reduced shear strength because of reduced suction	-frost susceptible and water sensitive
>16	>150	-wet or water saturated base	-adequate shear strength, no positive pore water pressure under dynamic load	-may form ice lense
>16	>150	-wet or water saturated base	-under a dynamic load, plastic deformation may occur because of high pore water pressure and low shear strength	-extemely frost susceptible

UNSATURATED SOILS

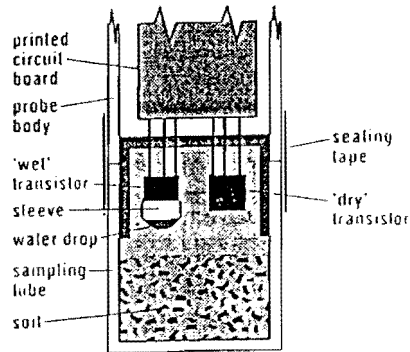


Figure 5.10a. The Probe Tip Containing the Sensing Elements (Transistors)

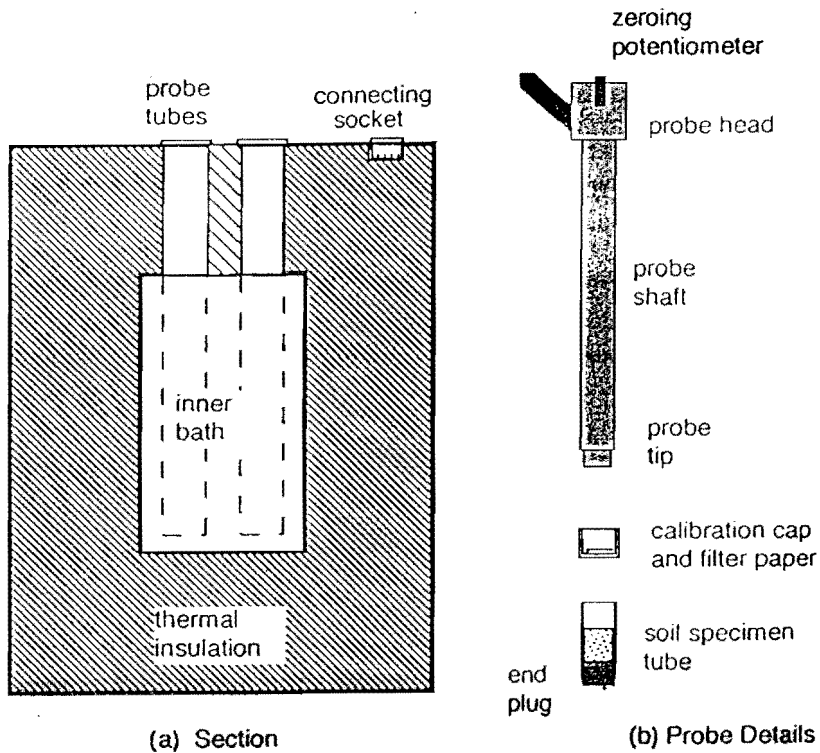


Figure 5.10b. The Probe and Thermally Insulated Container

After approximately 16 hours had elapsed, the probes were zeroed by turning the screw-type potentiometers within the probe heads by a screw driver. The probes were then calibrated using standard salt solutions prepared to give equivalent relative humidities between pF 3.0 to 5.0. The calibration cap containing filter papers impregnated by pF 2.0 solution was replaced by another calibration cap containing filter papers impregnated by pF 3.5 solution. The probe was sealed with electrical tape similarly and inserted into the container. The output from the probe in millivolt was recorded after approximately an hour when the reading became stable. The procedure was repeated for pF 4.0, 4.5, and 5.0 solutions. A typical calibration curve for a probe is shown in Figure 5.11.

Measurement of suction in soil samples was performed in a similar way to the calibration procedure but using the small 35 mm long sampling tubes. Samples were trimmed to 10 mm high by a sampling ring and then cut using the sample tubes. When the sample was in position at the bottom of the sampling tube, an end plug was carefully pushed into the tube, forcing the sample into the center of the tube. Each sampling tube was then placed on the end of a transistor probe. The probe was sealed with electrical tape and inserted into the container. The output in millivolt was recorded after approximately an hour when the reading became stable. The suction of the sample was then determined from the calibration curve of the probe.

Soil samples of the seven different aggregates were prepared by compaction at respective optimum moisture contents. The compacted samples were allowed to absorb water freely before they were prepared for suction measurements. After soil suctions of these samples were measured at high water contents, they were weighed immediately. They were allowed to be air-dried for a few hours to lower water contents. Suction measurements were then made again, and weights of the samples were recorded. The procedure was performed three to four times for each aggregate. The dry weights of the samples were determined at the conclusion of the experiment. The relationship between water content and soil suction was thus determined from a single set of samples.

Volume Change Due to Freezing and Thawing

Several methods are available for the study of the volume change characteristics of compacted aggregates resulting from freezing. From the perspective of availability of water, the testing system can be an open system or a closed system. An open system allows the sample free

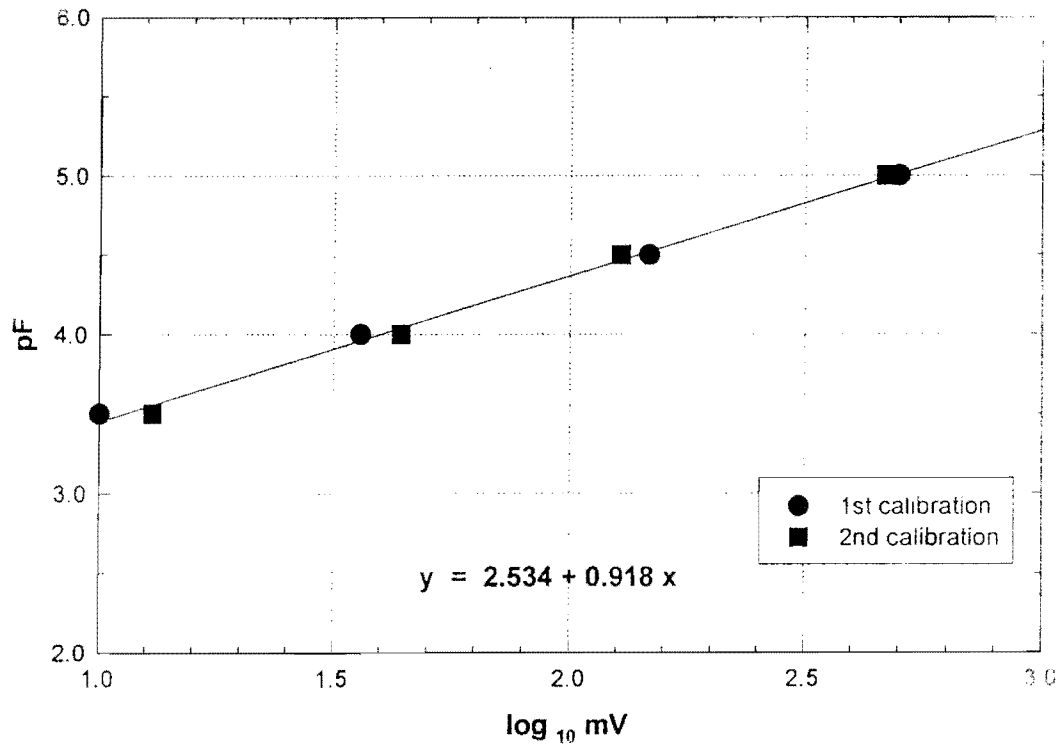


Figure 5.11. Calibration of Probe 9-Transistor Psychrometer

access to water during the freeze-thaw process. This is usually achieved by putting one end of the sample in water. A closed system does not allow the sample free access to water and is designed to maintain a constant moisture in the sample during the freeze-thaw process. From the perspective of temperature control, the sample can be frozen by unidirectional freezing or all-round freezing. The method of uni-directional freezing exposes only one end of the sample to the freezing temperature, allowing the advancement of a freezing front through the sample as a function of time. The sample, other than the exposed end, has to be thermally insulated to ensure that heat exchange only takes place at the exposed end [Hamilton 1966]. The insulation increases the difficulty and

complexity of making accurate volume measurements at different temperatures. It models the in situ freeze-thaw process better, but it takes a considerably longer period of time to expose the sample to cyclic freeze/thaw. The method of all-round freezing exposes the sample to an all-round uniform temperature. It takes considerably less time for the sample to reach thermal equilibrium with the all-round temperature. It is also much simpler to make volume measurements at different temperatures, as all measurements can be made at the all-round temperature, and there is no insulation to remove and to re-install.

A closed system simulates the conditions for a base course in west Texas better as the water table will have negligible direct influence on the pavement. In fact, results from a previous study conducted by Carpenter and Lytton [1975] indicate that the water content of base course in west Texas is actually lower than the as-compacted water content. The compacted aggregate is thus losing water rather than gaining water during the process. Unidirectional freezing of samples is of prime importance when studying the formation of ice lenses and frost heave that require a freezing front to advance through the sample. This phenomenon usually requires a fine-grained saturated material with free access to capillary water and a closed water table. This situation does not apply to base courses in west Texas [Carpenter and Lytton 1975]. Moreover, previous studies have not found any significant structural damage, such as moisture migration or loss, formation of ice lenses, etc., in samples of similar materials frozen in closed systems. Thus, a closed system with all-round freezing was selected for this study.

The samples were compacted in accordance with the TEX-113-E compaction procedure at different moisture contents to obtain samples of different degrees of saturation at room temperature. After the sample was weighed, it was covered by a plastic wrap immediately to minimize any moisture loss. Five small flat-headed nails were hammered into the top surface of each sample to provide bench marks for height measurements. The top surface was covered by a plastic cap. A gage made of graph paper was attached vertically to the cylindrical surface of the sample to mark the five locations for diameter measurements. Each sample was placed on a base plate of known height and mass. The sample and the base plate were separated by a plastic wrap. Two handles were installed onto each base plate so that no direct contact was made with the sample during the experiment. The sample was then placed in a large environmental chamber at 20 °C. The relative humidity of the chamber was kept at approximately 60%.

As the specific heat capacity of aggregate changes with temperature, it is impractical to use time as the criterion to determine whether the sample has reached thermal equilibrium with the air in the environmental chamber. To account for this effect, a control sample was prepared with a thermometer installed at the middle of the sample to measure the aggregate temperature as the specific heat capacity of the soil changed with water content and degree of saturation [Kersten 1949]. The temperature control (measurement) sample was compacted at a moisture content of 12% and a degree of saturation of 75%. This moisture content and degree of saturation were selected as they represent the highest of these values for all the samples except one. The preparation procedure of the temperature measurement sample was identical to that of the other samples, except for the insertion of a thermometer. When the sample temperature reached equilibrium with the air temperature of the chamber, it was assumed that all the samples had reached thermal equilibrium with the environment, as it takes less time to change the temperature of compacted aggregate samples at lower moisture contents.

After the samples reached thermal equilibrium with the environment, the heights of the samples at marked locations were measured by a dial gauge to the accuracy of 0.0254 mm and the diameters at marked locations measured by a pi tape to the accuracy of 0.0254 mm. The dial gauge and pi tape were in thermal equilibrium with the chamber temperature, and all measurements were made inside the chamber. Corrections for the thermal contraction of the dial gauge and pi tape were made to the measured values, as the linear thermal expansion coefficients of both measurement devices are known. The samples were weighed immediately after their dimensions had been measured to quantify any moisture loss during freezing and thawing. Measurements were made at approximately 20, 15, 10, 5, 1, -1, -5, -10, and -15 °C, as the temperature of the chamber cannot be set very precisely at a predetermined temperature. However, the chamber can maintain the variation of temperature within 0.5 °C. The actual temperature was recorded. The temperature range of 20 to -15 °C was selected on the basis of the results obtained by Hamilton [1966], and Carpenter and Lytton [1975] that most volume changes occur in the temperature range of 0 to -7 °C. The samples were warmed to 20 °C in similar steps after they had been cooled to -15 °C. Afterwards, the samples were cooled to -15 °C again to investigate the effects of a second freezing cycle.

Strength Testing

Strength testing was performed in accordance with the Texas Triaxial method, TEX-117-E. Aggregate samples were fabricated at a representative gradation used in the field (and meeting item 247 grade 1 requirements) at optimum moisture content. The samples were then subjected to 10 days of capillary soak and then tested for triaxial strength at a minimal confining pressure of 7 kPa. The triaxial strength in essentially an unconfined condition after 10 days of capillary soak provides a direct measure of the shear strength of the aggregate system and is used to evaluate the suitability of the aggregate as a structural paving layer.

Mineralogical Testing and Index Testing to Evaluate Mineralogical Effects

It is well established that the fines fraction of the aggregate matrix strongly affects the ability of the matrix to attract and hold moisture. This, in turn, affects the sensitivity of the aggregate matrix to the effects of moisture on strength and stability. In order to ascertain the nature of the fines, Atterberg limits (liquid limit, plastic limit, and plasticity index) were determined on each aggregate system. Furthermore, selected representative aggregates were separated into sand, silt, coarse clay, and fine clay fractions, and these fractions were evaluated using x-ray diffraction (XRD) to determine the minerals present.

MATERIALS EVALUATED

Source Material and Site Specific Material

Laboratory testing was performed on materials collected from several TxDOT districts: Abilene, Amarillo, Atlanta, Lufkin, Pharr, San Angelo, and Yoakum. The testing was limited on the material received from the Atlanta and Pharr Districts due to logistics in receiving adequate quantities of material for the very material intensive testing performed. Work concentrated on source material from Abilene, Amarillo, San Angelo, and Yoakum. The general testing approach and sequence changed several times during the course of the research in an effort to adjust the research effort to accommodate new findings. For example, specific mineralogical and petrographic testing originally planned was done only on a limited level. The focus of the study shifted to tests that can be performed on a design and specification basis, such as the dielectric value test, strength testing, and suction tests. Furthermore, it is not necessary to perform detailed mineralogical and petrographic analyses on all material once the effect of mineralogy and soil texture was established on a selected suite of materials which represent a reasonable cross-section of the materials encountered.

Dielectric and Texas Triaxial strength testing were performed on materials from the Abilene, Amarillo, Lufkin, San Angelo, and Lufkin Districts. These materials are identified in Tables 5.4 through 5.8.

Table 5.4. Material Used in Laboratory Dielectric Testing from the Abilene District

Material	Designation	Description
Clements	ABC	Source pit caliche
Jordan	ABJ	Source pit caliche
Kemper	ABJ	Source pit caliche
Parmley	ABP	Source pit caliche
Tubbs	ABBT	Source pit caliche
FM 3438	AB3438	Limestone
US 84	AB 84	Limestone
US 83	AB83-1 AB83-2 AB63-3	Caliche Caliche Caliche

Table 5.5. Material Used in Laboratory Dielectric Testing from the Amarillo District

Material	Designation	Description
Buckles	AMB	Source pit caliche
Coons	AMC	River gravel
Johnson	AMJ	River gravel
Lindsay	AML	Source pit caliche
Buckles FM 287 (1)	AMB297(1)	Source pit caliche
Buckles FM 297(2)	AMB297(2)	Source pit caliche
Lindsey - Coulter (1)	AMLC1	Source pit caliche
Lindsey - Coulter (2)	AMLC2	Source pit caliche
Box Canyon (6-1)	AMBX-1	River gravel
Box Canyon (6-2)	AMBX-2	River gravel

Table 5.6. Material Used in Laboratory Dielectric Testing from the Lufkin and Bryan Districts

Material	Designation	Description
Welches (Lufkin)	LW	Glauconite
WFC (Lufkin)	LWFC	Glauconite
IOG (Lufkin)	LIOG	Iron Ore Gravel
TTI Control LS (Bryan)	TTILS	High Quality Limestone
Kosse Limestone (Bryan)	BK	High Quality Limestone

Table 5.7. Material Used in Laboratory Dielectric Testing from the San Angelo District

Material	Designation	Description
Loop 306-1	SA 306-1	Limestone
Loop 306-2	SA 306-2	Limestone
North of East 24 th -1	SA 24-1	Limestone
North of East 24 th -2	SA 23-3	Limestone
Stockpile 1	SA 1	Limestone
Stockpile 2	SA 2	Limestone

Table 5.8. Material Used in Laboratory Dielectric Testing from the Yoakum District

Material	Designation	Description
Victoria	YV	Siliceous gravel
LP 463-1	YV (463-1)	Siliceous gravel with caliche fines
LP 463-2	YV (463-2)	Siliceous gravel with caliche fines
183 - Dry	183 d	Limestone
183 - Wet	183 w	Limestone
US 290	Y 290 (LS)	Limestone
Fayette Gravel	YRG	Lime-treated river gravel
Corpus Christi caliche pit	CCC	Caliche

Table 5.9. Study of the Effects on Additives and Selective Gradation Alterations on Selected Aggregates

Source	Additive or Alteration	Designation
Abilene - Clements	--- - 200 sieve size - 40 sieve size +1.5% Lime +3.0% Lime	ABC ABC (-200) ABC (-40) ABC (1.5 L) ABC (3.0 L)
Abilene - Jordan	--- +1.5% Lime +3.0% Lime	ABJ ABJ (1.5 L) ABJ (3.0 L)
Abilene - Kemper	--- +3.0% Lime	ABK ABK (3.0 L)
Abilene - Tubbs	--- +1.5% Lime +3.0% Lime +3.0% PC	ABT ABT (1.5 L) ABT (3.0 L) ABT (3.0 C)
Amarillo - Buckles	--- +1.5% Lime +3.0% Lime +1.5% PC +3.0% PC	AMB AMB (1.5 L) AMB (3.0 L) AMB (1.5 C) AMB (3.0 C)
Amarillo - Coons	-- + 1.5% Lime + 3.0% Lime	AMC AMC (1.5 L) AMC (3.0 L)
Amarillo - Johnson	-- +1.5% Lime +3.0% Lime +1.5% PC +3.0% PC +3.0% EA	ABJ ABJ (1.5 L) ABJ (3.0 L) ABJ (1.5 C) ABJ (3.0 C) ABJ (3.0 A)

Table 5.9. Study of the Effects on Additives and Selective Gradation Alterations on Selected Aggregates (continued)

Source	Additive or Alteration	Designation
Amarillo - Lindsey	-- +1.5% Lime +3.0% Lime +1.5% PC +3.0% PC	AML AML (1.5 L) AML (3.0 L) AML (1.5 C) AML (3.0 L)
Lufkin - Welches	-- +3.0% PC +4% LFA	LW LW (3.0 L) LW (4.0 LFA)
Yoakum - Victoria	-- +1.5% Lime +3.0% Lime +1.5% PC +3.0% PC +3.0% Asphalt	YV YV (1.5 L) YV (3.0 L) YV (1.5 C) YV (3.0 C) YV (3.0A)
Bryan - Kosse Limestone	-- +1.0% Lime +2.0% Lime	BK BK (1.0 L) BK (2.0L)
Corpus Christi Caliche	-- +1.0% Lime +2.0% Lime	CCC CCC (1.0 L) CCC (2.0 L)

Material Alteration by Scalping and Stabilizer Additives - The effect of additives and selective scalping of certain size fractions was determined on selected materials. The experiment to determine the effects of these additives and gradation alterations is presented in Table 5.9.

Selected Study to Determine Volumetric Effects of Freezing and Thawing

Seven aggregates from the aggregate library were selected for more detailed study of volumetric effects of freezing and thawing. Data concerning these materials are summarized in Table 5.10.

Table 5.10. Seven Aggregate Systems Selected for Volumetric Change Testing Due to Freeze-Thaw

Material	Designation	% Clay in - 75 Micron Fraction	Clay Mineralogy	LL, %	PI, %	DV_{max}
Box Canyon	AMBX	15	mica	--	--	5
Buckles Pit	AMB	--	mica/smectite	--	--	35
Coon Pit	AMC	17	cholorite/mica	--	--	9
Lindsay	AML	41	kaolinite/smectite/ mica	23	10	25
Victoria	YV	38	smectite/mica	21	21	18
US 290 (LS)	Y290 (LS)	41	kaolinite/mica/ smectite	--	--	20
Fayette gravel	(YFG)	27	smectite/mica	--	--	18

FINDINGS FROM LABORATORY TESTING

Source Material and Site Specific Studies

Tables 5.4 through 5.8 present the list of materials tested in this study for dielectric properties and strength properties from the Abilene, Amarillo, Bryan, Corpus Christi, Lufkin, and Yoakum Districts. Table 5.9 presents the alteration techniques and additives used with these aggregates in an effort to improve dielectric and strength properties of these selected aggregate systems.

As previously discussed, the testing approach first required that each aggregate gradation be reproduced to meet Item 247, grade 1 requirements and to match approximate district specifications based on the site specific pavement studies selected within the districts. Based on this aggregate gradation, the moisture-density properties of each aggregate system was determined. Samples were fabricated for dielectric and strength testing at optimum moisture content, maximum dry density, and at the representative gradation of similar materials used in the specific district in question.

Figures 5.13 through 5.17 summarize the dielectric values of the materials grouped by district. Figures 5.18 through 5.20 summarize Texas triaxial strength data for the same materials grouped by district.

Ranking of Sources and Variability Among Sources

A general finding of this study is that the dielectric value (DV) is a meaningful tool by which to evaluate the characteristics of a flexible base. This finding is based on: (1) a logical trend of DV and physical properties and mineralogical characteristics of the aggregates evaluated, (2) reproducibility of the test over three replicate samples for each test category, and (3) a suitable sensitivity of the DV to the addition of additives known to be able to alter and improve the properties of the fines fraction of the aggregate matrix.

The electrical conductivity property (EC) is not recommended at this time for screening aggregate properties. Although the test has great potential for use in conjunction with the DV parameter in determining specific properties of osmotic pore pressure and osmotic suction, we do not believe that the sensitivity, accuracy, and precision of the test as currently performed warrants adaptation for specification-type testing. Furthermore, acceptance or evaluation criteria cannot be established at this time.

The DV and strength properties of the aggregates evaluated are discussed in the following paragraphs under the heading of the specific district from which the material was obtained.

Abilene District - The DV properties of aggregates from the Abilene District are summarized in Figure 5.12, and the strength properties are summarized in Figure 5.17. From these figures and the criteria summarized in Table 5.2, one can determine the general character of the aggregates collected for this district. Each of the source materials are caliches. However, the quality as measured by DV varies considerably.

Based on the DV criteria, the following conclusions are pertinent to the Abilene aggregates:

1. The caliches ranked from best to worst as follows: Kemper, Clements, Parmley, Tubbs, and Jordan. The Kemper and Clements caliches are apparently considerably better than the Parmley, Jordan, or Tubbs materials.
2. The addition of 1.5% hydrated lime is generally effective in reducing the DV.

However, the use of 3.0% hydrated lime may be too much as the DV increases from the DV determined when 1.5% hydrated lime was added. This effect could mean that the 1.5% additive rate was sufficient to react with the fines materials, and the additional lime acts simply as a fines filler. The effects of a longer curing period for the lime should be investigated as the curing period in this experiment was seven days at 38 °F.

3. The addition of 1.5% portland cement and 3.0% portland cement both register solid improvements in the DV. This is likely because the portland cement hydration occurs much more rapidly than that of the lime, and the cementitious properties of the cement do not require a reaction with the soil fines. The cement acts to encapsulate the aggregate fines. The effects of long-term curing between the lime and cement will be important to evaluate. This point is addressed in more detail in the section entitled Curing Effects on Aggregates Stabilized with Hydrated Lime and Lime-Fly Ash.
4. The strength improvement, Figure 5.17, offered by the addition of lime at both the 1.5% and 3.0% rates for all caliches demonstrated a strength improvement of from about 150% to 400%. This is an attractive level of strength improvement without transforming the flexible base to a rigid system. This concept must be considered in rehabilitation and recycling operations.
5. It is interesting that most of the caliche aggregates in the district have DVs greater than the upper limit of 16 established by Saarenketo and Scullion.
6. The sensitivity of the DV test is verified in Figure 5.12 as the DV increases substantially when the non-plastic -40 and -200 fines are scalped from the Clements pit material and replaced with Victoria clay fines.

The general trend for the Abilene caliches is a fair to poor ranking based on DV measurements. DVs can be substantially improved to the fair or good category by the addition of chemical stabilizers (1.5 to 3.0% by weight). The hydration properties of portland cement (3.0%) are quite effective in reducing DVs to the “good” level. The hydration effects of portland cements seem to effectively encapsulate fines, which adsorb water more actively when not agglomerated and encapsulated. The preferred additive rate for hydrated lime with the materials evaluated seems to

be 1.5%. Hydrated lime is, at this rule of addition, very effective with the Clements and Jordan aggregates but not effective with the Tubbs material. The effectiveness of hydrated lime in reducing moisture sensitivity as measured by the DV test is certainly related to the level of pozzolanic reactivity of the lime and the aggregate fines. Soil mineralogy controls this level of reaction.

Figure 5.17 illustrates the effectiveness of 1.5% hydrated lime in improving triaxial strength of all aggregates tested. A more complete study is needed to evaluate the effects of the slower curing rate of lime-soil reactions compared to the portland cement-soil reactions.

Amarillo District - The summary DV plots for the Amarillo District are presented in Figure 5.13, and the strength data are summarized in Figure 5.17. According to these data, the following conclusions are drawn:

1. The rank of the moisture susceptibility of these aggregates according to DV analysis from best to worst is: Box Canyon, Johnson, Coons, Lindsey, and Buckles. The river gravel aggregates are substantially better performers than the caliches based on the DV criterion.
2. The effect of chemical stabilizers (lime and cement) on the river gravel aggregates are marginal in terms of DV changes. This is probably because improvement is not needed as the fines are not deleterious in their natural state. The addition of lime (1.5%) and cement (3.0%) substantially improves the DV properties of the Buckles caliche. Lime is not effective in improving the DV properties of the Lindsey pit material. The only effective chemical additive in the Lindsey material is 3.0% portland cement. However, one should consider long-term curing and ultimate strength of the stabilized mixture before a final decision is made. Curing effects were not considered in this study, as all stabilized materials were cured identically (7 days at 40 °C). The importance of the effects of long-term curing cannot be over emphasized.
3. Hydrated lime was effective (1.5%) in substantially improving the Texas Triaxial strength of all Amarillo aggregates evaluated to well above grade 1 (Item 247) requirements. This is a curious effect for the Lindsey aggregate where a strength increase is evident without a corresponding positive DV shift. Once again, this is

probably due to curing effects as discussed on page 5.55 under the section entitled Curing Effects on Aggregates Stabilized with Hydrated Lime or Lime-Fly Ash.

Lufkin District - The materials in the Lufkin District are unique to the area. The glauconite is a calcareous material deposited in a reduced environment. Under the right conditions, glauconite can oxidize and weather to form iron ore gravel. Glauconite is very porous and has a physical potential to absorb water. Little [1990] describes the poor chemical and mechanical stability of glauconite and its high level of moisture sensitivity. Iron ore gravel has historically been widely used in the Lufkin District and in east Texas.

The most important findings from the DV (Figure 5.14) and strength (Figure 5.18) analysis of the Lufkin materials are:

1. Glauconite is characterized as a highly moisture susceptible and moisture sensitive material according to the DV criteria in Table 5.2. This is an accurate characterization based on Little [1990] and the Lufkin District's experience with this material [Button and Little 1997].
2. The iron ore gravel is characterized as a durable and good aggregate. This is documented by the performance history of iron ore gravel in east Texas.
3. Although the DV properties of glauconite are improved by hydrated lime at the 3.0% level, the additive rate of 3.0% cement provides a better reduction in DV. This is probably because the glauconite does not have a substantial reactive clay component with which the lime can react. Based on the results of the effectiveness of 1.5% hydrated lime with the Abilene and Amarillo aggregates, the 1.5% hydrated lime additive rate should be tried with glauconite. Perhaps the 3.0% hydrated lime additive rate provides excess fines over what is needed for reaction as discussed in the Abilene and Amarillo Districts. The effects of longer term curing (than 7 days) should also be evaluated for the hydrated lime additives.
4. 1.5% hydrated lime is effective in improving the DV properties of the iron ore gravel.
5. The addition of 3.0% hydrated lime was successful in improving the Texas Triaxial strength of the Welches pit glauconite and the iron ore gravel. The addition of hydrated lime improved the triaxial classification to grade 1 for the Welches pit

glaucanite and increased the triaxial strength of the iron ore gravel by approximately 100%. A 4% lime-fly ash (one-to-one) blend was successful in improving the triaxial strength of the Welches Ford Corner glauconite by approximately 100%. The lime-fly ash additive was more successful than either 3.0% hydrated lime, which was not effective with this aggregate, or 3.0% portland cements. Hydrated lime (3.0%), lime-fly ash (4.0%), and portland cement (3.0%) were all effective in increasing the triaxial strength of the iron ore gravel to that of a good quality grade 1 base. As previously mentioned with the Abilene and Amarillo materials, the effect of curing time was not considered. The rate of curing, time to ultimate strength gain, and ultimate strength and dielectric properties at full strength are important factors which should be considered in an extended study.

San Angelo District - In general, the limestone and caliche aggregates tested from within the San Angelo District have better DV properties than do the caliche aggregates in the Abilene or Amarillo Districts. As seen in Figure 5.15, the limestone aggregates collected from Loop 306 and north of East 24th street have DVs low enough to place them in the “good” category in terms of moisture and thermal sensitivity. The DVs of limestone material from stockpiles 1 and 2 have fair DVs, indicating acceptable resistance to moisture and thermal effects.

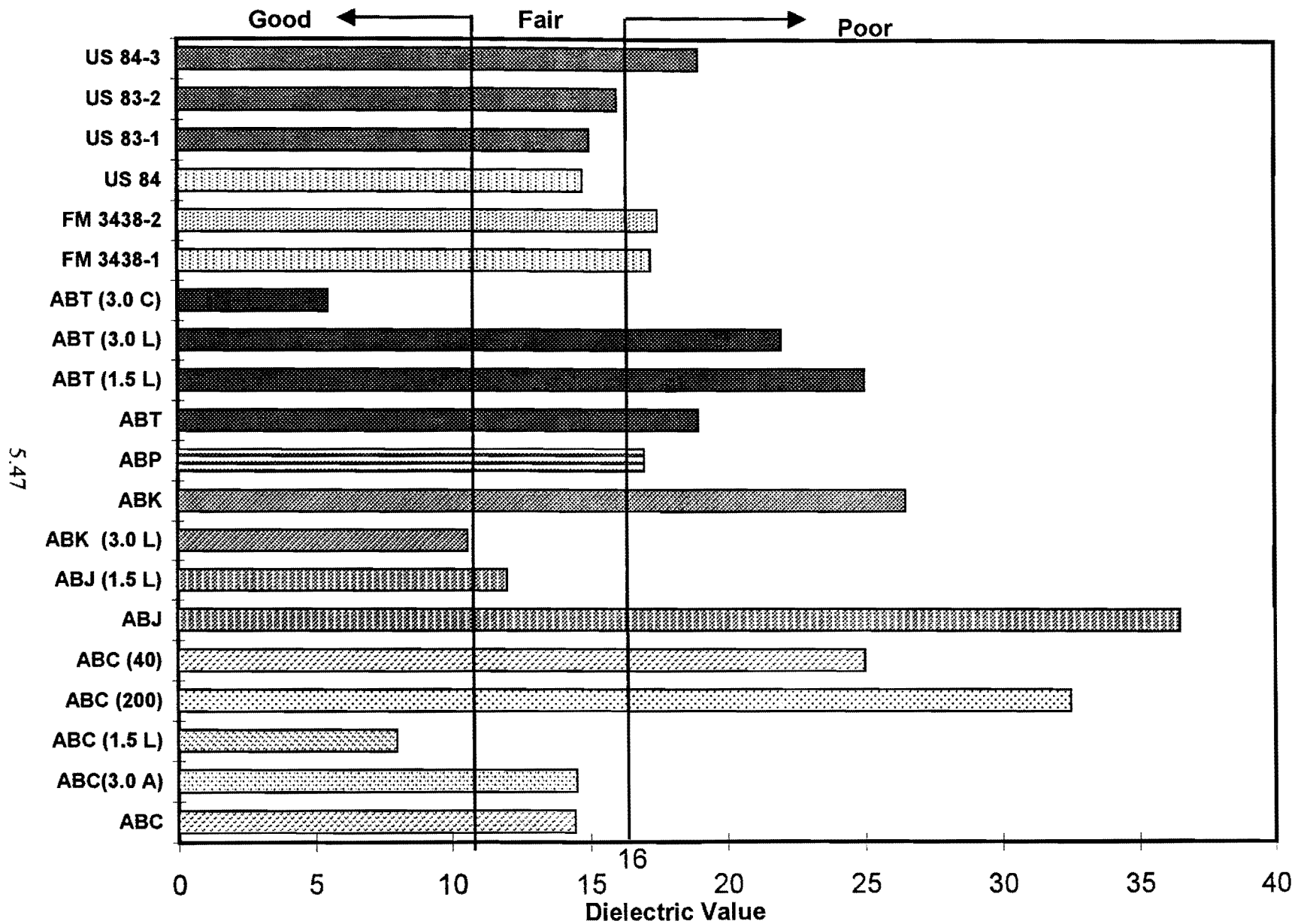


Figure 5.12. Plots of Average Dielectric Values for Source and Pavement Site Materials in the Abilene District

5.48

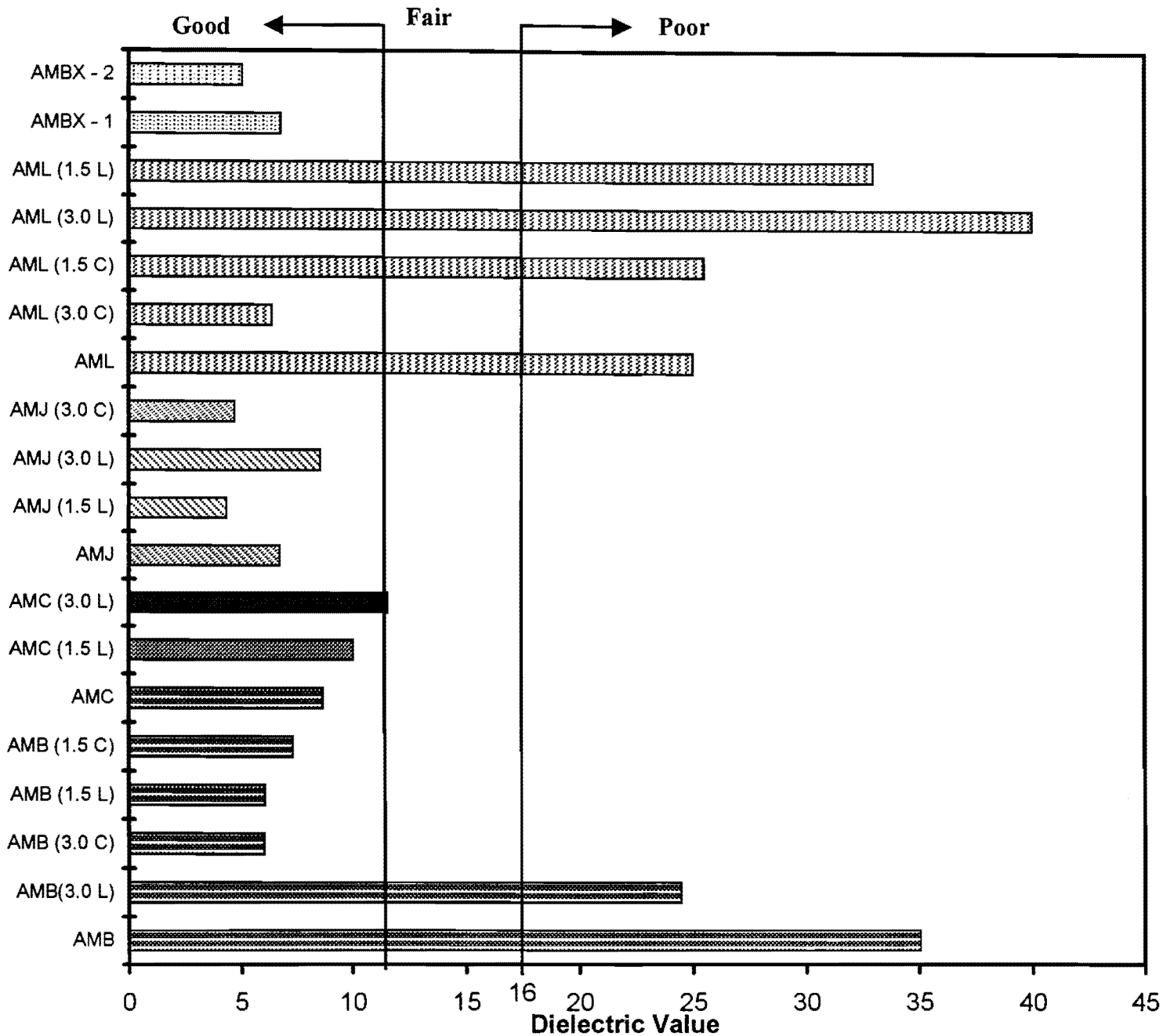


Figure 5.13. Plots of Average Dielectric Values for Source and Pavement Site Materials in the Amarillo District

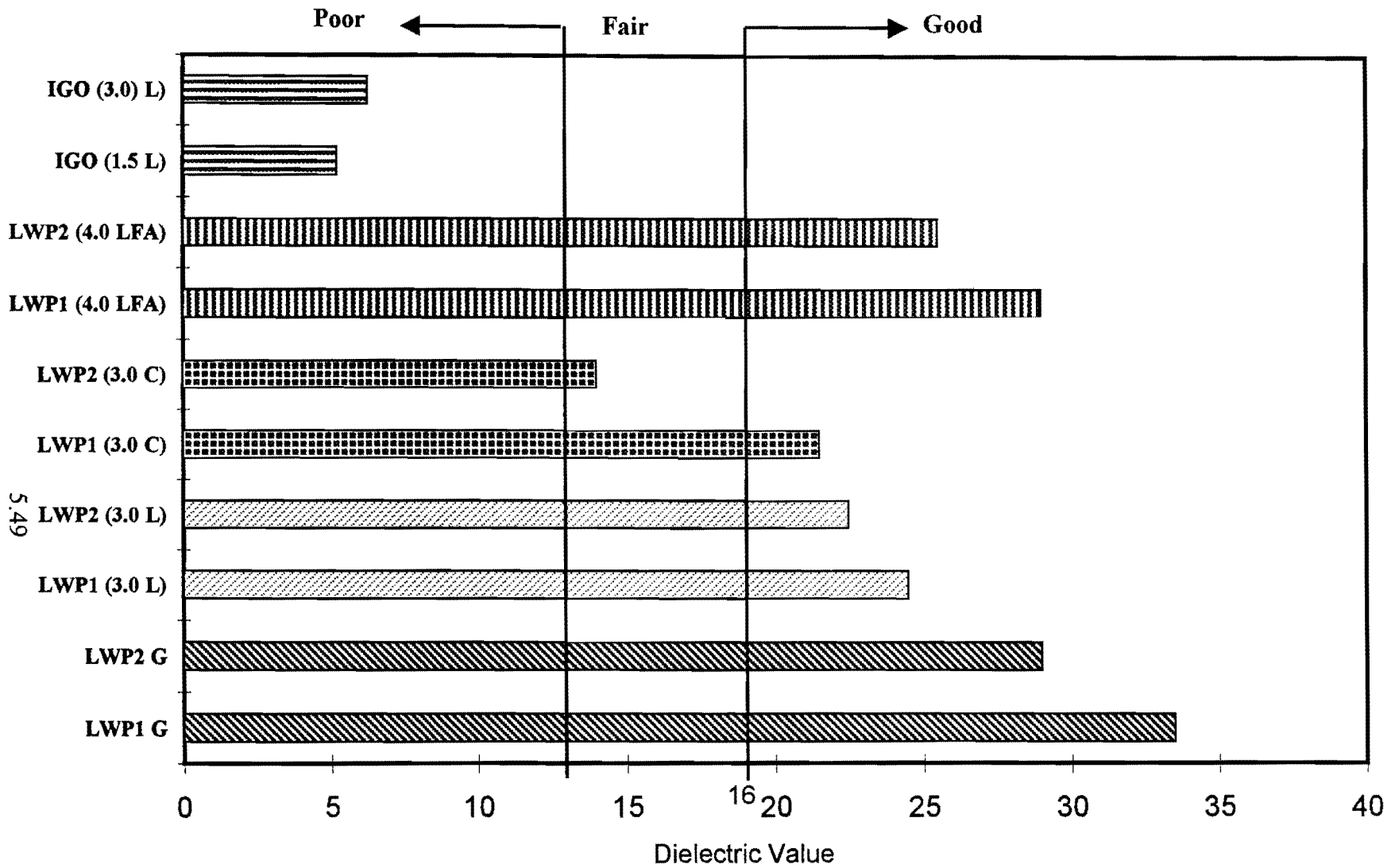


Figure 5.14. Plots of Average Dielectric Values for Source and Pavement Site Material in the Lufkin District

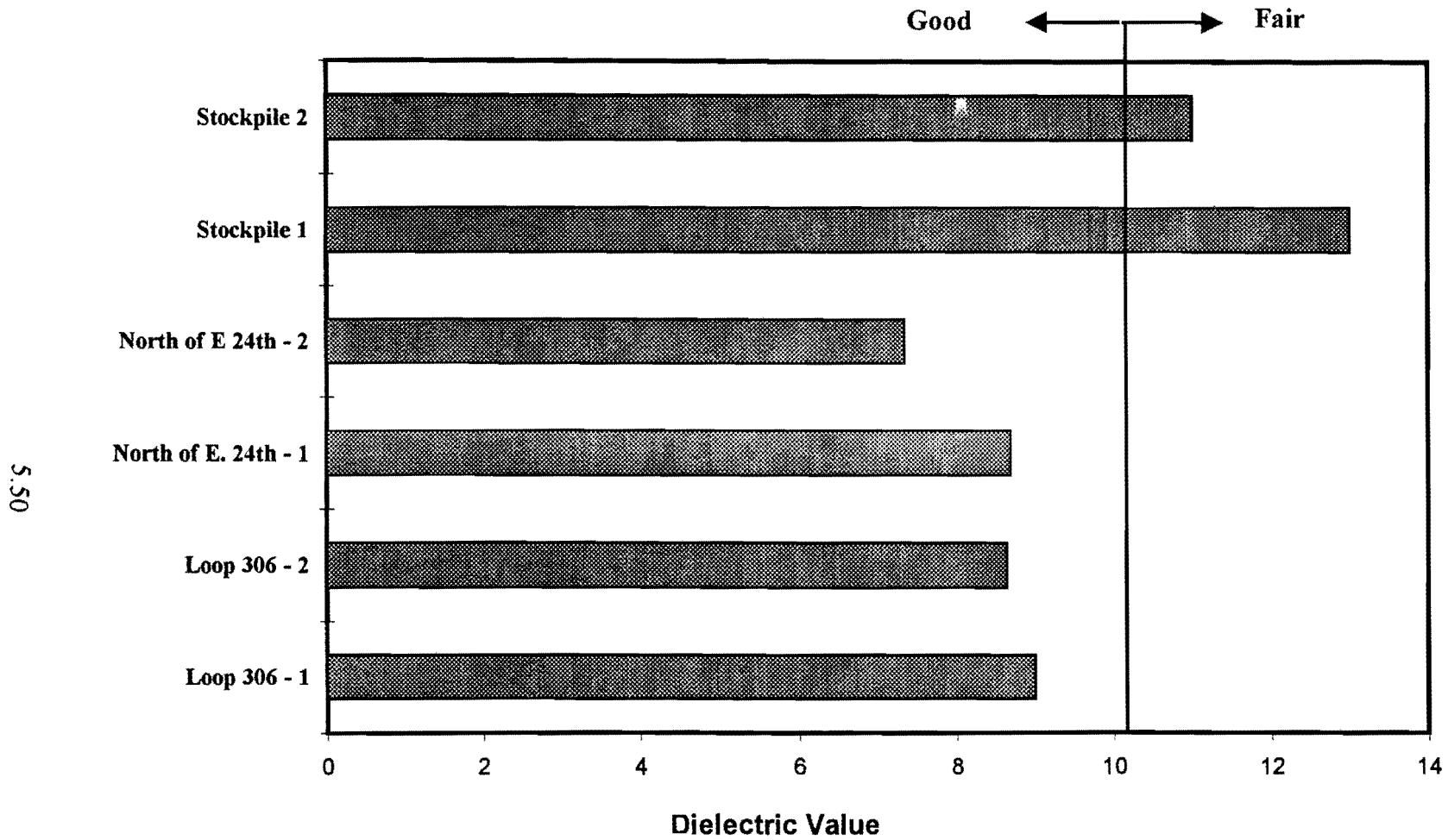


Figure 5.15. Plots of Average Dielectric Values for Source and Pavement Site Material in the San Angelo District

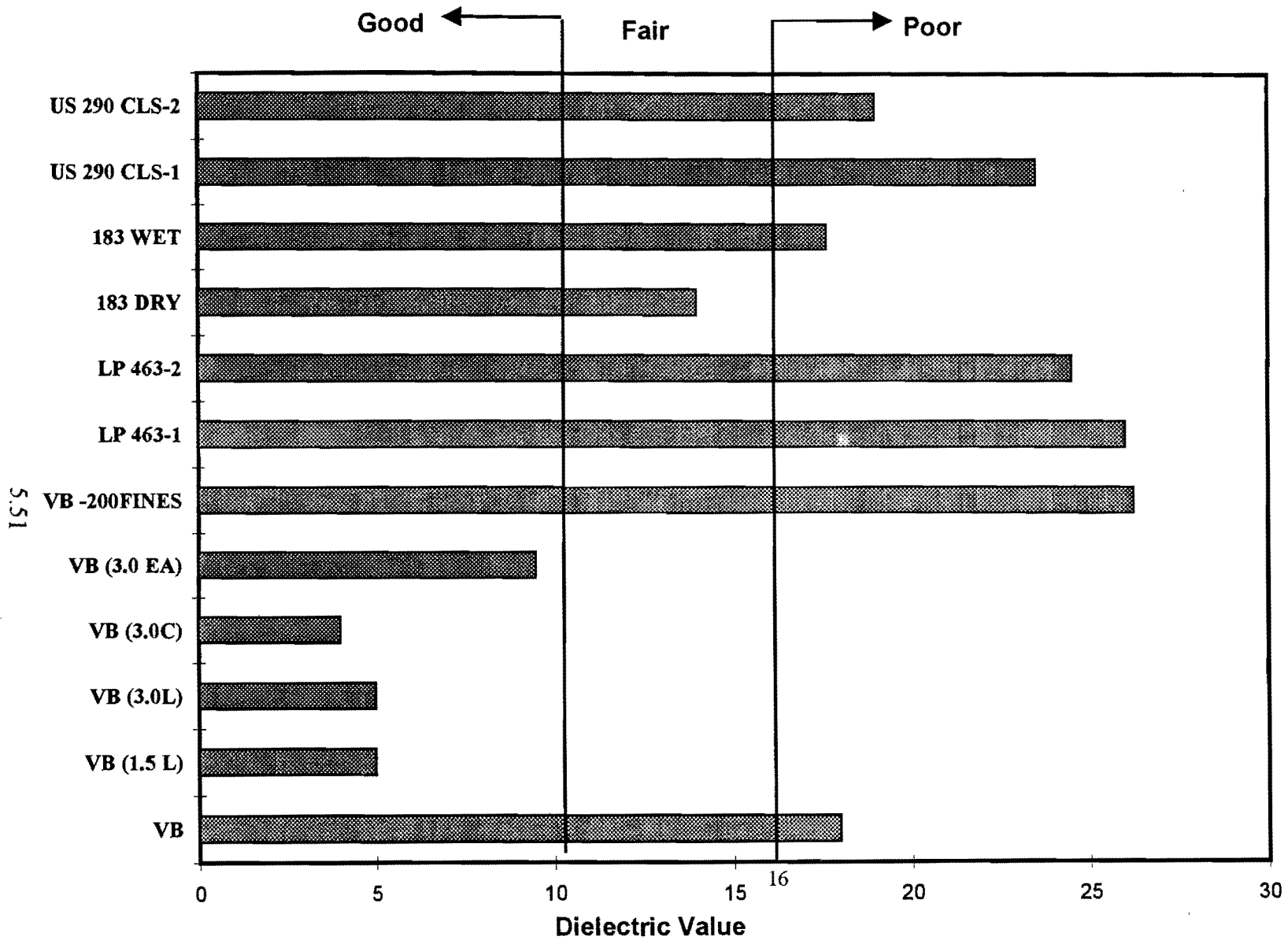


Figure 5.16. Plots of Average Dielectric Values for Source and Pavement Site Materials in the Yoakum District

5.52

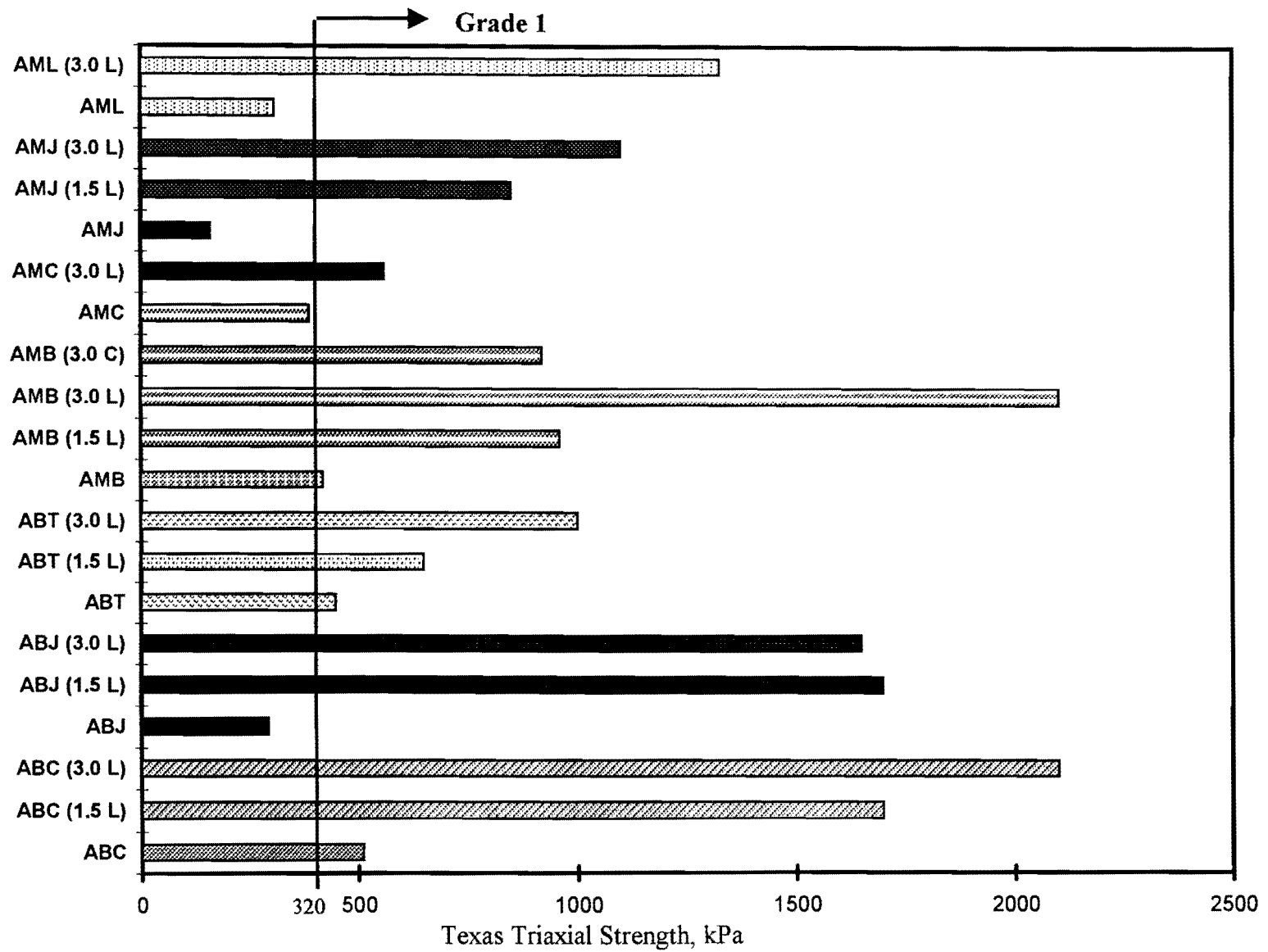


Figure 5.17. Plots of Average Texas Triaxial Strength Plots (7kPa confinement) for Materials from the Abilene and Amarillo Districts

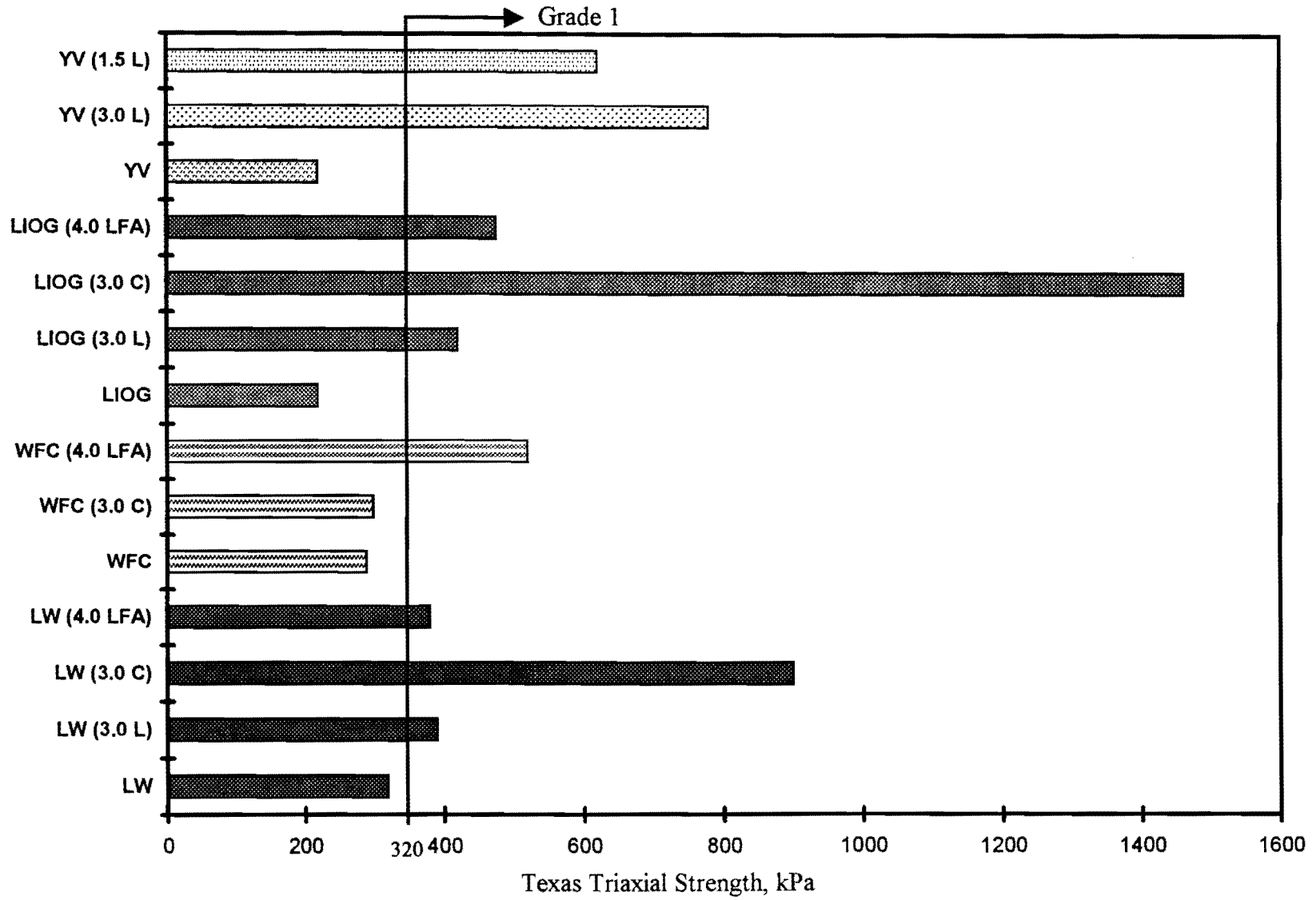


Figure 5.18. Plot of Average Texas Triaxial Strengths (7 kPa confinement) for Material from the Lufkin and Yoakum Districts

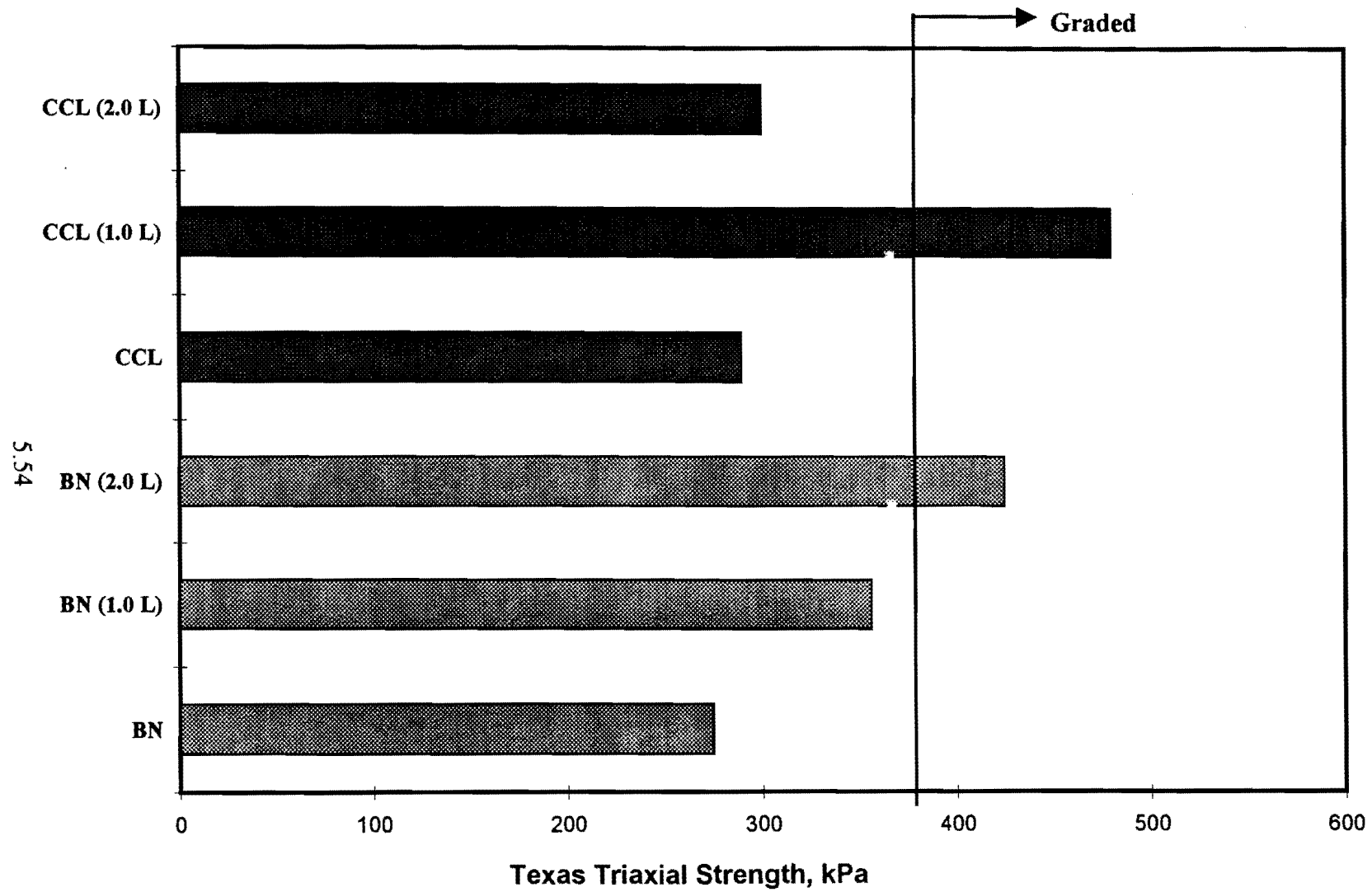


Figure 5.19. Plot of Average Texas Triaxial Strengths (7 kPa confinement) for Materials from the Bryan and Corpus Christi Districts

Yoakum District - The materials tested from the Yoakum District are summarized in Table 5.7. These materials represent a wide range of mineralogies and properties. As seen in Figure 5.19, the DVs of the Victoria base are above 16. This VB base (Figure 5.17) is a silicious river gravel with some clay fines. The Loop 463 material is similar with the exception that it is a blend of silicious river gravel aggregate and caliche fines. The caliche fines obviously have a deleterious effect on the moisture sensitivity of the river gravel aggregate.

The materials collected from US 183 and US 290 are limestone aggregates with fair to poor moisture sensitivity properties, as indicated by the dielectric values.

The VB aggregate is successfully treatable with hydrated lime (1.5%) or 3.0% portland cement. Emulsified asphalt (8%) is not effective in reducing moisture sensitivity. The significance of the addition of hydrated lime (1.5%) in improving the properties of the VB aggregate is verified by the Triaxial strength data summarized in Figure 5.18. The addition of 1.5% hydrated lime increased the Texas triaxial strength by almost 300%.

As has been seen from data from the various materials evaluated in this study, hydrated lime can have a significant and positive influence on improving strength and reducing moisture sensitivities when added at approximately 1.5% by weight. The effectiveness of hydrated lime is material dependent and certainly dependent on the curing conditions and pozzolanic reactivity with these fines fraction of the aggregate. Little et al. [1995] discuss the pozzolanic and carbonation reactions that are important in these aggregate systems. In that study, two calcareous aggregates with essentially no detectable clay content (by x-ray diffraction) were tested with 1.0% and 2.0% hydrated lime. Little et al. [1995] discuss that the strength and modulus improvements of these aggregates, when treated with hydrated lime, are primarily due to the formation of a calcium carbonate cement matrix. The Texas Triaxial strength data in Figure 5.19 illustrates this effect.

Curing Effects on Aggregates Stabilized with Hydrated Lime or Lime - Fly Ash

The authors have alluded several times in this section to the effects of curing on strength and moisture retention properties of aggregates stabilized with lime and lime-fly ash (LFA). Unlike portland cement which gains strength primarily through a cementitious reaction, lime and LFA mixtures rely primarily on a pozzolanic reaction between the lime and clay minerals within the soil

or aggregate and between pozzolans within the ash and lime. The pozzolanic reaction is much slower than the hydration reaction in portland cement. A recent study at TTI on lime and LFA curing rates on several western U. S. soils demonstrated that the ability of the lime and LFA stabilized soils to resist moisture effects continues to improve with time of curing. This also happens with portland cement stabilized soils and aggregates, but the time effects are more pronounced in pozzolanic reactions. In the long-term cure study of lime and LFA mixtures, the compressive strength and moisture absorption properties of soils and aggregates stabilized with various percentages of lime and LFA were evaluated. The study revealed that a substantial curing time (greater than 60 days at 25 °C) is usually required to realize substantial benefits from the stabilization process in terms of reduction of moisture sensitivity. As a specific example of the study, a clayey sand fine aggregate from southwestern Arizona was stabilized with 2% hydrated lime and 2% class C fly ash. Although short term (7 day, 40 °C) strength gains were substantial, the ability of the soil to absorb moisture in capillary soak testing did not show substantial improvement until the sample was allowed to cure for over 30 days at 25 °C. The absorption capacity decreased by more than 50% when the 7 day 40 °C cure and the 30 day 25 °C cure periods were compared. Based on this and similar evidence, the authors recommend a study of the extended curing effect of all chemical stabilizers: portland cement, hydrated lime, and lime-fly ash and cement-fly ash combinations.

Application to Material Selection and Pavement Design and Analysis and Implications to Rehabilitation and Recycling

This study focuses on identification of aggregate moisture and thermal sensitivity, particularly that which results in volume changes that cause cracking and strength loss. This study does not focus on mix design with various chemical stabilizers. Nevertheless, the trend is apparent that the DV screening test can be effectively utilized together with strength testing to: (1) assess the need to alter physicochemical properties of aggregates and (2) assess the effectiveness of chemical stabilizers. In this context, the DV test can be effectively used in the forensic analysis of existing aggregate bases and in assessing the role of chemical stabilizers — or other modification measures — in pavement rehabilitation.

The authors feel that the DV test and interim criteria, Table 5.2, should be included in the design protocol for recycled or rehabilitated aggregate bases. A viable scenario would be to include the DV measurement along with strength testing in the analysis of the existing base. Once the deficiencies (strength and moisture sensitivity) of the existing base are identified, the DV test can be used together with strength testing to identify: (1) the appropriate chemical stabilizer, (2) the appropriate amount of stabilizer, and (3) the appropriate level and amount of curing required to achieve the required result.

It is also appropriate to supplement the DV and strength testing with a measure of linear shrinkage potential of the selected aggregate-stabilizer or aggregate (without stabilizer) mixture. Tex-107-E can be adapted for this purpose when performed on the minus No. 40 sieve size fraction of the aggregate.

Selected Study to Determine Volumetric Changes During Freezing and Thawing Cycles

General Findings - The materials selected for this evaluation are presented in Table 5.9. Samples of these materials were compacted at different water contents. Both the heights and diameters of the samples were measured at different temperatures ranging from 20 to -15 °C. The compaction characteristics of these samples are shown in Figure 5.20. The masses of the samples were also measured after each dimension measurement. The volumes of these samples at different temperatures were calculated from the measured heights and diameters. Typical results of these measurements (e.g., for material from the Amarillo - Coon pit) are presented in Figures 5.21 through 5.23. There was no transfer of moisture into and out of the samples during the experiment, and any inadvertent loss of moisture to the atmosphere was quantified.

During the first cycle of freezing, the measured volume changes of most samples before freezing are within $\pm 0.5\%$, which can be considered to be the limits of experimental error of the test. Upon freezing, the volume changes follow the same trend demonstrated before freezing for samples compacted at relatively low degrees of saturation. For samples compacted at relatively high degrees of saturation, volumes increased by amounts up to approximately 4%. Most expansions occur in the temperature range of 0 to -5 °C. Samples that expanded more than 0.5% during freezing are denoted by an outlined symbol in Figure 5.20. The two samples of Yoakum District-Victoria lime-

treated gravel compacted at water contents of 12.4% and 13.0% were not used in the volume change study. One of the two samples was used as a dummy sample for temperature measurement, and the other was accidentally destroyed before reaching freezing temperature. The limiting degree of saturation is soil specific and ranges from approximately 55% to 85%. As some of the aggregates studied do not have well-defined optimum water contents, as shown in Figure 5.20; the significance of compaction water content relative to the optimum water content cannot be fully evaluated.

After the samples thawed, the volumes of all samples compacted at a low degree of saturation, except Box Canyon, rebounded practically to the original volumes or decreased slightly in volume before freezing. For samples compacted at a high degree of saturation, the volumes of the samples decreased. A similar phenomenon was reported by Carpenter and Lytton [1975]. The volumes of all Box Canyon samples increased after the first freeze-thaw cycle.

During the second cycle of freezing, the volume change trends are very similar to those of the first cycle. However, the percent volume change can increase or decrease in comparison to that of the first cycle of freezing. It is evident that the samples were “loosened” by the first cycle of freezing when there are significant volume changes.

These samples were not allowed access to free water during freezing and thawing. Therefore, the behavior observed is at the compaction water content. As discussed earlier, the volume change behavior of compacted aggregates depends primarily on two mechanisms: (1) volume reduction due to a increase in soil suction and (2) expansion due to transformation of water into ice. Thermal expansion or contraction of the aggregates is negligible. As discussed earlier, suction is primarily a function of water content. The higher the water content is, the lower is the suction. When the water transforms into ice, it increases the suction of the unfrozen water in the soil. However, the ice formed prevents excessive shrinkage of the compacted aggregate. Moreover, the higher the water content is, the higher is the frozen water content. When more ice exists in the soil, volumetric expansion is greater. When the degree of saturation approaches unity, there are no air voids in the compacted aggregate to accommodate the increase of volume resulting from freezing of pore water. Therefore, the increase in volume is significant. On the other hand, a low water content induces a high suction in the compacted aggregate before freezing. An increase in suction during freezing may cause a reduction in volume. However, as the suction is already high, a further

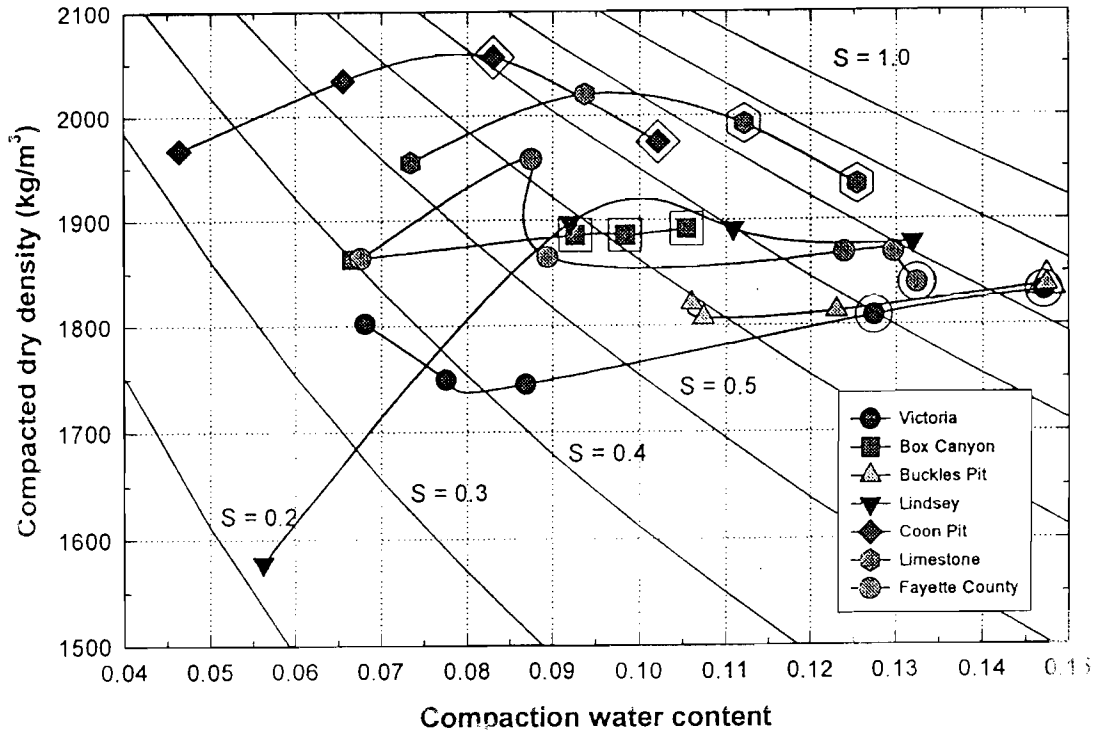


Figure 5.20. Compaction Moisture-Density Relationships for Selected Aggregates Used in the Freeze-Thaw Volume Change Analysis

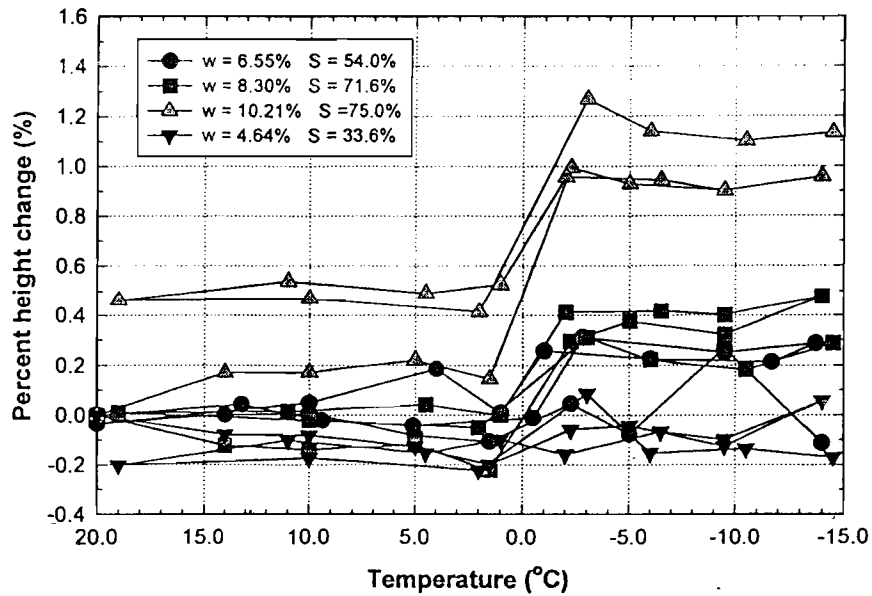


Figure 5.21. Percent Height Change of Coon Pit Aggregate versus Temperature

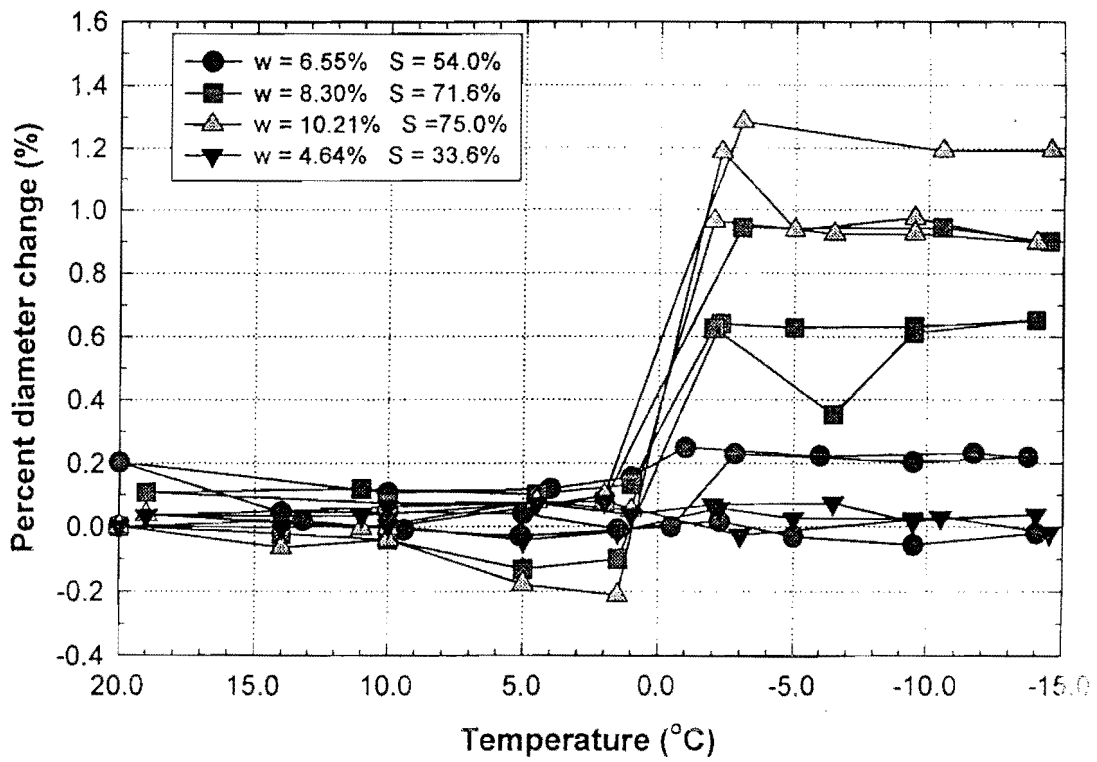


Figure 5.22. Percent Diameter Change of Coon Pit Aggregate versus Temperature

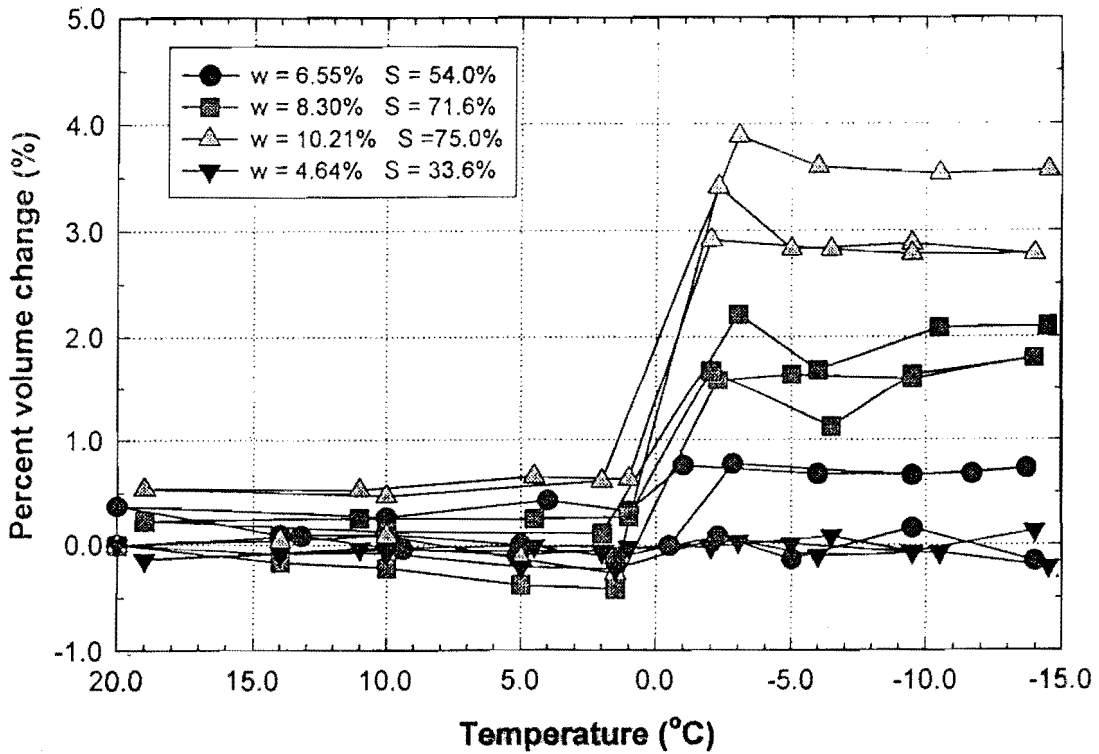


Figure 5.23. Percent Volume Change of Coon Aggregate versus Temperature

increase in suction may not cause too much shrinkage. A low water content also decreases the potential for expansion resulting from the formation of ice. When the degree of saturation is low, there are many air voids in the soil to accommodate the volume increase resulting from the freezing of a small amount of pore water. Therefore, a small reduction in volume results. The two mechanisms are thus competing with each other at all water contents; i.e., the compacted aggregates expand when they are frozen if the degree of saturation is high and vice versa.

A careful study of the suction-moisture content relationships and the volume change characteristics of the samples during freezing reveals that there is no significant expansion during freezing if the water content of the sample is lower than the water content corresponding to a soil suction of pF 4. Therefore, the suction-moisture content relationship can be used to determine the threshold water content for volume expansion during freezing. It should be noted that these relationships were determined during drying. Moreover, this moisture content should be the equilibrium moisture content of the compacted aggregate, which may not necessarily be the compaction water content if moisture exchange with the environment is allowed after compaction. If no moisture is allowed to migrate into the compacted aggregate, then the aggregate should be compacted dry of this threshold water content to prevent detrimental volumetric expansion during freezing.

It should also be noted that the samples used in this study were allowed to expand three-dimensionally. However, compacted aggregates in a base course can only rise in the vertical direction if they expand. The lateral confinement may reduce the total volume change. However, the vertical movement may still be detrimental to the pavement. For samples of water contents lower than the threshold water contents, the amount of thermal shrinkage is not very significant. Therefore, low temperature thermal cracking induced by shrinkage is probably not very influential [Carpenter et al. 1974, Carpenter and Lytton 1975].

Application to Material Selection and Pavement Design and Analysis

Use of pF v Moisture Content - The relationships between soil suction and water content during drying were determined for seven aggregates (Table 5.10). The soil suction increases with a decrease in water content. Results from previous studies have proposed different relationships

between water content and soil suction. In this study, it is interesting to note that the relationships between the logarithm of suction and water content are approximately linear for practical purposes. The linear relationship measured is not surprising as it has been found that volume change of soil is a linear function of water content or logarithm of suction [Lytton 1994]. Linear regression of the experimental data yields the relationships tabulated in Table 5.11.

Table 5.11. Relationship between Suction and Water Content

Aggregate	Relationship
Victoria (YV)	$y = 5.282 - 0.0877 x$
Box Canyon (AMBX)	$y = 4.962 - 0.1137 x$
Buckles Pit (AMB)	$y = 4.950 - 0.0649 x$
Lindsey (AML)	$y = 5.176 - 0.0772 x$
Coon Pit (AMC)	$y = 4.932 - 0.0841 x$
Crushed limestone (Y290(LS))	$y = 5.006 - 0.0988 x$
Fayette County river gravel (YFG)	$y = 5.336 - 0.142 x$
All seven aggregates	$y = 5.0 - 0.08 x$
Note: y = measured soil suction (pF); and x = water content (%).	

As the samples used in these soil suction measurements were compacted at the optimum water content, the results indicate that the soil suction of a compacted aggregate can change dramatically after it has been compacted if transfer of moisture into and out of the aggregate is allowed. Compaction water content is a significant factor affecting the structure of the compacted aggregate which may affect the pore size. Results from Carpenter and Lytton [1975] also indicate suction increases with decrease in compaction water content. The effect is more prominent in samples compacted dry of optimum than those compacted wet of optimum. However, the increase in suction may be caused by a decrease in water content, a change in soil structure, or both. The answer is probably both, but which is the dominant mechanism causing the increase in suction of compacted aggregates has yet to be fully investigated. The pore size of aggregate compacted dry

of optimum is considerably larger than that compacted wet of optimum. However, when the water content of a compacted aggregate is low, water also exists in small pores. Thus, it is postulated that the dominant factor for soil suction is the water content of the compacted aggregate. The postulation is also supported by experimental data presented by Ho et al. [1992], and Marinho and Chandler [1993]. Experimental data on compacted London clay/fine sand mixtures by Marinho and Chandler [1993] indicate that the relationships between water content and the logarithm of suction are linear and unique. Moreover, they are independent of compaction water content. Similar conclusions have also been reached by Ho et al. [1992].

As the relationships between soil suction and moisture content are approximately linear, it is very easy to use the moisture equilibrium model developed at the University of Illinois [Dempsey et al. 1986] to determine the moisture content in a compacted aggregate. This is particularly useful in cohesive soils as well as granular materials with a high percentage of fines as their strength and modulus are very sensitive to even a small change in moisture content, say $\pm 1\%$. The model assumes that the subgrade or base cannot receive moisture by infiltration through the pavement. Any precipitation will drain quickly through the drainage layer to the side ditch or longitudinal drain. Therefore, the only water in the subgrade is the capillary water fed by the water table. The model has been indicated to be a reasonable and practical choice for design purposes.

When there is no loading or overburden pressure, suction equals the negative pore water pressure. When a load or overburden pressure is applied to an unsaturated soil with a given moisture content or suction, the suction or moisture content remains the same, but the pore pressure becomes less negative. The relationship between soil suction and pore water pressure can be expressed as

$$u = S + \alpha p \quad [5.7]$$

where u = pore water pressure when the soil is loaded (kPa); S = soil suction (kPa) which is a negative pressure; p = applied pressure or overburden (kPa); and α = compressibility factor. The compressibility factor α varies between 0 for unsaturated cohesion less soils and 1 for saturated soils. For unsaturated cohesive soils, α is related to the plasticity index by [Black and Cronney 1957]

$$\alpha = 0.03 \times PI \quad [5.8]$$

where PI = plasticity index (%). The pore pressure in a soil depends solely on its distance above the groundwater table,

$$u = -z\gamma_w \quad [5.9]$$

where z = distance above the groundwater table (m); and γ_w = unit weight of water (kN/m^3). This simple fact can be explained by considering the soil as a bundle of capillaries with varying radii. Water will rise in these capillaries to various heights depending on the radius of the capillary. At the distance z above the groundwater table, a large number of menisci will form at the air-water interfaces, thus resulting in a tension at that elevation corresponding to the height of capillary rise. Combining Equations 5.8 and 5.9 yields

$$S = -z\gamma_w - \alpha p \quad [5.10]$$

The procedures for determining the equilibrium moisture content at any point in a pavement system can be summarized as follows:

1. Determine the distance z from the point to the water table.
2. Determine the loading or overburden pressure p .
3. Determine the Atterberg limits of the soil.
4. Determine the compressibility factor α by Equation 5.8.
5. Determine the suction at the point S by Equation 5.10.
6. Determine the moisture content from the suction-moisture relationship in Table 5.10.

This simple algorithm fits nicely in a layered pavement design or analysis scheme. By knowing the simple linear moisture - suction relationship of the aggregate base, the moisture content within the base is determined. The resilient modulus and deformation properties of the aggregate base are strongly related to the stress state (Equation 5.1) and moisture content of the base. In fact, accounting for the state but discounting the moisture effects on the flexible base is folly as these effects are so profound.

Approach to the Evaluation of Thermal Volume Change Potential - The development of the relationship between moisture content and soil suction (pF) can be effectively used to help avoid large freeze-induced expansion. If this initial freeze expansion can be held in check, then cyclic

damage can also be mitigated or eliminated. As previously discussed, the threshold moisture content of aggregate bases is the moisture content that corresponds to a pF of 4.0. When the soil or aggregate moisture reaches or exceeds the threshold moisture (ω_T), the aggregate is subject to considerable expansion upon freezing (see Figure 5.20). On the other hand, at moisture contents below the threshold value, thermally induced volume change is considerably less than 1%. Although these lower strains can and do cause cracking and degradation of the aggregate base after many cycles, they are not nearly as destructive as the approximately 4% strain that can occur upon freezing of an aggregate base at above 70% saturation. Furthermore, the effect of cyclic damage is dependent on the initial expansion volume change. Therefore, the control of this initial level of expansion is important.

The most straightforward way to determine ω_T is to develop the pF versus moisture content relationship. Figures 5.24 through 5.30 provide such relationships for several aggregates analyzed in this study. A master curve of these data for the seven aggregate systems studied is presented in Figure 5.31. However, if suction measuring equipment is not available, a relationship can be developed from the maximum moisture content obtained in the capillary rise tube test. In the development of this relationship, a master plot (for all seven aggregates) of pF versus moisture content normalized for suction capacity was used, Figure 5.32. In this plot, suction capacity is simply the slope of the pF versus moisture content relationship for each aggregate type. In Figure 5.32, it can be seen that the pF value of 4.0 occurs at a water content to suction capacity ratio of approximately 1.1. Figure 5.33 presents the relationship between suction capacity and maximum water content for the seven aggregates. The maximum water content is simply the equilibrium water content for each aggregate as illustrated in Figures 5.34 through 5.40. By entering Figure 5.33 with the maximum water content after long-term capillary soak, the suction capacity can be determined. The ω_T value is quickly calculated as $1.1 \times$ the suction capacity.

Since it is important to keep not only compaction moisture but also equilibrium moisture below ω_T , one must evaluate the range of equilibrium moisture within the aggregate base to determine whether the upper limit of the seasonal moisture variation, ω_U , will exceed ω_T .

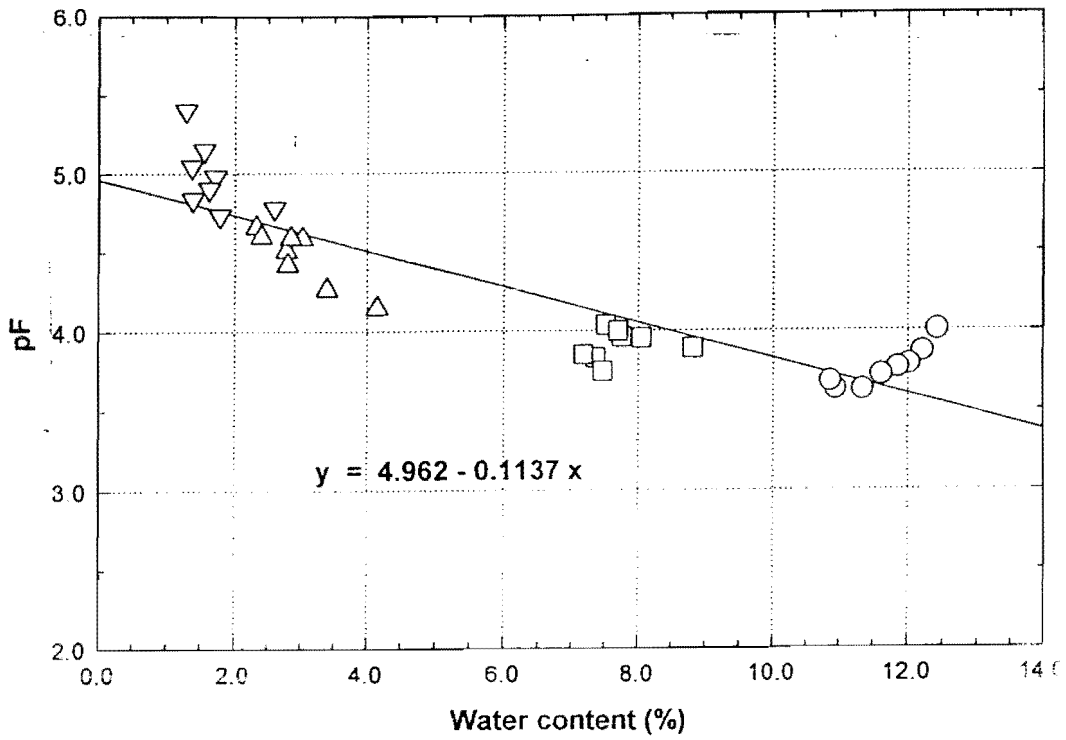


Figure 5.24. Suction versus Water Content of Box Canyon Aggregates

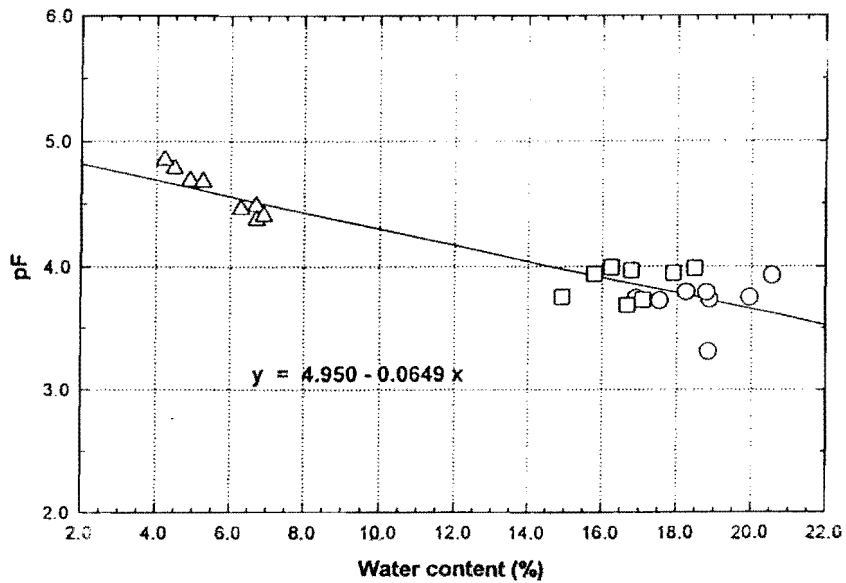


Figure 5.25. Suction versus Water Content of Buckles Pit Aggregates

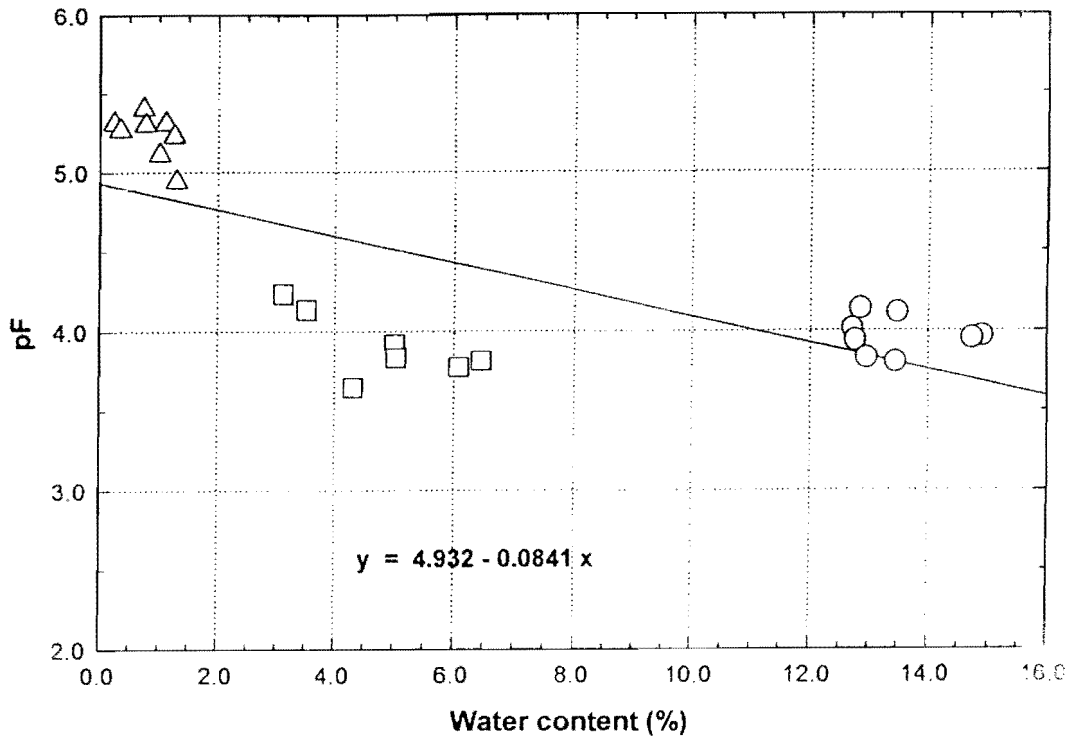


Figure 5.26. Suction versus Water Content of Coon Pit Aggregates

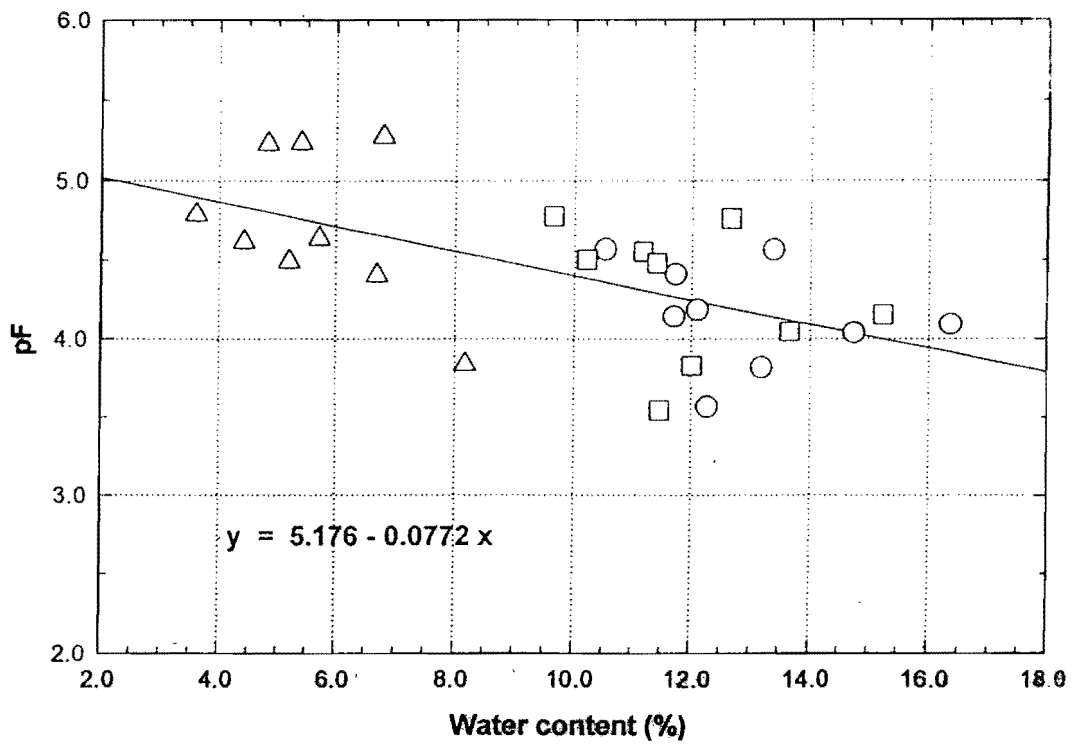


Figure 5.27. Suction versus Water Content of Lindsey Aggregates

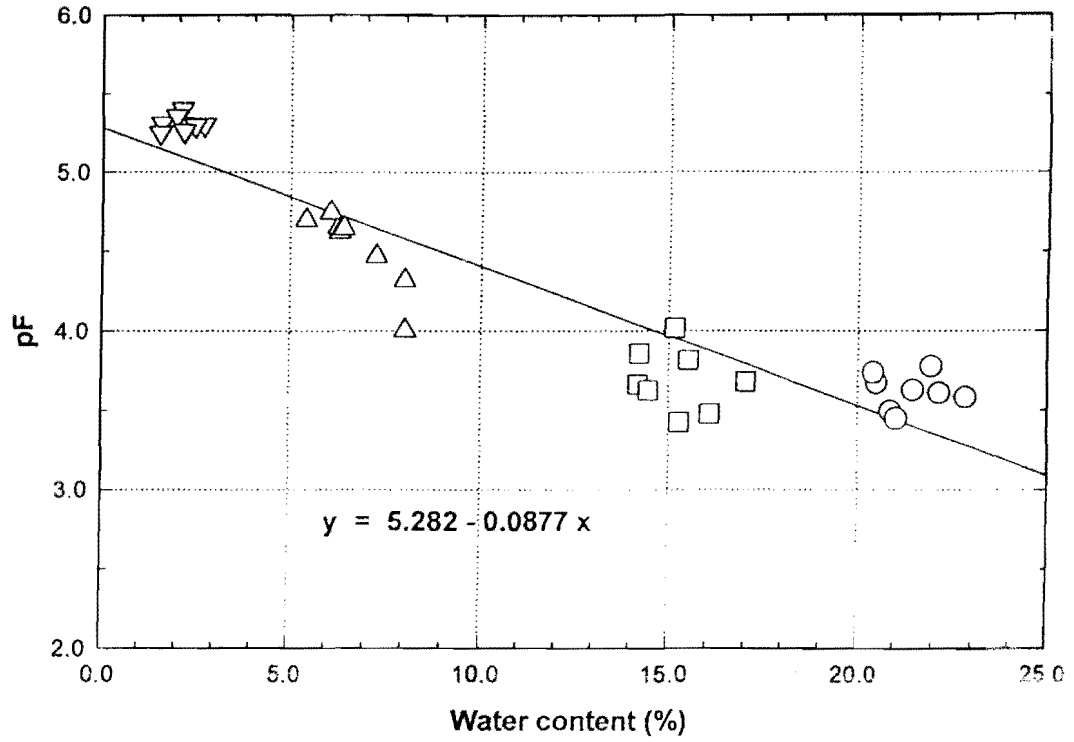


Figure 5.28. Suction versus Water Content of Victoria Aggregates

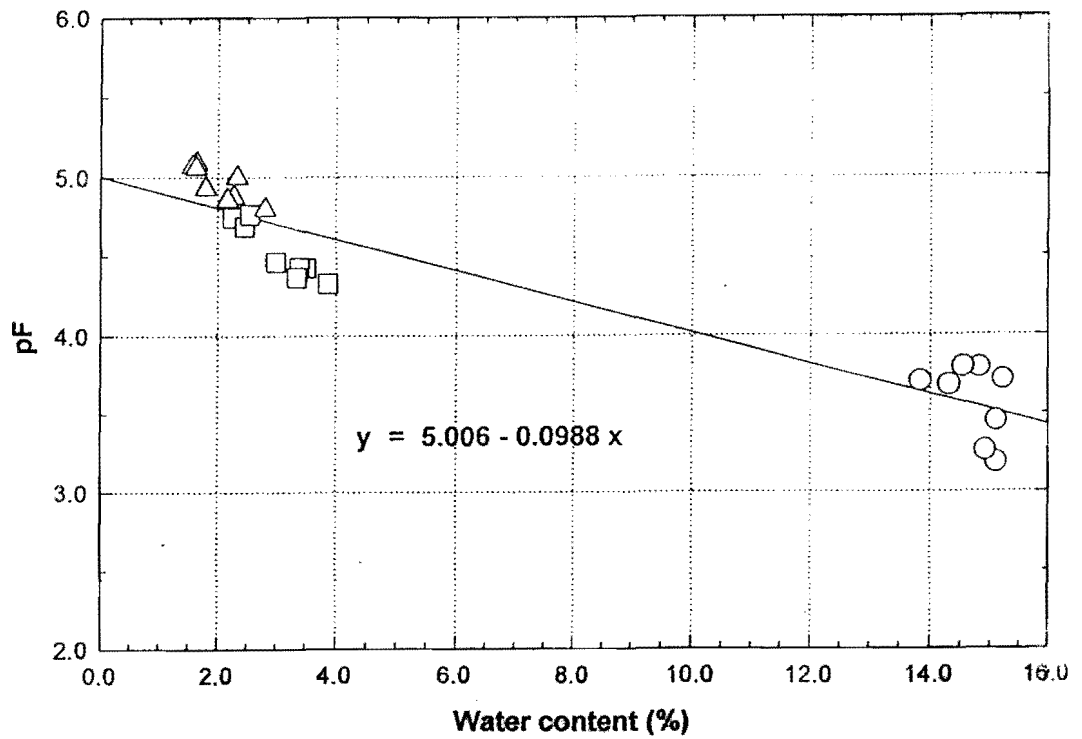


Figure 5.29. Suction versus Water Content of Yoakum Crushed Limestone

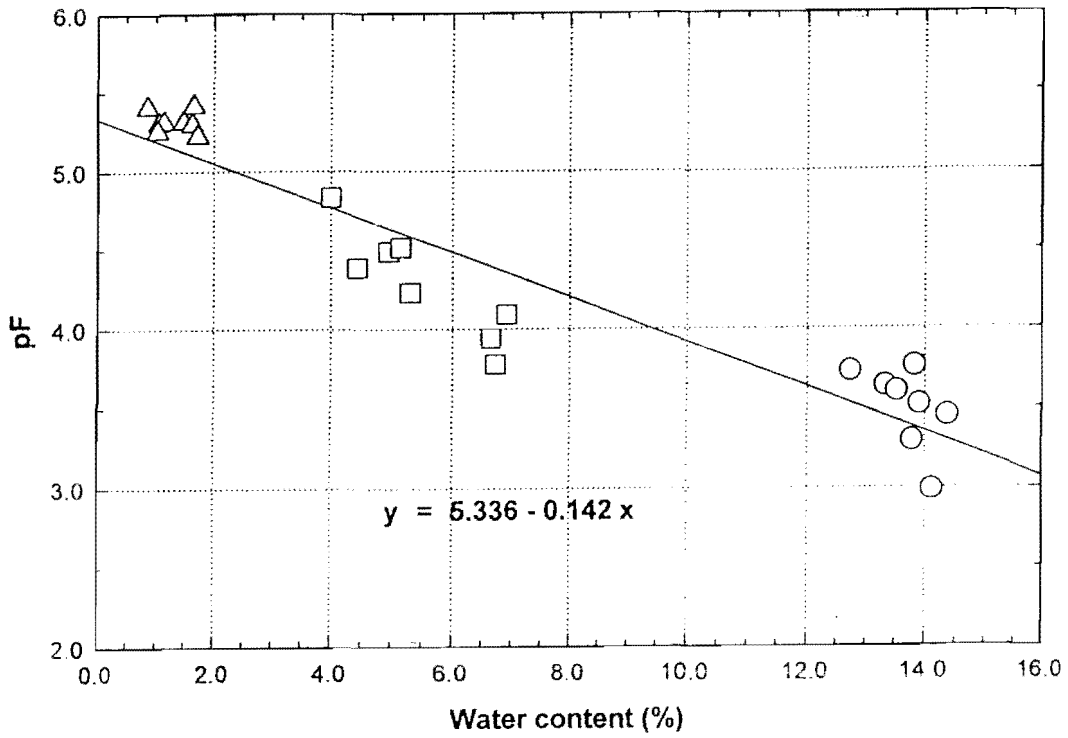


Figure 5.30. Suction versus Water Content of Lime Treated Fayette County Gravel

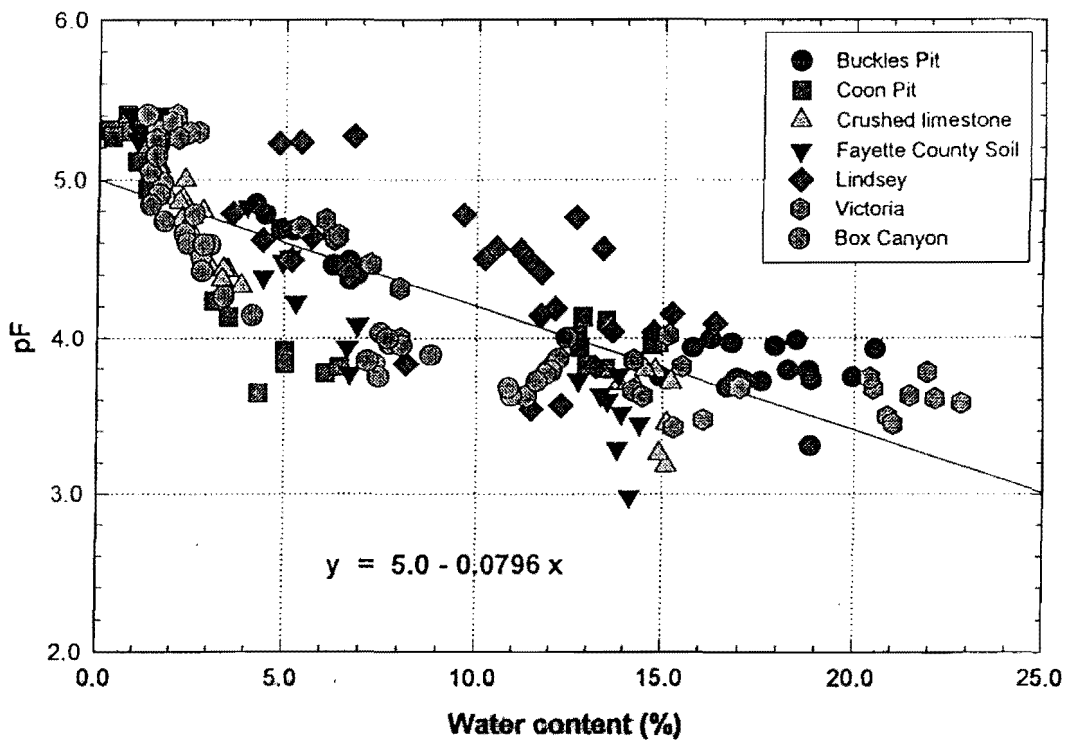


Figure 5.31. Master Curve of Suction versus Water Content for All Seven Aggregates

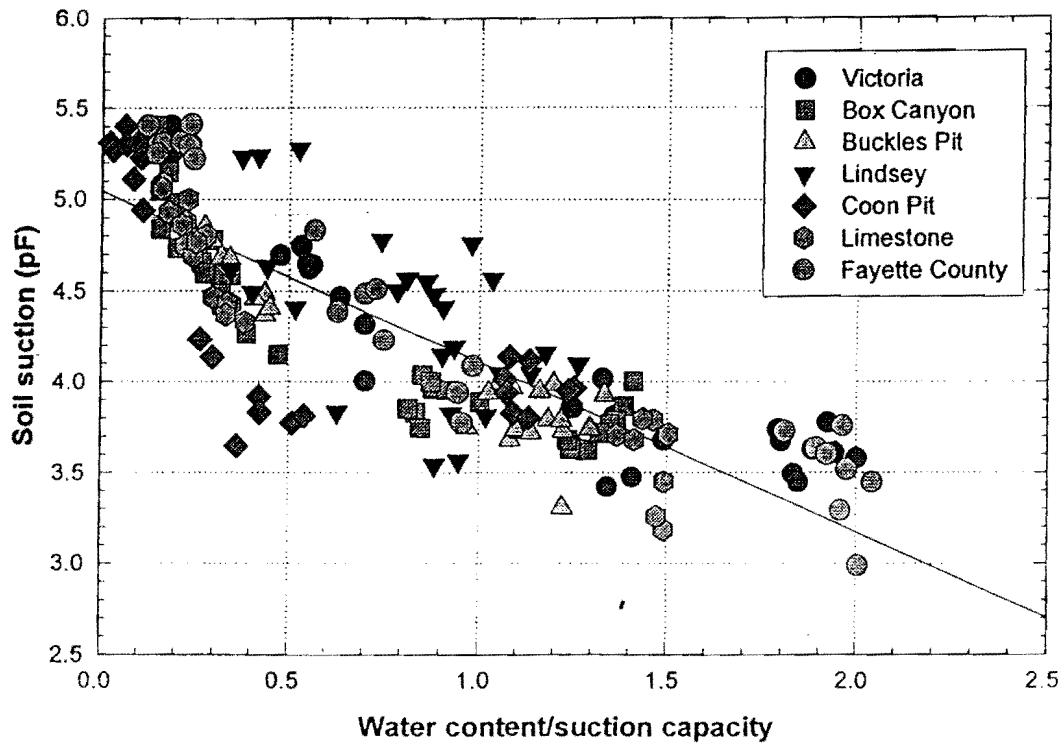


Figure 5.32. Master Curve of Soil Suction versus Water Content Normalized

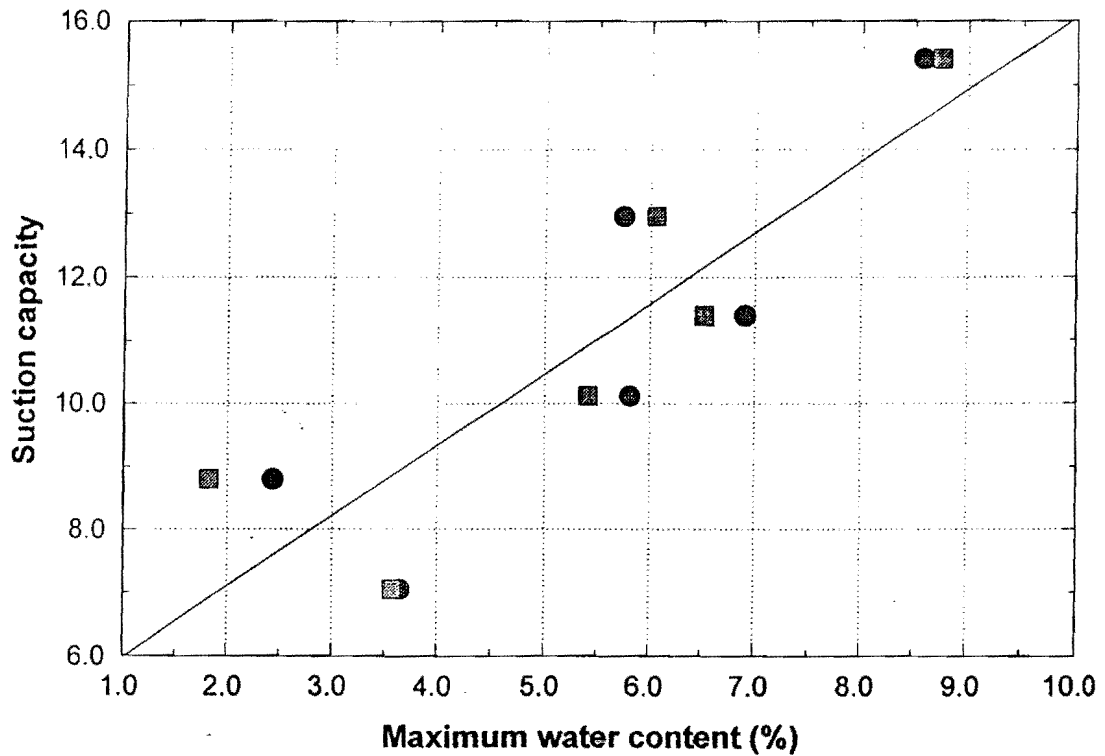


Figure 5.33. Variation of Suction Capacity with Maximum Water Content

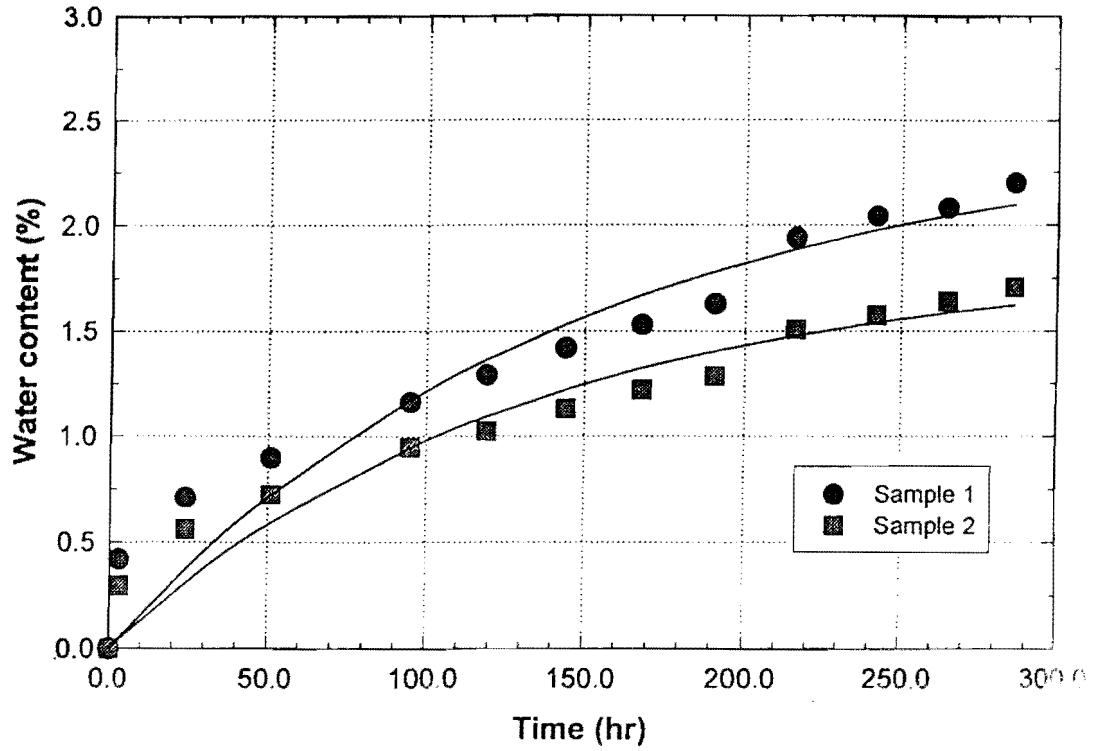


Figure 5.34. Variation of Water Content with Time during Suction Test for Box Canyon Aggregate

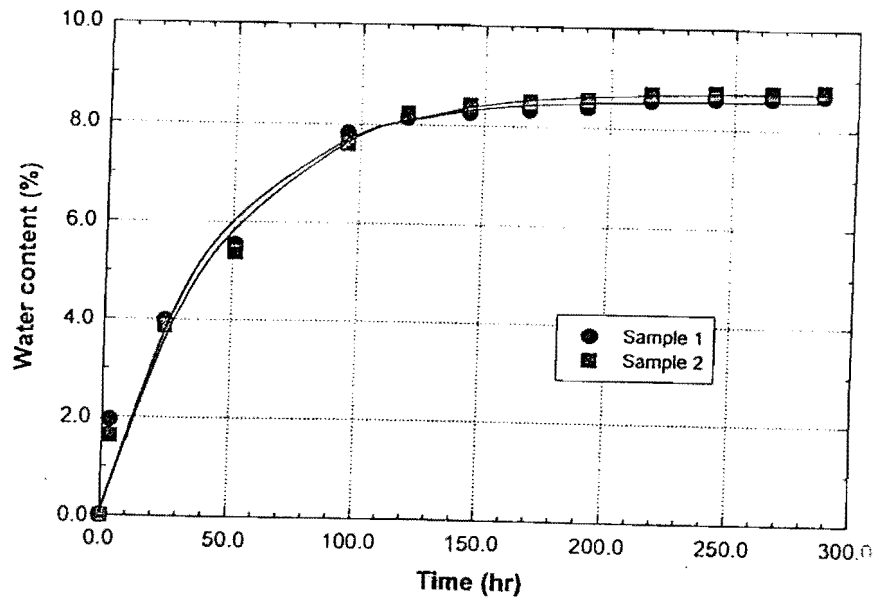


Figure 5.35. Variation of Water Content with Time during Suction Test for Buckles Pit Aggregate

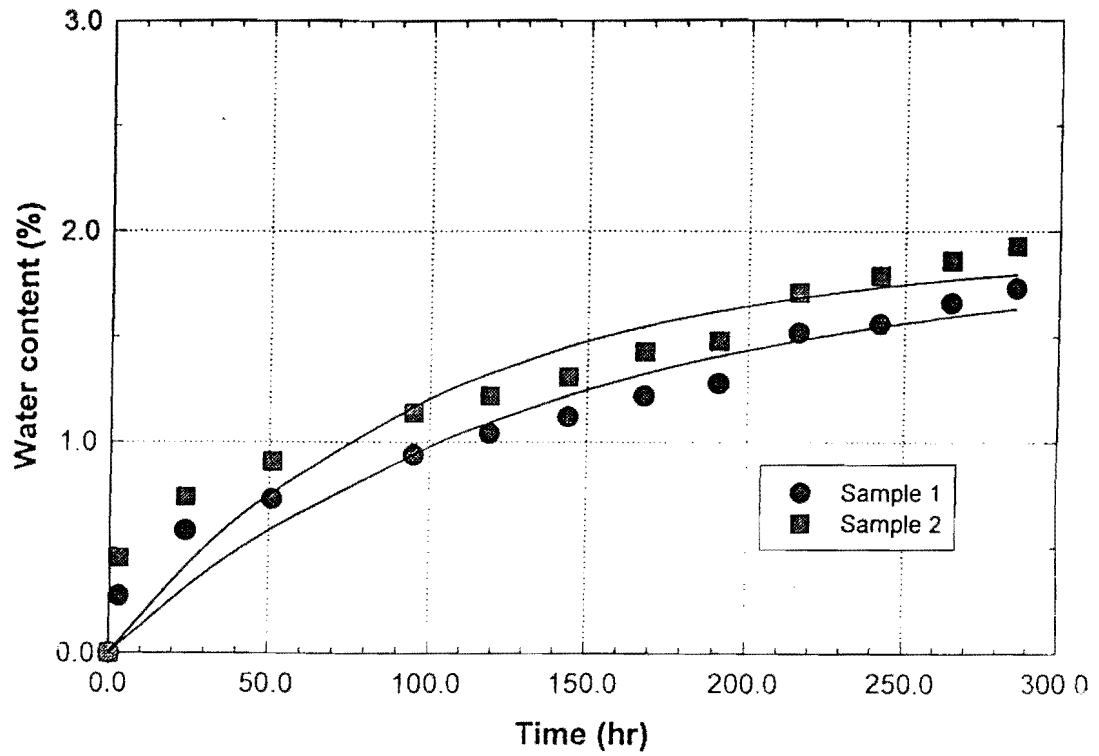


Figure 5.36. Variation of Water Content with Time during Suction Test for Coon Pit Aggregate

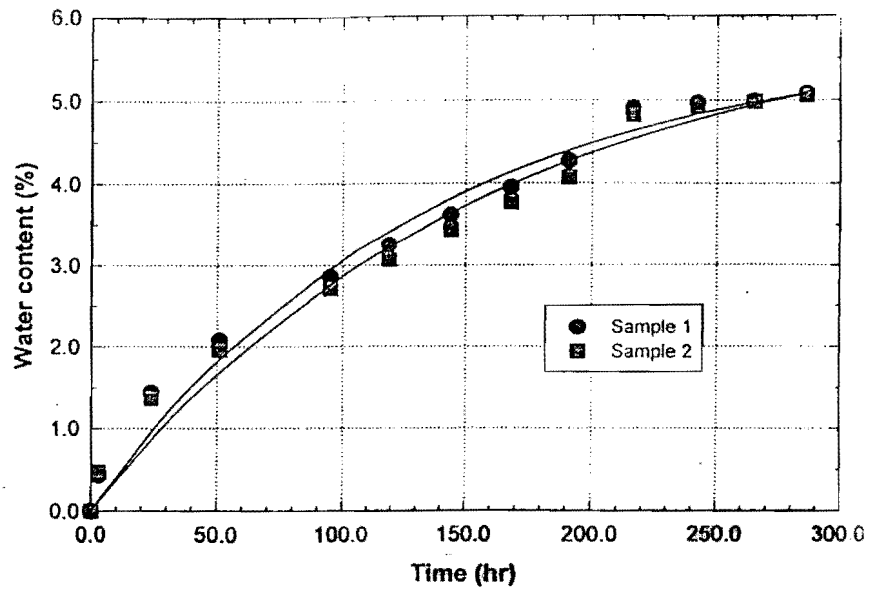


Figure 5.37. Variation of Water Content with Time during Suction Test for Lindsey Aggregate

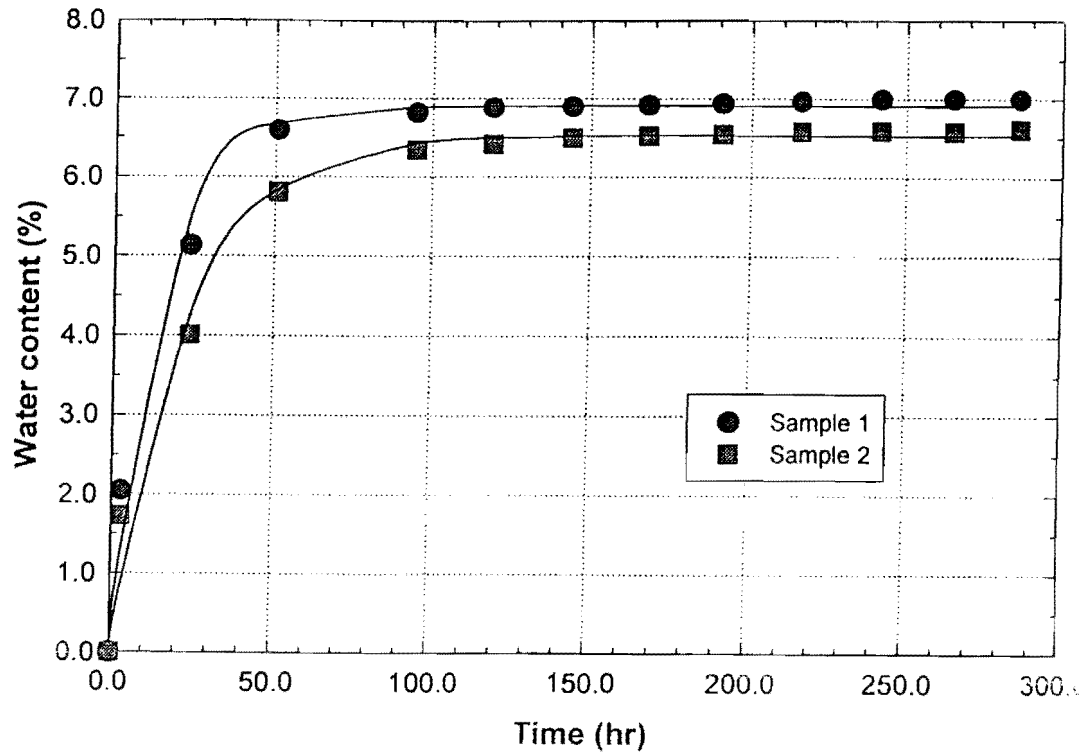


Figure 5.38. Variation of Water Content with Time during Suction Test for Victoria Aggregate

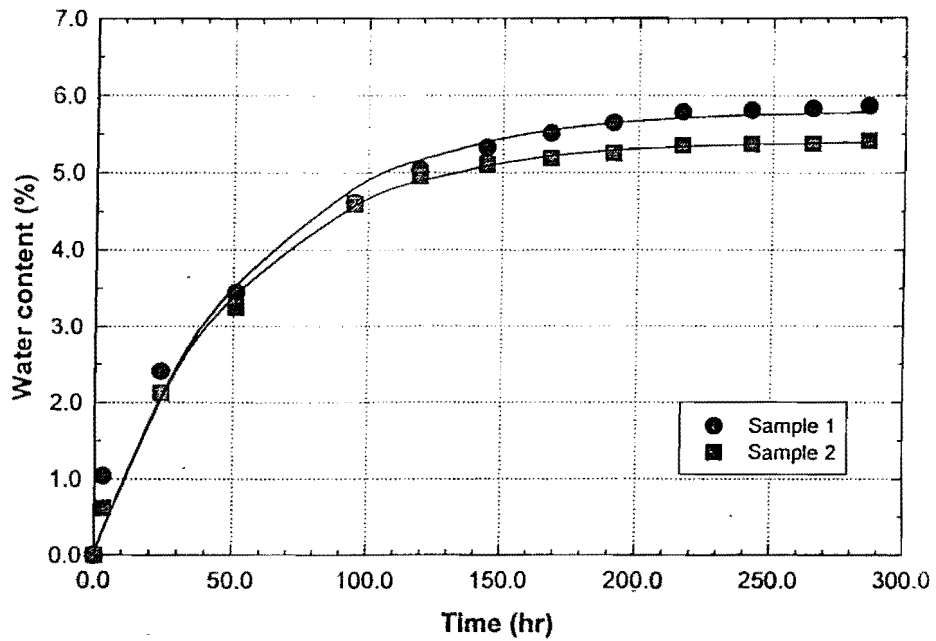


Figure 5.39. Variation of Water Content with Time during Suction Test for Yoakum Limestone

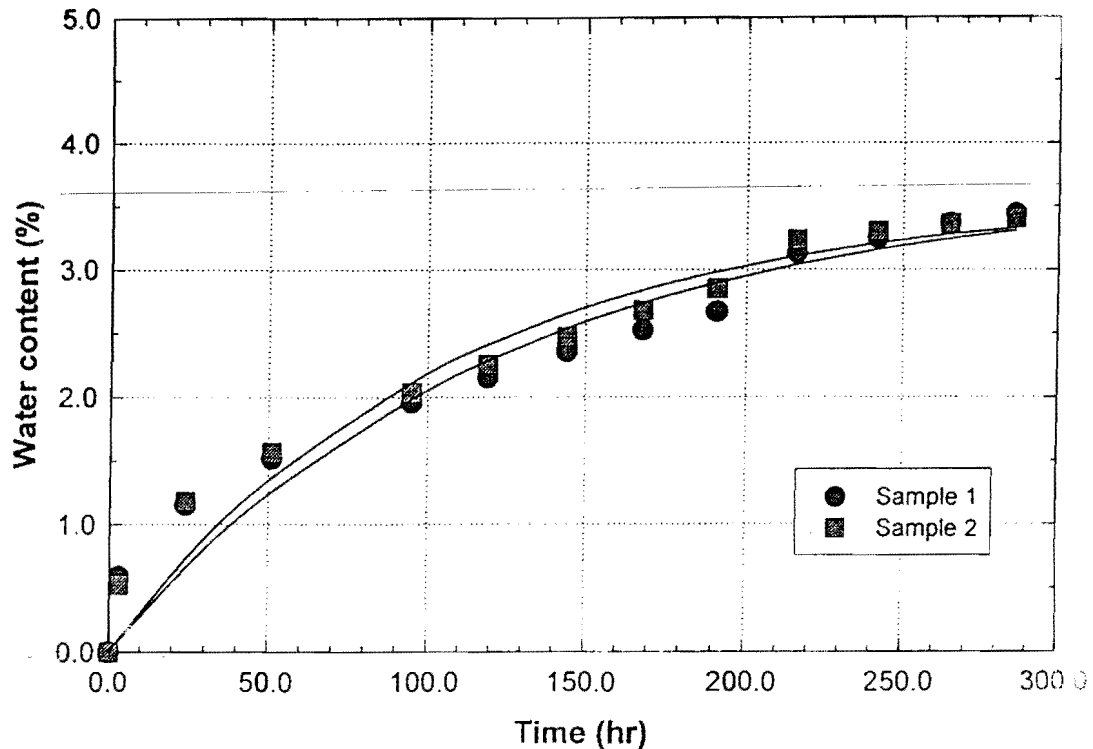


Figure 5.40. Variation of Water Content with Time during Suction Test for Yoakum Lime-Treated Limestone

Determining Effects of Environmental Change on Moisture Content of Flexible Bases in a Specific Environment - During the service life of a pavement, water may penetrate into or evaporate from the base course and subgrade depending on the environmental conditions. If the suction in the subgrade is higher than that of the compacted aggregate, water will be driven from the compacted aggregate to the subgrade. If the suction in the subgrade is lower than that of the compacted aggregate, water will migrate from the subgrade to the compacted aggregate. As a result, the water content of the compacted aggregate changes as a function of time regardless of the placement water content. These variations of moisture content must be taken into account when selecting an appropriate aggregate to minimize detrimental damage caused by environmental effects.

Since the thickness of a pavement is small relative to its length and width, the water flow in the system can be considered to be one-dimensional. Consider a covered ground surface with the

groundwater table located at a specified depth, as shown in Figure 5.41. As the permeability of the base course is considerably higher than that of the subgrade, the vertical water flow characteristics are dictated by the flow parameters of the subgrade. Therefore, the effects of the base course on the flow characteristics of the system are neglected for the sake of simplicity without sacrifice of accuracy.

When the ground surface is perfectly covered, there is no vertical flow of water through the ground surface. The pore water pressures are negative under static equilibrium conditions with respect to the groundwater table. The negative pore water pressure, i.e., suction, has a linear distribution with depth (i.e., line 1), and its magnitude is equal to the gravitational head (i.e., elevation head) measured relative to the elevation of the groundwater table. As a result, the total hydraulic head, i.e., the sum of pressure head and gravitational head, is zero throughout the soil profile resulting in no water flow in the vertical direction.

If the cover is removed from the ground surface, the soil surface will be exposed to the environment. Environmental changes can produce water flow in the vertical direction and alter the negative pore water pressure or suction profile. Computation of the transient suction profile as a function of time and environmental conditions is a very involved process [Gay 1994]. However, the transient suction profile is bracketed by two steady states: (1) steady state evaporation and (2) steady state infiltration.

Steady state evaporation, i.e., moisture leaving the system at a constant rate, causes the pore water pressure to become more negative, as shown by line 2 in Figure 5.41. The total hydraulic head changes to a negative value since the gravitation head remains constant. The hydraulic head has a nonlinear distribution from a zero value at the groundwater table to a negative value at the ground surface. An assumption is made in the analysis that the elevation of the groundwater table remains unchanged. The non-linearity of the hydraulic head profile is caused by the spatial variation in the coefficient of permeability. Even if the soil is homogeneous, the coefficient of permeability is a function of the degree of saturation and level of suction. As water flows in the direction of decreasing total hydraulic head, it flows upward from the groundwater table to the ground surface.

Steady state infiltration causes a downward flow of water. The negative pore water pressure increases from the static equilibrium condition, as shown by line 3 in Figure 5.41. The hydraulic head has a nonlinear distribution from a zero value at the groundwater table to a positive value at

the ground surface. Therefore, water flows downward with constant flux.

For design purposes, it is desirable to understand the variation of water content that occurs between the two extreme steady state suction profiles. Steady state flow conditions are given by Darcys law,

$$v = -k \left(\frac{\partial H}{\partial Z} \right) \quad [5.11]$$

where v = flow velocity (mm/s); k = coefficient of permeability (mm/s); H = total hydraulic head (mm); and Z = elevation head (mm). The total hydraulic head has two components,

$$H = h + Z \quad [5.12]$$

where h = total suction head (mm). The hydraulic gradient is thus

$$\frac{\partial H}{\partial Z} = \frac{\partial h}{\partial Z} + 1 \quad [5.13]$$

Solving for the change of suction as a function of the change in elevation gives

$$\partial h = -\partial Z \left(1 + \frac{v}{k} \right) \quad [5.14]$$

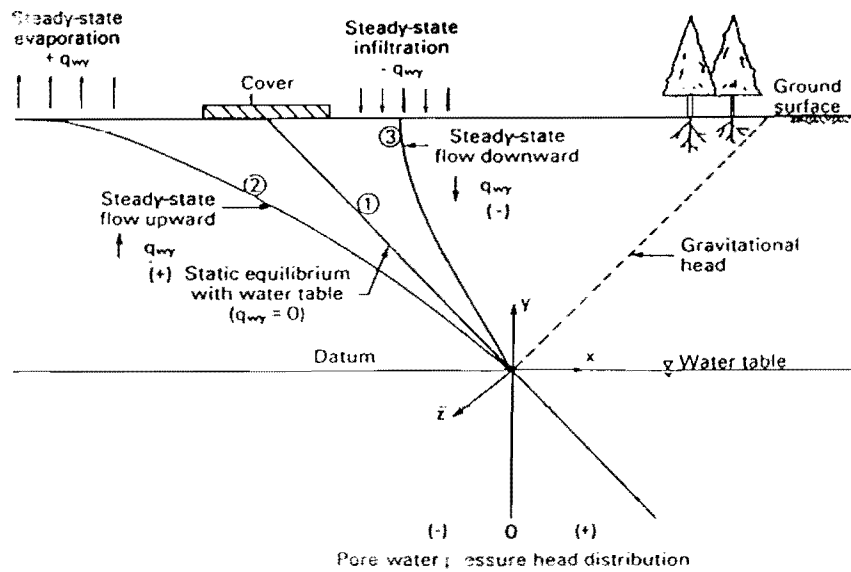


Figure 5.41. Static Equilibrium and Steady-State Flow Conditions in the Zone of Negative Pore-Water Pressure

The variation of the coefficient of permeability can be estimated by the Gardner equation or Mitchell's equation. Use of Gardner's equation for the unsaturated permeability gives

$$\Delta h = -\Delta Z \left(1 + \frac{v}{k_o} (1 + a|h|^n) \right) \quad [5.15]$$

where $a = 10^{-9}$ typically; $n = 3$ typically; and $k_o =$ saturated permeability (mm/s). The sign of the velocity, v , is positive for water leaving the soil (evaporation) and negative for water entering the soil (infiltration). Using Mitchell's equation for the unsaturated permeability gives

$$\Delta h = -\Delta Z \left(1 + \frac{v h}{k_o h_o} \right) \quad [5.16]$$

where $h_o = -100$ mm in clays. Mitchell's expression takes into account, to some extent, the increased permeability of the soil mass due to the cracks that become open at high suction levels. The velocity of water entering or leaving the soil may be estimated from Thornthwaite Moisture Index moisture balance computations.

A diffusion equation was developed by Mitchell to describe unsaturated moisture flow. Detailed derivation of the equation is given by Jayatilaka [1993]. Mitchell also modeled the effects of rainfall and evapotranspiration by a sinusoidal change in suction with time at the soil surface,

$$U(0,t) = U_e + U_o \cos(2\pi nt) \quad [5.17]$$

where $U(0,t)$ = suction at the surface at time t ; U_e = equilibrium matrix potential (pF); U_o = amplitude of matrix potential (pF); n = frequency (Hz); and t = time (s). For this boundary condition, the suction $u(Z,t)$ at any time t and depth Z is determined as

$$U(Z,t) = U_e + U_o \exp\left(-Z\sqrt{\frac{n\pi}{\alpha}}\right) \cos\left(2\pi nt - Z\sqrt{\frac{n\pi}{\alpha}}\right) \quad [5.18]$$

where $\alpha = (\gamma_w |S| P)/\gamma_d$ = Mitchell diffusion coefficient (mm^2/s); S = slope of the pF-water content line; $P = k_o h_o / 0.4343$ = Mitchell's unsaturated permeability (mm^2/s); γ_w = unit weight of water; and γ_d = dry unit weight of soil.

Mitchell's unsaturated permeability formulation has been used in finite element simulations to determine U_e and U_o by trial and error. The wet suction profile is controlled by U_e and U_o values that vary with soil type and Thornthwaite Moisture Index. The Thornthwaite Moisture Index is a number that indicates the moisture condition at a particular location. It is calculated on an annual basis by a procedure which involves: (a) determination of the potential evapotranspiration, (b) allocation of available water to storage, deficit, and runoff, and (c) computation of the annual summation. The parameters involved in this calculation procedure are the precipitation, potential evapotranspiration, and depth of available moisture. The depth of available moisture is the maximum depth of moisture that may be stored within the rooting depth of the soil profile [Thornthwaite 1948].

Typical values are given in Table 5.12 [Jayatilaka et al. 1993]. Thornthwaite Moisture Indexes of different locations in Texas can be obtained from Carpenter et al. [1974], as shown in Figure 5.42.

Table 5.12. Estimates of Wet Suction Values

Thornthwaite Moisture Index	Mitchell diffusion coefficient (cm²/s)	U_e (pF)	U_o (pF)
-46.5	0.0060	4.47	0.32
	0.0025	4.37	0.22
	0.0002	4.26	0.11
-21.3	0.0060	4.18	1.48
	0.0025	3.77	1.07
	0.0002	3.40	0.70
-11.3	0.0060	3.65	1.65
	0.0025	3.20	1.20
	0.0002	2.80	0.80
14.8	0.0060	3.58	1.58
	0.0025	3.14	1.14
	0.0002	2.76	0.76
26.8	0.0060	3.58	1.58
	0.0025	3.14	1.14
	0.0002	2.76	0.76

The minimum suction at a particular location of known TMI is thus $U_e - U_o$. If this lowest suction is higher than pF 4, compacting the aggregate base at a water content with pF higher than 4 will prevent the problem of expansion during freezing as the water content of the compacted aggregate will not be high enough to cause the compacted aggregate to expand during freezing throughout its service life. This situation applies to most locations in west Texas.

However, the pF of the subgrade may go below 4 during that part of the year when the base course can take water from the subgrade, resulting in an increase of water content and a decrease in suction. The transfer of moisture will eventually stop when the suction gradient reaches curve -1, as shown in Figure 5.41. The equilibrium suction profile in the base course can be estimated by

the suction versus water content curves of both the base course material and the subgrade, and moisture balance. If the suction versus water content curve of the subgrade material is not available, an approximate suction versus volumetric water content curve can be constructed as follows. The construction is illustrated in Figure 5.43. First, point A is located at the intersection of the field capacity volumetric water content ($= 0.88 \theta_{sat}$) and a pF of 2.0. Second, a line with a slope of S (γ_w/γ_d) is drawn from point A to its intersection with the vertical axis. Third, point C is located at a volumetric water content of $0.10 \theta_{sat}$ and the tensile strength of water (pF = 5.3). Fourth, point D is located at zero water content and a pF of 7.0, corresponding to oven dry. Fifth, a straight line is drawn between points C and D to its intersection with the first line. Ranges of saturated volumetric water content by the Unified Soil Classification System are [Lytton 1994] presented in Table 5.13.

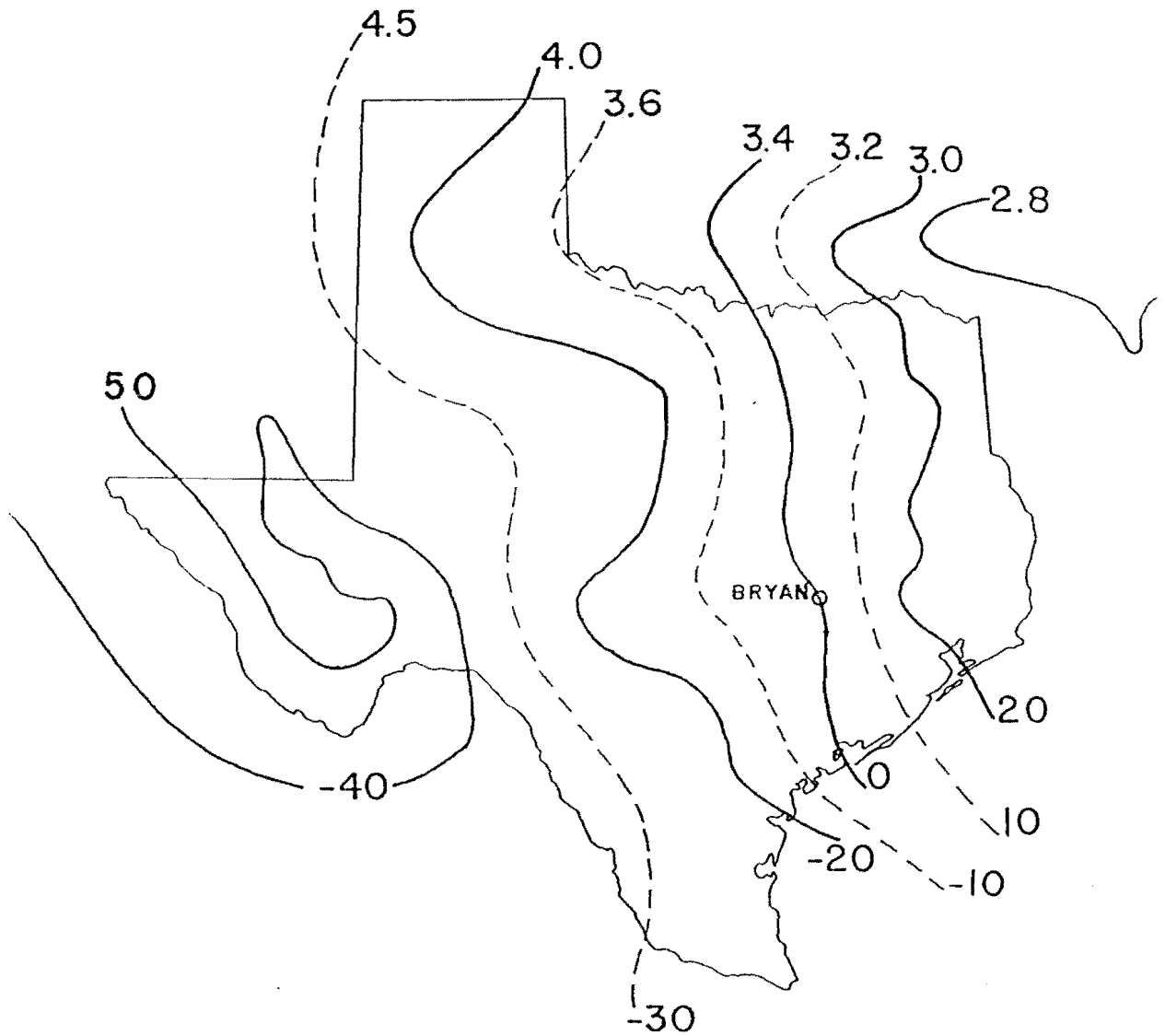


Figure 5.42. Predicted Suction in Subgrade below a Pavement (Upper Value), $pF = \log$ (mm of H_2O) Based on Thornthwaite Moisture Index (Lower Value) for a Clay Subgrade

Table 5.13. θ_{sat} for Various Soil Classifications

Soil type by the Unified Soil Classification System	Range of θ_{sat}
GW	0.31-0.42
GP	0.20
GM	0.21-0.38
GM-GC	0.30
SW	0.28-0.40
SP	0.37-0.45
SM	0.28-0.68
SW-SM	0.30
SP-SM	0.37
SM-SC	0.40
ML	0.38-0.68
CL	0.29-0.54
ML-CL	0.39-0.41
ML-OL	0.47-0.63
CH	0.50

$\theta_{sat} = n$ (porosity)

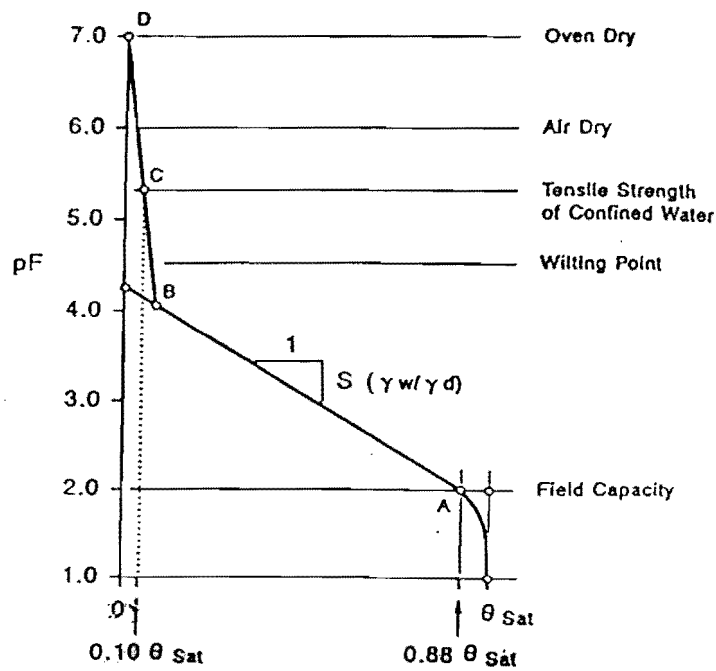


Figure 5.43. Approximate Construction of a Suction (pF) versus Volumetric Water Content Curve

The value of S is negative and can be estimated from:

$$S = -20.29 + 0.1555(LL \%) - 0.117(PI \%) + 0.0684(\% - \#200) \quad [5.19]$$

Extreme care must be exercised not to place a base course on a wet subgrade if the location is susceptible to freezing. Moreover, the increase in the water content of compacted aggregate can also worsen its strength characteristics.

Synthesis of Design and Construction Techniques to Minimize Cracking and Strength Loss -

Based on this research, the authors recommend the use of three tests to evaluate the thermal susceptibility of flexible bases: (1) the capillary soak tube test with dielectric value measurement as a function of time, (2) pF versus moisture content test, and (3) a determination of surface dielectric value and water content of the aggregate determined at each molding moisture content used in the development of the moisture-density relationship.

The maximum dielectric value (DV_{max}) determined after 250 hours of capillary soak in the capillary soak test, provides necessary information by which to evaluate moisture susceptibility and hence potential for stability loss due to moisture absorption. The criteria developed by Saaraketo and Scullion [1993] should be used as specified in Table 5.3. The value of DV_{max} must never exceed the selected criterion for DV_{max} in Table 5.3 in order to maintain acceptable strength and deformation resistance within the flexible base.

Once the strength and deformation resistance is addressed in accordance with Table 5.3, the potential of the flexible base to lose strength and expand due to freezing is addressed. As explained in the preceding section, the threshold moisture content of the base course leading to significant expansion and strength loss potential upon freezing is the moisture content at which the suction (pF) equals 4.0. At this threshold point, and at pFs below 4.0, sufficient moisture exists within the aggregate matrix to freeze and cause expansion. Since the moisture content within the aggregate or flexible base is not simply a function of compaction at the time of construction but also environmental equilibrium, the seasonal conditions of the subgrade are important in determining the threshold moisture content of the aggregate base.

The first step in this process is to determine the threshold moisture content of the aggregate base. This can be done most directly by establishing a pF versus moisture content curve, such as those shown in Figures 5.24 through 5.30, and simply identifying the moisture content corresponding to pF 4.0. Alternatively, a good estimate of the threshold moisture content can be made by entering Figure 5.33 with the moisture content of the aggregate corresponding to DV_{max} (maximum moisture content) to determine the suction capacity of the aggregate. The suction capacity is multiplied by 1.1 to arrive at the threshold moisture content. It is important to note that the maximum moisture content derived from the DV capillary soak test is an average moisture content of the 200 mm by 150 mm cylindrical samples prepared and tested in accordance with the protocol previously discussed. As such, the maximum moisture content is not the moisture content at the surface of the test sample, where the DV probe measures the dielectric properties, but is an average moisture content throughout the 200 mm by 150 mm sample. Therefore, the relationships and protocols discussed are specific to the capillary scale test on the 150 mm diameter by 200 mm high sample.

The next step is to determine the seasonal variation and critical value of subgrade suction. This can be accomplished by simply estimating the critical subgrade suction from Table 5.12 based on the Thornthwaite Index of the region in question. In this case, the critical pF is the difference between U_e and U_o in Table 5.12. Alternately, the subgrade suction can be estimated by using Figure 5.42 on the basis of the Thornthwaite Index. If this value of subgrade pF is higher than 4.0, then the base will not suck moisture from the subgrade when the flexible base is compacted at a moisture content corresponding to a pF of 4.0. If the flexible base is compacted at a pF lower than 4.0 (wetter) and the subgrade pF greater than 4.0, then the subgrade will suck moisture from the base until the pF of the base and subgrade reach equilibrium, but the water content of the flexible base may still be above the threshold value which could result in damaging freeze expansion. A more precise way to estimate subgrade suction is by establishing a suction versus water content relationship for the subgrade. The protocol for establishing this relationship is explained on pages 5.81 through 5.83. Once this pF versus moisture content relationship is established for the subgrade, expected seasonal variations in moisture content should be determined based on field records or county soil survey reports from the USDA's Soil Conservation Service.

Finally, a DV versus compaction moisture content relationship can be established during the development of the moisture density relationship for the aggregate base. This relationship can be effectively used as a quality control device for field construction operations.

Example Problem (Aggregate Evaluation) - The approach discussed in the preceding paragraphs can best be illustrated by an example problem.

Consider the Coon Pit river gravel aggregate (AMC) in the Amarillo District. The maximum dielectric value (DV_{max}) from this test is 10, which is acceptable as a good material (Figure 5.13) based on its resistance to moisture and thermal effects. If the DV_{max} of the Coon Pit aggregate was in excess of 16, the aggregate could either be rejected or altered or stabilized prior to use. However, since the DV_{max} did satisfy the criterion, it is appropriate to proceed to the analysis of the threshold moisture content for moisture damage due to the effects of volume increase during freezing.

The next step is to find the threshold moisture content corresponding to a pF of 4.0. Figure 5.26 shows the pF versus moisture content relationship for the Coon Pit material. Although a linear relationship equation is shown on the figure between pF (y) and moisture content (x), it is obvious that the suction versus moisture content relationship is quite nonlinear. The nonlinearity of this particular relationship for the aggregate in question makes the analysis more difficult and less precise. However, from the plot of data, the threshold moisture content at pF 4.0 is approximately 6.0% to 7.0%. If the relationship between pF and water content is not available, the suction capacity of the aggregate can be determined from Figure 5.33. This value is determined by entering Figure 5.33 with the maximum water content determined in capillary soak testing. From Figure 5.26, this value is 1.75%, and the corresponding suction capacity from Figure 5.33 is 7.0%. The threshold water content is thus 1.1 times 7.0% or 8.0%. Experimental evidence in Figure 5.23 reveals that the Coon Pit aggregate will suffer expansion, which can be deleterious at moisture contents of 8.0% and above. The two approaches are in reasonable agreement.

Finally, Figure 5.42 shows that the equilibrium subgrade suction in the Amarillo area is approximately 4.0. This level of suction, associated with a TMI of -20, means that a Coon Pit flexible base compacted at a moisture content of 8.0% or below should not suffer from freeze expansion under typical conditions. If, however, this same flexible base were placed in a freezing environment in east Texas, for example the Paris District where the pF is near 3.0, the propensity

of the base to take on moisture from the wet subgrade could lead to freeze expansion. The relationship between DV and soil moisture content determined during the development of the moisture-density relationship can now be used to monitor the field compaction operations as a form of quality control. Such a quality control protocol requires field DV measurements.

Example Problem (Rehabilitation Evaluation) - As a second example, consider a poorly performing flexible base from the Amarillo District. The pavement cross section consists of 75 mm of hot mix asphalt concrete surface and 600 mm of caliche flexible base from the Buckles Pit. The pavement rests over a silty sand subgrade just west of Amarillo. The pavement is highly distressed with severe thermal cracking and advanced alligator cracking in the wheel paths. A forensic investigation determined that the weak and moisture-sensitive base is largely responsible for the distress, and cold in-place recycling is the preferred approach. Capillary soak testing and DV measurement have shown that the DV max for the buckles materials is over 30, which is unacceptable and probably the reason for the poor performance. Similar testing with 1.5% hydrated lime added to the aggregate or 3.0% portland cement added to the mixture substantially improve the DV max to below 10, Figure 5.13. Based on this assessment, detailed mix designs were completed for lime, lime- fly ash (LFA), and portland cement. A 2% hydrated lime and 2% class F fly ash proved to provide the best target triaxial strength properties. This blend provides a slow rate of strength gain and an expected design strength after a long-term cure of 1,600 kPa. This strength is considered adequate for stability yet not so high that it will lead to shrinkage cracking induced by excessive pozzolanic or cement stress reaction. The DV max of the Buckles-LFA mixture is 6. A pF versus moisture content relationship was developed for Buckles-LFA mixture, and the moisture content at pF = 4.0 was determined to be 14%.

Based on this analysis, a decision was made to mill off the existing concrete, stabilize the existing base with 2% lime and 2% fly ash, and recompact at 14% moisture. The subgrade equilibrium suction in the area is approximately 4.0, which indicates that the stabilized base compacted at 14% moisture will not be susceptible to wetting and freeze-induced volume change.

CHAPTER 6. FALLING WEIGHT DEFLECTOMETER (FWD) TESTING AND DATA COLLECTION

The second part of the field evaluation program consisted of the performance of falling weight deflectometer (FWD) testing at the selected case study projects, as listed in Table 3.4. The FWD testing was used to evaluate the structural adequacy of the pavements and to investigate what effects, if any, the premature cracking had on the structural capacity of the pavements. This chapter provides a general description of FWD testing and analysis. It also describes the testing protocol we developed for this study. Chapters 7 and 8 discuss the FWD data analysis and the main factors considered.

FALLING WEIGHT DEFLECTOMETER APPARATUS

The FWD apparatus includes a known mass, a base plate, and foot plate connected by a spring buffer system, plus seven seismic deflectors (Geophones) [Uddin et al. 1985]. The mass is dropped from a specified height onto the foot plate, producing an impulse load on the pavement. Load is measured by a load cell located between the foot and base plates; the drop height of the mass is typically specified to achieve an approximate load on the pavement.

The geophones measure the dynamic deflection response of the pavement when a load is applied. The first geophone (Geophone #1) is located directly beneath the base plate, and the remaining six geophones may be positioned at variable distances along a raise/lower bar in front of the base plate. The geophones can be moved forward or backward along this bar at any distance 0.3 m (1 ft) to 2.1 m (7 ft) from the center of the base plate (the location of Geophone #1). The remaining six geophones are typically placed at 0.3 m (1 ft) intervals, beginning 0.3 m from Geophone #1. This positioning of the geophones is referred to as “normal.” A rear extension bar can also be installed to mount a geophone behind the load plate.

ANALYSIS OF FWD DEFLECTION DATA

Geophone #1 measures the maximum deflection (referred to as Y_1), and the deflection measurements typically decrease with increasing distance from the loading plate (i.e., Y_2 , Y_3 ,

... , Y_7). A deflection bowl can be generated using the measured deflections (Figure 6.1). Several types of analyses can be utilized to evaluate pavement structural capacity based on FWD deflection data. The three types which were considered for this study involve a structural type evaluation of the pavement, backcalculations of moduli, and a statistical analysis of the deflection data. Each type of analysis is described in the following sections, along with our reasons for focusing or not focusing on each.

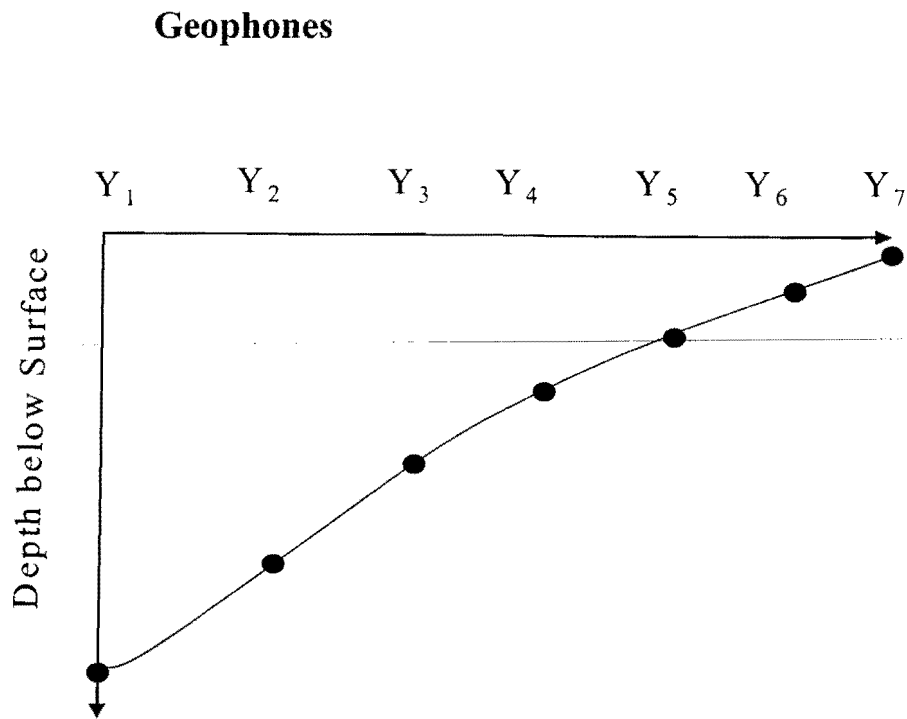


Figure 6.1. Typical Deflection Bowl from FWD Deflection Data

Structural Evaluation of Pavement

This type of analysis involves using the deflection measurements directly for a structural evaluation. Deflection data/deflection bowls are utilized to calculate certain parameters. These parameters have been related to the structural capacity of pavements. Y_1 and Y_2 (measurements at or near the base plate) are generally representative of the structural capacity of surface layers, while deflection measurements further away from the load are

influenced by the stiffness of underlying layers. Although there are various measurements and parameters that can be obtained from deflection bowls, only the following four are discussed, since they are the most pertinent to our evaluation.

Maximum deflection: Y_1

The maximum deflection (also surface deflection) is generally related to the strength of the surface layer of the pavement. High Y_1 measurements are representative of a weak surface layer. (Y_1 and Y_7 are typically the only measurements which are examined independently of any other deflections.)

Surface Curvature Index: $SCI = Y_1 - Y_2$

SCI is generally related to the strength of the top 200 mm (8 in) of the pavement structure. High SCI values are representative of weaker surface layers.

Base Curvature Index: $BCI = Y_2 - Y_3$

BCI is generally related to the strength from 200 to 400 mm (8 to 15 in) below the surface. High BCI values are representative of weaker base layers.

Load Transfer Efficiency: $LTE = (Y_2 / Y_1) * 100$

Expressed as a percentage, LTE is usually used in evaluations of jointed concrete pavements. Higher percentages represent good load transfer; however, it is difficult to establish a cut-off percentage at which a pavement is not exhibiting sufficient load transfer. LTE is more appropriate when performing evaluations at the project level, while SCI values are typically used for network level evaluations.

Backcalculation of Moduli

The second type of analysis typically performed using FWD deflection data involves using the measured deflections to backcalculate the approximate elastic moduli of each pavement layer. Backcalculation procedures are simple in methodology, but the process can become complex. The accuracy of results is highly dependent on the quality and amount of available data on the pavement. Backcalculation procedures typically do not produce unique results.

Although this type of analysis permits evaluation of individual layers, the limitations of the backcalculation process must be considered. Also, this type of analysis is more meaningful for project level type analysis than network level analysis.

Initially, the plan was to utilize this type of analysis for our study; however, based on the nature of the data, modulus backcalculation would not have been practical. As explained in the sections detailing our testing protocol, a high percentage of the data was collected at cracked locations. Moduli backcalculated using FWD measurements obtained at such locations usually yield inconsistent and questionable results.

Statistical Analysis

A statistical analysis focuses on the same parameters calculated for structural evaluations. To perform a statistical analysis, the assumption that the measured deflections and/or calculated parameters do, in fact, give accurate representations of the stiffness or structural adequacy of the pavement layers must be made. These parameters are considered to be the dependent variables. Any information or data (collected for all the pavements being studied) which influence the pavements' serviceability can then be considered as independent variables.

Models can be developed and/or an analysis of variance (ANOVA) can be performed to determine how well the independent variables explain the variance in the deflection data. This type of analysis is therefore more suited for network level type analysis, since the majority of data available at each drop will be the same across an entire test section.

FWD TESTING PROTOCOL FOR PROJECT

FWD deflection measurements are susceptible to seasonal variations. Perrone et al. [Perrone 1994] reported that such seasonal variations in deflection measurements are due to changes in average temperature and moisture content in the pavement layers. With the diverse environmental conditions experienced in the four distinct climatic zones of Texas, the net effect that seasonal variations will have on deflection measurements should also be expected to vary.

Although the effect of such seasonal changes cannot be quantified, it necessitated the performance of FWD testing during several seasons representing extreme conditions. Therefore, the first step in developing the FWD testing protocol was to plan two phases of testing, one during the winter months and the second during summer months.

Our original plan was to follow the same testing protocol during both phases of testing and to perform drops at the exact same locations. This would allow for meaningful comparisons of the two sets of data. After running some preliminary analysis on data from the first phase of testing, the protocol was, however, slightly altered; drops were still made as close to the exact locations of the first phase of testing as possible.

The second step in developing the testing protocol was to determine the frequency and locations of FWD measurements within each test section. As previously mentioned, structural efficiency estimates for both cracked and uncracked sections were the primary objectives of FWD testing. To achieve this goal, FWD drops had to be performed both at transverse cracks and at areas free from any cracks within each test section.

Using the distress maps developed as part of the visual condition surveys, a total of 20 test locations were identified within each 500 m test section. All test locations were within the outside lane of multiple lane project sites and within east or northbound lanes of single lane undivided highway projects. The testing apparatus was always positioned such that the load plate and geophones rested on the outside wheelpath of the testing lane.

The following sections explain the process by which the test locations were selected and the placement of the FWD apparatus.

Tests in Areas Free of Distress

These tests were performed within areas free of transverse cracks and preferably minimal or no other distress. Using the distress maps developed as part of the visual condition surveys, a total of 15 test locations were selected within each test section. The testing crew was, however, given the freedom to relocate the apparatus as actual field conditions demanded.

Measurements performed at these distress free locations and with the geophones in “normal” position were labeled as **Case 1** and are illustrated in Figure 6.2a. The parameters

calculated are also identified in the illustration. At each of these locations, a total of three drops were performed, with data from only the last two drops recorded. Each drop height was sufficient to achieve approximately 4082 kg (9000 lb) force on the pavement. Case 1 type measurements were made during both the winter and summer phases of testing and followed the same protocol.

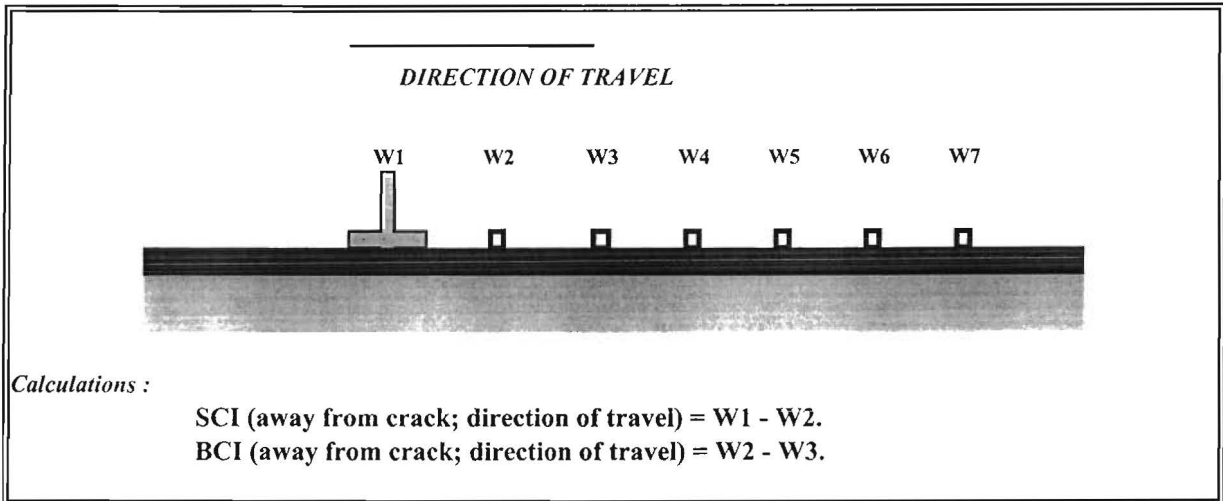


Figure 6.2a Case 1 : No Visible Cracks in Pavement - (Phases 1 and 2)

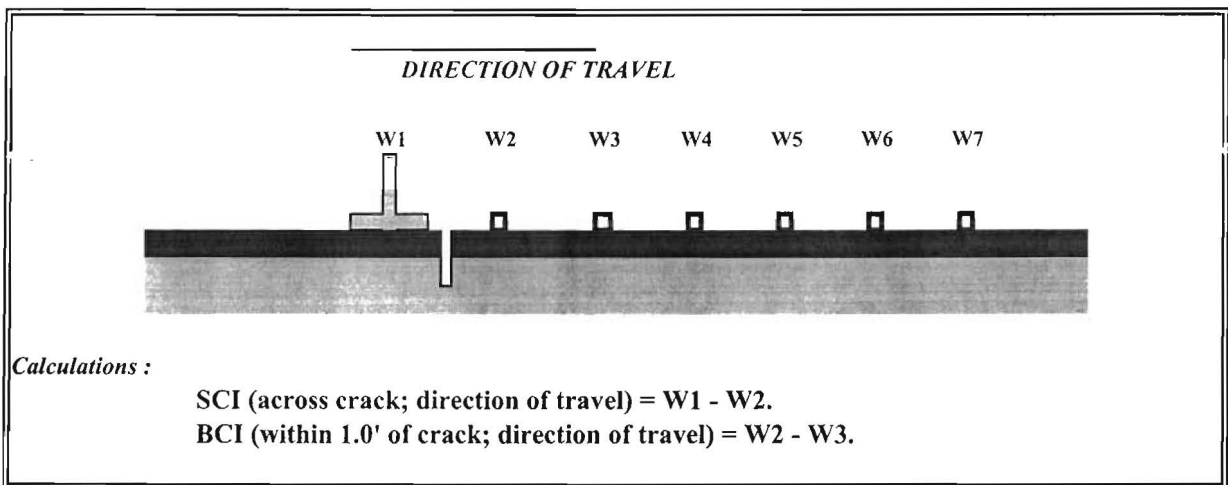


Figure 6.2b Case 2 : Crack between Loading Plate (Sensor #1) and Sensor #2 - (Phases 1 and 2)

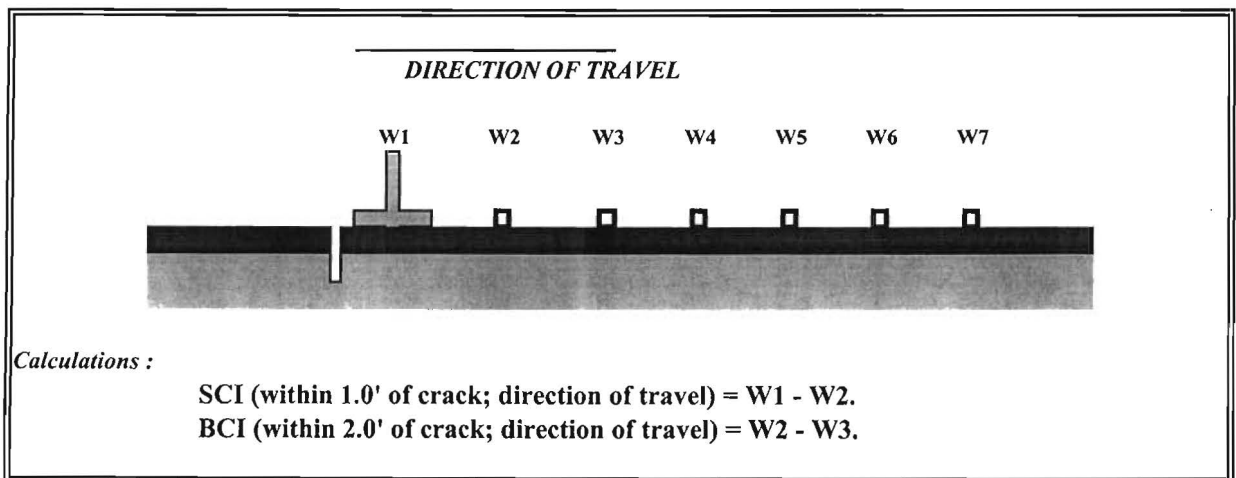


Figure 6.2c Case 3 : Crack behind Loading Plate (Sensor #1); Normal Sensor Positioning - (Phases 1 and 2)

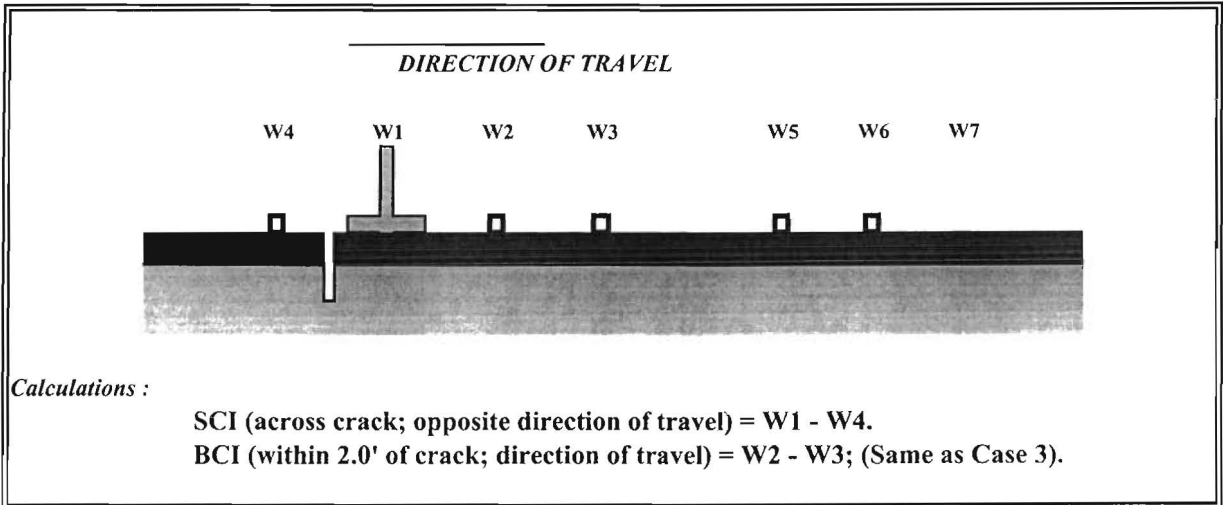


Figure 6.2d. Case 4 : Crack behind Loading Plate (Sensor #1) and Additional (Sensor #4) - (Phase 1 only)

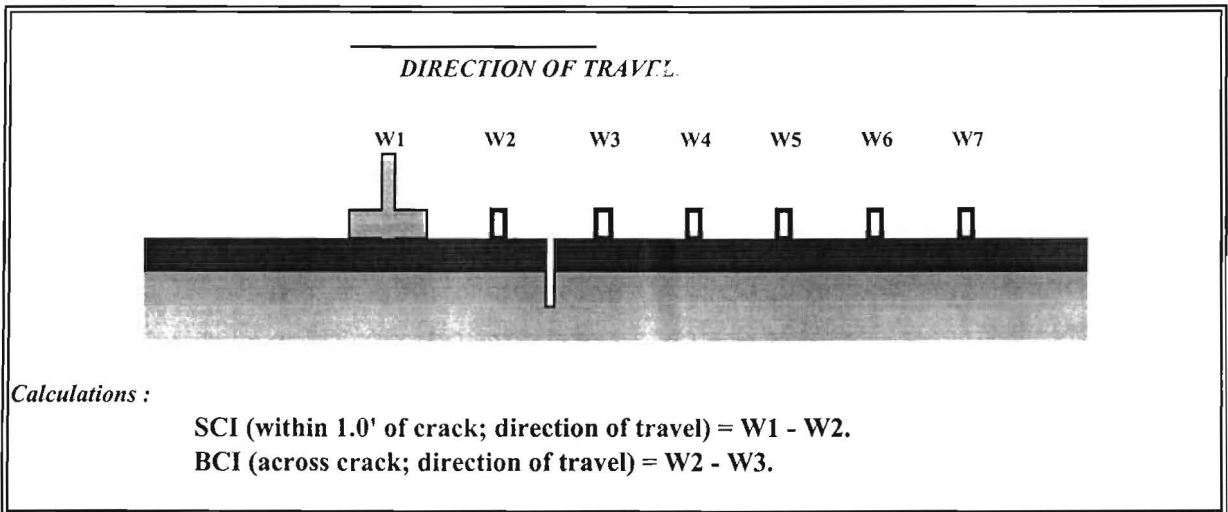


Figure 6.2e. Case 5 : Crack between Sensor #2 and Sensor #3 - (Phase 2 only)

Tests at Cracked Locations

As explained in *Distress Mapping* of Chapter 4, actual distress data for each test section was available only within the first 15 m of each 100 m subsection. It was within those 15 m that FWD drops at cracked locations were originally located.

Within each test section, a minimum of five prominent transverse cracks were identified. Once again, the testing crews were allowed the flexibility to relocate the testing apparatus if necessary.

At each of the cracked locations identified, drops were made with several different configurations. The configurations either varied in the location of the transverse crack (with relation to the loading plate) or in the positioning of the geophones. This testing was performed in an effort to determine how great an effect the cracks have on the pavement structural adequacy and to what approximate depths the cracks were having some effect.

Winter Phase

During winter testing, one measurement was made with the geophones in “normal” position and the transverse crack located between the loading plate and geophone #2. This testing configuration was labeled as **Case 2** and is illustrated in Figure 6.2b. Parameters calculated from Case 2 configurations are also defined in the illustration. At each of these locations, a total of three drops were performed, with data from only the last two drops recorded. Each drop height was sufficient to achieve approximately 4082 kg (9000 lb) force on the pavement.

The second configuration at cracked locations performed during winter testing placed an additional geophone behind the load plate. The transverse crack was then located between the loading plate and the additional geophone; i.e., behind the loading plate. (For this testing configuration, the computers read the deflection measurements from the additional geophone through the fourth available channel. Those deflection readings are therefore labeled as W_4 . Deflection measurements from the fourth geophone in front of the loading plate could, therefore, not be recorded.) This testing configuration was labeled as **Case 4** and is illustrated in Figure 6.2d. At each of these locations, a total of three drops was performed, with data from

only the last two drops recorded. Each drop height was sufficient to achieve approximately 4082 kg (9000 lb) force on the pavement.

Parameters calculated from Case 4 configurations are also defined in Figure 6.2d. This configuration allowed for calculations of two different SCIs; ‘near cracks’ in the direction of travel and ‘across cracks’ opposite the direction of travel. SCI calculations ‘across cracks’ from Case 4 could be compared to SCI calculations ‘across cracks’ in Case 2.

Summer Phase

During the summer phase of testing, measurements with four different type configurations were used; however, each of the configurations had the geophones in “normal” position but varied the distance of the identified crack from the loading plate.

The same configuration used for **Case 2** type measurements during winter testing was repeated during this phase of testing. Case 2 measurements from either phase could be directly compared.

The same crack location configuration used in **Case 4** type measurements during the winter phase was also used in the summer phase; i.e, with the transverse crack located behind the loading plate. However, due to some confusion during the first phase of testing, the installation of the additional geophone behind the loading plate was omitted. This configuration was labeled as Case 3 and is illustrated in Figure 6.2c. At each of these locations, a total of three drops was performed, with data from only the last two drops recorded. Each drop height was sufficient to achieve approximately 4082 kg (9000 lb) force on the pavement.

Parameters calculated from Case 3 configurations are also defined in Figure 6.2c. This configuration did not allow calculations of SCI ‘across cracks’ opposite to the direction of travel. However, Case 3 SCI calculations ‘near cracks’ in the direction of travel can still be compared to Case 4 (winter only) SCI calculations ‘near cracks’ in the direction of travel.

The fourth configuration used during summer testing located the transverse crack between geophone #2 and geophone #3. This configuration was labeled as Case 5 and is illustrated in Figure 6.2e. As always, a total of three drops were performed, with data from only the last two drops recorded. Each drop height was sufficient to achieve approximately

4082 kg (9000 lb) force on the pavement.

Parameters calculated from Case 5 configurations are also defined in Figure 6.2d. This was the only testing configuration which allowed BCI calculations ‘across cracks’.

DATA COLLECTION

With 11 test sections and two phases of testing, a total of 22 sets of data should have been collected. Unfortunately, problems encountered in performing and/or collecting the data resulted in only 15 sets of data being useful for our study. A seal coat was placed on one of the sections in Amarillo after completion of the condition survey and before any FWD testing could be done. At some other locations, coordination problems lead to some testing being performed differently from the testing protocol adopted for the study, and essentially rendering the data useless for analytical purposes.

Data from the following test sections could not be considered in our analysis:

- US 87/287 (AM2) - Winter Phase
- FM 1541 (AM2) - Winter and Summer Phases
- US 281 (PH1) - Winter and Summer Phases
- FM 2128 (PH2) - Winter and Summer Phases

Siddharthan et al. [Siddharthan 1972] reports that it cannot be expected that the many sources of error associated with FWD measurements can be totally eliminated. However, reducing the intervals of testing can help in eliminating the variability associated with changes within the pavement itself, and repeated testing and averaging can help in eliminating variability associated with human error and deviations in the geophone measurements. Our attempts to reduce variability in these data are described below.

Variability within the Pavement Structure and Material

Reducing the intervals between test measurements was the most effective method available to help reduce variability in measurements associated with variability in the pavement structure and materials. Deflection measurements for our study were typically made

at 25 m (85 ft) intervals, with tests measurements at uncracked locations being a maximum of 33 m (100 to 110 ft) apart. FWD measurements for the PMIS database are typically made at 160 m (530 ft) intervals [FWD Operator's Manual 1996].

Variability Associated with the Testing Apparatus

The repeated drops made at each location were an attempt at investigating the consistency of the geophone measurements. Measurements from both drops were, however, remarkably similar for a large majority of locations, indicating a high degree of precision within the geophone measurements. In the few cases where the measurements did vary, average values were used in the analysis.

Normalization and correction of FWD data is essential before any analysis can be made. Each drop height was supposed to be sufficient to achieve approximately 4082 kg (9000 lbs) force on the pavement; load readings, however, were usually not exactly 4082 kg. A simple linear correction was applied to each set of measurements for load normalization. We did not correct our data based on temperature readings since deflection measurements are typically not corrected when the asphalt cement layer is less than or equal to 75 mm (3 in). Measurements made on any asphalt layers greater than 75 mm (3 in) must be corrected to 21 °C (70 °F) based on the Corps of Engineer procedure [Modulus 5.0 : User's Manual 1995].

Variability Associated with Human Error

As with most experiments, the control over human error was limited. The establishment of a well-defined testing protocol which each testing crew could follow was the extent of our control over a variability which might be introduced due to human error.

CHAPTER 7. STRUCTURAL EVALUATION OF CASE STUDY PAVEMENTS USING FWD DATA

As mentioned in Chapter 6, the authors focused on two types of analysis for this study. The structural type evaluation of the case study pavements is presented in this chapter. Chapter 8 details the statistical analysis.

PARAMETERS CONSIDERED IN THE EVALUATION

Because the research focused on base and surface layer performance, deflection measurements representative of underlying layers were not as significant as those representative of surficial layers. Which measurements are correlated with the strength of the separate layers, however, depends on the pavement structure. The base layers of our case study projects typically extended to 300 mm (12.5 in) below the pavement surfaces, with the deepest base layer extending to a depth of 400 mm (15.5 in). Therefore, measurements W_1 , W_2 , and W_3 were the most pertinent to our study.

The focus of the analysis, therefore, was limited to parameters calculated using those measurements (as described in Chapter 6) W_1 , SCI, BCI, and LTE. Calculations for these parameters were made for each drop performed as part of the study. The results of calculations for SCI and BCI are shown in Figures C.1 through C.15 in Appendix C. As previously mentioned, only mean values were considered in the analysis. The mean values, along with their standard deviations, are also shown in the tables.

The high standard deviations reported in the tables suggest that regardless of the efforts, there was still a significant amount of variability experienced in the deflection measurements. Mean values and standard deviations of W_1 for Case 1 configurations only are presented in Table 7.1.

GROUND PENETRATION RADAR ANALYSIS

Ground penetration radar (GPR) analysis was performed on each of the pavement sections tested in the FWD analysis. The GPR analysis was performed in the winter months (between late January and mid March) and in the summer (August and early September). GPR data verified the pavement layer thicknesses very effectively. However, the GPR study

did not reveal significant moisture level variation between the summer and winter months. Furthermore, all bases tested appeared to have good dielectric properties, and there were no significant differences among the properties of the flexible bases tested.

STRUCTURAL EVALUATION

It is reasonable to assume that the magnitude of a crack's effect on pavement strength will depend on the severity and depth of the crack. Therefore, without any information regarding the nature and severity of each crack, it will be impossible to predict the magnitude of a crack's effect on a pavement's strength. However, the usefulness of this determines if there was any effect on the deflection measurements caused by the cracks.

Table 7.1. Y_t Mean and Standard Deviation for Case 1 Configurations

Test Section & Phase	Number Of Drops	Y_t	
		Mean	Standard Deviation
AB1 (winter)	15	7.72	1.36
AB2 (winter)	15	12.57	3.53
AT1 (winter)	16	17.28	4.12
SA1 (winter)	15	15.94	6.02
SA2 (winter)	15	15.61	4.51
YO1 (winter)	15	8.28	2.80
YO2 (winter)	15	8.77	3.92
AB1 (summer)	15	10.88	3.67
AB2 (summer)	15	14.22	3.50
AM1 (summer)	14	19.64	6.03
AT1 (summer)	17	17.06	3.86
SA1 (summer)	15	15.56	6.23
SA2 (summer)	15	12.84	3.63
YO1 (summer)	15	7.02	2.19
YO2 (summer)	15	8.68	3.97

For some analyses, it was convenient to group all FWD data from areas which exhibited some distress together. This allowed for general comparisons of data from uncracked locations (Case 1) to all data from cracked locations (Cases 2, 3, 4, and 5). Within this report, referrals to data at "cracked locations" will incorporate all data from such locations

regardless of case. When specific configurations are being discussed, they will either be referenced by case or by proximity to the crack; i.e., 'near crack' or 'across crack'.

Although the researchers were uncertain as to how the pavements would be affected, there was a general trend they expected the calculations to follow. The anticipated results of each of the parameters are explained below.

Maximum Deflection (Y₁): It was anticipated that the average Y₁ would be worse, i.e., higher deflections, at cracked locations than at uncracked locations. This would be an indication that the presence of cracks adversely affects pavement performance and that the surficial layers are carrying more of the applied loads than anticipated during design.

Surface Curvature Index (SCI): Average SCI calculations should be the best, i.e., lowest values for Case 1 configurations. We anticipated that the calculations for configurations 'across cracks', i.e., Case 2 and Case 4 would be the worst and calculations from Case 3, only 'near cracks' would be somewhere between. This general trend would indicate that the visible cracks do not allow proper load transfer within the pavement, thereby reducing its structural capacity.

Base Curvature Index (BCI): It is assumed that the majority of cracking within the selected test sections originates in the base layers and propagates up through the surface layers. It was, therefore, anticipated that BCI calculations would also be affected by the cracks, i.e., lower average BCI calculations in uncracked areas. However, it is also likely that if there is poor load transfer in the surficial layers, any effect in the load transfer of the underlying layers may not be reflected in the deflection measurements. Therefore, the confidence in BCI values obtained is related to SCI and LTE values.

Load Transfer Efficiency (LTE): If the cracks have a significant effect on the structural integrity of the pavements, it would be expected that the average LTE calculations would follow a trend similar to SCI. The best LTE calculations, i.e., high values, should be associated with Case 1, and worst values should be associated with calculations 'across cracks',

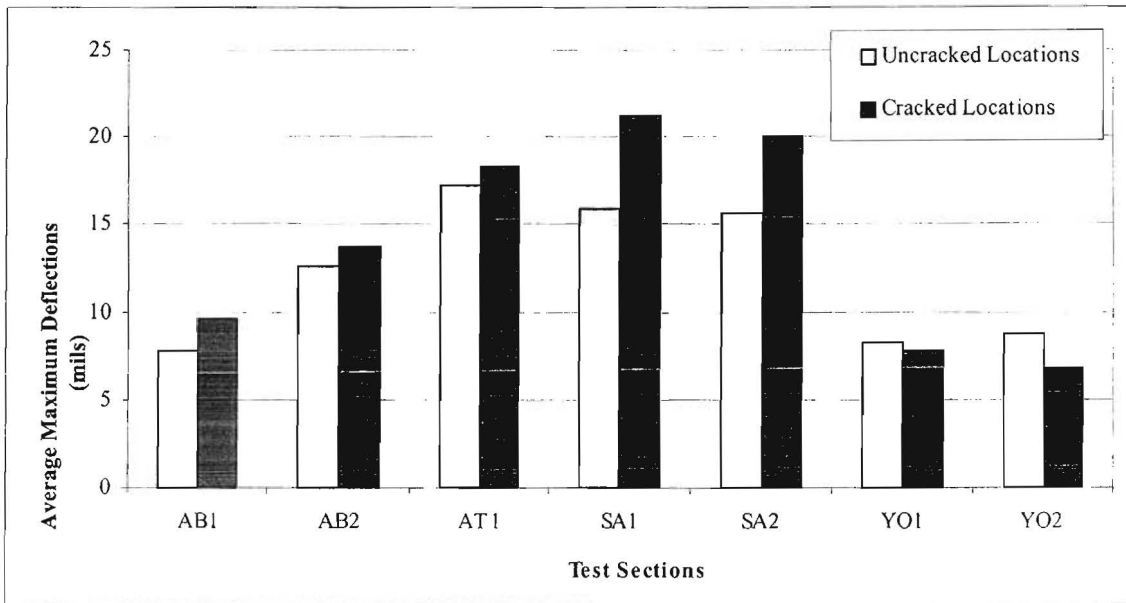


Figure 7.1. Average Maximum Deflections (Y₁) for Winter Phase of Testing

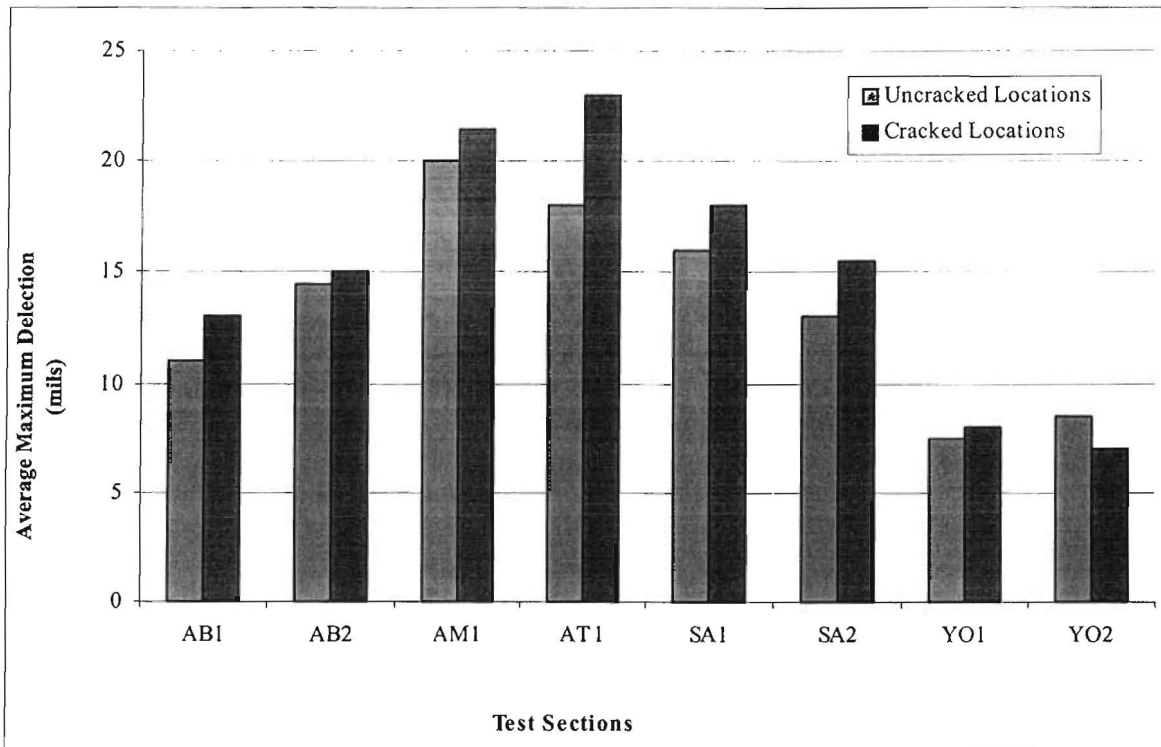


Figure 7.2. Average Maximum Deflections (Y₁) for Summer Phase of Testing

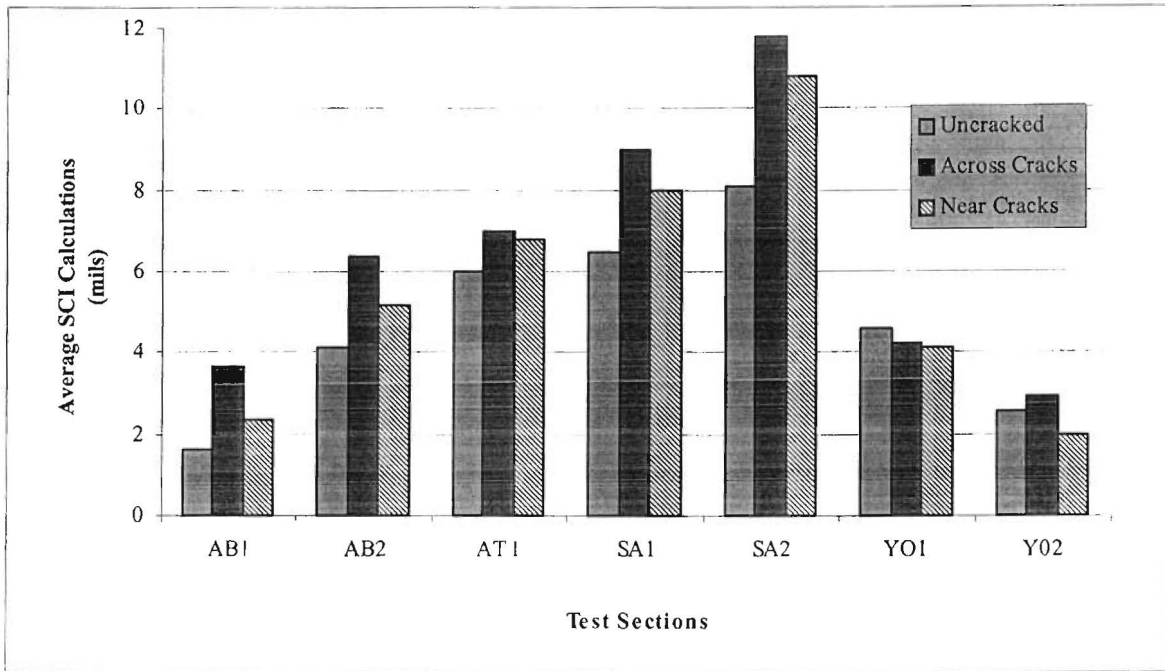


Figure 7.3 Average SCI Calculations for Winter Phase of Testing

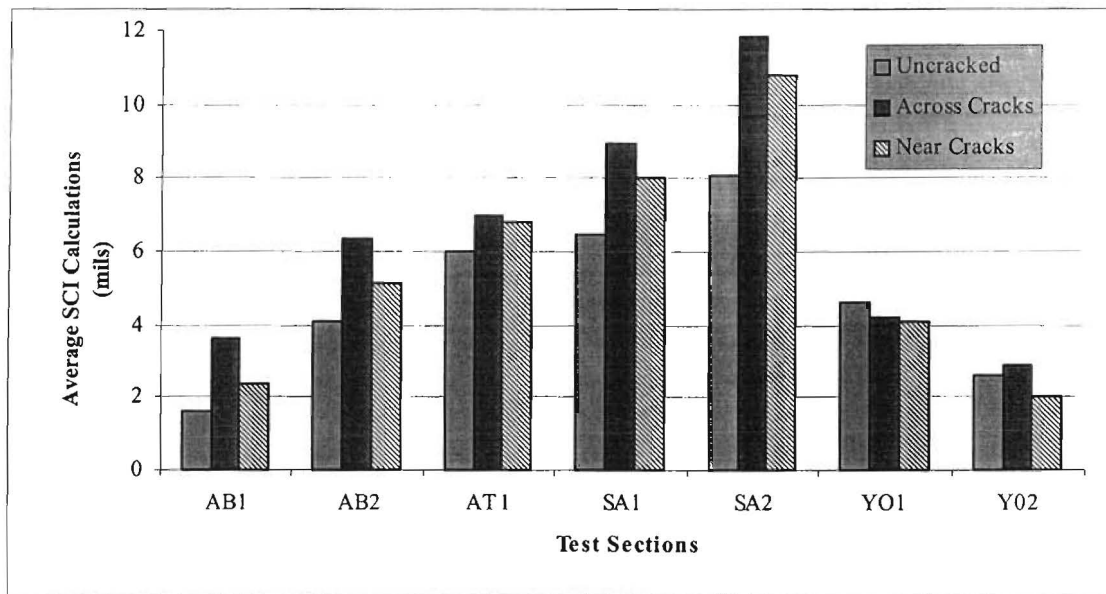


Figure 7.4. Average SCI Calculations for Summer Phase of Testing

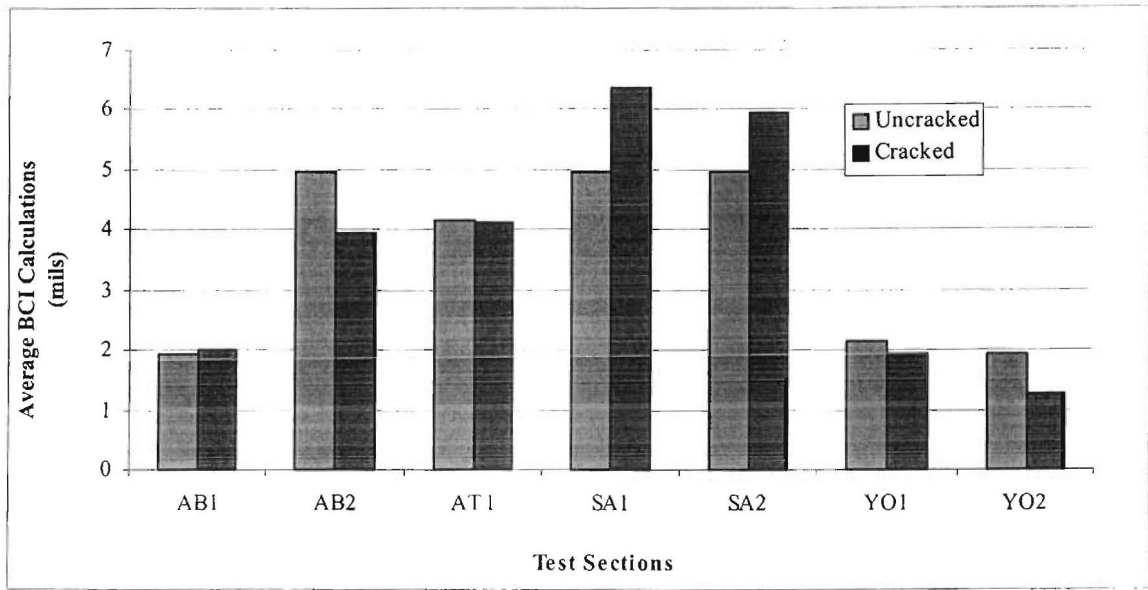


Figure 7.5. Average BCI Calculations for Winter Phase of Testing

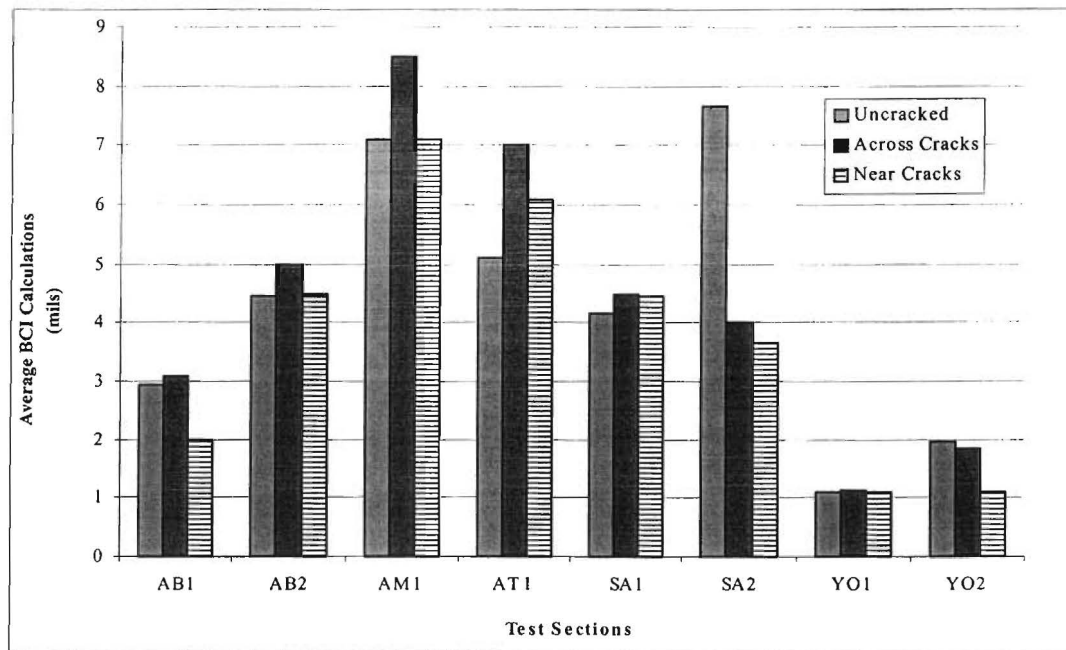


Figure 7.6. Average BCI Calculations for Summer Phase of Testing

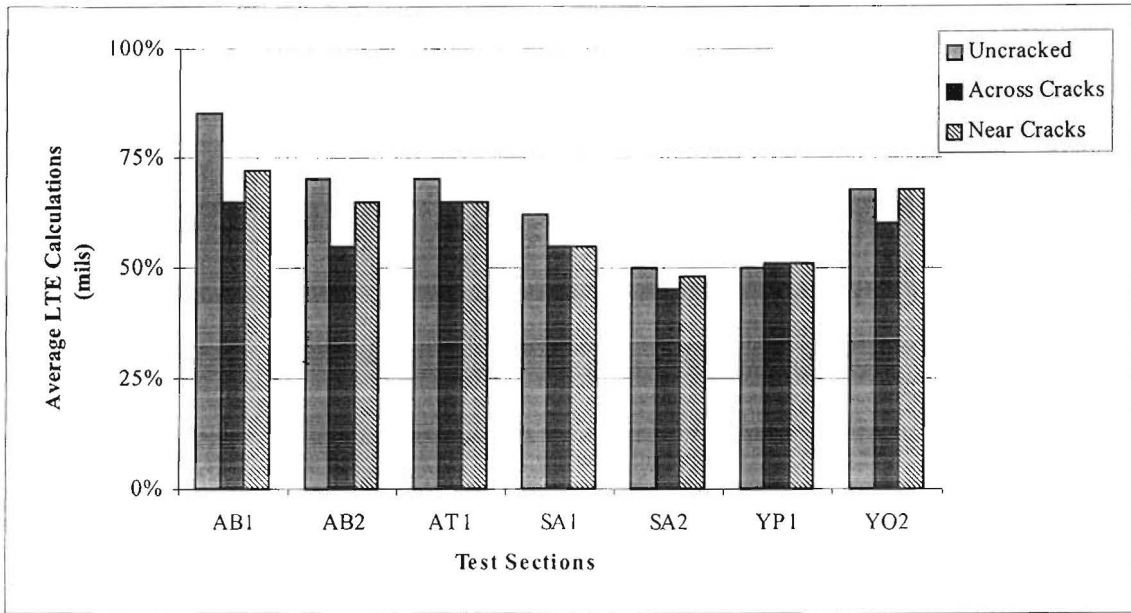


Figure 7.7. Average LTE Calculations for Winter Phase of Testing

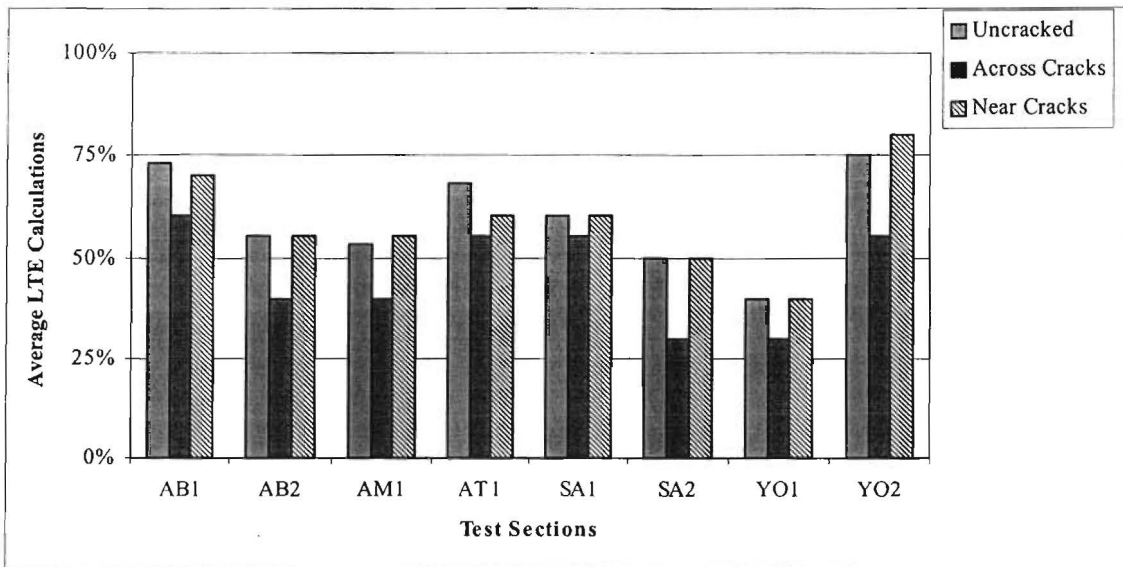


Figure 7.8. Average LTE Calculations for Summer Phase of Testing

Cases 2 and 4. If the LTE and SCI calculations do not follow the same general trend, at least within an individual test site, several interpretations can be made.

RESULTS OF ANALYSIS

With the exception of the two test sites in Yoakum, calculations of all of the parameters followed the expected trends, indicating that the observed cracks were having some effect on the in situ strength of the case study pavements. Plots of each of the parameters are provided in Figures 7.1 through 7.8. Each of the figures represents average values for a parameter during one phase of testing.

Analyzing any one of the parameters on its own may be misleading and may not give enough information to make conclusions about a pavement. Therefore, it is important to analyze all of the figures before making conclusions about pavement strength based on the parameters. Below is a discussion of results from several of the case study pavements.

Test Section AB1: Both sections in the Abilene District fall within the Dry/Freeze region. The base layer thickness of US 83 is approximately 250 mm with a 150 mm underlying subbase. The surface strength of this pavement appears to be adequate, as indicated by the low Y_1 s shown in Figure 7.2. There is a large difference between SCI and LTE calculations when comparing uncracked locations with 'across cracks'. The difference in LTE during winter was 23% and 13% during the summer. This indicated poor load transfer 'across cracks' and a significant loss of structural strength due to the cracks. Although our confidence in BCI values is low due to the SCI and LTE values obtained from cracked locations, the BCI values could indicate that the underlying layers are in relatively good condition. Of course, based on the depths associated with BCI values, those results have to be correlated with the subbase layer. The GPR analysis indicated that the flexible base was dry during both summer and winter test periods. Laboratory $D_{v_{max}}$ values for this material were between 15-20.

Test Section AB2: US 83B, also in the Abilene District, contains a 340 mm flexible base. Based on surface deflection, the asphalt surface and base layers appear to function well. The cracks have some effect, as evident by the SCI and LTE calculations. The differences

between the values for uncracked compared to 'across cracks' are small. Both sets of values were worse during the summer testing phase, i.e, average LTE at uncracked during the winter was 67% but dropped to 54% during the summer. This trend indicates some deterioration in the pavement's strength, even in uncracked areas, from the time of winter testing to the time of summer testing.

LTE values were too low, particularly in the summer (54%), to consider BCI calculations an accurate representation of the underlying layer strengths. Laboratory Dv_{max} values for this material was in the 16-20 range.

Test Section AM1: Only data from the summer phase of testing could be utilized for US 87/287. This was unfortunate, since Amarillo falls within the Dry/Freeze region and experiences more freeze/thaw cycles than most other climatic regions in the state. The pavement's base layer is 235 mm thick with a 100 mm underlying gravel subbase. This section yielded some of the highest summer W_1 values and the worst summer SCI values, indicating poor strength, particularly in the surface layers. (The distress surveys also indicated a high number of cracks at this test section.) Once again, there was a significant difference between SCI and LTE values at uncracked locations when compared to 'across crack' values, indicating a loss in strength related to the cracks. Our confidence in BCI values are representative of in situ strength was again low, but at this test section, the large difference in BCI values at cracked and uncracked locations may indicate that the cracks extend relatively deep. Field GPR data for both summer and winter periods revealed acceptable dielectric properties and bases with acceptable moisture contents.

Test Section AT1: SH 08 in Atlanta was the only one of our test sections located in the Wet/Freeze region of the state. Average W_1 s at this test site were also very high, indicating poor surface strength. Additionally, W_1 measurements at uncracked locations were approximately the same during both phases, but the measurements at cracked locations increased an average of 2.5 mils during the summer, a significant increase, indicating a greater loss in surface strength at the cracked locations. All of the other three parameters indicated a similar trend, a larger negative effect due to the cracks during the summer phase of testing.

Test Section SA1: Both pavements in the San Angelo District fall within the Dry/Freeze region of the state. The base layer of US 67 is 380 mm thick and is tied with section YO2 (LP 463) for the deepest base layer of our case study projects. Coincidentally, W_1 measurements from these two pavements, SA1 and YO2, displayed the worst standard deviations, based on a percentage of their respective means (see Table 7.1). This may have been due to increased possibility of variability with the thicker pavement structures. In these situations, percentage type calculations, i.e., LTE, are probably more reliable.

The ‘across cracks’ LTE values and the uncracked LTE values were relatively similar, indicating that the cracks are probably not yet contributing to any loss of in situ strength.

Test Section SA2: SH 208 has a 200 mm thick base layer. Y_1 measurements followed the expected trends during both phases of testing, but the Y_1 measurements during the winter were significantly higher than measurements during the summer. Since it is not likely that the pavement’s strength improved between testing, the higher deflections measured in the winter may have been caused by a higher moisture content in the pavement’s underlying layers and/or a highly moisture/thermal susceptible base material. However, GPR testing did not reveal high dielectric values in either summer or winter measurements, nor was a significant difference in GPR dielectric values recorded between the two seasonal measurements. Laboratory Dv_{max} values all fell in the good range, indicating, little or no moisture sensitivity.

The LTE values were relatively low during both phases of testing, never above 49% with any configuration, indicating very poor load transfer at this test site. The LTE values also indicated an increased loss of in situ strength due to the cracks during the summer.

Test Section YO1: As previously mentioned, values from neither of the two Yoakum test sites followed all of the expected trends. They are also the only two case study projects from any single district that fall within different climatic zones. This project, US 290, falls within the Wet/No Freeze region. The section has the thickest pavement structure, when considering the 300 mm gravel subbase and the 260 mm base.

The cracks appear to have little effect on this case study’s pavement during either phase of testing. During the summer phase of testing, however, the maximum deflections measured at uncracked locations were actually higher than those measured at cracked

locations. All of the LTE values were relatively low during the winter and dropped even further during the summer phase of testing, indicative of very poor load transfer along the entire test section. Laboratory Dv_{\max} values range from 18 to 24, indicating a high level of moisture sensitivity.

Test Section YO2: This project, on LP 463, falls within the Dry/No Freeze region. As previously mentioned, the base is one of the thickest, and the Y_1 measurements yielded the worst standard deviations. The SCI values were still relatively good, low numbers and not significantly affected by the cracks. However, the LTE values, which were also relatively good, did appear to be affected by the cracks. These results combined with low BCI values and a high number of cracks (Table 4.2) may be representative of a pavement with adequate in situ strength and mostly surface cracks. It is also likely that those cracks will steadily begin to lower the pavement's strength. Laboratory Dv_{\max} values averaged 18 for the material, indicating high moisture sensitivity.

DISCUSSION

As mentioned in the discussion of test section SA2, the maximum deflections measured during the winter were larger than those measured during the summer. Although this was the only section where there was a significant decrease in W_1 from winter to summer, several other sections had slightly lower deflections during the summer phase of testing. Because we expect a steady decline in pavement strength, barring any rehabilitation, the improved deflections may be a result of higher moisture contents during the winter phase of testing. One focus of this study was to examine the susceptibility of the existing bases to moisture and/or thermal effects. Although it is difficult to come to such conclusions, deflection data certainly indicate that the time of testing had a significant effect on the results. As mentioned earlier, without specific information about each individual crack, it would be impossible to predict the magnitude of the effect of each crack on a pavement's strength. However, collecting and analyzing data in the presented herein manner provides a reasonable protocol by which to determine if and/or how surface cracks are affecting strength and possibly to what approximate depths. Such results could be useful in developing maintenance strategies; a possible methodology is outlined in the recommendations section of Chapter 10.

CHAPTER 8. STATISTICAL ANALYSIS OF FWD DATA

It is important to establish the researchers' expectations of the statistical analysis and to understand the limitations of such an analysis, particularly given the limited data available for the analysis. This analysis was not an attempt to develop a model which could be used to accurately predict the measured deflections but rather an attempt to determine, from a statistical point of view, which factors had the most influence on the measurements.

We must also remember that if a certain factor does not have a significant statistical effect on the parameters, it does not mean that the factor is unimportant. Obviously, any factor which was considered in the analysis must have some engineering significance.

MAIN EFFECTS CONSIDERED

As with the structural evaluation, the statistical analysis focused on Y_1 , SCI, and LTE; in statistical terms, those parameters were the dependent variables. BCI calculations were not examined as thoroughly in the statistical analysis for two reasons: (1) with the exception of Case 5, all of the configurations for BCI calculations are relatively the same and (2) with increasing distance from the transverse crack, the probability that the deflection measurement is indicative of actual in situ strength decreases.

The independent variables, inputs made by the researchers, usually fall into two groups: classification variables and continuous variables.

Classification (Class) Variables

These variables can be considered to be categorical or qualitative variables. The values of class variables are called levels. All of these factors were either established as part of the experiment design or by the testing protocol. Each of the variables are listed below with their corresponding levels:

Moisture Region	-	Dry, Wet
Temperature Region	-	Freeze, No Freeze

Subgrade Soil Type	-	<p>CL – Clays, Silty clays, Silty clay loams, Sandy clay loams.</p> <p>CH – Clays (highly plastic clays)</p> <p>GM – Caliche with Loam texture</p> <p>(Symbols based on Unified Soil Classification System.)</p>
Base Material Type	-	Caliche, Limestone, Gravel
Phase	-	Winter, Summer
Case	-	Case 1, Case 2, Case 3, Case 4, Case 5 (In some of the analyses, Cases 2 through 5 were grouped together as tests at cracked locations.)

Continuous Variables

These variables have to be numeric and are used for response variables or covariates. Values for each of these variables were either measured during testing or determined through existing structural drawings. Each of the variables are listed below along with their source:

Pavement Temperature	-	measured during testing
Total Transverse Cracks	-	estimated during visual condition surveys
Asphalt Thickness	-	determined using design drawings
Base Thickness	-	determined using design drawings
Subbase Thickness	-	determined using design drawings

INTERACTIONS

There were also some interactions of the variables which were reasonable to consider as part of this analysis. These interactions are listed below with a brief description of why each was considered.

Moisture Region * Temperature Region: Instead of only considering the regions separately, this interaction, when included, would capture the effect of the distinct climatic zones.

Pavement Temperature * Phase of Testing: This interaction was included to evaluate the effect different phases of testing have on the deflection measurements.

Base Thickness * Base Material: With the base layer being the primary focus of the study, this interaction explains the additional effect of the combination.

Pavement Temperature * Asphalt Thickness: As previously mentioned, temperature correction factors were not applied to the data due to the relatively thin asphalt surface layers. However, with such vast differences in the average temperature readings from the winter and summer phase (18 °C and 43 °C, respectively), this interaction would help in determining if the pavement temperatures have some effect.

Total Trans. Cracks * Asphalt Thickness; Total Trans. Cracks * Base Thickness: These interactions include the total estimated transverse cracks, which are the only available quantitative measure of the pavements' present condition. The significance of these interactions can be compared and could be used in determining which of the layers, if either, is correlated to the severity of cracking.

Total Trans. Cracks * Base Material: This interaction can also be useful in relating the severity of cracking to the base layer.

MODELS

The researchers used the SAS system for the statistical analysis. Based on the nature of the data, the researchers decided to use the SAS procedure **GLM**; General Linear Model.

The GLM procedure is particularly useful for data that is “unbalanced,” i.e., models where there are an unequal numbers of observations of the different combinations of class variables. GLM has the ability to provide tests for hypotheses for the effects of a linear model reasonably, with few missing cells.

Another feature of the GLM procedure that made it appropriate for this analysis is that it provides for certain degrees of interaction, including class by continuous and continuous by continuous effects. Interactions considering class by class effects are usually more meaningful, particularly in analyses such as these where the amount of data is limited. Most of the interactions that were considered were not class by class effects, and therefore, the researchers have to be cautious in drawing conclusions from the results that were

obtained in those situations.

After analyzing the results obtained, the researchers had to establish what the null hypotheses would be for each model. They defined the null and alternate hypothesis based on what they were trying to prove with the data; which was that the independent variables have some effect on the dependent variables. The hypotheses are defined below.

$$H_0 : \text{Effect of } \beta_k \text{ on } Y_i = 0;$$

$$H_a : \text{Effect of } \beta_n \text{ on } Y_i = 0;$$

β_n = Independent variable n

Y_i = Dependent variable i

Hence, a high F statistic yields a low probability of rejecting H_0 when, in fact, it should be accepted. Essentially, reject H_0 and accept H_a when encountering probabilities lower than some confidence level chosen. For this analysis, a confidence level of 0.1 was accepted.

STATISTICAL ANALYSIS

As with the structural evaluation, it was sometimes convenient to group together all data obtained at cracked locations. This reduced the levels of classes and typically improved the model. This also allowed for a general comparison of data from uncracked locations to all data from cracked locations. The researchers accomplished this by defining a dummy variable 'C', which was set equal to 1 for Case 1 and set equal to 0 otherwise. 'C' was then used as a class variable, and the case was deleted from the model.

The first analysis on each dependent variable included 'C' as a variable and utilized all of the data. This initial analyses did not include interactions. Tables 8.1 through 8.3 present the results of the analyses. The two columns give the probabilities, which are the basis for rejecting or accepting H_0 , associated with two different types of estimable functions. For the purpose of this discussion, the primary difference between the two types

is that Type I is order dependent while Type III is not.

A Type III analysis always considers the effect of that independent variable after the effect of all the other variables have been accounted. Therefore, a single analysis yielded all of the results in the second column. A Type I analysis considers the effect of each independent variable in the order that they appear in the model. We decided to perform

Table 8.1. Significance of Main Effects on Y_1

Variable	Type I Prob. > F	Type III Prob. > F
Base Material Type	0.0001	--
Moisture Region	0.4708	--
Temperature Region	0.0001	--
Phase (of testing)	0.0811	0.1462
Subgrade Soil Type	0.0001	--
C (case)	0.0091	0.0091
Pavement Temperature	0.0001	0.1439
Total Transverse Cracks	0.0001	--
Asphalt Thickness	0.0009	--
Base Thickness	0.4164	--
Subbase Thickness	0.0001	--

$$R^2 = 0.896165$$

Table 8.2. Significance of Main Effects on SCI

Variable	Type I Prob. > F	Type III Prob. > F
Base Material Type	0.0001	--
Moisture Region	0.8279	--
Temperature Region	0.0001	--
Phase (of testing)	0.0071	0.1632
Subgrade Soil Type	0.0001	--
C (case)	0.0294	0.0091
Pavement Temperature	0.0008	0.1439
Total Transverse Cracks	0.3413	--
Asphalt Thickness	0.0001	--
Base Thickness	0.0009	--
Subbase Thickness	0.0001	--

$R^2 = 0.844967$

Table 8.3. Significance of Main Effects on LTE

Variable	Type I Prob. > F	Type III Prob. > F
Base Material Type	0.0001	--
Moisture Region	0.0023	--
Temperature Region	0.6913	--
Phase (of testing)	0.0046	0.7616
Subgrade Soil Type	0.0313	--
C (case)	0.0001	0.0313
Pavement Temperature	0.0961	0.8870
Total Transverse Cracks	0.5713	--
Asphalt Thickness	0.0013	--
Base Thickness	0.0001	--
Subbase Thickness	0.6362	--

$R^2 = 0.742997$

an analysis, almost the opposite of Type I, introducing each of the independent variables first into the model. This would allow evaluation of the significance of that variable before any other effects were removed.

The R^2 given below each table is an indication of the confidence with which that model describes the variance in the dependent variable. Note that the R^2 is the same, regardless of the order in which the variables enter the model. The large number of blank cells in the Type III column is evidence of the limited data being used in an analysis with a large factorial.

The second series of analyses that were performed were similar to the previous analyses except that the interactions were included. Each interaction was introduced as the first variable into the models with no other interactions included. The R^2 's of each of the new models were then evaluated. If the R^2 was unchanged, it was assumed that including that specific interaction did not improve the model.

The following interactions did not appear to have any statistical influence on the model: Moisture Region*Temperature Region, Base Thickness*Base Material, Transverse Cracks*Base Material, Transverse Cracks*Asphalt Thickness, Transverse Cracks*Base Thickness. Tables from those analyses are not included in this report.

The remaining two interactions, Pavement Temperature*Phase and Pavement Temperature*Asphalt Thickness, did have some influence on the models. Tables 8.4 and 8.5 provide the R^2 for each of the new models and give the Type I and Type III probabilities for the interactions. Tables D.1 through D.6, included in Appendix D, provide all probabilities associated with each independent variable for each model.

Table 8.4. Significance of Effect of Pavement Temperature * Phase

Dependent Variable	Type I Prob. > F	Type III Prob. > F	R^2
Y ₁	0.0001	0.0120	0.909072
SCI	0.0001	0.0013	0.875125
LTE	0.0095	0.1727	0.752862

Table 8.5. Significance of Effect of Pavement Temperature * Asphalt Thickness

Dependent Variable	Type I	Type III	R ²
	Prob. > F	Prob. > F	
Y ₁	0.1093	0.0147	0.908385
SCI	0.0030	0.0007	0.878099
LTE	0.0105	0.0211	0.770219

After the analysis where each interaction was introduced separately, an analysis was performed where all of the interactions were included, although it was anticipated that only the same interactions would show significance. Only Type III results were considered in these analyses; those results are provided in Table 8.6.

Table 8.6. Significance of Main Effects and Interactions on Y₁, SCI, and LTE

Variable	Type III		
	Prob. > F		
	Y ₁	SCI	LTE
Base Material Type	--	--	--
Moisture Region	--	--	--
Temperature Region	--	--	--
Phase (of testing)	0.7509	0.3068	0.0182
Subgrade Soil Type	--	--	--
C (case)	0.6035	0.0056	0.0228
Pavement Temperature	0.2460	0.0236	0.0750
Total Transverse Cracks	--	--	--
Asphalt Thickness	--	--	--
Base Thickness	--	--	--
Subbase Thickness	--	--	--
Moist. Reg. * Temp. Reg.	--	--	--
Pavm't. Temp. * Phase	0.0054	0.0001	0.1243
Base Thick. * Base Material	--	--	--
Pavm't. Temp * Asp. Thick.	0.0065	0.0001	0.0165
Trans. Cracks * Base Material	--	--	--
Trans. Cracks * Asp. Thick.	--	--	--
Trans. Cracks * Base Thick.	--	--	--

R² = 0.92249 (for Y₁); R² = 0.911169 (for SCI); R² = 0.92249 (for LTE)

Once the analyses using all data were complete, the researchers decided to perform some analyses on specific samples of our data. Case was reintroduced as a variable, and an analysis was performed on a case by case basis. For this study, however, we decided that the only meaningful sample for this analysis would be Case 1 data.

This was because Case 1 configurations were the only drops performed at areas free of distress. Researchers were uncertain how, exactly, cracks would affect the deflection measurements, but as is evident from the structural evaluation, the cracks do have some effect. Measurements from other locations, therefore, would experience an even greater amount of variability and produce inconsistent results. Once again, only Type III probabilities were considered. Results from these analyses are provided in Table 8.7.

Table 8.7. Significance of Main Effects and Interactions on Y_1 , SCI, and LTE Using Only Case 1 Data

Variable	Type III Prob. > F		
	Y_1	SCI	LTE
Base Material Type	--	--	--
Moisture Region	--	--	--
Temperature Region	--	--	--
Phase (of testing)	0.0676	0.1775	0.2204
Subgrade Soil Type	--	--	--
Pavement Temperature	0.0673	0.2077	0.2678
Total Transverse Cracks	--	--	--
Asphalt Thickness	--	--	--
Base Thickness	--	--	--
Subbase Thickness	--	--	--

$$R^2 = 0.976788 \text{ (for } Y_1\text{); } R^2 = 0.957627 \text{ (for SCI); } R^2 = 0.956990 \text{ (for LTE)}$$

CHAPTER 9. SYNTHESIS OF RESULTS

The objectives of this research are clearly stated in Chapter 1. These objectives are centered around the development of improved construction and design specifications for flexible bases. The development of the improved design and construction specifications was based primarily on laboratory testing to define how the thermal and moisture susceptibility of flexible bases can be efficiently and effectively measured in specification type testing. This effort was successful. However, we also placed a major emphasis in this research on the collection of field performance data in terms of deflection measurements, GPR measurements, and visual distress measurements. A field testing protocol using the FWD was successfully developed to evaluate the structural effects of transverse cracking. An unstated objective of the research effort was to synthesize the coordinated laboratory and field efforts in order to provide a protocol for laboratory testing verified by nondestructive field testing.

Although both the laboratory and field studies were successful in the development and application of important information in their own right, the synthesis effort was only marginally successful. A major reason for this marginal success is that in order to properly coordinate laboratory and field testing, the testing methodology must be developed, to a substantial level, prior to initiating the coordinated effort. A significant part of the study was spent developing the testing protocol and evaluating the sensitivity of the tests. On the other hand, field testing must be done with enough frequency and over a long enough time period to measure the effects of significant seasonal changes and significant episodes of moisture accumulation and thermal activity. Therefore, in this project, it was necessary to select project field test sites or case histories before the test protocol could be fully developed and before knowing the sensitivity of the testing protocol. This means that the window of time during which the lab and field testing protocols were fully developed and during which they could be evaluated on field “case history” projects to adequately assess their sensitivity to important variables was very small — perhaps too small.

This research has provided laboratory tests and a testing and evaluation protocol that can effectively be used to enhance design and construction specifications for the use of aggregate bases. This testing can help to assure that bases, which are highly sensitive to thermal and moisture effects, are either not selected or are altered or treated in a manner to reduce thermal and moisture sensitivity

to an acceptable level. This research has provided a field testing protocol using the FWD and GPR which has the potential to define the structural capacity and deficiencies in flexible bases due to moisture and thermal damage. An important step at this time is to establish a list of test pavements with established flexible base moisture and/or thermal-moisture related deficiencies in selected districts that can be monitored over a long period of time. The flexible bases represented in the field case history studies should have similar properties (DV, suction, etc.) to the aggregates deemed problematic in the laboratory study and should cover the range of these properties. The selected field case history pavements must then be evaluated using the FWD and GPR techniques described in this report. This evaluation must occur over a sufficient period of time and through significant seasonal and weather episode variations. FWD and GPR testing should be done several times a year over at least a two-year period.

In this proposed implement or monitoring study, it is imperative to test exactly the same material in that lab that was used in the field for the flexible base. It is equally important to monitor the field sections over at least a two-year period and frequently enough to assess the effects of significant swings in moisture state and significant thermal effects. The experiment design for the field testing and the approach for selecting the case history site locations presented in Chapters 3, 4, and 6 should be followed.

CHAPTER 10. SUMMARY AND CONCLUSIONS AND RECOMMENDATIONS

GUIDELINES FOR DESIGN OF FLEXIBLE BASES

As discussed in detail in Chapter 5, the design and construction specifications for flexible bases are discussed in item 247 of the *Standard Specifications for Construction of Highways, Streets and Bridges* (1995). The design aspects of these specifications adequately address: (1) general classification of geological type and degree of crushing (Types A through D), (2) strength according to Tex-117-E based on the Texas triaxial test, (3) gradation limits (Tex-110-E), (4) Atterberg limits (Tex-104-E and Tex-106-E), (5) wear resistance according to the wet ball mill test (Tex-116-E), and (6) linear shrinkage (Tex-107-E). These specifications are based on a considerable experience base, and the Texas triaxial test remains one of the best and most realistic methods of characterizing strength properties of aggregate bases available in any testing methodology. The construction aspects of these specifications address: (1) subgrade preparation, (2) application of the first flexible base course and successive flexible base courses, and (3) compaction of the flexible base to the density requirements of Tex-113-E. This study has identified a testing and analysis protocol to supplement the item 247 design specifications.

The first test recommended to supplement the item 247 design specifications as outlined in the above paragraph is the *dielectric value (DV)* measurement. In this test, the DV is measured during a 250-hour period of capillary soak of a 150 mm diameter by 300 mm high sample compacted at optimum moisture content according to Tex-113-E. The sample is “cured” in an oven at 60 °C for 24 hours before it is subjected to the 250-hour period of capillary soak. The dielectric value is measured by a probe at the surface of the sample. Therefore, the surface DV is not an average DV within the sample but is a property specific to the test geometry. The 300 mm sample height was selected as a representative thickness of a typical aggregate base. The test geometry specificity is indeed a present limitation of this test. We would much prefer a test that evaluates a true material property which is independent of test configuration. This is an area of needed improvement and should be pursued in future research.

A plastic container was used for fabrication and testing of the initial specimens in this study; it is, however, clear that the container must be rigid enough to resist significant deflection or

permanent deformation during sample compaction and fabrication. A plastic container was selected partially because it does not interfere in any way with the DV probe. However, further analysis is necessary to insure that the plastic casing is stiff enough not to deform during compaction.

The dielectric value determined at the end of the 250-hour period or at the time that the value reaches a maximum or asymptotic level is the design value - designated DV_{max} . This value must not exceed the criteria established in Table 5.3 of Chapter 5. If DV_{max} exceeds the upper limit deemed acceptable in Table 5.3, then the base is too moisture sensitive for use as an effective flexible base. The authors recommend an upper limit of 10 for DV_{max} . The testing program on 24 different aggregate sources from seven districts determined that the capillary soak test with DV monitoring is reproducible, precise, and efficient for routine specification testing.

If the maximum dielectric value is within criteria, then the next step to supplement the item 247 design specifications is to determine the limits on the construction moisture content for the flexible base. This approach is based on the ability of a specific aggregate to gain and hold water through its suction potential and a critical level of moisture that will aggravate expansion damage in a freeze-thaw environment. The protocol involves determining a relationship between the water content of the aggregate and the suction. This can be done by direct testing and measurement, as described in Chapter 5 on pages 5.82 through 5.85, or it can be done indirectly through a correlation between DV_{max} and the critical pF, as described in the same paginated section of Chapter 5. Both methods described in Chapter 5 can effectively define the critical or threshold moisture content that an aggregate should never exceed if it has the potential of being subjected to a freezing environment. This critical or threshold moisture content is associated with a pF (suction) of the aggregate equal to 4.0. In fact, the water content of the aggregate during construction compaction or afterward (while achieving in situ equilibrium) should never be high enough to push the pF above 4.0.

Once the critical or threshold water content is determined for the specific aggregate, the next step is to determine how that construction moisture content will be affected by the environment. This is done by determining the suction of the natural subgrade soil, which is a function of the soil type (secondarily) and the Thornthwaite Index (primarily). Chapter 5, pages 5.82 through 5.85, describes two methods to determine the subgrade equilibrium suction. The indirect or approximate method is based simply on selecting an approximate map location of the project and from this location identifying the Thornthwaite Index and associated equilibrium pF of the subgrade in that region. The

more exact and more precise method is to construct a pF versus field moisture content relationship, as described on pages 5.79 through 5.82. From this relationship, a pF seasonal profile can be established for the subgrade. This is accomplished by measuring the moisture content of the subgrade throughout the year to obtain a weighted average moisture content or a critical high moisture content. From this, a weighted average pF or a critical low pF can be established by the moisture versus pF relationship already established.

A DV versus moisture content relationship for the aggregate can be established during the development of the moisture density relationship (Tex-113-E). This can be achieved by simply using the DV probe to record the surface DV on each sample used to develop the moisture - density curve. This DV versus moisture relationship can be used for quality control field testing to monitor the constructed aggregate base.

SELECTION OF ALTERATION OR STABILIZATION STRATEGIES TO ELIMINATE OR MITIGATE MOISTURE AND THERMAL PROBLEMS IN FLEXIBLE BASES

Texas triaxial strength testing coupled with DV testing can effectively be used to assess the potential to alter or stabilize a specific aggregate base and therefore upgrade its ability to resist moisture or thermally induced damage. The protocol for this is simple and employs the same protocol as discussed in the preceding paragraphs. The effectiveness of the additive or alteration technique is judged on the basis of its ability to alter DV_{max} and triaxial strength values so that they meet specification requirements. As pointed out in Chapter 5, it is critical to consider the appropriate mix design and long-term curing protocols for the stabilizer in question in order to successfully evaluate that stabilization process. This point is illustrated for a lime-fly ash stabilized aggregate in Chapter 5. In the example, the DV is only slightly altered after an accelerated curing period of 7 days at 40 °C. However, with additional, long-term curing, the DV is significantly reduced to an acceptable level.

FIELD TESTING PROTOCOL TO EVALUATE THE STRUCTURAL EFFECTS OF TRANSVERSE CRACKING

The major shortcoming of this study, as identified in Chapter 9, is the lack of field data required to fully assess the effects of different variables (subgrade, flexible base, pavement

structural, and climatic) on the degree and severity of thermally induced cracks in the flexible bases as determined by field measurements. The difficulties caused by these limited data are reflected in the analysis of field testing data as discussed in Chapter 8.

Chapter 9, however, discusses a recommended approach to orchestrate field, “case history” testing to evaluate and verify laboratory and field testing protocols developed in this study.

During the field FWD structural evaluations, the following conclusions were drawn:

1. For project level FWD evaluations, it is important to consider more than just one deflection parameter, i.e., Y_1 , SCI, BCI, or LTE. The maximum deflection, Y_1 , is the most meaningful value if examined independently and should be one of the parameter considered in a field deflection study.
2. The parameters selected for the FWD analysis must reflect the load transfer efficiency of the critical pavement layers: surface and base. This should be based on a load transfer efficiency factor (LTE). This value is the percentage of load transferred across the crack as defined by the ratio of the maximum deflection (Y_1) to the second deflection (Y_2) expressed as a percentage. The methodology for performing the LTE evaluation is explained in Chapters 6 and 7.

RECOMMENDATIONS

The authors recommend implementation of the supplementary laboratory tests to item 247 as discussed in the first section of this chapter. These tests are expedient, reproducible, and precise and are meaningfully related to moisture sensitivity and thermal sensitivity of flexible bases. A recommended approach for the synthesis of field FWD and GPR data with laboratory data on selected flexible bases within selected pavement sections in selected climatic regions and the field verification of the laboratory testing protocol is presented in Chapter 9, pages 9.1 through 9.2.

The authors also recommend additional development of the laboratory capillary soak test with DV measurement so that sample geometry can be eliminated from the test and a DV as a material property can be measured from the test. The authors also suggest a more detailed investigation into the effects of the required stiffness of the mold used in the capillary soak test. This container should be stiff enough not to deform or warp during compaction.

Finally, the authors recommend an extended study on the effects of long-term curing of chemically stabilized aggregate base materials. Evidence is presented that short-term curing, even if accelerated, for lime and lime-fly ash mixtures, may not adequately reveal long-term dielectric properties. This is because the pozzolanic reactions can be significantly longer than cementitious - hydration reactions and cannot necessarily be mimicked by short-term, accelerated testing. Since slow pozzolanic reactions can be beneficial in the stabilization and upgrade of flexible base material (i.e., as it may relate to reduced shrinkage cracking potential), this study is important.



REFERENCES

- Adu-Osei, Alex, Lytton, R. L., Little, D. N., and Allen, J. J., (1997), "Structural Evaluation of Unbound Aggregate Bases, Volume I: Literature Synthesis and Testing and Characterization Protocol," ICAR Research Report.
- Aitchison, G. D., (1965), Ed., "Moisture Equilibria and Moisture Changes in Soil Beneath Covered Areas," Butterworths, Sydney, Australia.
- Allen, J. J., (1973), "The Effect of Non-Constant Lateral Pressures on Resilient Response of Granular Materials," Ph.D. Dissertation, University of Illinois at Urbana-Champaign, Illinois.
- Anderson, D. M., and Tice, A. R. (1972), "Predicting Unfrozen Water Contents in Frozen Soils from Surface Area Measurements," *Frost Action in Soils*. Highway Research Record 393, Highway Research Board, Washington, D.C., pp.12-18.
- Anderson, D. M., and Morgenstern, N. R., (1973), "Physics, Chemistry, and Mechanics of Frozen Ground: A Review," *Proceedings, Permafrost 2nd International Conference*, Yakutsk, U.S.S.R., pp. 257-288.
- Anderson, D. M., Pusch, R., and Penner, E., (1978), "Physical and Thermal Properties of Frozen Ground," *Geotechnical Engineering for Cold Regions*, O. B. Andersland, and D. M. Anderson, eds., pp. 37-102.
- Anderson, D. M., and Williams, P. J., (1985), Eds., "Freezing and Thawing of Soil-Water Systems: A State of the Practice Report," Technical Council on Cold Regions Engineering Monograph, ASCE, New York, New York.
- Anderson, T. M., (1989), "Frost Heave Properties of Soils," In *Frost in Geotechnical Engineering, Volume I, International Symposium*, Saariselka, Finland, March 13-15, 1989, Ed. by Hans Rathmayer, Espoo 189, pp. 105-125.
- Black, W. P. M., and Croney, D., (1957), "Pore Water Pressure and Moisture Content Studies Under Experimental Pavements," *Proceedings, 4th International Conference on Soil Mechanics and Foundation Engineering*, Vol. 2, pp. 94-103.
- Button, Joe, and Little, D.N., (1997), "Evaluation of Unstabilized Glauconite Aggregate from the Lufkin District," Research Report 3901-1F, Texas A&M University, College Station, Texas.

Carpenter, S. H., Lytton, R. L., and Epps, J. A., (1974), "Environmental Factors Relevant to Pavement Cracking in West Texas," *Research Report No. TTI-2-8-73-18-1*, Texas Transportation Institute, College Station, Texas.

Carpenter, S. H., and Lytton, R. L., (1975), "Thermal Activity of Base Course Material Related to Pavement Cracking," *Research Report No. TTI-2-8-73-18-2*, Texas Transportation Institute, College Station, Texas.

Carpenter, S.H., and Lytton, R. L., (1977), "Thermal Cracking in West Texas," Texas Transportation Institute, Texas A&M University, *TxDOT Research Report 18-4*.

Dempsey, B. J., Herlache, W. A., and Patel, A. J., (1986), "Climatic-Materials-Structural Pavement Analysis Program," *Transportation Research Record 1095*, Transportation Research Board, pp. 111-123.

Distress Identification Manual for the Long-Term Pavement Performance Studies, (1990), SHRP-LTTP/FR-90-001, Strategic Highway Research Program (SHRP), Washington, D.C.

Dillon, H. B., and Andersland, O. B., (1966), "Predicting Unfrozen Water Contents in Frozen Soils," *Can. Geotech. J.*, 3(2), pp. 53-60.

Edlefsen, N. E., and Anderson, A. B. C., (1943), "Thermodynamics of Soil Moisture," *Hilgardia*, 15(2), pp. 31-298.

Falling Weight Deflectometer Operator's Manual, (1996), TxDOT.

Fredlund, D. G., and Rahardjo, H., (1993), "Soil Mechanics for Unsaturated Soils," John Wiley & Sons, New York, New York.

Gay, D. A., (1994), "Development of a Predictive Model for Pavement Roughness on Expansive Clay," Ph. D. Dissertation, Texas A&M University, College Station, Texas.

General Soils Map of Texas, published by Texas Agricultural Experiment Station, Texas A&M University, (1973).

Hamilton, A. B., (1966), "Freezing Shrinkage in Compacted Clays," *Can. Geotech. J.*, 3(1), pp. 1-17.

Ho, D. Y. F., Fredlund, D. G., and Rahardjo, H., (1992), "Volume Change Indices During Loading and Unloading of an Unsaturated Soil," *Can. Geotech. J.*, 29(2), pp. 195-207.

Hudec, P.P., and Achampong, F., (1994), "Improving Aggregate Quality by Chemical Treatment," *Report on the 2nd International Aggregates Symposium*, Erlangen, Germany, Ed. By G. W. Luttwig, pp. 135 - 146.

Hudson, C. S., (1906), "The Freezing of Pure Liquids and Solutions Under Various Kinds of Positive and Negative Pressure and the Similarity Between Osmotic and Negative Pressure," *Physical Review*, 22(5), pp. 257-264.

Jayatilaka, R., Gay, D. A., Lytton, R. L., and Wray, W. K., (1993), "Effectiveness of Controlling Pavement Roughness Due to Expansive Clays with Vertical Moisture Barriers," *Research Report 1165-2F*, Texas Transportation Institute, College Station, Texas.

Jumikis, A. R., Jr., (1966), "Thermal Soil Mechanics," Rutgers University Press, New Brunswick, New Jersey.

Jumikis, A. R., Jr., (1977), *Thermal Geotechnics*. Rutgers University Press, New Brunswick, New Jersey.

Jumikis, A.R., (1978), *Thermal Geotechnics*, Rutgers University Press, New Jersey.

Kersten, M. S., (1949), "Thermal Properties of Soils," Bulletin No. 28, Engineering Experiment Station, Institute of Technology, University of Minnesota, Minneapolis, Minnesota.

Konrad, K. M., and Morgenstern, N. R., (1980), "A Mechanistic Theory of Ice Formation in Fine Grained Soils," *Can. Geotech. J.* pp. 473-486.

Kujjala, K., (1991), "Factors Affecting Frost Susceptibility and Heaving Pressure in Soils," *Acta University Oul.*, C 57, pp. 99.

Ladanyi, B., and Shen, M., (1989), "Mechanics of Freezing and Thawing in Soils," In *Frost in Geotechnical Engineering, Volume I International Symposium*, Saariselka, Finland, pp. 13-15, Ed. by Hans Rathmayer, Espoo., pp. 73-103.

Little, D.N., (1990), "Back-Calculated Moduli of Aggregate Base Courses, Stabilized with Low Percentages of Lime," Special Technical Publication (STP) 1135 American Society for Testing Materials (ASTM), Symposium on Innovative Use of Limestone.

Little, D. N., Lytton, R. L., and Williams, D., (1995), "Propagation and Healing of Microcracks in Asphalt Concrete and Their Contributions to Fatigue," *Asphalt Science and Technology*, pp.149-195.

Lytton, R. L., (1994), "Prediction of Movement in Expansive Clays," *Vertical and Horizontal Deformations of Foundations and Embankments*, Geotech. Spec. Publ. No. 40, A. T. Yeung and G. Y. Felio, Eds., ASCE, New York, New York, 2, pp. 1827-1845.

Marinho, F. A. M., and Chandler, R. J., (1993), "Aspects of the Behavior of Clays on Drying," *Unsaturated Soils*, S. L. Houston and W. K. Wray, Eds., Geotech. Spec. Publ. No. 39, ASCE, New York, New York, pp. 77-90.

Michalak, C.H., and T. Scullion, (1995), *Modulus 5.0: User's Manual*, Research Report 1987-1, Texas Transportation Institute, Texas A&M University.

Miller, R. D., (1972), "Freezing and Heaving of Saturated and Unsaturated Soils," Frost Action in Soils, *Highway Research Record 393*, Highway Research Board, Washington, D.C., pp.1-11.

Miller, R. D., (1973), "Soil Freezing in Relation to Pore Water Pressure and Temperature," *Proceedings, Permafrost 2nd International Conference*, Yakutsk, U.S.S.R., pp- 344-352.

Mindess, S., and Young, J. F., (1981), "Other Properties of Concrete," *Concrete*, Prentice Hall, Englewood Cliffs, New Jersey, pp. 521-543.

Mitchell, J. K., (1993), "Fundamentals of Soil Behavior," 2nd ed., John Wiley & Sons, New York, New York.

PMIS Rater's Manual, TxDOT, (1995).

Petterson, D. E., and Smith, M. W., (1981), "The Measurement of Unfrozen Water Content by Time Domain Reflectometry: Results from Laboratory Tests," *Can. Geotech. J.*, 18(1), pp. 131-144.

Perrone, E., Dossey, T., and Hudson, W. R, (1994), "Network-Level Deflection Data Collection for Rigid Pavements," Research Report 1908-3, CTR, University of Texas at Austin.

Ruiz-Herta, J.M., and McCullough, B.F, (1994), "Development of a Jointed Concrete Pavement Database for the State of Texas," Research Report 1342-2, CTR, University of Texas at Austin.

Saarenketo, T., and Little, D., (1995), Unpublished report, Texas Transportation Institute, Texas A&M University.

Saarenketo, T., and Scullion, T., (1995), "Using Electrical Properties to Classify the Strength Properties of Base Course Aggregates," Texas Transportation Institute, Report 1341-2.

Schofield, R. K., (1935), "The pF of the Water in Soil," *Trans. 3rd International Congress of Soil Science*, Oxford, 2, pp. 37-48.

Shanin, M.Y., and McCullough, B.F., (1972), "Prediction of Low Temperature and Thermal Fatigue Cracking in Flexible Pavements," CTR, University of Texas at Austin, TxDOT Research Report 123-14.

Siddharthan, R., Sebaaly, P. E., and Javaregowda, M., (1972), "Influence of Statistical Variation in FWDs on Pavement Analysis," TRB No. 1377, Transportation Research Board, Washington, D.C.

Spaans, E. J. A., and Baker, J. M., (1996), "The Soil Freezing Characteristic: Its Measurement and Similarity to the Soil Moisture Characteristic," *Soil Sci. Soc. Am. J.*, 60(1), pp. 13-19.

Thorntwaite, C. W., (1948), "An Approach Toward a Rational Classification of Climate," *The Geophysical Review*, Vol. 38. No. 1, pp. 55 -94.

Tutumlur, E., Garg, N., and Thompson, M. R., (1997), "Granular Material Radial Deformation Measurements Using a Circumferential Extensometer in Repeated Load Triaxial Testing," 77th Annual Meeting of the Transportation Research Board Specialty Session on "Local Strain Measurement in Laboratory Determination of Soil and Rock Stiffness," Soil and Rock Properties Committee, A2L02, TRB, National Research Council, Washington, D.C.

Uddin, W., Meyer, A. H., Hudson, W. R., and Stokoe, K. H. II., (1985), "A Structural Evaluation Methodology for Pavements Based on Dynamic Deflections," Research Report 387-1, CTR 01-4.

Urry, D. W., (1995), "Elastic Biomolecular Machines," *Scientific American*, pp. 64-69.

Uzan, J., (1985), "Characterization of Granular Material," *Transportation Research Record*, 1022, Transportation Research Board, National Research Council, Washington, D.C.

Verbeck, G. J., and Hass, W. E., (1951), "Dilatometer Method for Determination of Thermal Coefficient of Expansion of Fine and Coarse Aggregate," *Proceedings 30th Annual Meeting*, Highway Research Board, Washington, D.C., pp.187-193.

Williams, P. J., (1963), "Suction and Its Effects in Unfrozen Water of Frozen Soils," *Proceedings Permafrost International Conference*, Lafayette, pp. 225-229.

Williams, P. J., (1964), "Unfrozen Water Content of Frozen Soils and Soil Moisture Suction," *Géotechnique*, London, England, 14(3), pp. 231-246.

Woodburn, J. A., Holden, J. C., and Peter, P., (1993), "The Transistor Psychrometer: A New Instrument for Measuring Soil Suction," *Unsaturated Soils*, S. L. Houston, and W. K. Wray, Eds., Geotech. Spec. Publ. No. 39, ASCE, New York, New York, pp. 91-102.

Yong, R. N., (1963), "Soil Freezing Considerations in Frozen Soil Strength," *Proceedings Permafrost International Conference*, Lafayette, Louisiana, pp. 315-319.

Yong, R. N., (1965), "Soil Suction Effects on Partial Soil Freezing," *Highway Research Record*, No. 68, Highway Research Board, Washington, D.C., pp. 31-42.

Yong, R. N., and Warkentin, B. P., (1966), "Introduction to Soil Behavior," The Macmillian Company, New York, Collier-Macmillan Limited, London.

APPENDIX A
PROJECT INFORMATION SHEET

Project Code: AM1
District: Amarillo **County:** Potter **Highway:** US 87/287
Control - Section - Job: 41 - 7 - 41 **Direction:** NB
Facility Type: Divided highway, two lanes in each direction
Reference Marker - Project: Begin at Sta 1365+50, end at Sta1618+50
Reference Marker - Test Section: Mile post 136, (after FM 2176 overpass)
Project Length (km): 7.67 (4.76 mile)
Completion Date: October 1968

Pavement Structure:

Layer	Asphalt	Base	Subbase	Subgrade
Thickness	1.5"	8"	4"	6"
Material Type	N/A	Gravel	Gravel	N/A
Stabilization	N/A	N/A	N/A	1.5% Lime

Figure A.1. Identification and design information for project AM1

Project Code: AM2
District: Amarillo **County:** Randall **Highway:** FM 1541
Control - Section - Job: 1480 - 2 - 15 **Direction:** NB/SB
Facility Type: Undivided highway, one lane in each direction
Reference Marker - Project: Between Loop 335 and SH 217 (Sta 185+00 to Sta 25+14)
Reference Marker - Test Section: End near FM 1151
Project Length (km): 15.4 (9.55 mile)
Completion Date: June 1987

Pavement Structure:

Layer	Asphalt	Base	Subbase	Subgrade
Thickness	1.5"	11"	N/A	N/A
Material Type	N/A	Caliche	N/A	N/A
Stabilization	N/A	N/A	N/A	N/A

Figure A.2. Identification and design information for project AM2

Project Code: AB1
District: Abilene **County:** Taylor **Highway:** US 83/84
Control - Section - Job: 34 - 1 -36 **Direction:** SB
Facility Type: Divided highway, two lanes in each direction
Reference Marker - Project: Begin at Sta 652+77, end at Sta 1211+82
Reference Marker - Test Section: Mile post 338 (after Clark Road intersection)
Project Length (km): 16.45 (10.2 miles)
Completion Date: August 1966
Pavement Structure:

Layer	Asphalt	Base	Subbase	Subgrade
Thickness	2"	8"	6"	N/A
Material Type	N/A	Limestone	Unknown	N/A
Stabilization	N/A	N/A	N/A	N/A

Figure A.3. Identification and design information for project AB1

Project Code: AB2
District: Abilene **County:** Taylor **Highway:** US 83 BU
Control - Section - Job: 33 - 8 - 28 **Direction:** NB
Facility Type: Undivided highway, two lanes in both direction
Reference Marker - Project: Begin at Sta 147+80, end at Sta 603+30
Reference Marker - Test Section: End near IH 20 overpass
Project Length (km): 13.6 (8.5 mile)
Completion Date: January 1991
Pavement Structure:

Layer	Asphalt	Base	Subbase	Subgrade
Thickness	1.5"	12"	N/A	N/A
Material Type	N/A	Limestone	N/A	N/A
Stabilization	N/A	N/A	N/A	N/A

Figure A.4. Identification and design information for project AB2

Project Code: SA1
District: San Angelo **County:** Tom Green **Highway:** US 67
Control - Section - Job: 77 - 6 - 54 **Direction:** NB
Facility Type: Divided highway, two lanes in each direction
Reference Marker - Project: Begin at Loop 306 (Sta 93+75 to Sta 274+94)
Reference Marker - Test Section: Between Loop 306 and Arden Road
Project Length (km): 5.5 (3.43 mile)
Completion Date: October 1983
Pavement Structure:

Layer	Asphalt	Base	Subbase	Subgrade
Thickness	2"-3"	12.5"	N/A	8"
Material Type	N/A	Limestone	N/A	N/A
Stabilization	N/A	N/A	N/A	2% Lime

Figure A.5. Identification and design information for project SA1

Site Code: SA2
District: San Angelo **County:** Tom Green **Highway:** SH 208
Control - Section - Job: 454 - 2 - 28 **Direction:** NB
Facility Type: Undivided, two lanes in each direction
Reference Marker - Project: Between 19th and 28th Streets, (Sta 00+00 to Sta 37+50)
Reference Marker - Test Section: End before 28th street, TxDOT area engineer office
Project Length (km): 1.6 (1 mile)
Completion Date: December 1977
Pavement Structure:

Layer	Asphalt	Base	Subbase	Subgrade
Thickness	1.5"	6.5"	N/A	4"
Material Type	N/A	Limestone	N/A	N/A
Stabilization	N/A	N/A	N/A	N/A

Figure A.6. Identification and design information for project SA2

Project Code: AT1
District: Atlanta **County:** Bowie **Highway:** SH 08
Control - Section - Job: 60-2-23 **Direction:** NB/SB
Facility Type: Undivided highway, one lane in each direction
Reference Marker - Project: From IH 30 to Bowie county line
Reference Marker - Test Section: One mile north from IH 30 intersection
Project Length (km): 5.98 (3.74 mile)
Completion Date: April 1993
Pavement Structure:

Layer	Asphalt	Base	Subbase	Subgrade
Thickness	2"	10"	N/A	N/A
Material Type	N/A	Gravel	N/A	N/A
Stabilization	N/A	1% Lime + 2% Flyash	N/A	N/A

Figure A.7. Identification and design information for project SA2

Project Code: YO1
District: Yoakum **County:** Fayette **Highway:** US 290
Control - Section - Job: 0114 - 08 - 022 **Direction:** WB
Facility Type: Divided, two lanes in each direction
Reference Marker - Project: Begin at Lee/Fayette county line
Reference Marker - Test Section: Sta 152+10, Reference marker 654+0.53, MP 6.559
Project Length (km): 11.2 (7 mile)
Completion Date: August 1991
Pavement Structure:

Layer	Asphalt	Base	Subbase	Subgrade
Thickness	2.5"	8"	12"	6"
Material Type	ACP	Limestone	Gravel	N/A
Stabilization	N/A	N/A	1.5% Lime	4% Lime

Figure A.8. Identification and design information for project YO1

Project Code: YO2
District: Yoakum **County:** Victoria **Highway:** LP 463
Control - Section - Job: 2350 - 1 - 10 **Direction:** EB/WB
Facility Type: Undivided highway, one lane in each direction
Reference Marker - Project: 590+0.860/14.860 (from US 77 to US 59)
Reference Marker - Test Section: West end 691+50, East end 907+90
Project Length (km): 9.55 (5.97 mile)
Completion Date: Will be provided later
Pavement Structure:

Layer	Asphalt	Base	Subbase	Subgrade
Thickness	1.5"	14"	N/A	8"
Material Type	N/A	Gravel	N/A	N/A
Stabilization	N/A	2% Lime	N/A	5% Lime

Figure A.9. Identification and design information for project YO2

Project Code: PH1
District: Pharr **County:** Hidalgo **Highway:** US 281
Control - Section - Job: 255 - 8 - 52 **Direction:** NB
Facility Type: Divided highway, two lanes in each direction
Reference Marker - Project: Begin at Sta 93+75, end at Sta 274+94
Reference Marker - Test Section: Begin before Trinten Road overpass
Project Length (km): 7.3 (4.56 mile)
Completion Date: Year 1978
Pavement Structure:

Layer	Asphalt	Base	Subbase	Subgrade
Thickness	2"	10"	N/A	12"
Material Type	N/A	Caliche	N/A	N/A
Stabilization	N/A	N/A	N/A	3% Lime

Figure A.10. Identification and design information for project PH1

Project Code: PH2
District: Pharr **County:** Hidalgo **Highway:** FM 2128
Control - Section - Job: 2450 - 1 - 12 **Direction:** EB
Facility Type: Undivided highway, two lanes in each direction
Reference Marker - Project: Begin at St 797+22, end at Sta 1033+16
Reference Marker - Test Section: Between US 281 and US 281 BU
Project Length (km): 7.15 (4.47 mile)
Completion Date: May 1987
Pavement Structure:

Layer	Asphalt	Base	Subbase	Subgrade
Thickness	2"	8"	N/A	12"
Material Type	N/A	Caliche	N/A	N/A
Stabilization	N/A	1%	N/A	3% Lime

Figure A.11. Identification and design information for project PH2

APPENDIX B

CONDITION SURVEY RESULTS



Tables B.1 to B.22 show the distribution of distresses among low, medium, and high severity levels; Table B.23 shows the distribution of half and full transverse cracks for all projects.

Table B.1. Distress distribution in outside lane in Project AM1

Distress Severity Levels	Transverse Cracking (No. / km)	Longitudinal Cracking (Lin. m / m)	Random Cracking (No. / km)	Alligator Cracking (% wheel path)
Low	200	0.472	214	7.8
Moderate	93	0.072	93	2.4
High	0	0	0	0
Total	293	0.544	307	10.2

Table B.2. Distress distribution in inside lane in Project AM1

Distress Severity Levels	Transverse Cracking (No. / km)	Longitudinal Cracking (Lin. m / m)	Random Cracking (No. / km)	Alligator Cracking (% wheel path)
Low	53	0	0	0
Moderate	0	0	0	0
High	0	0	0	0
Total	53	0	0	0

Table B.3. Distress distribution in outside lane in Project AM2

Distress Severity Levels	Transverse Cracking (No. / km)	Longitudinal Cracking (Lin. m / m)	Random Cracking (No. / km)	Alligator Cracking (% wheel path)
Low	0	0	53	3.40
Moderate	67	0.248	53	0
High	26	0.032	0	0
Total	93	0.28	106	3.40

Table B.4. Distress distribution in inside lane in Project AM2

Distress Severity Levels	Transverse Cracking (No. / km)	Longitudinal Cracking (Lin. m / m)	Random Cracking (No. / km)	Alligator Cracking (% wheel path)
Low	13	0	0	0
Moderate	27	0	0	0
High	27	0.02	0	0
Total	67	0.02	0	0

Table B.5. Distress distribution in outside lane in Project AB1

Distress Severity Levels	Transverse Cracking (No. / km)	Longitudinal Cracking (Lin. m / m)	Random Cracking (No. / km)	Alligator Cracking (% wheel path)
Low	40	0	27	0
Moderate	94	0	0	0
High	0	0	0	0
Total	134	0	27	0

Table B.6. Distress distribution in inside lane in Project AB1

Distress Severity Levels	Transverse Cracking (No. / km)	Longitudinal Cracking (Lin. m / m)	Random Cracking (No. / km)	Alligator Cracking (% wheel path)
Low	13	0	0	0
Moderate	40	0	0	0
High	0	0	0	0
Total	53	0	0	0

Table B.7. Distress distribution in outside lane in Project AB2

Distress Severity Levels	Transverse Cracking (No. / km)	Longitudinal Cracking (Lin. m / m)	Random Cracking (No. / km)	Alligator Cracking (% wheel path)
Low	54	0.056	80	3.40
Moderate	173	0.192	80	0
High	40	0.024	0	0
Total	267	0.272	160	3.40

Table B.8. Distress distribution in inside lane in Project AB2

Distress Severity Levels	Transverse Cracking (No. / km)	Longitudinal Cracking (Lin. m / m)	Random Cracking (No. / km)	Alligator Cracking (% wheel path)
Low	0	0.52	13	0
Moderate	107	0.104	13	2
High	27	0	0	0
Total	134	0.624	26	2

Table B.9. Distress distribution in outside lane in Project SA1

Distress Severity Levels	Transverse Cracking (No. / km)	Longitudinal Cracking (Lin. m / m)	Random Cracking (No. / km)	Alligator Cracking (% wheel path)
Low	40	0.72	80	6
Moderate	0	0.34	13	0
High	0	0	0	0
Total	40	1.06	93	6

Table B.10. Distress distribution in inside lane in Project SA1

Distress Severity Levels	Transverse Cracking (No. / km)	Longitudinal Cracking (Lin. m / m)	Random Cracking (No. / km)	Alligator Cracking (% wheel path)
Low	40	0.32	0	0
Moderate	0	0.2	0	10
High	0	0	0	0
Total	40	0.52	0	10

Table B.11. Distress distribution in outside lane in Project SA2

Distress Severity Levels	Transverse Cracking (No. / km)	Longitudinal Cracking (Lin. m / m)	Random Cracking (No. / km)	Alligator Cracking (% wheel path)
Low	13	0.02	107	0
Moderate	147	0	27	1.8
High	40	0	0	0
Total	200	0.02	134	1.8

Table B.12. Distress distribution in inside lane in Project SA2

Distress Severity Levels	Transverse Cracking (No. / km)	Longitudinal Cracking (Lin. m / m)	Random Cracking (No. / km)	Alligator Cracking (% wheel path)
Low	0	0	13	0
Moderate	147	0	27	1.6
High	80	0	0	0
Total	227	0	40	1.6

Table B.13. Distress distribution in outside lane in Project AT1

Distress Severity Levels	Transverse Cracking (No. / km)	Longitudinal Cracking (Lin. m / m)	Random Cracking (No. / km)	Alligator Cracking (% wheel path)
Low	187	0.308	0	2
Moderate	0	0	0	0
High	0	0	0	0
Total	187	0.308	0	2

Table B.14. Distress distribution in inside lane in Project AT1

Distress Severity Levels	Transverse Cracking (No. / km)	Longitudinal Cracking (Lin. m / m)	Random Cracking (No. / km)	Alligator Cracking (% wheel path)
Low	13	0	0	0
Moderate	0	0	0	0
High	0	0	0	0
Total	13	0	0	0

Table B.15. Distress distribution in outside lane in Project YO1

Distress Severity Levels	Transverse Cracking (No. / km)	Longitudinal Cracking (Lin. m / m)	Random Cracking (No. / km)	Alligator Cracking (% wheel path)
Low	93	0.68	120	0
Moderate	40	0.188	13	0
High	0	0	0	0
Total	133	0.868	133	0

Table B.16. Distress distribution in inside lane in Project YO1

Distress Severity Levels	Transverse Cracking (No. / km)	Longitudinal Cracking (Lin. m / m)	Random Cracking (No. / km)	Alligator Cracking (% wheel path)
Low	80	0.056	13	0
Moderate	0	0	0	0
High	0	0	0	0
Total	80	0.056	13	0

Table B.17. Distress distribution in outside lane in Project YO2

Distress Severity Levels	Transverse Cracking (No. / km)	Longitudinal Cracking (Lin. m / m)	Random Cracking (No. / km)	Alligator Cracking (% wheel path)
Low	307	1.188	213	0
Moderate	0	0	0	0
High	0	0	0	0
Total	307	1.188	213	0

Table B.18. Distress distribution in inside lane in Project YO2

Distress Severity Levels	Transverse Cracking (No. / km)	Longitudinal Cracking (Lin. m / m)	Random Cracking (No. / km)	Alligator Cracking (% wheel path)
Low	240	1.764	133	0
Moderate	0	0	0	0
High	0	0	0	0
Total	240	1.764	133	0

Table B.19. Distress distribution in outside lane in Project PH1

Distress Severity Levels	Transverse Cracking (No. / km)	Longitudinal Cracking (Lin. m / m)	Random Cracking (No. / km)	Alligator Cracking (% wheel path)
Low	53	0.04	53	0
Moderate	0	0	0	22.60
High	0	0	0	18
Total	53	0.04	53	40.60

Table B.20. Distress distribution in inside lane in Project PH1

Distress Severity Levels	Transverse Cracking (No. / km)	Longitudinal Cracking (Lin. m / m)	Random Cracking (No. / km)	Alligator Cracking (% wheel path)
Low	0	0.072	0	0
Moderate	0	0	0	0
High	0	0	0	0
Total	0	0.072	0	0

Table B.21. Distress distribution in outside lane in Project PH2

Distress Severity Levels	Transverse Cracking (No. / km)	Longitudinal Cracking (Lin. m / m)	Random Cracking (No. / km)	Alligator Cracking (% wheel path)
Low	67	0.332	93	3.8
Moderate	40	0.3	107	1.4
High	0	0	0	3
Total	107	0.632	200	8.20

Table B.22. Distress distribution in inside lane in Project PH2

Distress Severity Levels	Transverse Cracking (No. / km)	Longitudinal Cracking (Lin. m / m)	Random Cracking (No. / km)	Alligator Cracking (% wheel path)
Low	27	0.04	40	0
Moderate	213	0.352	104	5.60
High	0	0	0	0
Total	240	0.392	147	5.60

Table B.23. Summary statistics for full and half transverse cracks in both lanes of projects

Case Study Projects	Outside Lane			Inside Lane		
	Full Lane Trans. Cracking (No. / km)	Half Lane Trans. Cracking (No. / km)	Total Trans. Cracking (No. / km)	Full Lane Trans. Cracking (No. / km)	Half Lane Trans. Cracking (No. / km)	Total Trans. Cracking (No. / km)
Amarillo, US 87, NB	107	186	293	40	13	53
Amarillo, FM 1541, NB/SB	53	40	93	27	40	67
Abilene, US 83, SB	67	67	134	40	13	53
Abilene, US 83 BU, NB	200	67	267	133	0	134
San Angelo, US 67, NB	27	13	40	40	0	40
San Angelo, SH 208, NB	160	40	200	200	27	227
Atlanta, SH 08, NB/SB	80	107	187	13	0	13
Yoakum, US 290, WB	120	13	133	80	0	80
Yoakum, LP 463, EB/WB	160	147	307	173	67	240
Pharr, US 281, NB	13	40	53	0	0	0
Pharr, FM 2128, EB	67	40	107	53	187	240

APPENDIX C

FWD TEST RESULTS AND CALCULATIONS

Figure A.1 - Calculations from FWD Test Data (Phase 1)
US 83 (AB1)

	SCI at Test Location																				Mean	St. Dev.
	1	2	3	4	5	6	7	8	9	10	11	12	13	14	15	16	17	18	19	20		
CASE 1	--	1.37	0.89	0.71	--	1.58	1.79	0.96	--	1.06	1.01	1.11	--	1.39	0.77	1.16	--	0.99	0.97	2.52	1.22	0.47
CASE 2 (across crack)	5.01	--	--	--	3.20	--	--	--	3.58	--	--	--	3.98	--	--	--	3.29	--	--	--	3.81	0.74
CASE 3 (w/in 1.0' of crack)	2.42	--	--	--	1.79	--	--	--	2.15	--	--	--	2.16	--	--	--	2.04	--	--	--	2.11	0.23
CASE 4 (across crack)	3.97	--	--	--	1.99	--	--	--	2.71	--	--	--	2.35	--	--	--	2.57	--	--	--	2.72	0.75

C-3

	BCI at Test Location																				Mean	St. Dev.
	1	2	3	4	5	6	7	8	9	10	11	12	13	14	15	16	17	18	19	20		
CASE 1	--	1.89	1.21	1.09	--	1.92	2.19	1.50	--	1.40	1.36	1.55	--	1.67	1.26	1.37	--	1.36	1.42	2.19	1.56	0.34
CASE 2 (w/in 1.0' of crack)	1.65	--	--	--	1.24	--	--	--	1.58	--	--	--	1.46	--	--	--	1.56	--	--	--	1.50	0.16
CASE 3 (w/in 2.0' of crack)	2.32	--	--	--	1.81	--	--	--	1.75	--	--	--	1.66	--	--	--	2.00	--	--	--	1.91	0.26

Experimental Design Region : Dry / Freeze
 Test Date : 02/10/97
 Pavement Test Temperature : 73 Deg.
 Test Section Definition : Outside Southbound Lane
 Projected Distress Distribution : 134 Transverse Cracks / km
 in testing lane 0.0 lin. meter / meter; longitudinal cracks
 0 % Alligator Cracking (crk'd. whl. path / Tot. whl. path)

Pavement Structure : 2.0 " Asphalt
 8.0 " Limestone Base
 6.0 " Subbase

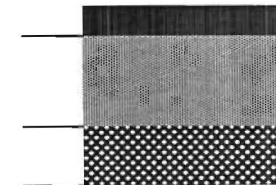


Figure A.2 - Calculations from FWD Test Data (Phase 1)
US 83 BU (AB2)

	SCI at Test Location																				Mean	St. Dev.
	1	2	3	4	5	6	7	8	9	10	11	12	13	14	15	16	17	18	19	20		
CASE 1	--	2.61	2.01	2.94	--	3.75	9.54	3.22	--	4.90	3.94	6.40	--	3.08	3.67	4.37	--	3.61	2.96	4.97	4.13	1.85
CASE 2 (across crack)	8.28	--	--	--	8.59	--	--	--	3.89	--	--	--	4.21	--	--	--	6.29	--	--	--	6.25	2.20
CASE 3 (w/in 1.0' of crack)	5.98	--	--	--	5.93	--	--	--	2.80	--	--	--	4.19	--	--	--	5.16	--	--	--	4.81	1.34
CASE 4 (across crack)	8.25	--	--	--	7.61	--	--	--	3.79	--	--	--	4.32	--	--	--	5.43	--	--	--	5.88	1.97

C-4

	BCI at Test Location																				Mean	St. Dev.
	1	2	3	4	5	6	7	8	9	10	11	12	13	14	15	16	17	18	19	20		
CASE 1	--	3.03	2.48	3.90	--	3.89	6.07	3.96	--	4.24	3.75	4.83	--	3.13	4.06	2.72	--	2.50	2.38	3.27	3.61	1.00
CASE 2 (w/in 1.0' of crack)	3.09	--	--	--	3.23	--	--	--	4.49	--	--	--	3.29	--	--	--	2.36	--	--	--	3.29	0.77
CASE 3 (w/in 2.0' of crack)	4.03	--	--	--	5.33	--	--	--	4.93	--	--	--	2.65	--	--	--	2.58	--	--	--	3.91	1.27

Experimental Design Region :	Dry / Freeze	Pavement Structure :	1.5 " Asphalt
Test Date :	02/10/97		
Pavement Test Temperature :	57 Deg.		12.0 " Limestone Base
Test Section Definition :	Outside Northbound Lane		
Projected Distress Distribution :	267 Transverse Cracks / km		
in testing lane	0.272 lin. meter / meter; longitudinal cracks		
	3.4 % Alligator Cracking (crk'd. whl. path / Tot. whl. path)		

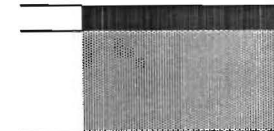


Figure A.3 - Calculations from FWD Test Data (Phase 1)
SH 08 (AT1)

	SCI at Test Location																				Mean	St. Dev.
	1	2	3	4	5	6	7	8	9	10	11	12	13	14	15	16	17	18	19	20		
CASE 1	--	4.03	2.55	5.13	--	5.09	8.16	6.33	--	8.07	5.46	5.46	--	3.26	1.68	4.02	--	7.69	6.41	6.64	5.33	1.96
CASE 2 (across crack)	7.02	--	--	--	5.51	--	--	--	6.14	--	--	--	8.07	--	--	--	4.63	--	--	--	6.28	1.33
CASE 3 (w/in 1.0' of crack)	5.75	--	--	--	4.28	--	--	--	5.48	--	--	--	8.55	--	--	--	5.03	--	--	--	5.82	1.63
CASE 4 (across crack)	4.24	--	--	--	4.61	--	--	--	5.67	--	--	--	9.08	--	--	--	4.69	--	--	--	5.66	1.98

C-5

	BCI at Test Location																				Mean	St. Dev.
	1	2	3	4	5	6	7	8	9	10	11	12	13	14	15	16	17	18	19	20		
CASE 1	--	3.13	2.33	4.73	--	4.48	5.03	5.34	--	5.44	5.03	3.80	--	2.29	1.50	2.81	--	4.99	4.66	4.78	4.02	1.28
CASE 2 (w/in 1.0' of crack)	4.62	--	--	--	2.94	--	--	--	4.37	--	--	--	4.97	--	--	--	2.83	--	--	--	3.94	0.99
CASE 3 (w/in 2.0' of crack)	3.81	--	--	--	3.53	--	--	--	4.37	--	--	--	5.71	--	--	--	2.52	--	--	--	3.99	1.17

Experimental Design Region : Wet / Freeze
 Test Date : 03/06/97
 Pavement Test Temperature :
 Test Section Definition : Northbound Lane
 Projected Distress Distribution : 187 Transverse Cracks / km
 in testing lane 0.308 lin. meter / meter; longitudinal cracks
 2 % Alligator Cracking (crk'd. whl. path / Tot. whl. path)

Pavement Structure : 2.0 " Asphalt
 10.0 " Gravel Base
 (1% Lime, 2% Flyash)

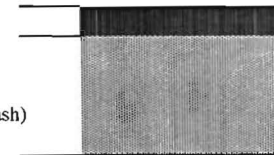


Figure A.4 - Calculations from FWD Test Data (Phase 1)
US 67 (SA1)

	SCI at Test Location																				Mean	St. Dev.
	1	2	3	4	5	6	7	8	9	10	11	12	13	14	15	16	17	18	19	20		
CASE 1	--	9.30	10.85	8.24	--	8.30	9.87	6.72	--	6.05	5.31	8.71	--	4.23	4.40	3.74	--	5.84	5.34	2.99	6.66	2.42
CASE 2 (across crack)	10.07	--	--	--	7.01	--	--	--	9.23	--	--	--	--	--	--	--	--	--	--	--	8.77	1.58
CASE 3 (w/in 1.0' of crack)	8.29	--	--	--	7.65	--	--	--	8.32	--	--	--	--	--	--	--	--	--	--	--	8.09	0.38
CASE 4 (across crack)	9.67	--	--	--	8.32	--	--	--	9.40	--	--	--	--	--	--	--	--	--	--	--	9.13	0.71

C-6

	BCI at Test Location																				Mean	St. Dev.
	1	2	3	4	5	6	7	8	9	10	11	12	13	14	15	16	17	18	19	20		
CASE 1	--	7.80	7.12	6.24	--	5.84	7.35	4.57	--	3.46	3.22	6.57	--	2.78	2.31	1.90	--	4.16	3.50	1.82	4.58	2.08
CASE 2 (w/in 1.0' of crack)	7.75	--	--	--	4.73	--	--	--	6.03	--	--	--	--	--	--	--	--	--	--	--	6.17	1.51
CASE 3 (w/in 2.0' of crack)	6.67	--	--	--	4.92	--	--	--	6.86	--	--	--	--	--	--	--	--	--	--	--	6.15	1.07

Experimental Design Region : Dry / Freeze
Test Date : 02/18/97
Pavement Test Temperature : 80 Deg.
Test Section Definition : Outside Northbound Lane
Projected Distress Distribution : 40 Transverse Cracks / km
 in testing lane 1.06 lin. meter / meter; longitudinal cracks
 6 % Alligator Cracking (crk'd. whl. path / Tot. whl. path)

Pavement Structure : 3.0 " Asphalt
 12.5 " Limestone Base
 8.0 " Stabilized Subgrade (2% Lime)

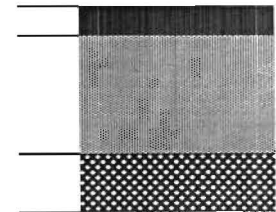


Figure A.5 - Calculations from FWD Test Data (Phase 1)
SH 208 (SA2)

	SCI at Test Location																				Mean	St. Dev.
	1	2	3	4	5	6	7	8	9	10	11	12	13	14	15	16	17	18	19	20		
CASE 1	--	3.89	4.75	10.80	--	12.11	12.18	5.33	--	8.85	7.03	11.91	--	4.76	8.11	10.17	--	8.14	11.85	9.16	8.60	2.92
CASE 2 (across crack)	7.18	--	--	--	15.70	--	--	--	9.69	--	--	--	10.85	--	--	--	20.71	--	--	--	12.83	5.39
CASE 3 (w/in 1.0' of crack)	9.19	--	--	--	14.09	--	--	--	7.13	--	--	--	10.47	--	--	--	15.11	--	--	--	11.20	3.35
CASE 4 (across crack)	9.58	--	--	--	14.53	--	--	--	6.90	--	--	--	11.80	--	--	--	14.34	--	--	--	11.43	3.25

C-7

	BCI at Test Location																				Mean	St. Dev.
	1	2	3	4	5	6	7	8	9	10	11	12	13	14	15	16	17	18	19	20		
CASE 1	--	1.83	2.37	5.66	--	6.07	5.75	2.35	--	4.56	5.03	5.59	--	2.88	5.33	5.07	--	4.48	6.81	5.06	4.59	1.52
CASE 2 (w/in 1.0' of crack)	4.85	--	--	--	7.28	--	--	--	3.54	--	--	--	4.59	--	--	--	5.70	--	--	--	5.19	1.40
CASE 3 (w/in 2.0' of crack)	4.83	--	--	--	8.28	--	--	--	3.09	--	--	--	5.32	--	--	--	8.62	--	--	--	6.03	2.36

Experimental Design Region : Dry / Freeze
 Test Date : 02/18/97
 Pavement Test Temperature : 78 Deg.
 Test Section Definition : Outside Northbound Lane
 Projected Distress Distribution : 200 Transverse Cracks / km
 in testing lane 0.02 lin. meter / meter; longitudinal cracks
 1.8 % Alligator Cracking (crk'd. whl. path / Tot. whl. path)

Pavement Structure : 1.5 " Asphalt
 6.5 " Limestone Base
 4.0 " Stabilized Subgrade

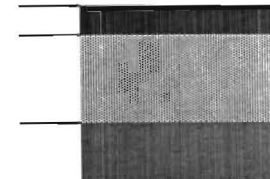


Figure A.6 - Calculations from FWD Test Data (Phase 1)
US 290 (YO1)

	SCI at Test Location																				Mean	St. Dev.
	1	2	3	4	5	6	7	8	9	10	11	12	13	14	15	16	17	18	19	20		
CASE 1	--	6.20	4.10	1.65	--	3.48	4.30	2.88	--	3.26	4.98	6.94	--	7.41	4.25	6.25	--	3.72	2.12	3.47	4.33	1.71
CASE 2 (across crack)	5.73	--	--	--	2.97	--	--	--	3.04	--	--	--	6.03	--	--	--	2.77	--	--	--	4.11	1.63
CASE 3 (w/in 1.0' of crack)	5.28	--	--	--	2.89	--	--	--	3.01	--	--	--	5.79	--	--	--	2.67	--	--	--	3.93	1.48
CASE 4 (across crack)	5.27	--	--	--	3.08	--	--	--	2.76	--	--	--	5.14	--	--	--	2.64	--	--	--	3.78	1.31

C-8

	BCI at Test Location																				Mean	St. Dev.
	1	2	3	4	5	6	7	8	9	10	11	12	13	14	15	16	17	18	19	20		
CASE 1	--	2.23	1.67	0.69	--	1.75	2.22	1.72	--	1.63	2.82	3.97	--	2.82	2.23	3.41	--	1.48	0.66	1.37	2.05	0.92
CASE 2 (w/in 1.0' of crack)	1.16	--	--	--	1.13	--	--	--	1.67	--	--	--	2.68	--	--	--	1.34	--	--	--	1.60	0.64
CASE 3 (w/in 2.0' of crack)	1.65	--	--	--	1.66	--	--	--	1.57	--	--	--	2.03	--	--	--	1.38	--	--	--	1.66	0.24

Experimental Design Region : Wet / No Freeze
 Test Date : 03/04/97
 Pavement Test Temperature : 50 Deg.
 Test Section Definition : Outside Westbound Lane
 Projected Distress Distribution : 133 Transverse Cracks / km
 in testing lane 0.868 lin. meter / meter; longitudinal cracks
 0 % Alligator Cracking (crk'd. whl. path / Tot. whl. path)

Pavement Structure : 2.5 " Asphalt
 8 " Limestone Base
 12 " Gravel Subbase
 (1.5% Lime)

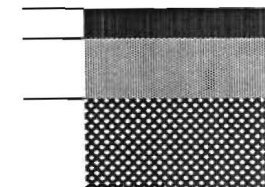


Figure A.7 - Calculations from FWD Test Data (Phase 1)
LP 463 (YO2)

	SCI at Test Location																				Mean	St. Dev.
	1	2	3	4	5	6	7	8	9	10	11	12	13	14	15	16	17	18	19	20		
CASE 1	--	3.18	2.38	1.84	--	1.33	1.85	2.10		0.00	3.71	4.00		1.01	1.68	0.45		2.46	2.85	5.08	2.42	1.25
CASE 2 (across crack)	2.38	--	--	--	2.01	--	--	--	2.85	--	--	--	2.18	--	--	--	3.46	--	--	--	2.58	0.59
CASE 3 (w/in 1.0' of crack)	1.39	--	--	--	1.02	--	--	--	1.84	--	--	--	1.92	--	--	--	2.68	--	--	--	1.77	0.62
CASE 4 (across crack)	1.46	--	--	--	1.48	--	--	--	2.98	--	--	--	3.45	--	--	--	2.70	--	--	--	2.41	0.90

C-9

	BCI at Test Location																				Mean	St. Dev.
	1	2	3	4	5	6	7	8	9	10	11	12	13	14	15	16	17	18	19	20		
CASE 1	--	3.16	2.86	1.27	--	0.84	1.38	2.16		0.00	2.38	3.27		0.50	0.71	0.86		1.37	1.75	3.19	1.84	0.99
CASE 2 (w/in 1.0' of crack)	1.30	--	--	--	0.72	--	--	--	0.85	--	--	--	0.57	--	--	--	1.27	--	--	--	0.94	0.33
CASE 3 (w/in 2.0' of crack)	1.48	--	--	--	0.92	--	--	--	1.19	--	--	--	1.02	--	--	--	1.24	--	--	--	1.17	0.21

Experimental Design Region :	Dry / No Freeze	Pavement Structure :	1.5" Asphalt
Test Date :	02/18/97		
Pavement Test Temperature :	60 Deg.		14.0" Gravel Base (2% Lime)
Test Section Definition :	Eastbound Lane		
Projected Distress Distribution :	307 Transverse Cracks / km		8.0" Subbase (5% Lime)
in testing lane	1.188 lin. meter / meter; longitudinal cracks		
	0% Alligator Cracking (crk'd. whl. path / Tot. whl. path)		

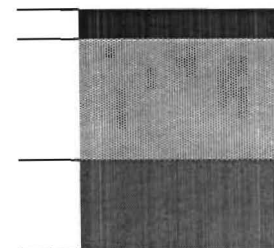


Figure A.8 - Calculations from FWD Test Data (Phase 2)
US 83 (AB1)

	SCI at Test Location																				Mean	St. Dev.
	1	2	3	4	5	6	7	8	9	10	11	12	13	14	15	16	17	18	19	20		
CASE 1	--	4.28	1.52	2.17	--	4.01	5.58	2.29	--	2.98	2.23	2.83	--	2.67	2.99	2.57	--	2.54	2.51	11.49	3.51	2.42
CASE 2 (across crack)	5.54	--	--	--	4.08	--	--	--	4.98	--	--	--	7.84	--	--	--	5.29	--	--	--	5.55	1.39
CASE 3 (w/in 1.0' of crack)	5.46	--	--	--	3.45	--	--	--	4.69	--	--	--	6.52	--	--	--	4.38	--	--	--	4.90	1.16
CASE 5 (w/in 1.0' of crack)	3.41				2.80				2.28				4.49				2.89				3.17	0.84

C-10

	BCI at Test Location																				Mean	St. Dev.
	1	2	3	4	5	6	7	8	9	10	11	12	13	14	15	16	17	18	19	20		
CASE 1	--	3.49	1.94	1.86	--	3.94	3.25	2.65	--	2.48	2.39	2.23	--	2.35	2.38	2.34	--	2.27	2.36	4.29	2.68	0.72
CASE 2 (w/in 1.0' of crack)	3.23	--	--	--	2.51	--	--	--	2.21	--	--	--	2.55	--	--	--	3.27	--	--	--	2.76	0.47
CASE 3 (w/in 2.0' of crack)	3.45	--	--	--	2.54	--	--	--	2.55	--	--	--	2.67	--	--	--	3.00	--	--	--	2.84	0.39
CASE 5 (across crack)	3.93				2.73				2.73				2.71				3.18				3.06	0.53

Experimental Design Region : Dry / Freeze
 Test Date : 07/07/97
 Pavement Test Temperature : 116 Deg.
 Test Section Definition : Outside Southbound Lane
 Projected Distress Distribution : 134 Transverse Cracks / km
 in testing lane 0.0 lin. meter / meter; longitudinal cracks
 0 % Alligator Cracking (crk'd. whl. path / Tot. whl. path)

Pavement Structure : 2.0 " Asphalt
 8.0 " Limestone Base
 6.0 " Subbase

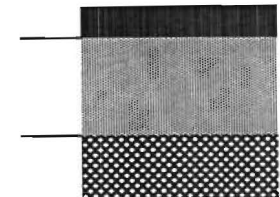


Figure A.9 - Calculations from FWD Test Data (Phase 2)
US 83BU (AB2)

	SCI at Test Location																				Mean	St. Dev.
	1	2	3	4	5	6	7	8	9	10	11	12	13	14	15	16	17	18	19	20		
CASE 1	--	5.80	4.92	7.67	--	8.79	11.53	7.22	--	7.95	6.60	5.56	--	3.98	6.65	5.90	--	6.63	6.88	7.95	6.93	1.79
CASE 2 (across crack)	8.94	--	--	--	13.31	--	--	--	7.51	--	--	--	3.88	--	--	--	6.95	--	--	--	8.12	3.44
CASE 3 (w/in 1.0' of crack)	8.62	--	--	--	12.93	--	--	--	6.66	--	--	--	4.55	--	--	--	6.00	--	--	--	7.75	3.24
CASE 5 (w/in 1.0' of crack)	5.75				8.80				7.71				3.06				5.89				6.24	2.19

C-11

	BCI at Test Location																				Mean	St. Dev.
	1	2	3	4	5	6	7	8	9	10	11	12	13	14	15	16	17	18	19	20		
CASE 1	--	4.60	4.14	5.89	--	5.42	6.54	6.12	--	5.48	4.18	3.74	--	2.67	4.09	2.37	--	2.42	3.10	3.79	4.30	1.35
CASE 2 (w/in 1.0' of crack)	4.26	--	--	--	4.90	--	--	--	6.10	--	--	--	2.27	--	--	--	2.11	--	--	--	3.93	1.72
CASE 3 (w/in 2.0' of crack)	4.68	--	--	--	6.90	--	--	--	6.26	--	--	--	2.24	--	--	--	2.39	--	--	--	4.50	2.15
CASE 5 (across crack)	5.76				7.07				6.09				2.75				2.48				4.83	2.08

Experimental Design Region : Dry / Freeze
 Test Date : 07/07/97
 Pavement Test Temperature : 100 Deg.
 Test Section Definition : Outside Northbound Lane
 Projected Distress Distribution : 267 Transverse Cracks / km
 in testing lane 0.272 lin. meter / meter; longitudinal cracks
 3.4 % Alligator Cracking (crk'd. whl. path / Tot. whl. path)

Pavement Structure : 1.5 " Asphalt
 12.0 " Limestone Base

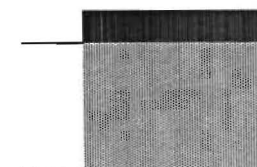


Figure A.10 - Calculations from FWD Test Data (Phase 2)
US 287 (AM1)

	SCI at Test Location																				Mean	St. Dev.
	1	2	3	4	5	6	7	8	9	10	11	12	13	14	15	16	17	18	19	20		
CASE 1	--	10.75	13.96	9.25	--	8.58	6.86	8.87	--	8.28	8.17	12.03	-	15.14	12.98	12.60	--	--	--	--	10.62	2.66
CASE 2 (across crack)	9.79	--	--	--	12.10	--	--	--	11.08	--	--	--	9.08	--	--	--	16.82	--	--	--	11.77	3.05
CASE 3 (w/in 1.0' of crack)	11.64	--	--	--	10.09	--	--	--	10.04	--	--	--	8.29	--	--	--	15.26	--	--	--	11.07	2.63
CASE 5 (w/in 1.0' of crack)	10.06				9.02				8.18				6.73				13.55				9.51	2.56

C-12

	BCI at Test Location																				Mean	St. Dev.
	1	2	3	4	5	6	7	8	9	10	11	12	13	14	15	16	17	18	19	20		
CASE 1	--	7.09	9.45	5.35	--	5.32	3.86	5.19	--	5.96	5.38	8.48	--	10.15	8.88	8.61	--	--	--	--	6.98	2.06
CASE 2 (w/in 1.0' of crack)	8.62	--	--	--	5.55	--	--	--	5.44	--	--	--	4.63	--	--	--	9.94	--	--	--	6.84	2.31
CASE 3 (w/in 2.0' of crack)	8.15	--	--	--	6.77	--	--	--	5.39	--	--	--	5.16	--	--	--	9.96	--	--	--	7.09	2.01
CASE 5 (across crack)	8.33	--	--	--	8.36	--	--	--	7.74	--	--	--	6.07	--	--	--	11.52	--	--	--	8.41	1.98

Experimental Design Region : Dry / Freeze
Test Date : 07/22/97
Pavement Test Temperature : 90 Deg.
Test Section Definition : Outside Northbound Lane
Projected Distress Distribution : 293 Transverse Cracks / km
in testing lane ??? lin. meter / meter; longitudinal cracks
 ??? % Alligator Cracking (crk'd. whl. path / Tot. whl. path)

Pavement Structure : 1.5 " Asphalt
 11.0 " Caliche Base
 4.0 " Gravel Subbase

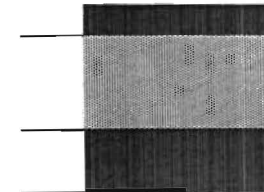


Figure A.11 - Calculations from FWD Test Data (Phase 2)
SH 08 (AT1)

	SCI at Test Location																				Mean	St. Dev.
	1	2	3	4	5	6	7	8	9	10	11	12	13	14	15	16	17	18	19	20		
CASE 1	--	7.73	8.20	7.70	--	6.87	9.65	8.06	--	8.62	7.03	6.67	--	4.26	1.66	6.85	--	7.13	8.24	8.19	7.13	1.93
CASE 2 (across crack)	12.93	--	--	--	12.65	--	--	--	9.09	--	--	--	11.33	--	--	--	6.17	--	--	--	10.53	2.87
CASE 3 (w/in 1.0' of crack)	7.30	--	--	--	12.03	--	--	--	7.55	--	--	--	10.92	--	--	--	5.15	--	--	--	8.59	2.82
CASE 5 (w/in 1.0' of crack)	9.86				13.15				7.08				10.15				5.47				9.14	2.97

C-13

	BCI at Test Location																				Mean	St. Dev.
	1	2	3	4	5	6	7	8	9	10	11	12	13	14	15	16	17	18	19	20		
CASE 1	--	4.59	4.68	7.29	--	5.56	7.14	5.78	--	5.88	5.36	3.54	--	2.98	1.75	5.25	--	6.07	4.96	5.31	5.08	1.46
CASE 2 (w/in 1.0' of crack)	7.12	--	--	--	7.29	--	--	--	6.57	--	--	--	5.78	--	--	--	3.55	--	--	--	6.06	1.52
CASE 3 (w/in 2.0' of crack)	6.13	--	--	--	7.11	--	--	--	6.61	--	--	--	5.90	--	--	--	3.79	--	--	--	5.91	1.27
CASE 5 (across crack)	10.29				7.51				6.27				6.13				3.98				6.84	2.31

Experimental Design Region :

Wet / Freeze

Pavement Structure :

2.0 " Asphalt

Test Date :

Pavement Test Temperature :

10.0 " Gravel Base

Test Section Definition :

Northbound Lane

Projected Distress Distribution :
in testing lane

187 Transverse Cracks / km

0.308 lin. meter / meter; longitudinal cracks

2 % Alligator Cracking (crk'd. whl. path / Tot. whl. path)

(1% Lime, 2% Flyash)

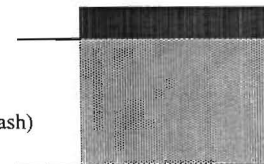


**Figure A.12 - Calculations from FWD Test Data (Phase 2)
US 67 (SA1)**

	SCI at Test Location																				Mean	St. Dev.
	1	2	3	4	5	6	7	8	9	10	11	12	13	14	15	16	17	18	19	20		
CASE 1	--	10.06	9.62	9.37	--	8.59	8.76	8.05	--	5.80	5.95	5.51	--	4.09	3.18	2.57	--	6.57	6.13	3.15	6.49	2.51
CASE 2 (across crack)	7.64	--	--	--	4.20	--	--	--	7.69	--	--	--	9.63	--	--	--	5.75	--	--	--	6.98	2.08
CASE 3 (w/in 1.0' of crack)	7.02	--	--	--	4.01	--	--	--	7.94	--	--	--	8.81	--	--	--	5.28	--	--	--	6.61	1.96
CASE 5 (w/in 1.0' of crack)	6.35				4.64				6.71				9.22				5.61				6.51	1.71

C-14

	BCI at Test Location																				Mean	St. Dev.
	1	2	3	4	5	6	7	8	9	10	11	12	13	14	15	16	17	18	19	20		
CASE 1	--	8.66	6.48	6.15	--	5.51	4.87	4.42	--	2.95	3.05	3.47	--	3.16	1.65	1.63	--	3.64	4.04	2.47	4.14	1.93
CASE 2 (w/in 1.0' of crack)	4.76	--	--	--	3.04	--	--	--	5.03	--	--	--	6.32	--	--	--	1.48	--	--	--	4.13	1.89
CASE 3 (w/in 2.0' of crack)	5.03	--	--	--	3.08	--	--	--	6.41	--	--	--	6.98	--	--	--	1.51	--	--	--	4.60	2.29
CASE 5 (across crack)	4.93				3.22				5.50				7.10				1.58				4.47	2.13

Experimental Design Region :
Test Date :
Pavement Test Temperature :
Test Section Definition :
Projected Distress Distribution :
in testing lane

Dry/Freeze
07/23/1997
129 deg
Outside Northbound Lane
40 Transverse Cracks / km
1.06 lin. meter / meter; longitudinal cracks
6 % Alligator Cracking (crk'd. whl. path / Tot. whl. path)

Pavement Structure :

3.0" Asphalt

12.5" Limestone Base

8.0" Stabilized Subgrade
(2% Lime)

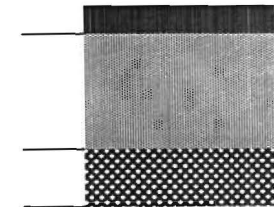


Figure A.13 - Calculations from FWD Test Data (Phase 2)
SH 208 (SA2)

	SCI at Test Location																				Mean	St. Dev.
	1	2	3	4	5	6	7	8	9	10	11	12	13	14	15	16	17	18	19	20		
CASE 1	--	3.27	4.64	5.50	--	10.36	7.84	3.53	--	7.55	7.60	7.68	--	6.24	6.73	9.10	--	8.38	9.97	9.04	7.16	2.18
CASE 2 (across crack)	6.44	--	--	--	11.69	--	--	--	3.91	--	--	--	6.51	--	--	--	9.64	--	--	--	7.64	3.04
CASE 3 (w/in 1.0' of crack)	6.67	--	--	--	11.73	--	--	--	3.29	--	--	--	5.13	--	--	--	9.79	--	--	--	7.32	3.43
CASE 5 (w/in 1.0' of crack)	6.02				10.35				3.65				5.70				8.37				6.82	2.59

C-15

	BCI at Test Location																				Mean	St. Dev.
	1	2	3	4	5	6	7	8	9	10	11	12	13	14	15	16	17	18	19	20		
CASE 1	--	1.59	1.76	3.19	--	4.23	3.06	1.80	--	4.37	5.02	3.57	--	3.74	3.91	4.36	--	4.66	4.20	3.97	3.56	1.08
CASE 2 (w/in 1.0' of crack)	3.04	--	--	--	5.48	--	--	--	2.04	--	--	--	3.54	--	--	--	3.87	--	--	--	3.59	1.26
CASE 3 (w/in 2.0' of crack)	3.29	--	--	--	5.74	--	--	--	1.87	--	--	--	3.18	--	--	--	4.32	--	--	--	3.68	1.44
CASE 5 (across crack)	2.86				5.57				2.59				4.39				4.11				3.91	1.21

Experimental Design Region : Dry / Freeze
Test Date : 07/23/97
Pavement Test Temperature : 127 deg.
Test Section Definition : Outside Northbound Lane
Projected Distress Distribution : 200 Transverse Cracks / km
in testing lane 0.02 lin. meter / meter; longitudinal cracks
1.8 % Alligator Cracking (crk'd. whl. path / Tot. whl. path)

Pavement Structure : 1.5 " Asphalt
6.5 " Limestone Base
4.0 " Stabilized Subgrade

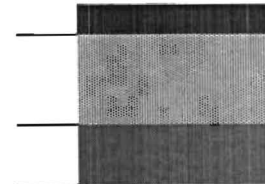


Figure A.14 - Calculations from FWD Test Data (Phase 2)
US 290 (YO1)

	SCI at Test Location																				Mean	St. Dev.
	1	2	3	4	5	6	7	8	9	10	11	12	13	14	15	16	17	18	19	20		
CASE 1	--	5.23	3.95	2.03	--	4.42	3.86	2.84	--	3.72	5.79	6.69	--	7.35	5.85	6.79	--	3.81	2.47	3.94	4.58	1.63
CASE 2 (across crack)	6.78	--	--	--	2.98	--	--	--	3.59	--	--	--	5.75	--	--	--	3.21	--	--	--	4.46	1.70
CASE 3 (w/in 1.0' of crack)	6.51	--	--	--	3.13	--	--	--	4.21	--	--	--	5.28	--	--	--	3.33	--	--	--	4.49	1.41
CASE 5 (w/in 1.0' of crack)	5.68				3.36				3.86				5.61				3.74				4.45	1.11

C-16

	BCI at Test Location																				Mean	St. Dev.
	1	2	3	4	5	6	7	8	9	10	11	12	13	14	15	16	17	18	19	20		
CASE 1	--	1.54	0.82	0.34	--	0.83	0.62	0.88	--	1.00	1.40	1.79	--	2.22	1.53	1.67	--	0.75	0.47	0.81	1.11	0.54
CASE 2 (w/in 1.0' of crack)	1.39	--	--	--	0.80	--	--	--	1.04	--	--	--	1.48	--	--	--	0.67	--	--	--	1.08	0.36
CASE 3 (w/in 2.0' of crack)	1.44	--	--	--	0.61	--	--	--	0.99	--	--	--	1.51	--	--	--	0.76	--	--	--	1.06	0.40
CASE 5 (across crack)	1.89				0.58				1.01				1.58				0.65				1.14	0.58

Experimental Design Region : Wet / No Freeze
 Test Date : 07/21/97
 Pavement Test Temperature : 99 deg
 Test Section Definition : Outside Westbound Lane
 Projected Distress Distribution : 133 Transverse Cracks / km
 in testing lane 0.868 lin. meter / meter; longitudinal cracks
 0 % Alligator Cracking (crk'd. whl. path / Tot. whl. path)

Pavement Structure : 2.5 " Asphalt
 8 " Limestone Base
 12 " Gravel Subbase
 (1.5% Lime)

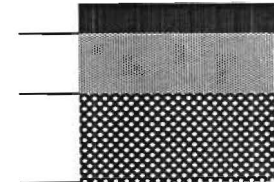


Figure A.15 - Calculations from FWD Test Data (Phase 2)
LP 463 (YO2)

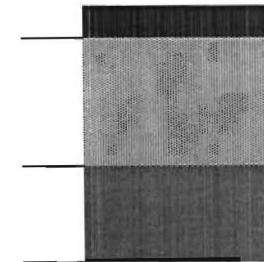
	SCI at Test Location																				Mean	St. Dev.
	1	2	3	4	5	6	7	8	9	10	11	12	13	14	15	16	17	18	19	20		
CASE 1	--	3.94	3.01	2.90	--	2.05	1.21	2.96	--	4.12	2.32	2.99	--	4.92	2.39	1.46	--	1.40	0.75	0.46	2.46	1.28
CASE 2 (across crack)	1.80	--	--	--	0.80	--	--	--	3.47	--	--	--	3.95	--	--	--	3.26	--	--	--	2.66	1.31
CASE 3 (w/in 1.0' of crack)	1.08	--	--	--	1.45	--	--	--	0.25	--	--	--	1.51	--	--	--	2.09	--	--	--	1.28	0.68
CASE 5 (w/in 1.0' of crack)	1.77				1.04				0.72				0.64				3.49				1.53	1.18

C-17

	BCI at Test Location																				Mean	St. Dev.
	1	2	3	4	5	6	7	8	9	10	11	12	13	14	15	16	17	18	19	20		
CASE 1	--	2.14	2.60	1.77	--	0.88	1.83	2.23	--	2.02	2.14	2.72	--	2.96	1.81	1.02	--	0.50	0.31	0.30	1.68	0.88
CASE 2 (w/in 1.0' of crack)	1.43	--	--	--	0.76	--	--	--	0.70	--	--	--	0.83	--	--	--	1.49	--	--	--	1.04	0.39
CASE 3 (w/in 2.0' of crack)	1.40	--	--	--	0.75	--	--	--	0.78	--	--	--	0.63	--	--	--	2.25	--	--	--	1.16	0.68
CASE 5 (across crack)	1.80				0.97				1.64				1.09				1.83				1.47	0.41

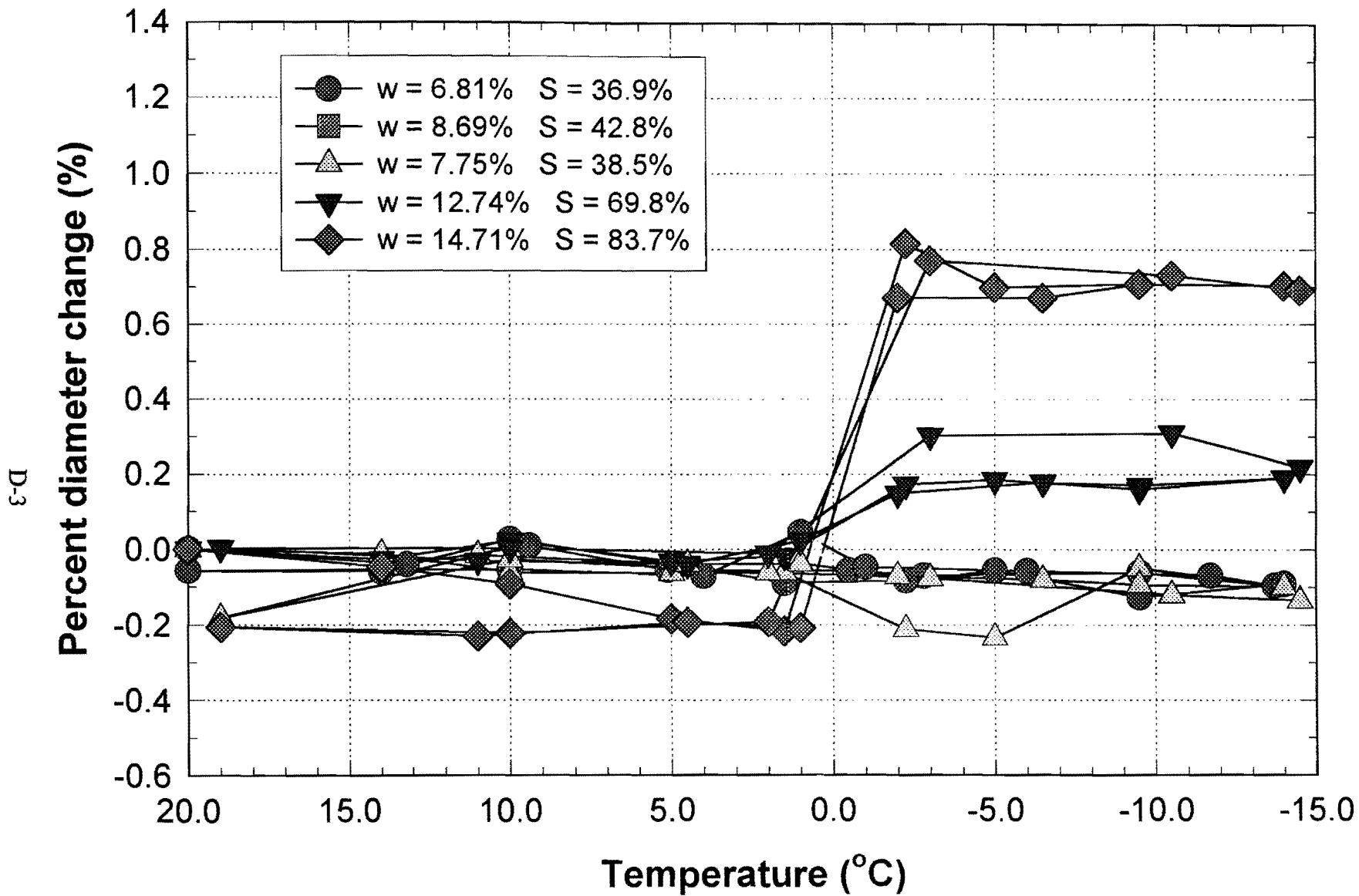
Experimental Design Region : Dry / No Freeze
Test Date : 07/21/97
Pavement Test Temperature : 105 deg.
Test Section Definition : Eastbound Lane
Projected Distress Distribution : 307 Transverse Cracks / km
in testing lane 1.188 lin. meter / meter; longitudinal cracks
 0 % Alligator Cracking (crk'd. whl. path / Tot. whl. path)

Pavement Structure : 1.5 " Asphalt
 14.0 " Gravel Base
 (2% Lime)
 8.0" Subbase
 (5% Lime)

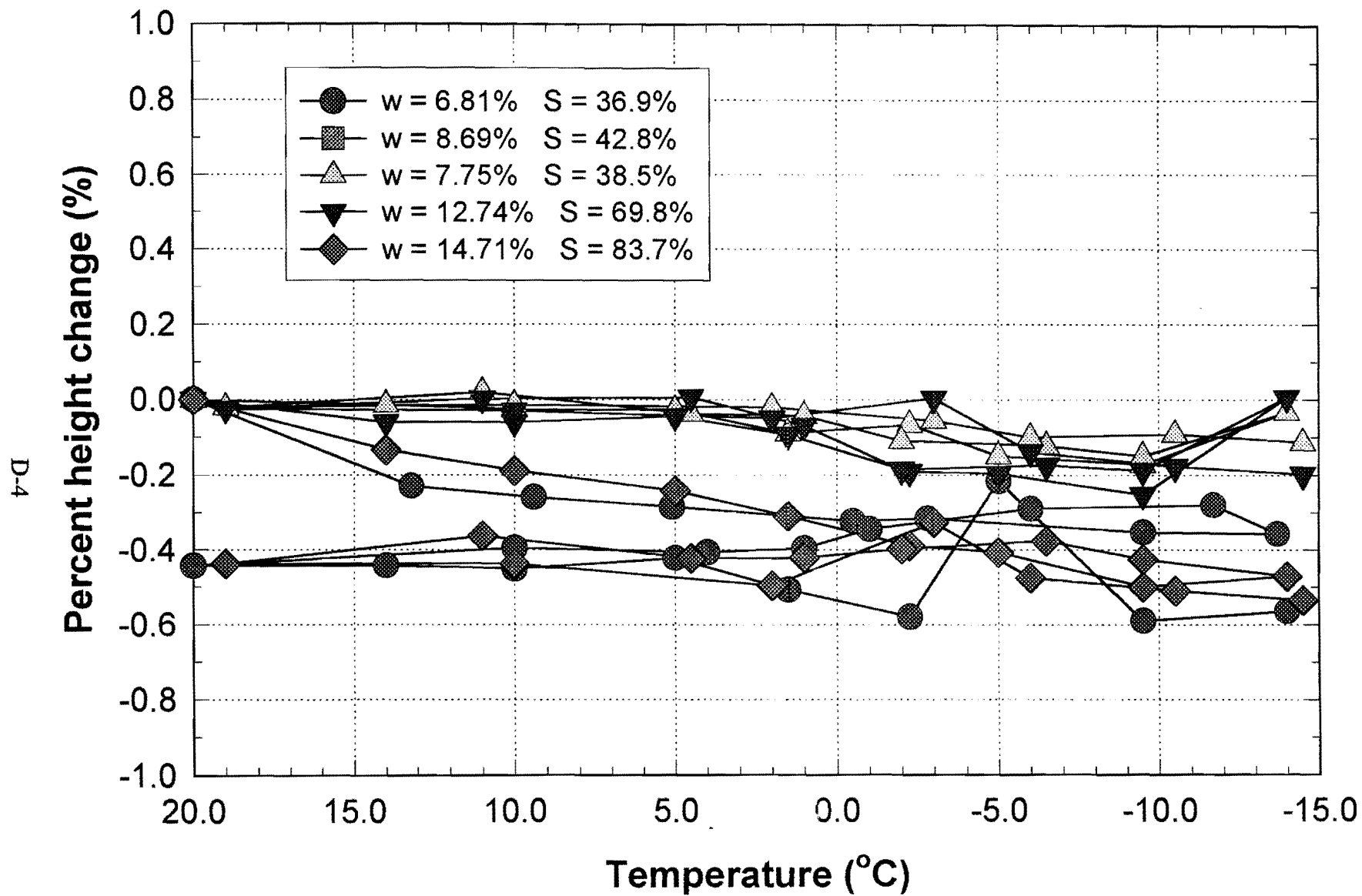


APPENDIX D

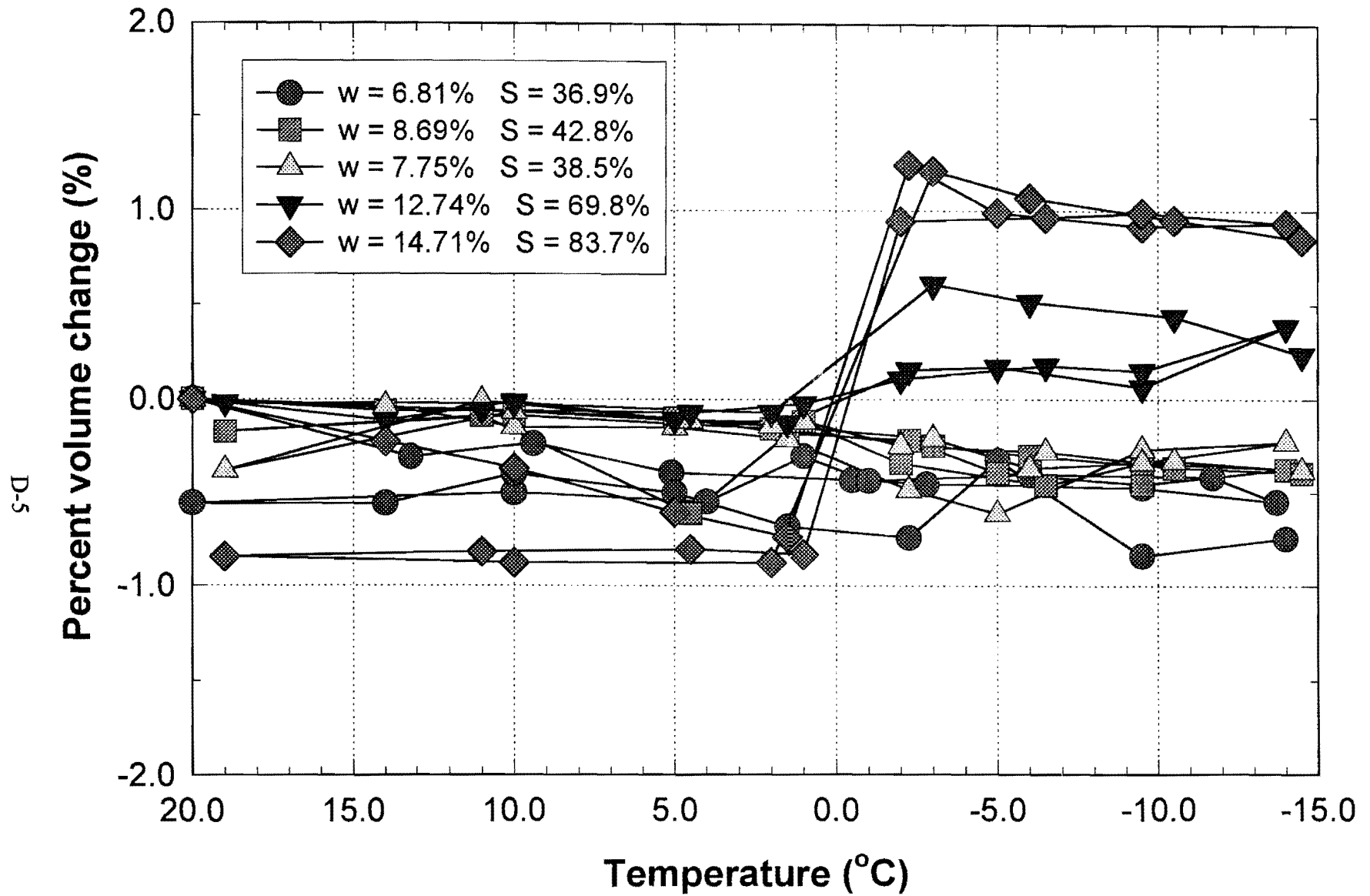
VOLUME CHANGE RELATIONSHIPS



Percent Diameter Change of Aggregate YV versus Temperature

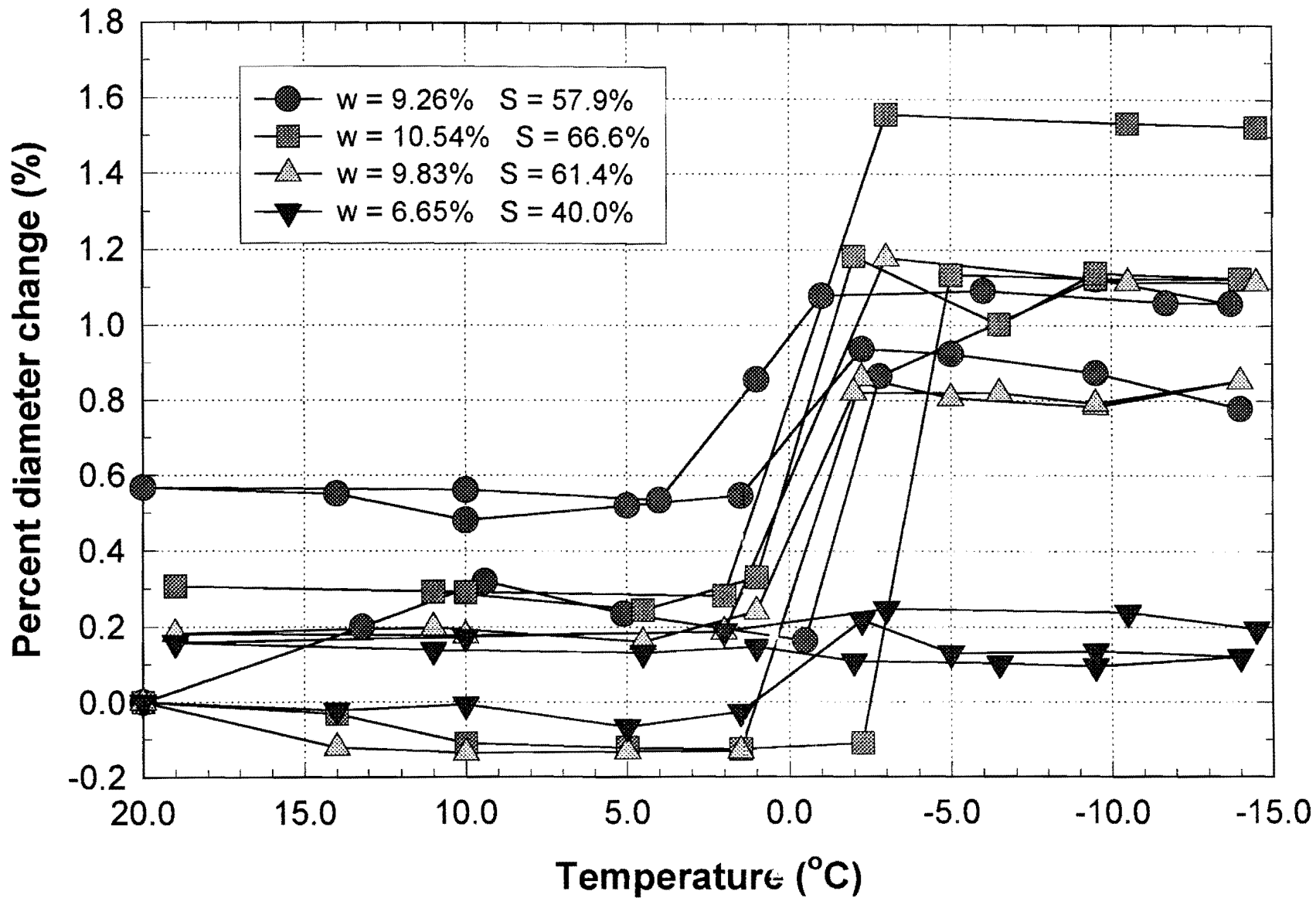


Percent Height Change of Aggregate YV versus Temperature

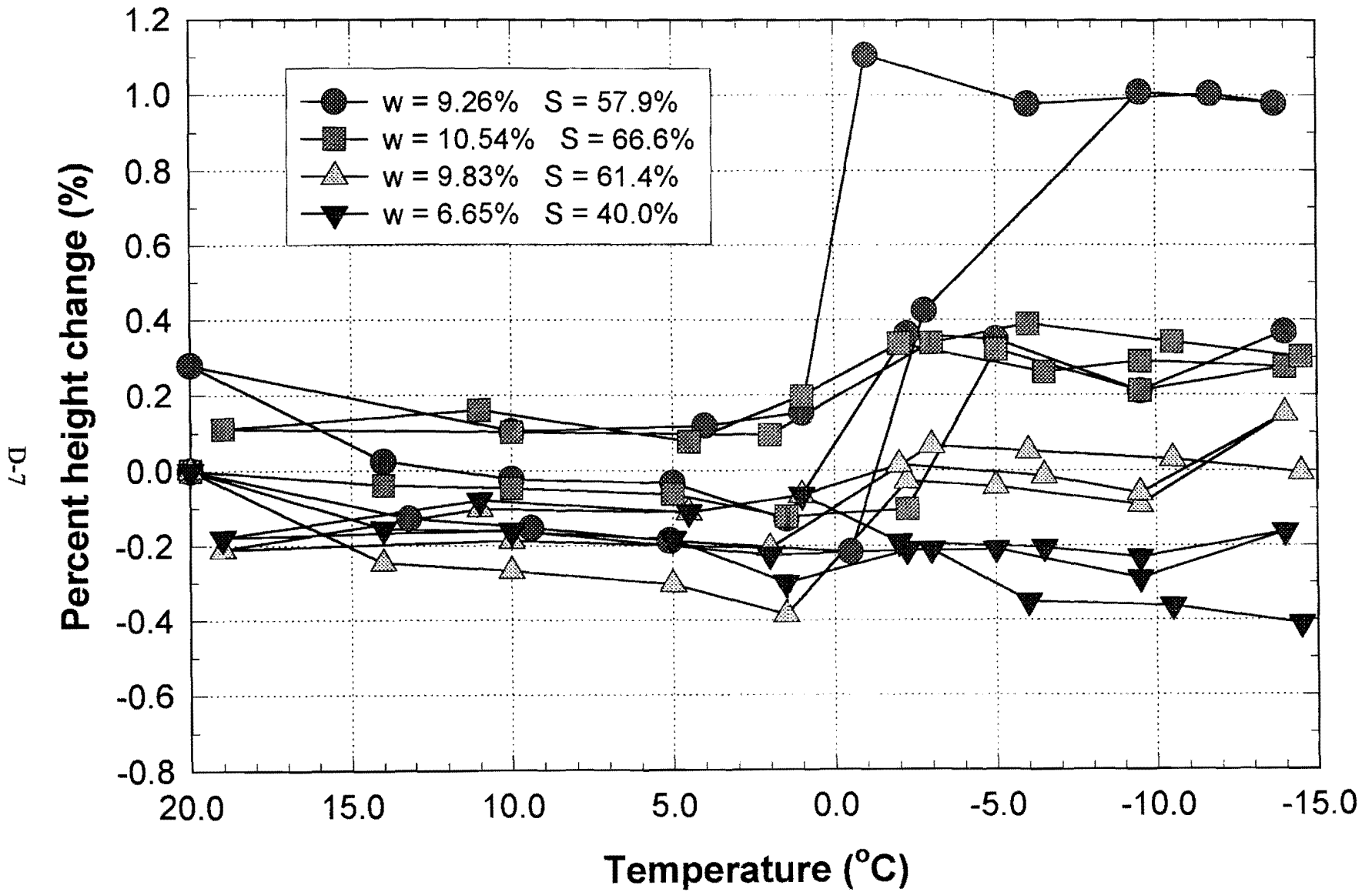


Percent Volume Change of Aggregate YV versus Temperature

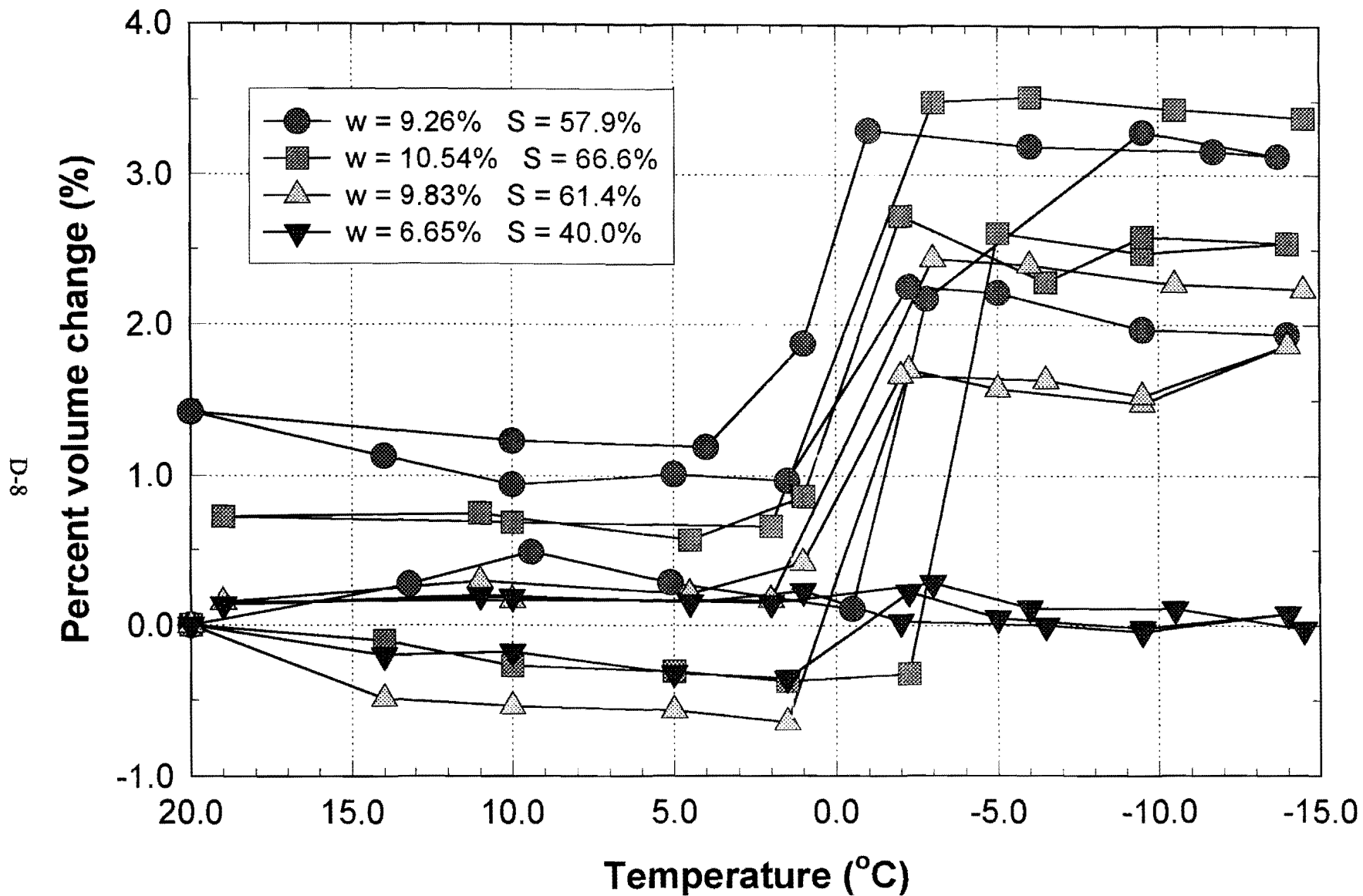
D-6



Percent Diameter Change of Aggregate AMBX versus Temperature

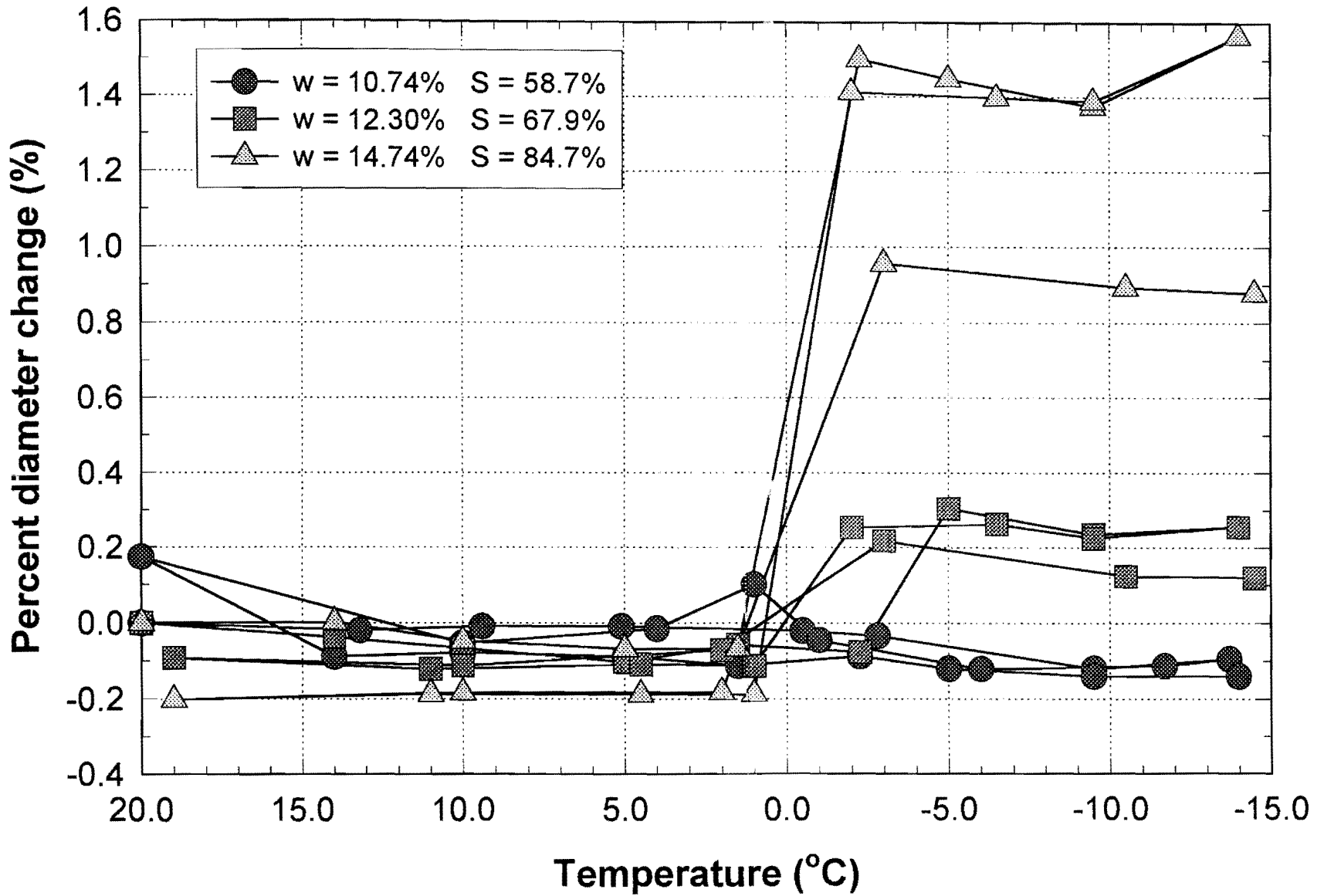


Percent Height Change of Aggregate AMBX versus Temperature

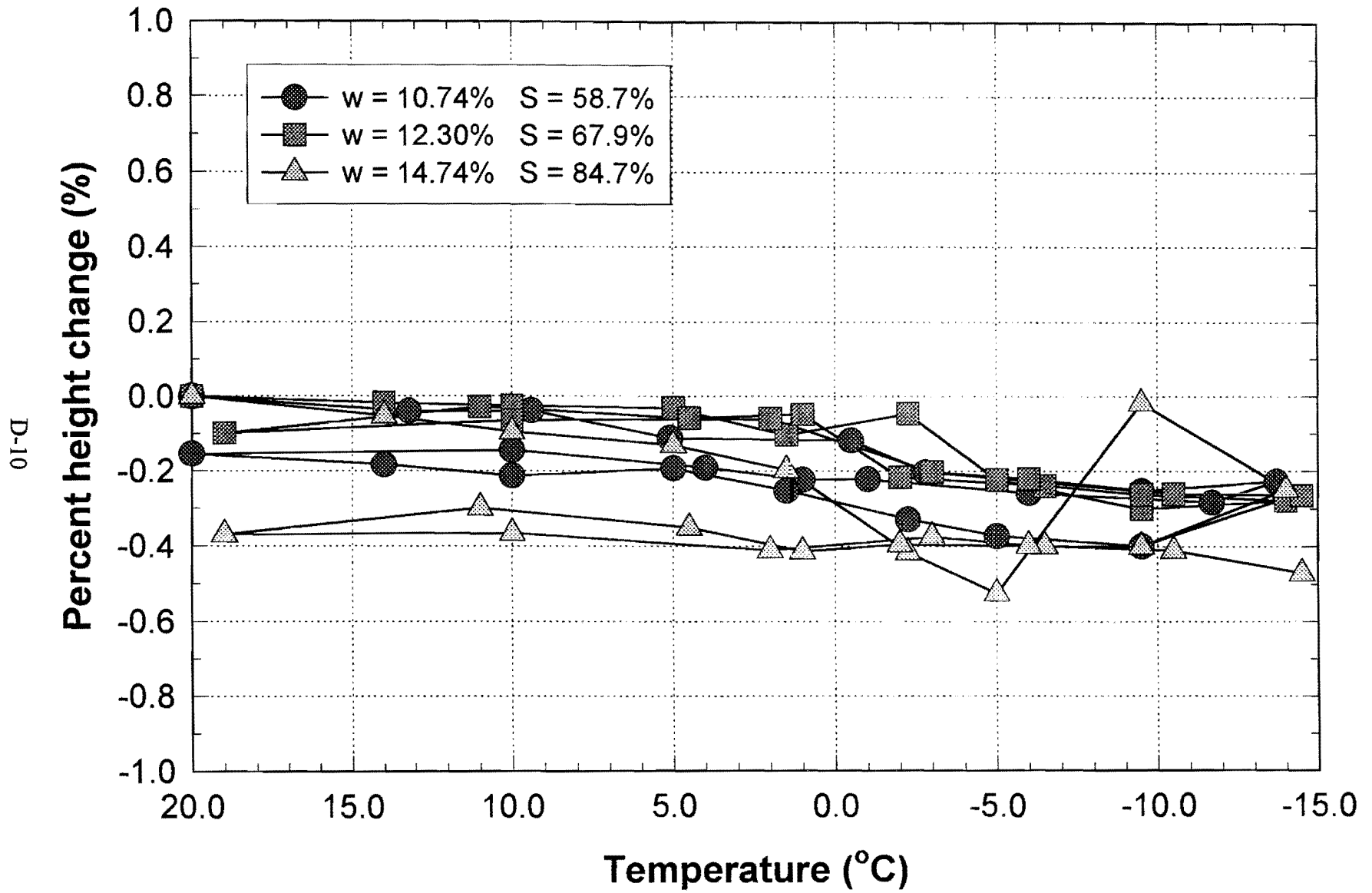


Percent Volume Change of Aggregate AMBX versus Temperature

D-9

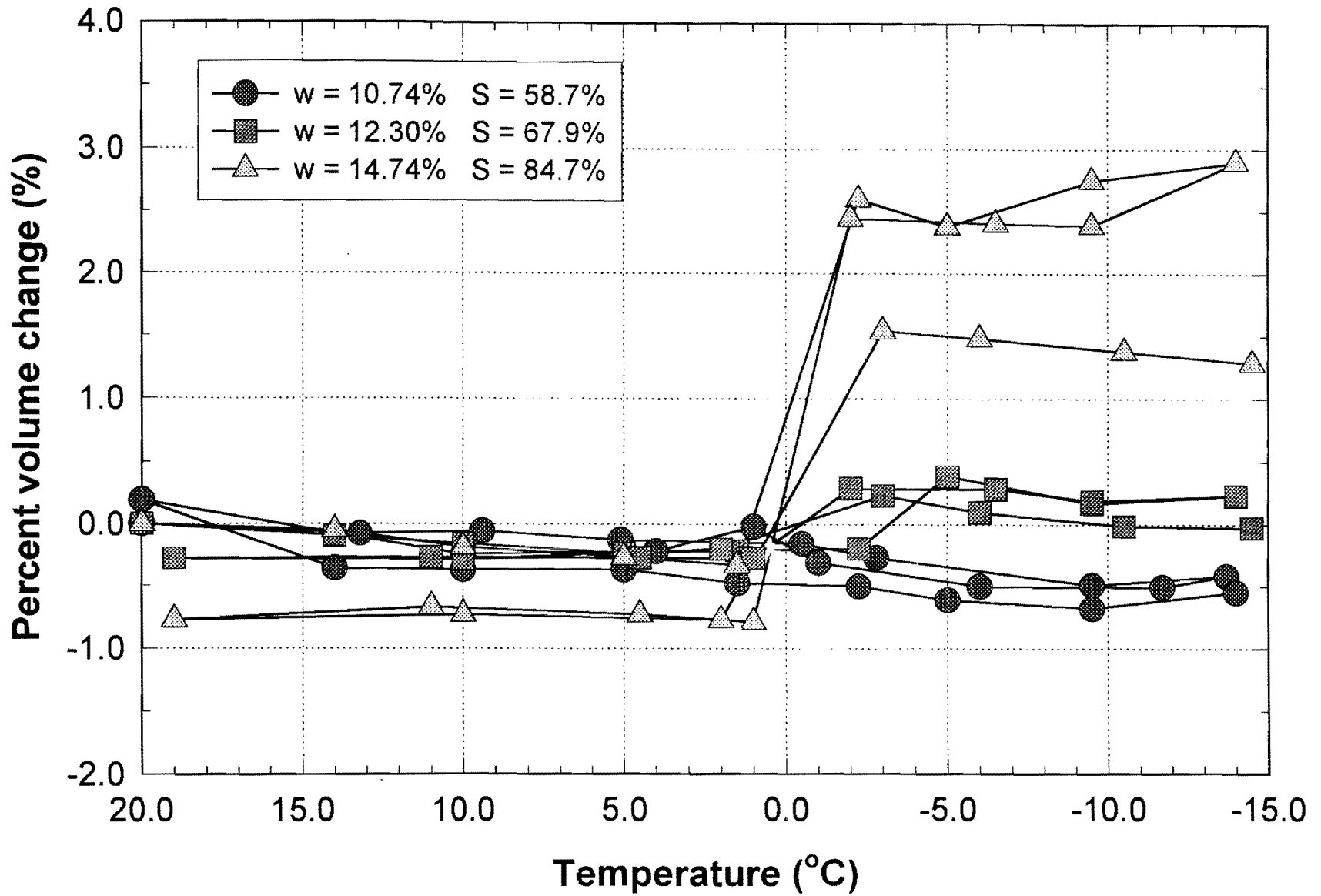


Percent Diameter Change of Aggregate AMB versus Temperature



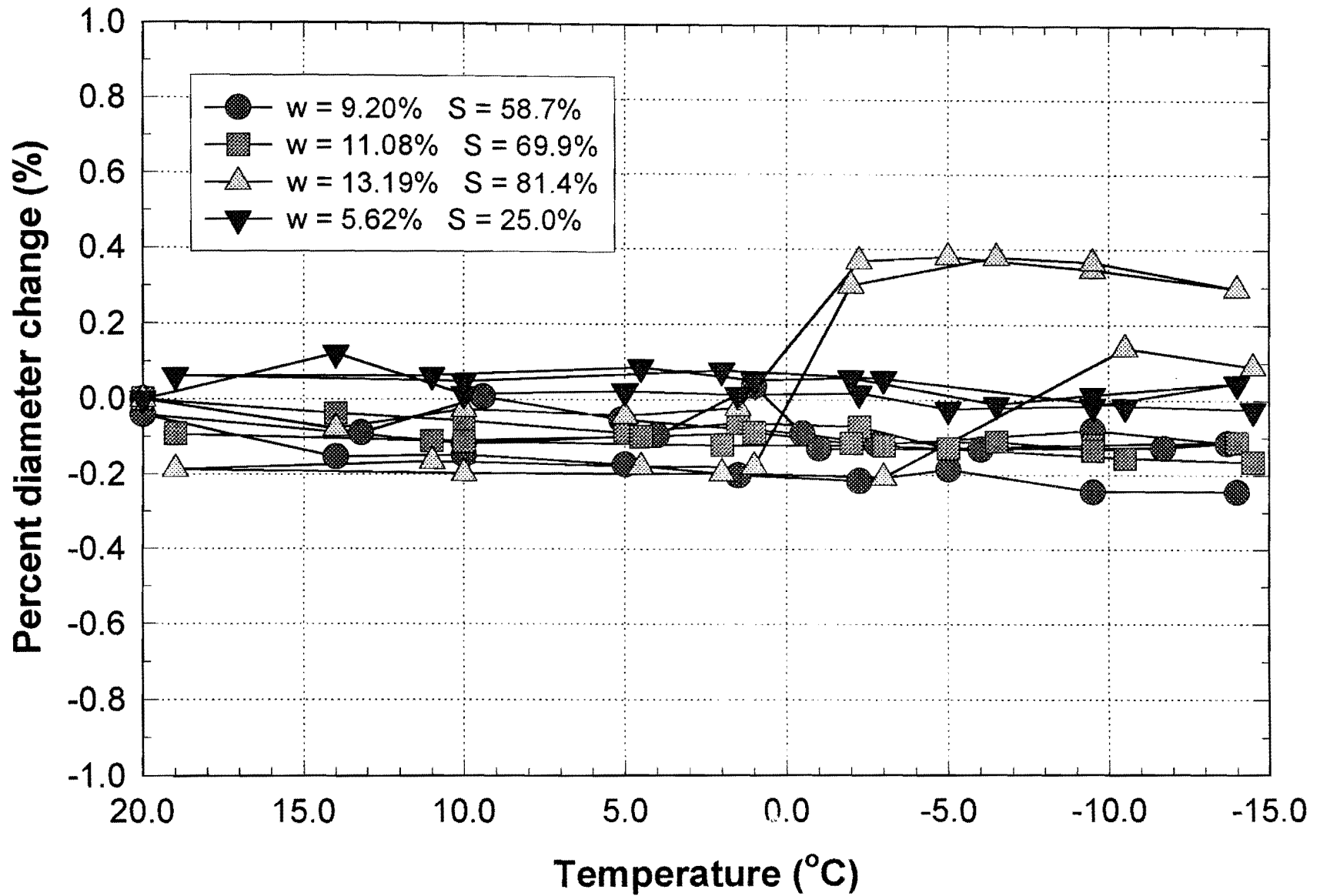
Percent Height Change of Aggregate AMB versus Temperature

D-11

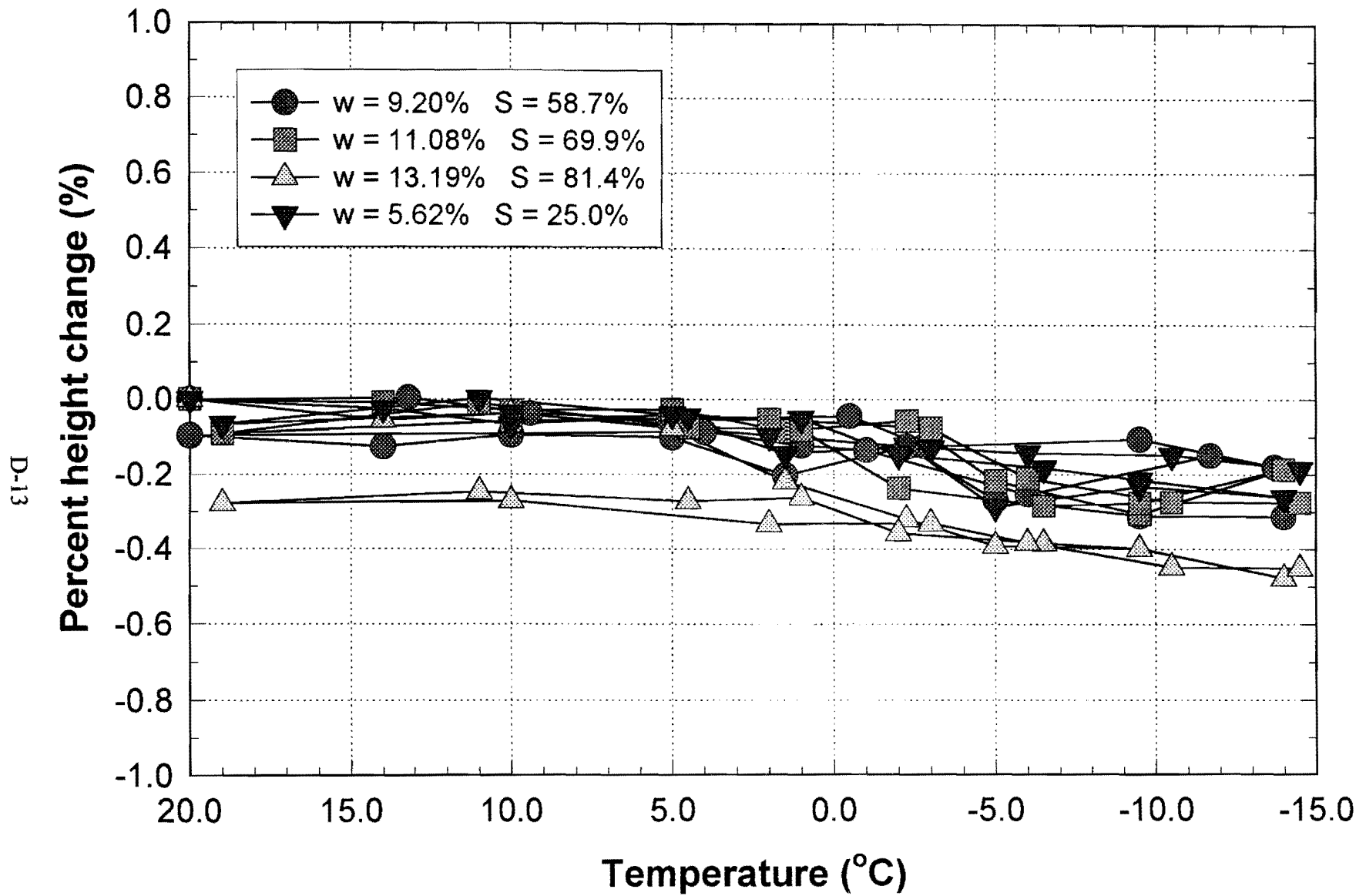


Percent Volume Change of Aggregate AMB versus Temperature

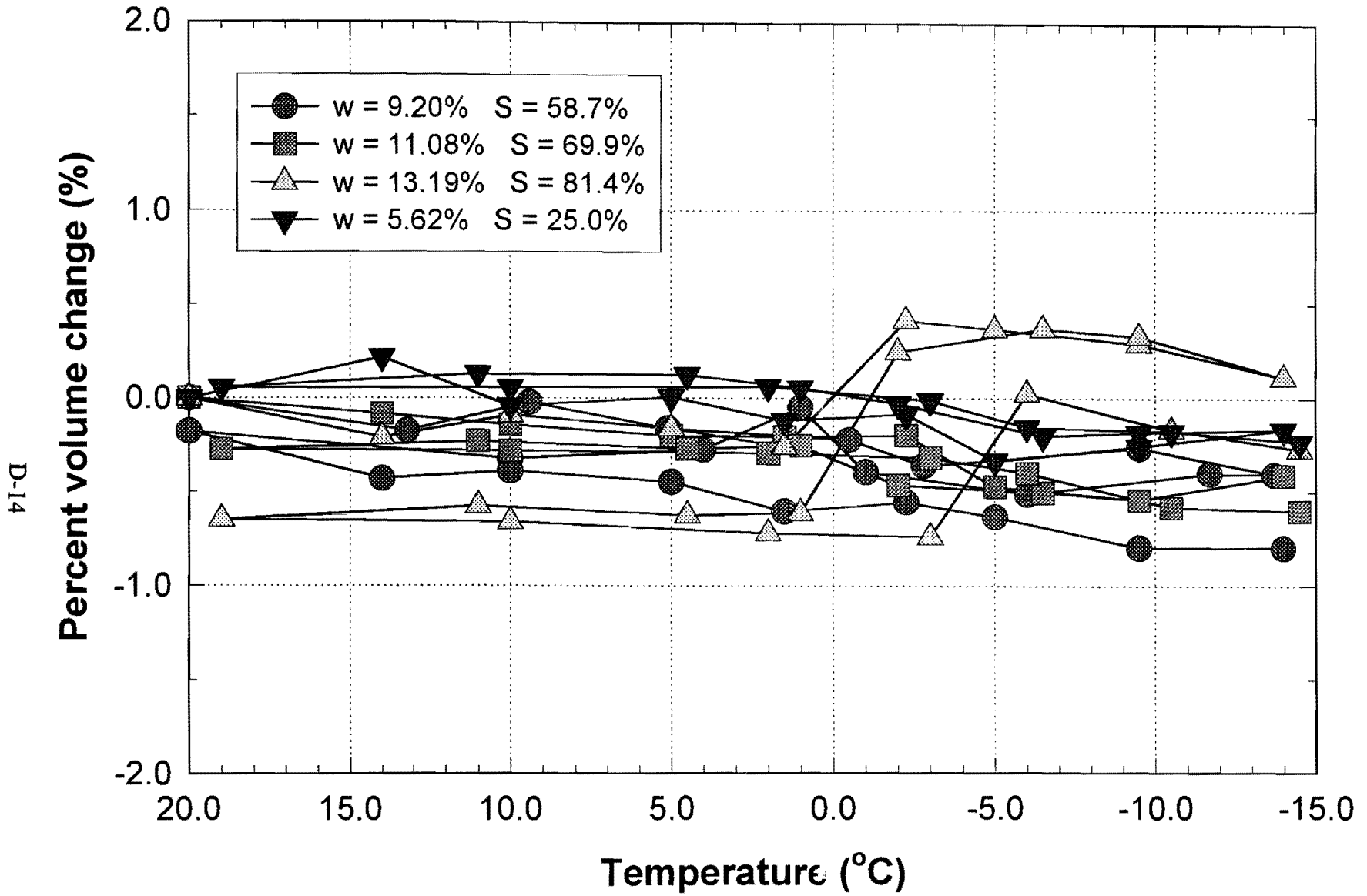
D-12



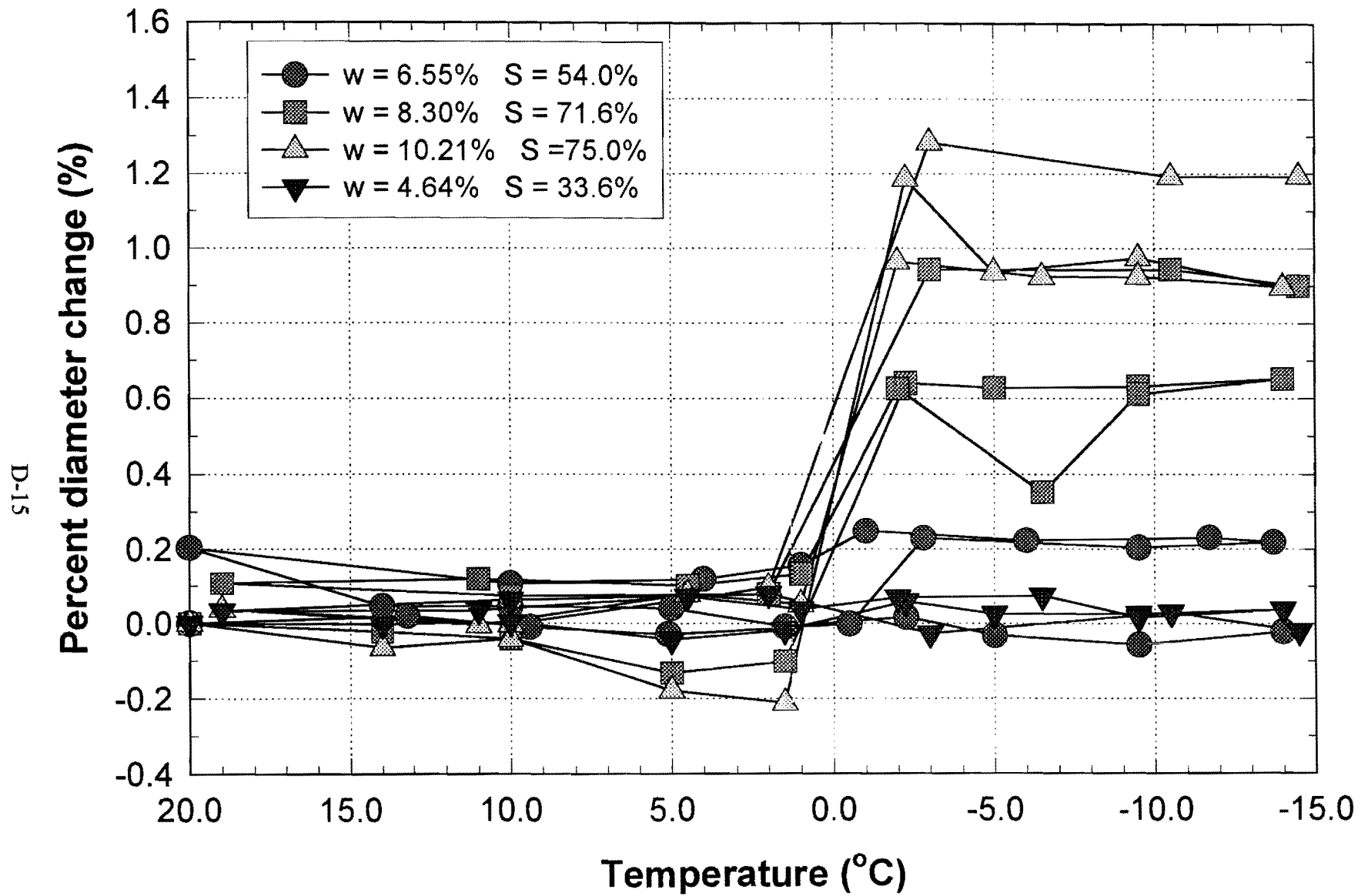
Percent Diameter Change of Aggregate AML versus Temperature



Percent Height Change of Aggregate AML versus Temperature

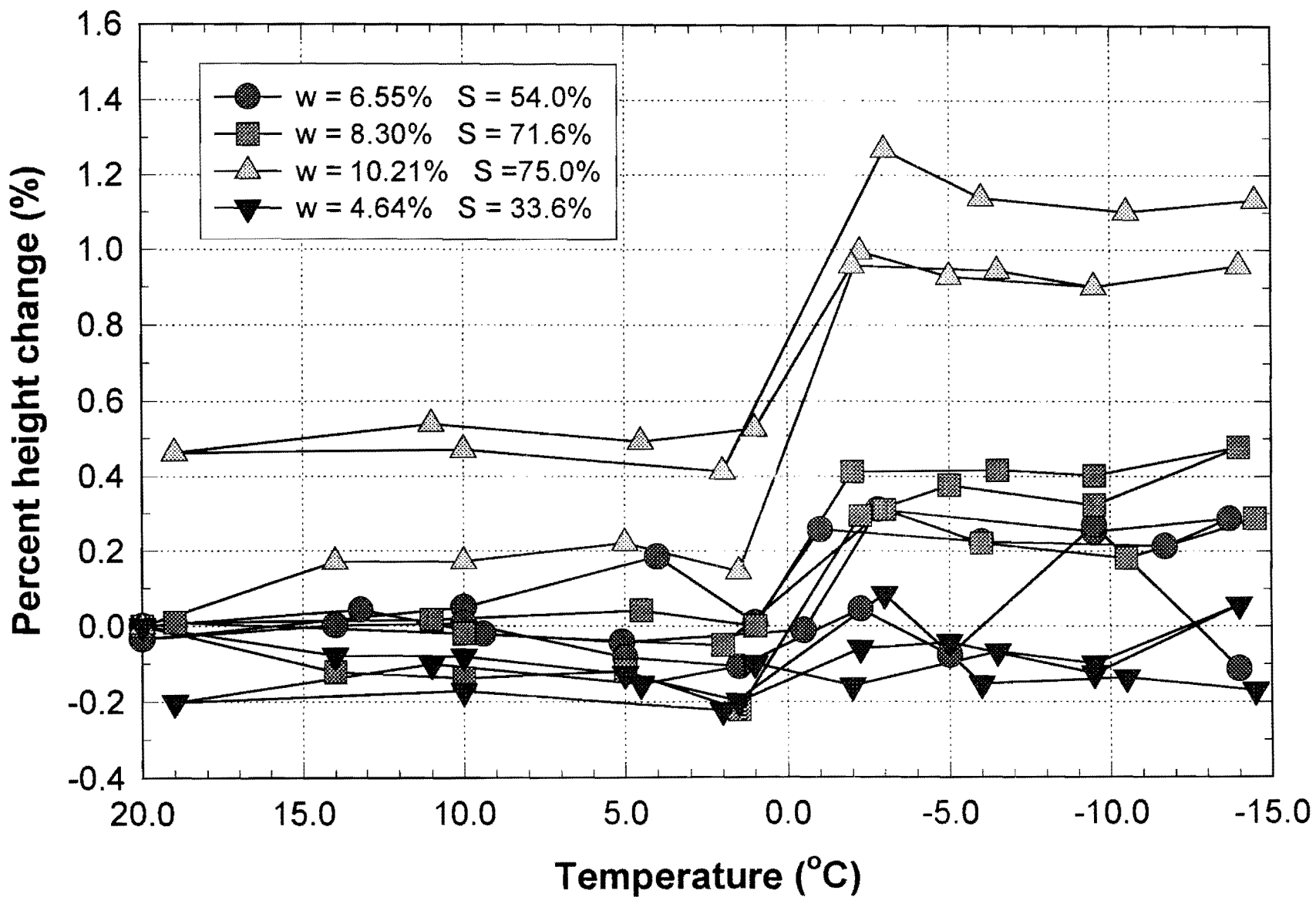


Percent Volume Change of Aggregate AML versus Temperature



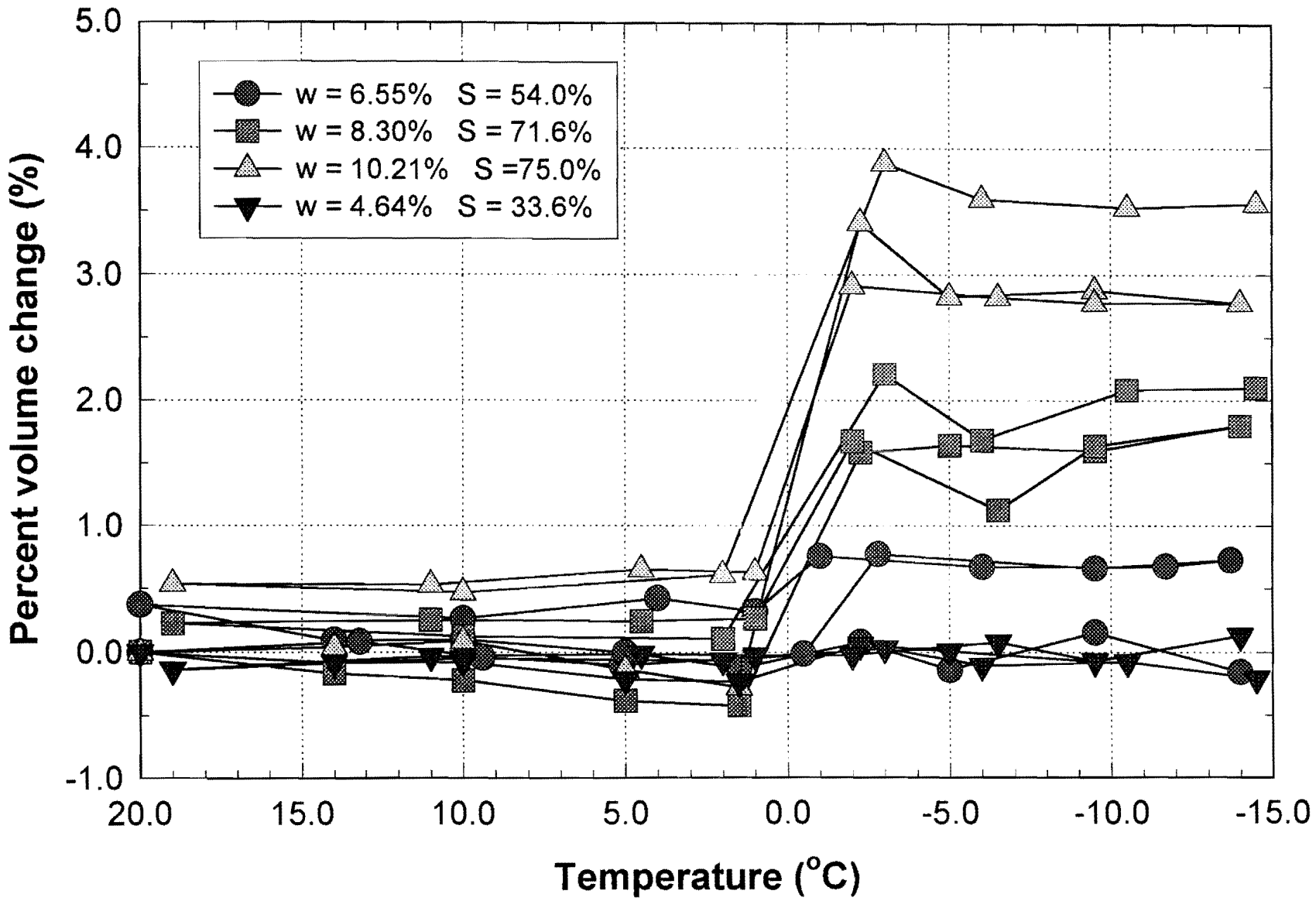
Percent Diameter Change of Aggregate AMC versus Temperature

D-16



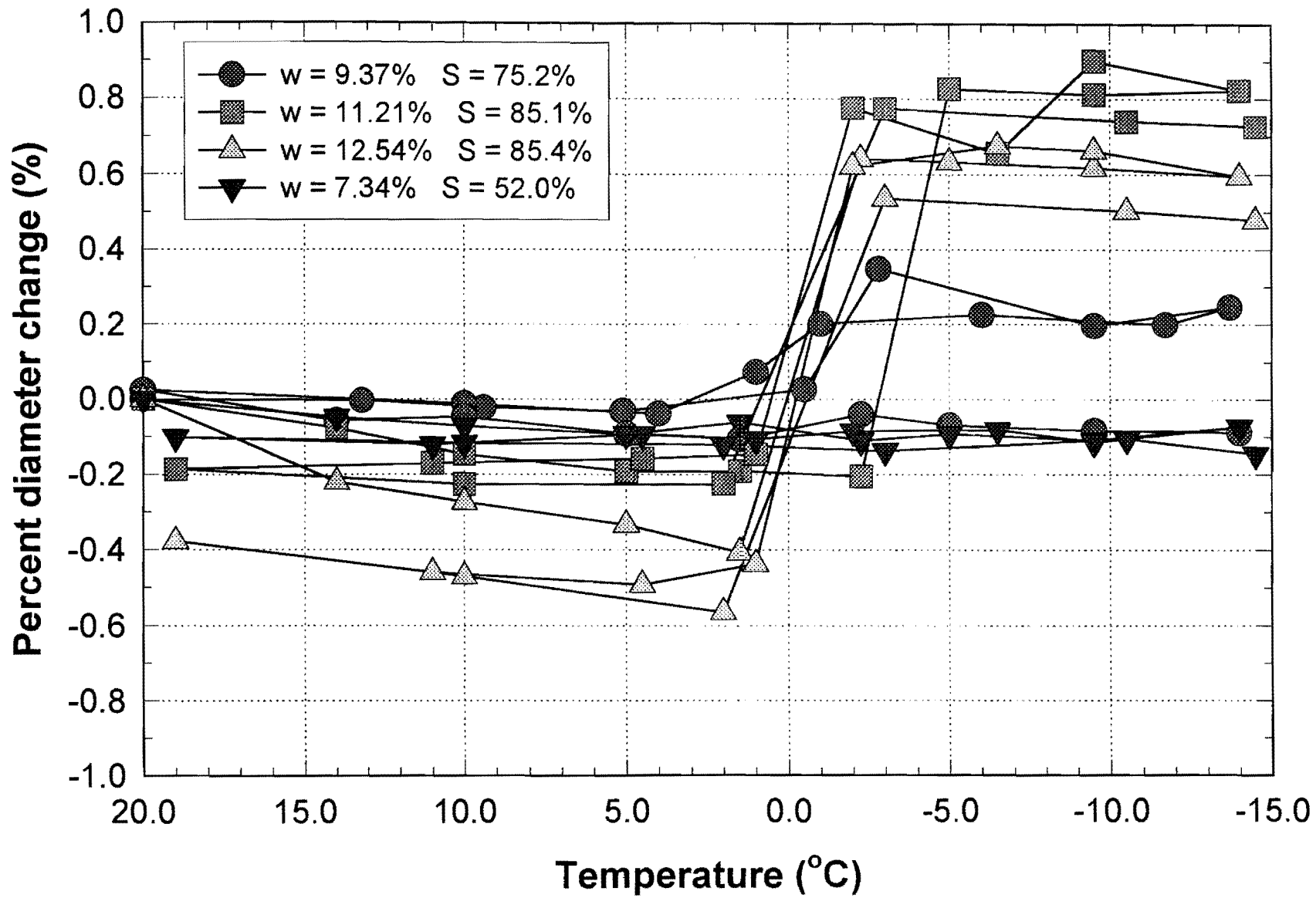
Percent Height Change of Aggregate Δ MC versus Temperature

D-17



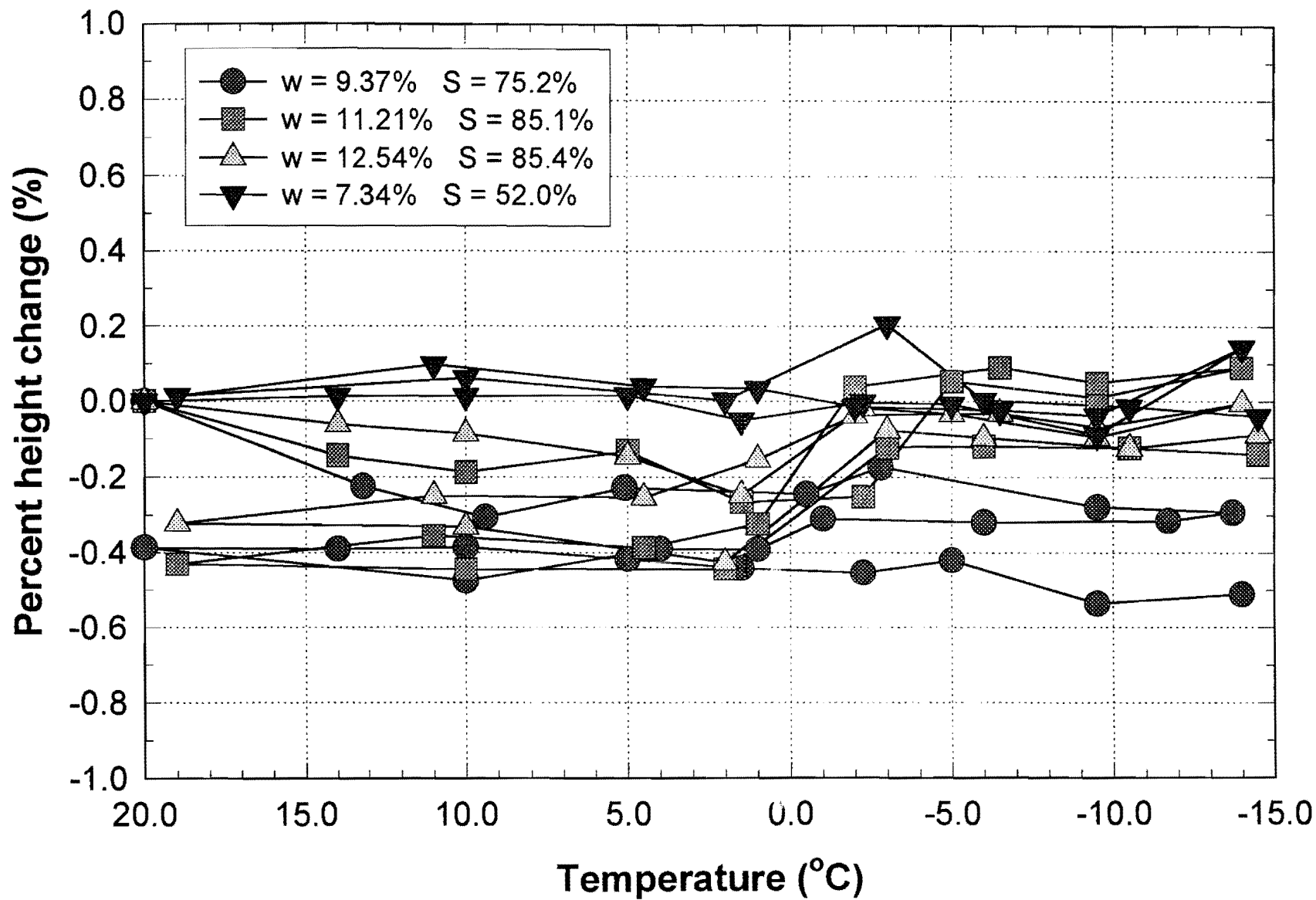
Percent Volume Change of Aggregate AMC versus Temperature

D-18

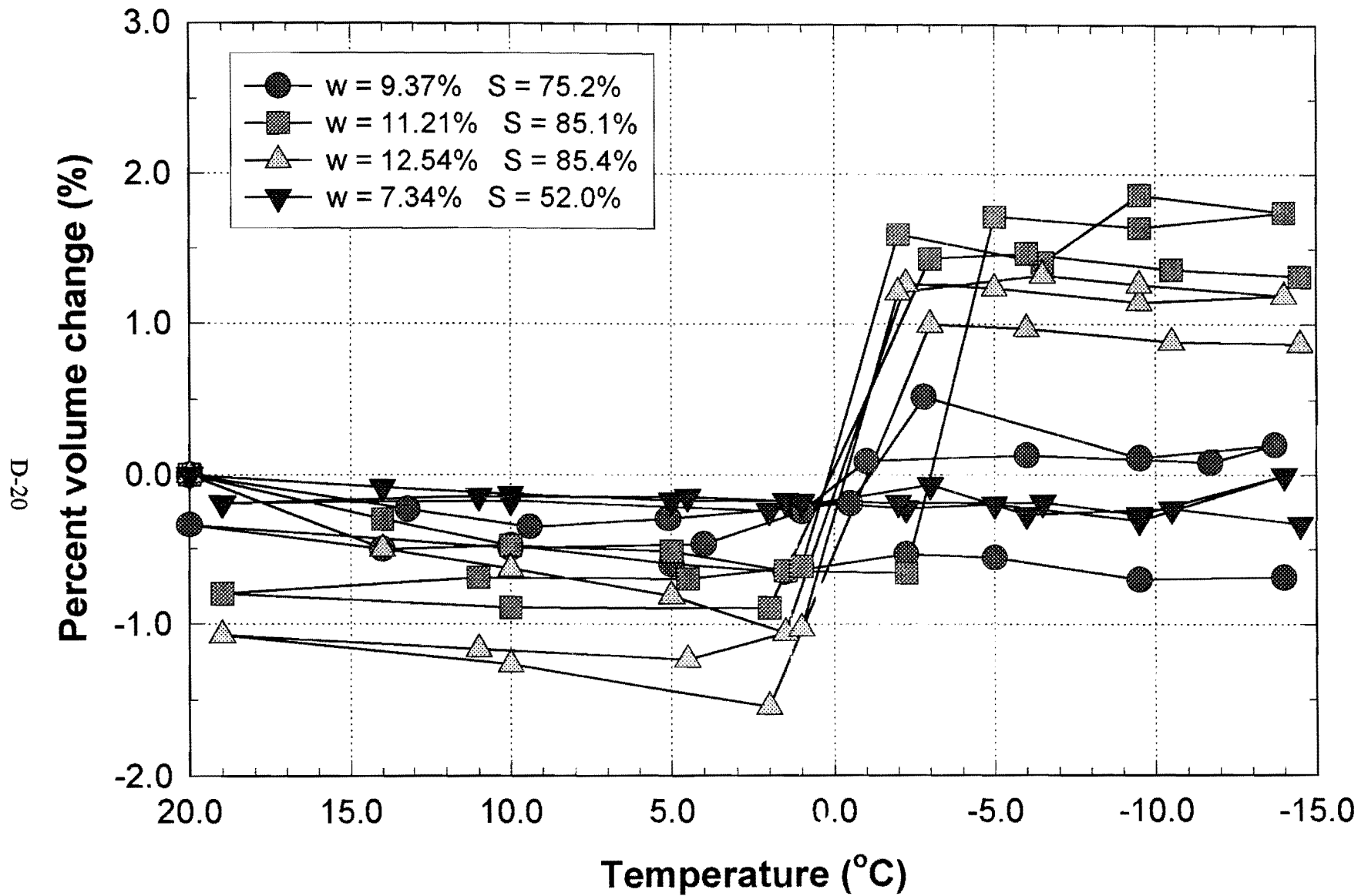


Percent Diameter Change of Aggregate Y290 (LS) versus Temperature

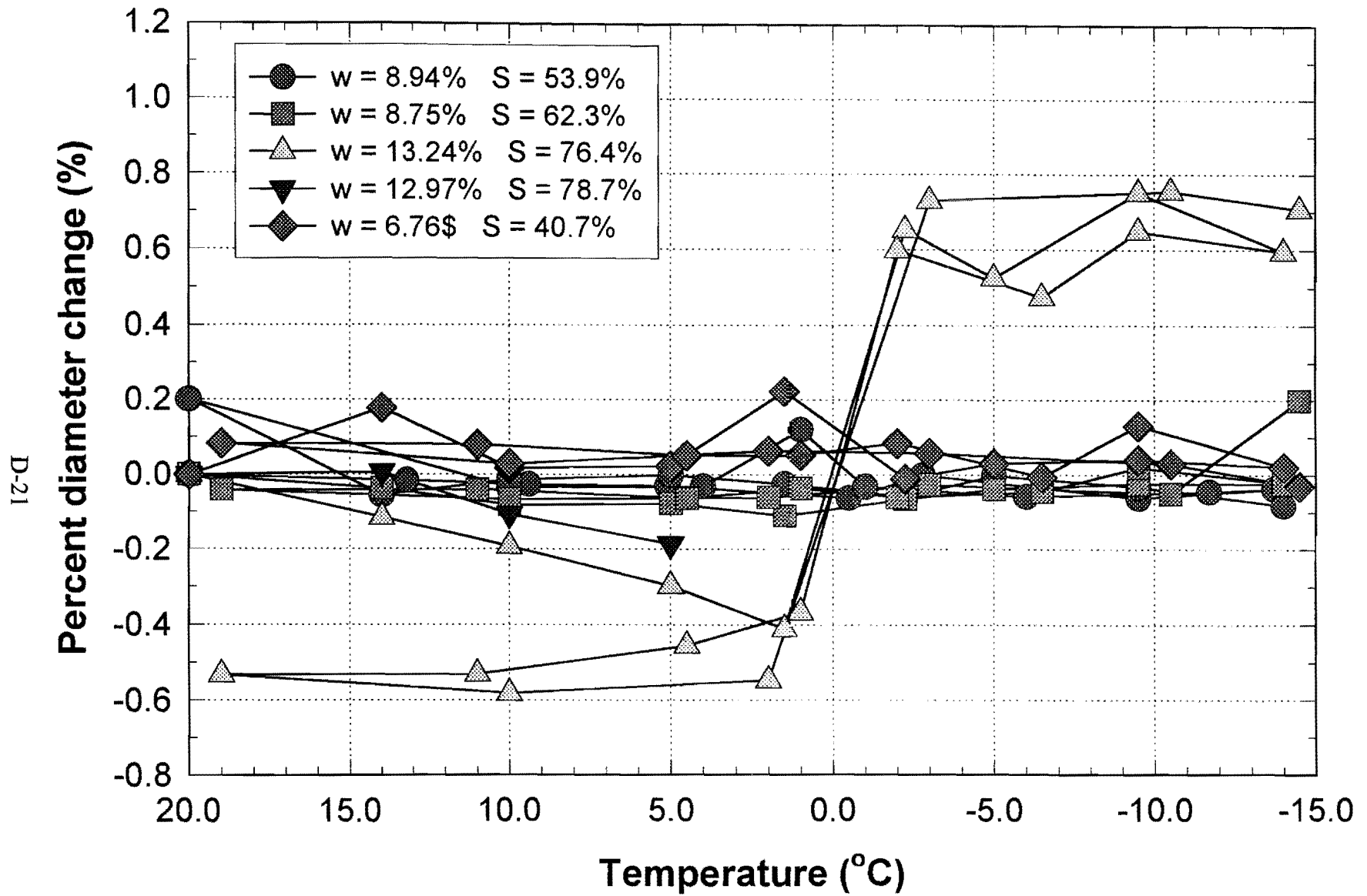
D-19



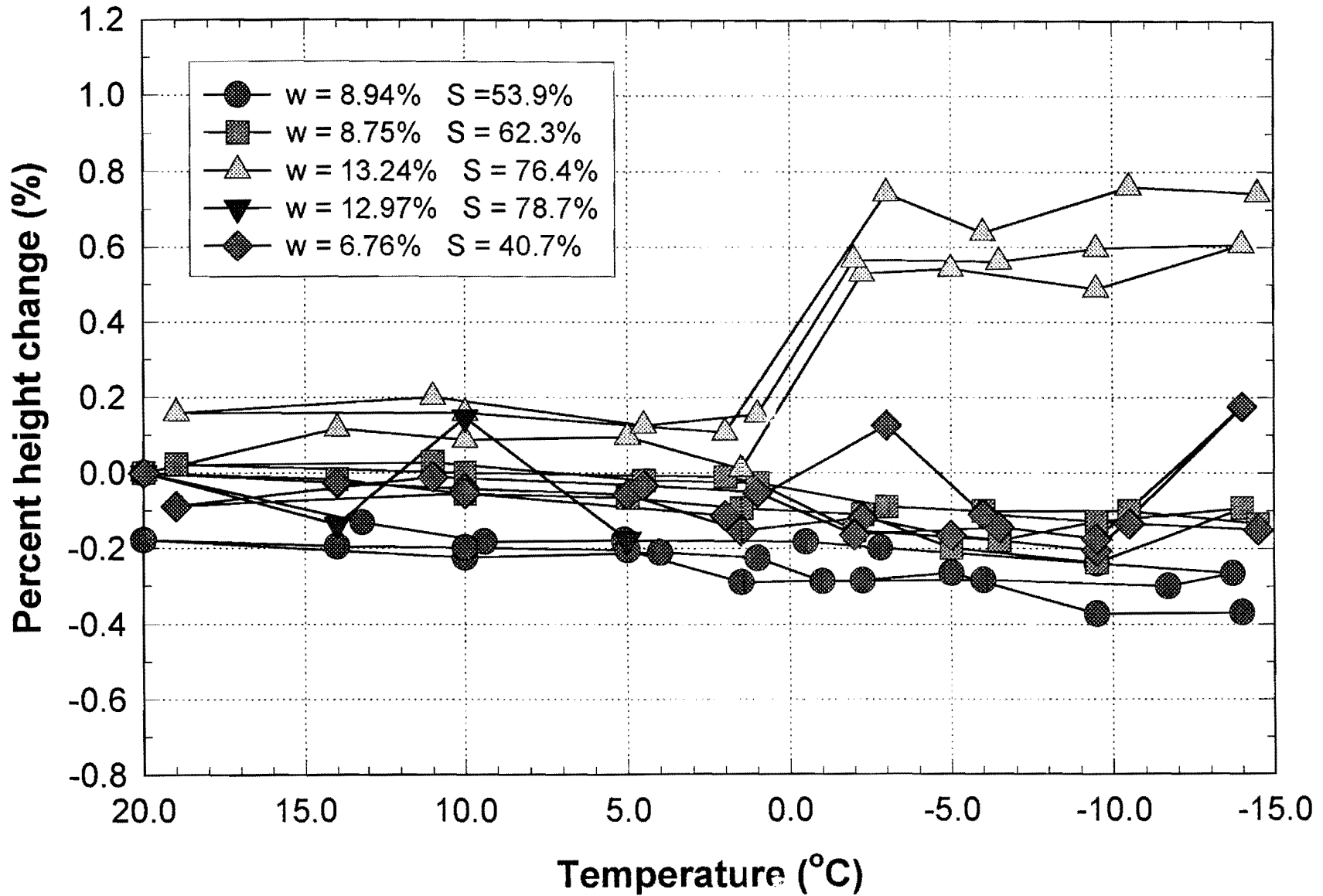
Percent Height Change of Aggregate Y290 (LS) versus Temperature



Percent Volume Change of Aggregate Y290 (LS) versus Temperature

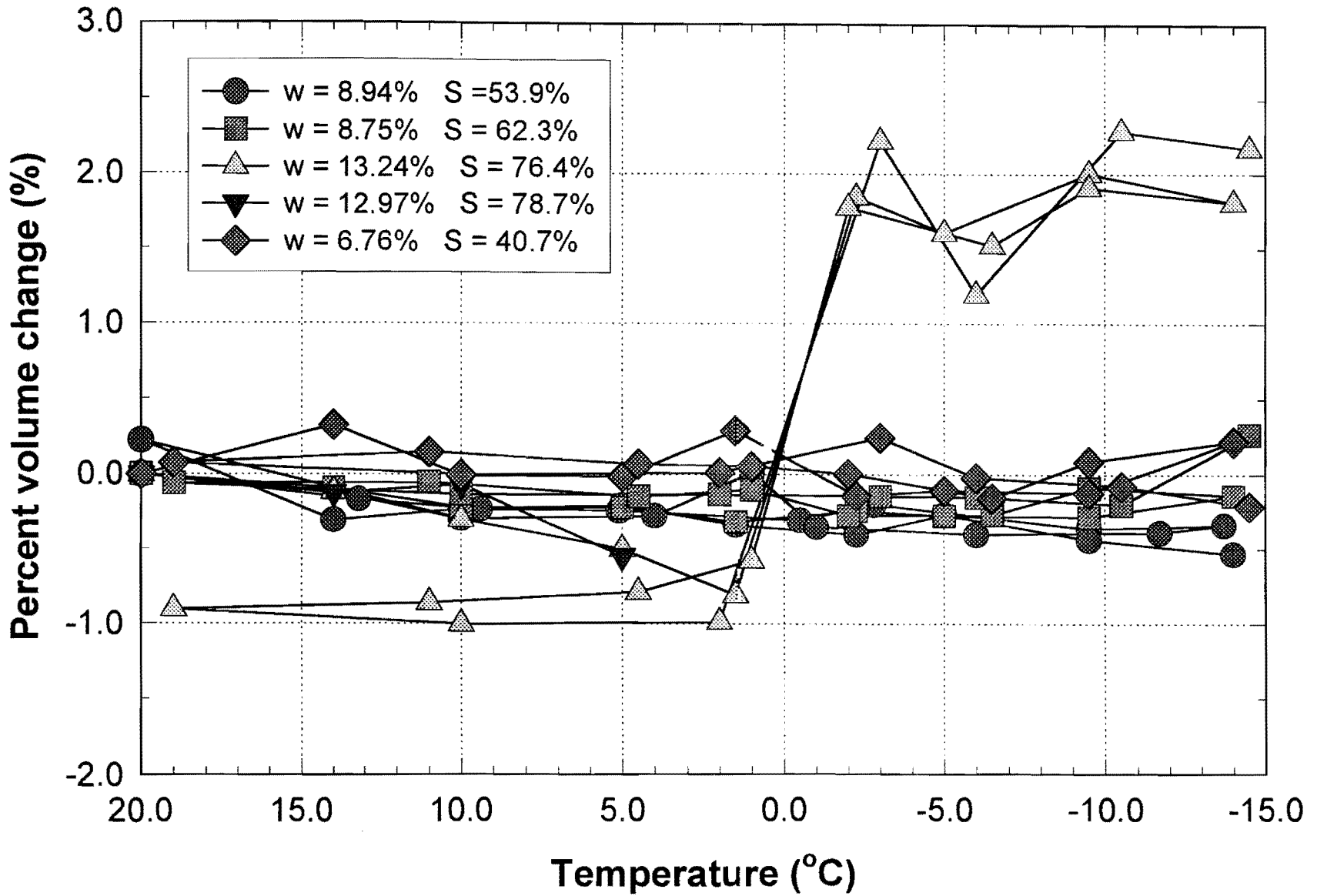


Percent Diameter Change of Aggregate YFG versus Temperature



Percent Height Change of Aggregate YFG versus Temperature

D-23



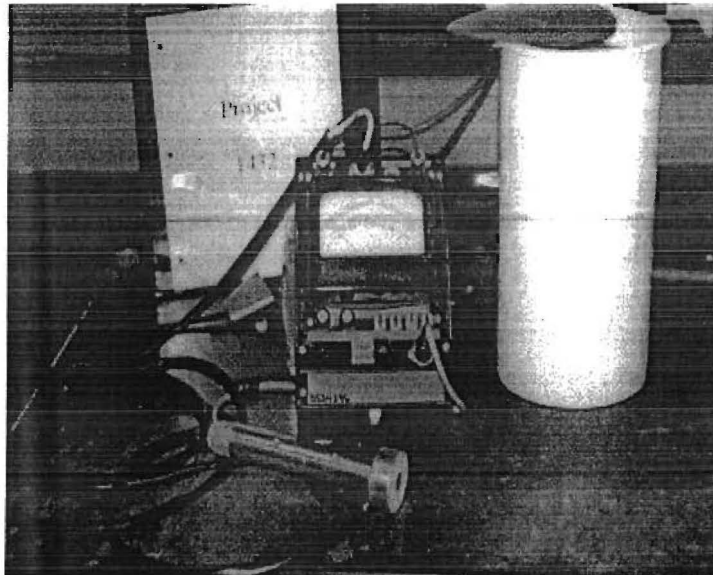
Percent Volume Change of Aggregate YFG versus Temperature

APPENDIX E
LABORATORY TESTING PROCEDURE

Laboratory Testing Procedure for the Tube Suction Test

What is the Dielectric Probe?

The Dielectric Meter and measurement probe are manufactured in Estonia, costing approximately five thousand dollars. The device itself is about the size of a shoebox, with a probe attached by a cord. The device contains a rechargeable battery, which allows it to be portable. The latest version has a digital output and comes with some standard material samples for calibration purposes.



What is the Dielectric Value and Electrical Conductivity?

The dielectric value is a measure of the volumetric moisture content and the state of molecular bonding in a material. Low dielectric values indicate the presence of tightly adsorbed and well-arranged water molecules; granular bases with low dielectrics would normally have optimum strength properties. Significantly higher values (> 16) would indicate the presence of substantial “free” moisture. With values such as these, the aggregate base would be suspected to be sensitive to both traffic loads and environmental freeze/thaw cycling. The electrical conductivity of a material is an indication of the amount of ions dissociated to the free water. The higher the electrical conductivity, the more ions present.

Purpose of the Tube Suction Test

The purpose of this lab testing procedure is to determine the moisture susceptibility of base course aggregates used in Texas. The test is a direct measure of how much moisture a base will absorb through capillary rise and the state of bonding of this absorbed moisture. From experience, the test results are primarily related to the amount and type of clay in the base, and secondarily to the water absorption properties of the coarse aggregate fraction.

Proposed base materials which fail this test would be anticipated to perform poorly under heavy wheel loads and when subjected to freezing and thawing conditions. The test is simple to perform and could be used as a screening test to identify sources which should be subjected to the full 10-day Texas Triaxial test. Alternatively, the test could be used to evaluate the impact of chemical stabilization on marginal base materials.

Preparation of the Material

The optimum moisture content must be determined using the Modified Proctor procedure. Prior to molding, the aggregate must be dried and prepared according to standard TxDOT methods (117 E).

Molding Procedure

Apparatus

- 10 lb drop hammer
- Plastic testing mold, with a height of 12 in and diameter of 6 in (standard concrete cylinder molds). The testing mold must have 1/16 in holes drilled at 1/2 in spacings, around the entire circumference, approximately 1/4 in from the bottom. An additional 4 holes are drilled in the base.
- Drying oven, maintained at 104 °F
- Large mixing bowl, capable of holding 12,000 grams of material

1. Weigh out 12,000 grams of aggregate and place in the large mixing bowl.

Note: When performing step one, it is necessary to discard all rocks larger than 1 in in diameter. This will assure a thorough consistency of the aggregate for molding.
2. Sprinkle water onto the material in increments. Thoroughly mix the specimen to ensure even distribution of water throughout. Adjust water content of the specimen in 2% increments until optimum water content is achieved.
3. Thoroughly re-mix the sample.
4. Place loose soil into the mold and spread into a layer of uniform thickness.
5. Compact the specimen in six 2 in thick lifts at 50 blows per lift.

Note: After compacting the sixth layer, it is necessary to achieve as smooth a surface as possible. This is achieved by placing some of the material fines on the surface.
6. Place the molded specimen on a bench for 12 hours at room temperature, then place in the drying oven. Weigh the sample every day until the weight becomes constant (typically 3 – 4 days).

Instructions for the Tube Suction Test

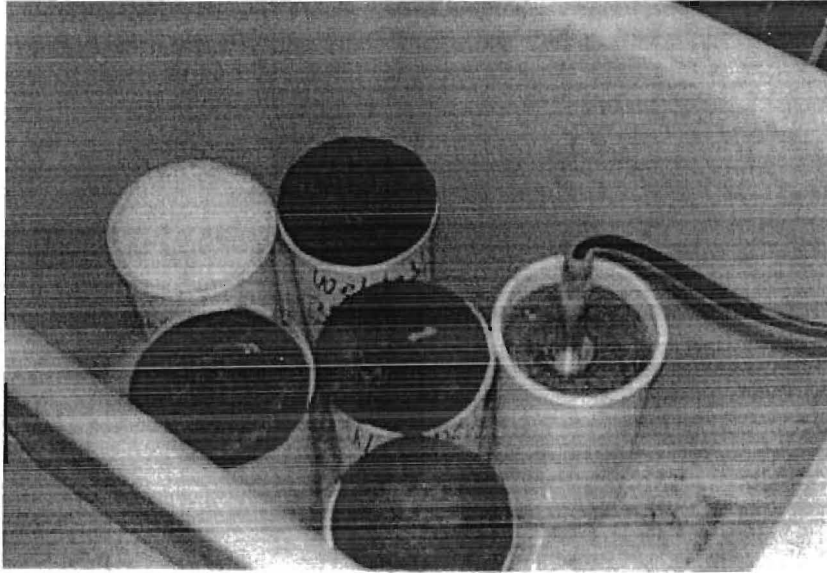
- A. Remove the molded specimen from the drying oven, and allow it to cool to room temperature. It will take around 4 hours. At this time, use a paperclip to dislodge any material that may be clogging the small holes around the base of the mold.

Equipment Needed

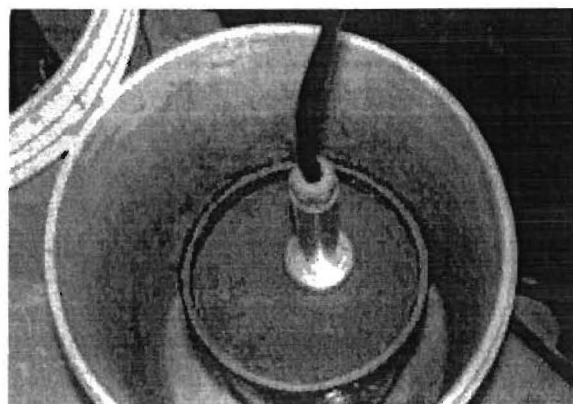
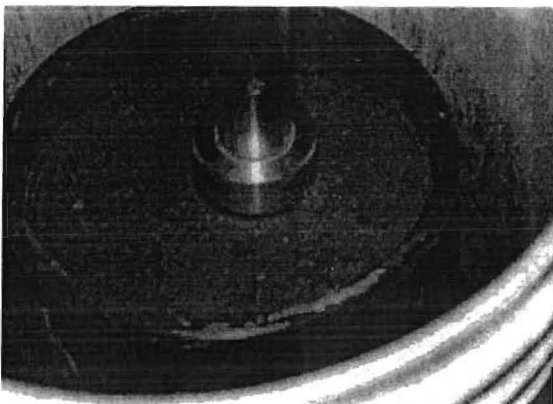
Dielectric Meter Probe
Container large enough to hold molded sample
Deionized water
Paper and pen to record measurements
Splash cap

- B. Begin by filling the container with 1/2 in of deionized water.

Note: It is important to monitor the level of deionized water in the container. The sample will absorb this water, and it is necessary to maintain a level of 1/2 in throughout the test.



- C. Begin by taking initial readings of the specimen before placing it in the deionized water. Measure the dielectric value and electrical conductivity of the dry sample surface. The probe must be placed firmly against the surface, in good contact with the test material. Avoid locations with protruding large aggregates. Take 4 readings of both Dielectric and Surface Conductivity from different locations on the surface. Weigh the sample. Then place the sample in the deionized water bath, and put the splash cap on the top of the cylinder.



Note: To compute the surface dielectric and conductivity, the high and low values in each case will be discarded and the remaining two averaged.

- D. Repeat step C at time intervals of 0.5, 1, 2, 4, 8, 12, and 24 hours and then every 24 hours for a total test period of 10 days.
- E. Stop the test after 10 days. Plot a graph of average dielectric and conductivity versus time. Note the typical curve will reach an asymptote after several days. The values below are used to classify materials based on these asymptotic values.

	<u>Good materials</u>	<u>Poor materials</u>
dielectric value	10 and below	16 and greater
electrical conductivity	200 and below	400 and greater

Conclusion

Once you have concluded the tube suction test, you will have a good indication of how the aggregate base will perform in the field. Based on the measurements taken, you can recommend whether or not that the particular aggregate base tested should be used for construction of a roadway structure.